Breiðdalur Central Volcano. What came first: The Central Volcano or The Fissure Swarm?

Robert A. Askew

Faculty of Earth Sciences
University of Iceland
2020

Breiðdalur Central Volcano. What came first: The Central Volcano or The Fissure Swarm?

Robert A. Askew

Dissertation submitted in partial fulfilment of a
Philosophiae Doctor degree in Earth Sciences

Advisor
Dr. Thorvaldur Thordarson, Professor in Volcanology and Petrology
University of Iceland

PhD Committee
Dr. Ármann Höskuldsson, Research Professor in Volcanology
University of Iceland

Dr. Phil Gans, Professor in Structural Geology and Argon Geochronology
University of California Santa Barbara

Opponents
Dr. Valentin Rudolf Troll, Professor in Igneous Petrology
Uppsala University, Sweden

Dr. Brian Bell, Lecturer at the School of Geographical and Earth Sciences
University of Glasgow, UK

Faculty of Earth Sciences
School of Engineering and Natural Sciences
University of Iceland
Reykjavik, January 2020

Breiðdalur Central Volcano. What came first: The Central Volcano or The Fissure Swarm?
Breiðdalur Volcano
Dissertation submitted in partial fulfillment of a *Philosophiae Doctor* degree in Earth Sciences

Faculty of Earth Sciences
School of Engineering and Natural Sciences
University of Iceland
Sturlugata 7, Reykjavík
101, Reykjavik
Iceland

Telephone: 525-4000

Bibliographic information:
Robert A. Askew, 2020, *Breiðdalur Central Volcano. What came first: The Central Volcano or The Fissure Swarm?*, PhD dissertation, Faculty of Earth Sciences, University of Iceland, 177 pp.

ISBN 978-9935-9412-6-8

Printing: Háskólaprent
Reykjavik, Iceland, January 2020

Abstract

The Breiðdalur volcanic system, eastern Iceland, comprises of a 600 km^3 central volcano, a 30 - 40 km long dyke swarm and plateau basalts erupted from this dyke swarm. The entire volcanic system was active from 10.1 to 7.8 Ma, the central volcano was only active from 10.1 to 9.1 Ma and the dyke swarm's activity continues for a further 1.3 My after this. The central volcano is predominantly basaltic (80-85 %) and basaltic lava formed the broad flanks of the volcano between 10.1 Ma and about 9.5 to 9.6 Ma. More evolved lavas of basaltic icelandite to icelandite composition also erupted onto the flanks during this time, a 400 m thick sequence of icelandites formed on the south east flank of Breiðdalur from 9.9 to around 9.7 Ma. These earliest evolved lavas probably formed through fractional crystallisation of basaltic magma, resulting the formation of a crustal magma storage zone/chamber below the south east flank of the volcano.

At around 9.6 to 9.5 Ma silicic magmatism began at Breiðdalur volcano, one of the earliest silicic events was a caldera forming event. This created the depression of Breiðdalur caldera, which was infilled by silicic pumice agglomerate, and further deformed by subsequent eruptions. This early silicic magma was most likely formed through partial melting of hydrated basaltic crust and drove the explosive volcanism. The Breiðdalur caldera was 8 to 10 km wide and around 500 m deep, it is infilled with the products of silicic explosive eruptions, silicic effusive eruptions and mafic to intermediate intrusions and eruptions. The loose deposits of the caldera material have been extensively reworked by water and there is evidence for caldera lakes and trace fossils of life within the lakes. The caldera is overlain by the summit group, a sequence of horizontal to sub-horizontal lavas, ignimbrite, tuffs and sediments that was erupted at around 9.3 Ma. At this time silicic lavas were erupted on the flanks of the volcano, most prominently the South East Rhyolites group in the south-east and the Fossárdalur composite lava in the south. Silicic magmatism ceases at 9.1 Ma.

The dyke swarm was active from at least 9.8 Ma to 7.8 Ma. The dykes are basaltic in composition and is likely related to the plateau basalts that envelope the central volcano. The central volcano was buried rapidly by plateau basalts, or within a few hundred thousand years and all activity ceases in the Breiðdalur area at 7.8 Ma.

The volcanic systems of Þingmúli, Breiðdalur and Álftafjörður were all active at a similar time from 11 to 8 Ma and thus featuring overlapping activity. Reyðarfjörður and Streitishvarf volcanic systems are older, or around 12 to 11 Ma. All systems are tholeiitic with a slight enrichment in incompatible trace elements when compared to Mid Ocean Ridge Basalts (MORB). Isotopic analysis was undertaken on a suite of samples from these volcanic systems and the results indicate that Breiðdalur, Þingmúli and Streitishvarf are isotopically indistinct and share similar deep magma sources, though the latter system is slightly older. Reyðarfjörður, the most northern system in this study, featured a more depleted magma source than the other systems, whereas the southernmost one, Álftafjörður, had a more enriched source. These characteristics appear to indicate a spatial variation in isotopic geochemistry, as can be seen in Holocene lavas, rather than a temporal variation. We present a renewed geochronological map of the east fjords and maps of the geochemical variation in East fjord lavas.

Útdráttur

Eldstöðvakerfið sem er kennt við Breiðdal á Austurlandi samanstendur af 600 km^3 megineldstöð, með rúmmál metið upp á, og 30-40 km löngum gangasveim sem framleiddi ofan og umliggjandi flæðibasalthraun. Eldstöðvakerfið var virkt á tímabilinu frá 10,1 til 7,8 milljónum ára (Ma), megineldstöðin frá 10,1 til 9,1 Ma. Gangasveimurinn byrjaði að myndast fyrir 9.9 Ma og var virkur næstu 2,3 milljónir ár. Megineldstöðin er að mestu gerð úr basalthraunum frá gosum á tímabilinu 10.1 Ma til 9,5/9,6 Ma og hlóðu upp ytri hlíðar fjallsins. Þróaðri hraun úr basaltísku íslandíti og íslandíti mynduðust einnig á þessum tíma og þá einkum á tímabilinu 9,9-9,7 Ma þegar 400 m þykk syrpa af íslandíthraunum staflaðist upp í suðausturhlíðum fjallsins. Þessar ísúru kvikur mynduðust sennilega við hlutkristöllun á kvikunni sem lagði til basísku hraunin í árdaga eldstöðvarinnar og benda til þess að einhvers konar kvikugeymsla (kvikuhólf?) hafi þá þegar myndast undir megineldstöðinni.

Rýólít eldvirkni byrjaði í Breiðdalsmegineldstöðinni fyrir um 9,6-9,5 Ma sem leiddi af sér myndun öskju í toppi fjallsins. Askjan, sem er að stórum hluta fyllt af vikurbrexíu, hélt áfram að þróast í þeim eldgosum sem fylgdu í kjölfarið. Rýólít kvikur Breiðdalseldstöðvarinnar virðast hafa myndast við hlutbráðnun á vatnaðri basaltskorpu og dreif áfram sprengigosavirknina í eldstöðinni. Askjan í Breiðdalseldstöðinni var 8- 10 km í þvermál og allt að 500 m djúp, og er fyllt af gosmyndunum súrra sprengigosa og hraungosa ásamt seint tilkomnum basískum og ísúrum innskotum. Gjóskumyndanirnar í öskjufyllunni urðu á þessum tíma fyrir verulegu rofi og endurflutningi, sennilega að mestu vegna úrkomu. Um tíma voru lítil „öskjuvötn“ inni í öskjunni og setið í öðru þeirra hefur varðveitt steinrunnin för eftir vatnalífverur. Ofan á gosmyndanir öskunnar leggst „Toppmyndunin“ (e. Summit Group), sem er syrpa af lárétt liggjandi stafla sem er byggður upp af hraunum, gjóskuhlaupaseti, og gjósku sem mynduðust í eldgosum í kringum 9,3 Ma og inniheldur í minna mæli setlagamyndanir. Á svipuðum tíma mynduðust rýólíthraun í hraungosum á ytri hlíðum eldstöðvarinnar og þar eru mest áberandi Suðaustur Rýólít Hraunasyrpan (e. South East Rhyolite Group) sem krýnir fjallagarðinn sem skilur að Berufjörð og Breiðdal og síðan samsetta hraunið (e. composite lava) neðarlega í suðurhlíðum eldstöðvarinnar og rekja má með Fossárfjalli og yfir í Fossárdal. Þessi rýólít eldvirkni var öll um 9.1 Ma.

Gangasveimurinn byrjaði að myndast tvö hundruð þúsund árum seinna en megineldstöðin og var virkur frá 9.8 Ma til 7,8 Ma. Berggangarnir eru að mestu basískir og eflaust tengist myndun sumra þeirra myndun flæðibasalthraunanna sem umlykja og leggjast ofan á Breiðdalseldstöðina. Eldstöðin grófst í hraun á nokkrum hundrað þúsund árum og virkni lognaðist út af í Breiðdal fyrir um 7,8 Ma.

Kulnuðu eldstöðvarkerfin Þingmúli, Breiðdalur og Álftafjörður voru öll virk á svipuðum tíma, eða á tímabilinu 11 Ma til 8 Ma og með til hlýðandi skörun í eldvirkninni. Kerfin sem eru kennd við Reyðarfjörð og Streitishvarf eru eldri, eða um 12-11 Ma. Öll kerfin eru þóleiítísk og framleiddu kvikur sem eru heldur auðugri af utangarðsefnum en dæmigerðar úthafshryggja kvikur (þ.e. MORB). Samsætugreiningar á sýnum sem var safnað innan þessara kerfa sýna að Breiðdals-, Þingmúla- og Streitishvarfskerfin eru óaðgreinanleg, sem bendir til þess að basaltkvikur þessara kerfa eiga rætur sínar að rekja til upptaka með sömu samsetningu og það þrátt fyrir aldursmuninn á síðastnefnda og hinum tveimur fyrrnefndu kerfum. Basaltkvikur Reyðarfjarðarkerfisins, sem liggur nyrst af þessum kerfum, virðast konar frá upptökum sem eru heldur snauðari í utangarðsefnum, á meðan basaltkvikur

syðsta kerfisins, sem er kennt við Álftafjörður, er heldur auðugari í utangarðsefnum. Þessar niðurstöður benda til þess að það er staðbundin munur á samsætusamsetningu upptakasvæða kvikunnar sem komu upp í þessum eldstöðvarkerfum á sínum tíma, ekki ósvipað þeim mun sem er til staðar í dag innan virkra gosbelta á Íslandi. Einnig fylgir með uppfært jafnaldurkort af Austfjarðarstaflanum og kort sem sýna svæðisbundnar breytingar í efnasamsetningu hraunlagastaflans.

Acknowledgements

Firstly, I would like to thank my supervisor, Thor. Without your valuable tuition from 1st year Undergraduate trips to Arthur's Seat, to MSc field courses and research in Iceland and now to supervision and mentoring in Ph.D. research, this project would not have been possible. It's also these skills that I've learnt through you and opportunities you provided that have allowed me to continue my work as a Field Geologist.

And to my co-supervisors, firstly Ármann, thank you for all your hard work and input. I'm extremely grateful to have had the opportunity to learn from you, especially during fieldwork from Reykjanes to the Holuhraun eruption. These are some of the most memorable fieldtrips and fieldwork of my time in Iceland, I've learnt the value of calm and decisive leadership in ever-so-slightly stressful situations. I'm also grateful for the contacts in Misasa, Japan and the opportunity to travel there. And to Phil, it was an honour to meet you and have had the opportunity to travel to California, learn the ins-and-outs of the Ar-Ar age dating technique and experience the California life!

Thanks go as well to those who helped out on fieldwork out east: Kate, Andy, Simon, Sibylla and Pippin. And special thanks to Christa and Martin at Breiðdalssetur for your input, accommodation and your help with everything in the east! Further thanks to Björn Björgvinsson in Breiðdalsvík for interesting stories, letting us stay in your house and for showing us many interesting sites in eastern Iceland.

Further gratitude is due to all those who helped with lab work and more! Nic Oddling and Godfrey Fitton at the University of Edinburgh; Sæmi and Guðrun for all of your help with lab work and valuable feedback; Dr. Katsura Kobayashi, Dr. Hiroshi Kitagawa and especially Dr. Chie Sakaguchi for all your help in the clean lab at PML, Misasa.

Ph.D.'s are tricky things and life in Iceland through the long, cold winters, is hard. It would be impossible to get through it without the support and friendship of everyone I've met here, especially those in Askja. From those who have shared an office: Hrönn, Guilia, Kate, Jónas, Will and Alberto. To those on the Geo-side of Askja, whose names are too many to list down here and also to those on the ´wrong' side of Askja, the biology crew. Thank you to everyone in the best running club in Iceland ´Da Running Club', to everyone who I've tied to the end of a rope with, to everyone I've shared a drink with, celebrated with, commiserated with and mostly complained to/with: Ágúst, Sydney, Hannah, Becca, Gro, Daniel, Paavo, Jed, Erla, Mike, Óli, Holly, Ryan, Gotje, Jake, Þóra, Birgir, Deirdre, Vincent, Joaquin, Mary, Spencer and so many more. Many thanks go to the folks I met in Santa Barbara, thanks for being great hosts, it was amazing getting to know you all.

Special thanks go to my partner, Kate. Without your support this would have been 1000 times harder, it's been amazing and a pleasure to share this part of life with you and here's to many more years exploring Iceland, the world and the future. We also couldn't have got through this without the therapy support of our little four-legged fluff-ball Pippin.

And final thanks go to my whole family and especially to my parents, thanks for giving me all of the opportunities you did, thankyou for raising me, teaching me and giving me a happy, loving life, and thankyou for putting up with my decision to go through this stressful and draining stage in life.

This project was funded by the University of Iceland Eimskip Research Fund, to whom I am grateful for accepting my application. The final years were supported by a teaching assistant position at the University of Iceland and a research position with the EVE project provided by Ármann Höskuldsson and Thorvaldur Thordarson, as well as funding from the Watanabe Trust Fund (Thanks Mr Watanabe) for a research visit to Misasa, Japan.

To those who's names are not written, you're not forgotten, there were so many people that I've had the pleasure of meeting in the past few years, thank you and I'm grateful you were there!

Abbreviations

BFT	Berufjarðatindur.
EM	Enriched Mantle.
EVZ	Eastern Volcanic Zone.
GPG	Grænavatn Porphyrytic Group.
ICP-MS	Inductively Coupled Plasma Mass Spectrometer.
ICP-OES	Inductively Coupled Plasma Optical Emission Spectrometer.
IES	Institute of Earth Sciences.
LA-ICP-MS	Laser Ablation Inductively Coupled Plasma Mass Spectrometer.
MC-ICP-MS	Multi Collector Inductively Coupled Plasma Mass Spectrometer.
NVZ	Northern Volcanic Zone.
PML	Pheasant Memorial Lab.
SER	South Eastern Rhyolites.
SVB	Snæfellsnes Volcanic Belt.
TIMS	Thermal Ionisation Mass Spectrometry.
WVZ	Western Volcanic Zone.
ÖVB	Öræfi Volcanic Belt.

Contents

List of Tables

List of Figures

Motivation and Objectives

The main objective of this project was to outline a definitive age relationship between a central volcano and dyke swarm within a single volcanic system. This has important implications for understanding volcanic systems across Iceland and the North Atlantic Igneous Province. Additionally, it provides a new insights to behaviour of Neogene volcanic systems in the North Atlantic as well as new views on future volcanic hazards in Iceland. It can also be beneficial in promoting geotourism in the area, in cooperation with the Walker Centre (i.e. Breiðdalssetur), Breiðdalsvík.

Chapter 1

Introduction

1.1 The evolution of Iceland and its volcanism

Iceland is the only part of the Mid-Atlantic Ridge (MAR) which is sub-aerial, a manifestation of the interplay between the MAR and the Iceland mantle anomaly, resulting in "excess" volcanism (Helgason, 1985; Martin et al., 2011). The current Iceland mantle anomaly, or mantle plume, is attributed to the creation a Large Igneous Province (LIP), the North Atlantic Igneous Province (NAIP), which today stretches from Eastern Greenland to North West Scotland (Figure 1.1a). The Paleogene Iceland mantle plume caused rifting, flood basalt volcanism and significant volcanic centres across eastern Greenland and north west Scotland. The resultant continental breakup lead to the formation of the North Atlantic ocean and the Iceland mantle plume became coupled with the MAR, an interplay which has continued to the present day. Iceland is in the centre of the NAIP, and the only section currently active (e.g. Saunders et al. (1997); Figure 1.1a and 1.1b).

The presence of a mantle anomaly beneath Iceland was suggested due to the elevated Iceland plateau and the symmetrical ridge connecting Greenland and Scotland (Vink, 1984; Morgan, 1971, Figure 1.1a). Further geochemical and geophysical evidence has strengthened this argument (e.g Thirlwall, 1995), with most authors suggesting the plume head is placed beneath western Vatnajökull (Figure 1.1a). It's thought that the plume is an upwelling of hot, wet (e.g. (Nichols et al., 2002)) or enriched mantle or a combination off all 3. The upwelling mantle plume mixes with Mid-Ocean Ridge basalt (MORB) from the spreading ridge, with a higher concentration of plume material close to the plume head and a decreasing amount away from it (Schilling, 1973; Sigmarsson et al., 2008). This dynamic is well documented along the Reykjanes Peninsula and Ridge, though a similar signal is not observed to the north of Iceland (Thirlwall, 1995; Thirlwall et al., 2004), most likely due to the presence of the Tjörnes fracture zone, which may act as a blocking feature to any plume material attempting to flow northwards from Iceland. The plume head also creates an irregular ridge architecture through Iceland; the MAR is moving westward relative to the semi-stationary Iceland mantle plume. The relative motion of the ridge away from the plume head causes eastward rift relocations on the order of 100's of km's approximately every 6 – 7 My (Jóhannesson, 1980; Steinþórsson, 1981; Helgason, 1984). Thus, the current configuration of the rift axes in Iceland is thought to be due to this interplay.

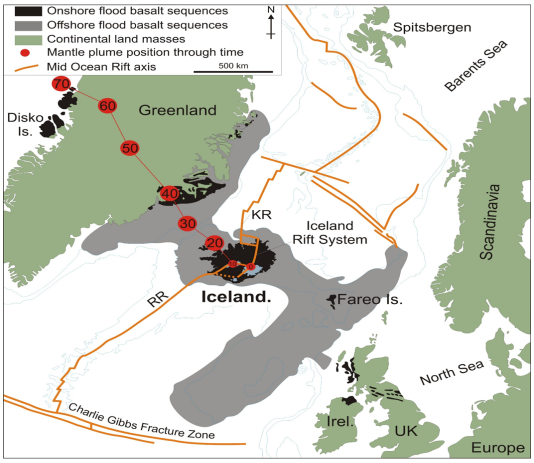

(a) NAIP from Thordarson and Larsen (2007) edited from Saunders et al. (1997).

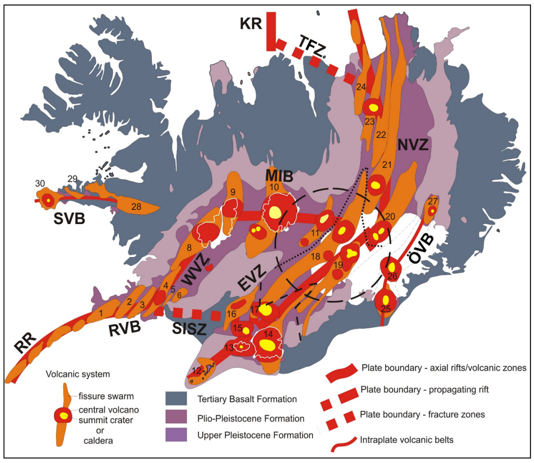

(b) Volcanic zones and systems in Iceland, from Thordarson and Höskuldsson (2008)

Figure 1.1: Regional geological context and crustal structure of Iceland

1.1.1 Volcanic Zones and Belts

Active volcanism in Iceland in is confined to two types of settings: i. along the axial rift and ii. intraplate belts (Figure 1.1b). The nomenclature follows the simple rule of relative geographic position within Iceland. Axial zones, shown in Figure 1.1b, consist of:

The Northern Volcanic Zone (NVZ), delineated by the Tjörnes Fracture zone (TFZ) to the north and southwards to the Eastern Volcanic Zone (EVZ). Typically the boundary between the NVZ and the EVZ is between the Askja volcanic system and the Bárðarbunga volcanic system (No. 21 and 18 in Figure 1.1b respectively; dotted line in figure; Thordarson and Larsen (2007); Thordarson and Höskuldsson (2008)). The NVZ includes the volcanic systems of Þeistareykir, Krafla, Fremrinámur, Askja and Kverkfjöll.

The Western Volcanic Zone (WVZ), an ultra slow spreading portion of the MAR system, as spreading is taken up across both the WVZ and EVZ. This zone contains the systems of Hengill, Hróðmundartindur, Grímsnes, Geysir, Prestahnjúkur and Hveravellir. Only Hengill, Prestahnjúkur and Hveravellir contain a central volcano. Rifting began here after a shift from the Snæfellsnes Volcanic Belt (SVB) around 6 Ma. Lavas erupted along the WVZ are mostly incompatible element depleted and tholeiitic in composition (Sinton et al., 2005).

The EVZ, located south of the NVZ, it includes the systems of Grímsvötn, Bárðarbunga, Torfajökull, Hekla, Tindfjöll, Katla, Eyjafjallajökull and Vestmannaeyjar. The northern part of the zone (dashed line Figure 1.1b) displays faster spreading rates (LaFemina et al., 2005) than to the south and has well defined volcanic systems (Thordarson and Höskuldsson, 2008), which are not represented as well in the south part. This geometry is reflected in the geochemistry of the magma erupted, with more tholeiitic compositions to the north and more alkalic magmas further south (Jakobsson, 1979b; Saemundsson, 1979). This volcanic zone began by propagating southwards between 1.5–3 Ma (Saemundsson and Jóhannesson, 1994) from the NVZ and it is thought this rift may take over from the WVZ as a major axial rift. The propagating front of the zone forms the southern portion of the EVZ, with major central volcanoes of Vestmannaeyar, Katla, Eyjafjallajökull and Tindfjöll. Notably, the volcanic systems of the southern EVZ display poorly developed or no fissure swarms. The EVZ is currently the most active segment of the Icelandic rift zones, producing around 80% of the erupted magma in historic times, with all 4 of the most productive systems (Katla 36%, Grímsvötn 30%, Hekla 19%, and Bárðarbunga 15%) being located on this zone (Thordarson and Larsen, 2007).

The TFZ (also called Húsavík-Flatey Zone (Einarsson, 2008)), a series of oblique strike-slip faults connecting the Kolbeinsey Ridge (KR) to the axial belts running through Iceland (Sæmundsson, 1974).

The Mid-Iceland Belt (MIB), connects the NVZ and WVZ through the centre of Iceland (Figure 1.1b). The is little information in the literature directly addressing the MIB (also called the Hofsjökull Zone (Sinton et al., 2005; Jakobsson et al., 2008)), it consists almost entirely of the large caldera volcano of Hofsjökull and its fissure swarms, the small volcanic centre of Kerlingarfjöll lies to the south of Hofsjökull. The MIB is joined to the WVZ by a series of fractures, thought to be connected to the Hofsjökull system, with a NNE orientation recently termed the Kjölur fissure swarm (Hjartardóttir et al., 2016). There are no mapped fissures across Sprengisandur, between Hofsjökull and Tungnafellsjökull in the NVZ though linear structures are visible on aerial photographs of the area, thus the connection between the two is unclear.

The South Iceland Seismic Zone (SISZ), connects the southern EVZ to the WVZ through a left lateral transform zone that manifests as en-échelon N-S trending right-lateral strike-slip faults (Ward, 1971; Einarsson et al., 1981; Einarsson and Eiríksson, 1982; Stefánsson et al., 1993; Gudmundsson, 1995; Árnadóttir et al., 2001). The transform is 'leaky' with respect to magmatism as evident from the volcanism at Grímsnes and late glacial eruption that formed Hestfjall (Sinton et al., 2005; Eason et al., 2015).

The Reykjanes Volcanic Belt (RVB) is delineated in the north by the Brennisteinsfjöll volcano and the south by the Reykjanes Ridge. The belt contains the fissure swarms of Reykjanes/Svartsengi, Krýusuvík and Brennisteinsfjöll. The RVB contains no central volcanoes, though active geothermal areas suggest that long-lived shallow magma chambers are present beneath the crust (Gudmundsson, 2000). The belt is either an oblique axial rift or a leaky transform, as suggested by the strong strike-slip component in its tectonic fabric (Clifton et al., 2003; Clifton and Kattenhorn, 2006; Einarsson et al., 2018). Geochemically the lavas erupted are tholeiitic (Jakobsson et al., 1978), olivines containing high He ratios are found in southern Reykjanes (Condomines et al., 1983).

Intraplate belts (Figure 1.1b), consist of:

The Öræfi Volcanic Belt (ÖVB), an intraplate volcanic zone with alkalic magmatism and distinct isotopic and incompatible element compositions (Prestvik, 1985; Prestvik et al., 2001; Kokfelt et al., 2006; Jakobsson et al., 2008; Torsvik et al., 2015; Manning and Thirlwall, 2014). It consists of 3 volcanoes, Snæfell to the north, Esjufjöll and Öræfajökull to the south, the latter is the only volcano on the belt to have erupted in historical times, having had two eruptions, the oldest in AD1362 and later a basaltic eruption in 1727 (Thorarinsson, 1958). The ÖVB is distinct in lying outside of the well defined rift zones, early studies suggested the belt may reside at the intersection of a fracture zone and a largely dormant rift zone (Thorarinsson et al., 1973; Walker, 1975; Prestvik, 1979, e.g.). More recently it's been suggested that ÖVB represents a site of incipient rifting at the fringe of the mantle plume (Hards et al., 2000; Peate et al., 2010).

The Snæfellsnes Volcanic Belt is another intraplate volcanic zone displaying alkalic magmatism (Jakobsson et al., 2008), and high Pb isotope ratios (Peate et al., 2010), it is thought to be the pre-rift to the WVZ active before 6 Ma. Magmatism is suggested to continue due to the topography of the base of the lithosphere, which channels plume material westwards beneath the old rift zone. One large strato-volcano is present on the peninsula, Snæfellsjökull volcano.

To the north of Iceland is the Kolbeinsey Ridge (KR), part of the submarine MAR. To the south is the Reykjanes Ridge (RR).

Petrology and Geochemistry

The volcanic zones and belts of Iceland can be broken up by their petrological and geochemical characteristics. Where the names of the zones and belts is purely geographical, their petrology and geochemistry fits, to some extent, these divisions. Iceland itself broadly erupts enriched Ocean Island Basalt (OIB) mixed with MORB (Oskarsson et al., 1982; Schilling, 1973; Thirlwall, 1995; Fitton et al., 1997). The composition of lavas is strongly contrasting between the axial zones of Iceland, and the off-axis or flank zones. The axial zones of the WVZ and NVZ as well as the northern portion of the EVZ display tholeiitic, or more incompatible element depleted magmatism compared to other zones on Iceland (e.g. Jakobsson et al., 2008; Sigmarsson et al., 2008; Peate et al., 2010). Whereas the off-axis zones and belts such as the ÖVB, SVB and the southern EVZ erupt more alkalic (Jakobsson et al., 2008) or more incompatible element enriched magmas. This distinction was noted early in petrological research into Icelandic volcanic systems and zones (Jakobsson, 1979a) and went so far as to distinguish the EVZ from the rest of the NVZ axial zone (Jakobsson, 1979b).

The main axial zones of Iceland, the WVZ and the NVZ are broadly tholeiitic in character. This characteristic, however, is carried down to the northern portion of the EVZ. These zones are the most evolved and matured rift systems in Iceland, thus they have high degrees of mantle melting resulting in this tholeiitic melt character. The southern EVZ is thought to be the propagating tip of the axial zone, which is breaking through older, cooler crust, resulting in slightly lower degrees of mantle melting than the true axial zones. This results in the more transitional or alkali character noted by Jakobsson et al. (2008). Transitional magmas are compositionally between those of tholeiitic and alkalic magmas, it is a fairly arbitrary delineation but indicates there is a compositional spectrum evident, rather than 2 distinct members. The off-axis belts of the ÖVB and SVB are distinctly alkaline in character, these belts are typified by low degrees of deep mantle melting, and most likely of an enriched mantle source (Prestvik, 1985; Prestvik et al., 2001; Fitton et al., 2003; Peate et al., 2010; Manning and Thirlwall, 2014).

Crustal thickness is a first order control on the composition of mafic magmas at these volcanic zones and belts in Iceland, thickness dictates the melt depth and thus some degree of mantle melt. Second order control is though to be the amount of plume material involved in the melt process, this is either hotter than the ambient mantle, more enriched than the ambient mantle or both. The plume material incorporated into the mafic melts rising to the surface in the neovolcanic zones is inferred to be related to the location of the melting, relative to the rising plume material (Thirlwall, 1995). Thus despite NVZ and WVZ lavas having similar tholeiitic compositions, their ratio of elements and isotopes that are incorporated in plume material (e.g. Nb (Fitton, 2007), $^{206/207/208}$Pb) decreases with distance from the plume head (e.g. Schilling, 1973; Thirlwall et al., 2004, for further details see Figure 4.18 and associated text). Further to this, the ÖVB has thick, relatively cool crust beneath it, meaning any melt produced is more alkalic than the main axial zones. The melting beneath the belt is promoted by the enriched mantle (with a relatively lower melting point) from the plume, a similar process is thought to occur along the SVB. However, some researchers have also pointed to the possibility of a sliver of continental crust ‘caught’ beneath south east Iceland, which is evidenced by high $^{207/208}$Pb/^{204}Pb ratios and Jurassic aged zircons found in eroded material from the volcano (Prestvik et al., 2001; Torsvik et al., 2015).

1.1.2 Volcanic Systems

Volcanic zones are divided into volcanic systems. Volcanic systems consist of a central volcano – a loci of evolved magmatism on the system, a fissure swarm or both. The original term is used prior to 1900 in volcanic areas around the world, though the first use in Iceland does not appear in the literature until Bodvarsson (1970) when referring to the "Reykjanes volcanic system" although he offers no further distinction. Volcanic systems were then outlined and defined by Saemundsson (1978, 1979) and this outline has essentially continued in the same manner into any research following on from this. Jakobsson et al. (1978) suggested to define fissure swarms mapped by Pálmason and Sæmundsson (1974); Jakobsson (1974) using the term ‘systems’ due to apparent petrological characteristics which were coupled with magnetic anomalies, geothermal anomalies and variations or gaps in faulting. Jakobsson (1979a) and Jakobsson (1979b) continued this distinction into the EVZ and the rest of Iceland respectively. 30 to 32 volcanic systems are considered to be active on land today. In reality it seems that the exact number and delineation of volcanic systems is still in question, this debate was sparked again after the Holuhraun/Bárðarbunga eruption of 2014, where magma sourced from Bárðarbunga, erupted within what was previously called the ‘Askja fissure swarm’ (e.g. Hjartardóttir et al., 2009; Hartley and Thordarson, 2013; Sigmarsson and Halldórsson, 2015). Outwith the active volcanic zones of Iceland extinct volcanic systems are scattered across the country, with up to 23 more in eastern Iceland alone (Figure 2.1 and table 2.1), and at least 28 more are shown on recent geological maps of Iceland (based on map data from Saemundsson (1979); Jóhannesson and Sæmundsson (2009); Jóhannesson (2014)). These volcanic systems presumably erupted on equivalent rift zones and belts in Iceland prior to the current arrangement c. 6 Ma.

Of the 30 active volcanic systems shown in Figure 1.1b, 6 do not contain central volcanoes, 9 do not contain a distinct fissure swarm, and 2 do not contain either (Grímsnes (6) and Hróðmundartindur (5)). The extinct systems are more difficult to quantify since many are poorly mapped or exposed. In the east fjords (i.e focus of this study) of the 22 systems presented in, Table 1.1 and shown in Figure 2.1, everyone has a central volcano bar Streitishvarf dyke swarm, which, if a central volcano existed, would be eroded and submerged. Nine of these systems are not known to have a dyke swarm, though this does not mean that one is not present since many of these systems are not fully mapped. Four of the named systems in Table 1.1 have a little mention available literature, though it can be assumed these have at least a central volcano.

Volcanic systems are relatively evenly distributed throughout the axial volcanic zones including the EVZ, the distribution of certain types of system however, does not follow this pattern. As shown in Figure 1.1b, the systems containing large caldera-type central volcanoes are Askja, Kverkfjöll, Hofsjökull, Bárðarbunga, Grímsvötn, Katla and Torfajökull. These volcanoes are scattered around the estimated position of the presumed mantle plume beneath western Vatnajökull (Wolfe et al., 1997) and the southern EVZ, where crustal thickness is also greatest (Darbyshire et al., 2000). Interestingly, there are no central volcanoes in the Siða highlands between Torfajökull and Grímsvötn-Bárðarbunga, and the northern NVZ contains only one central volcano, Krafla, which is split by its own fissure swarm (Sæmundsson, 1991). The central volcanoes of the propagating rift (i.e. EVZ), namely Eyjafjallajökull, Katla, Torfajökull, Hekla, Þórðarhyrna and Grímsvötn, which include some of the largest and/or most active volcanoes of Iceland, have no or very immature fissure swarms. In these situations it is clear that if these systems develop a fissure swarm, its development follows that of the central volcano. In contrast, the central volcanoes of the axial rift, such as Hengill, Bárðarbunga, Askja and Krafla are associated with well-developed Holocene fissure swarms. In these instances it is not clear which came first, the central volcano or the fissure swarm, although the splitting of the Krafla caldera (i.e central volcano) by the fissure swarms can be viewed as evidence that the central volcano came first.

1.1.3 Central Volcanoes

Central volcanoes are, when present, the focal point of evolved magmatism within a volcanic system. They vary in type, being either, stratovolcano, caldera volcano or shield volcano and are typically the largest and highest edifice within the system (Thordarson and Höskuldsson, 2008, e.g.). A mature central volcano is often considered to be one with a large caldera, and most show more evolved magmatism. They are of taken to represent the surface manifestation of a 'shallow' magma chamber. The volcanic edifice can reach a height of 1-2 km high, the lowest elevation central volcano being Krafla at 818 m a.s.l., to the highest peak in Iceland, Hvannadalshnjúkur at 2110 m a.s.l. on the edge of the Öræfajökull central volcano. Current volume estimates, where they are possible to measure, suggest a range of volumes between 14 – 474 km^3 though most sit in the range of 100 – 200 km^3 (Thordarson, unpublished data 2019).

A central volcano typically erupts once every few hundred years, however, the volcano may undergo periods of higher activity where multiple eruptions occur over a period of years (Thordarson and Höskuldsson, 2008). Their activity level is typically higher than that of the fissure swarms, but fissure swarms erupt a higher volume of lavas overall (Thordarson and Larsen, 2007).

Shallow magma reservoirs (1-5 km) are inferred to be present or have been present beneath several central volcanoes, believed to form due to the consistent high heat/magma input into the crust they are inferred using multiple methods including: geothermal activity, geophysical data (Einarsson, 1978), petro-geochemistry (Nicholson et al., 1991; Harðarson, 1993; Loughlin, 1995; Hards et al., 2000; Prestvik et al., 2001; Kuritani et al., 2011) and exposed volcanoes and magma chambers in the Neogene sequences (Walker, 1964; Blake, 1966;

Mattson et al., 1986; Åberg et al., 1987; Furman et al., 1992b; Gústafsson, 1992; Thorarinsson and Tegner, 2009; Berg et al., 2014; Padilla et al., 2016). It is commonly inferred that the presence of a persistent heat source in the shallow crust allows evolved magmas to be produced. The exact way in which silicic magmas are formed in Iceland is constantly being re-evaluated and often needs to be determined on an individual place-by-place scale. The two end-member methods are fractional crystallisation (FC) (MacDonald et al., 1990; Furman et al., 1992b) and partial melting of hydrothermally altered basaltic crust (PM) (Oskarsson et al., 1982, 1985; Sigmarsson et al., 1991; Gunnarsson et al., 1998). In the former, silicic magma is produced through the extensive crystallisation of a mafic magma body(ies) within the crust with the outcome that the parent magma becomes more enriched in silica and incompatible elements. The latter produces silicic magma through the melting of hydrothermally altered basaltic crust, the alteration decreasing the melting temperature of rock. In this method the high heat flux from basaltic magma heats the surrounding country rock, incompatible elements are enriched within the first melts produced and high silica rocks can be formed. The method suggested by Sigmarsson et al. (1991) is PM forms dacites with subsequent FC of feldspars forming rhyolites. Martin and Sigmarsson (2007) suggested that both methods of producing evolved melts occur depending on the tectonic setting, off-axis volcanoes form rhyolite through FC due to lower heat input and on-axis volcanoes through PM and subsequent FC. Gunnarsson et al. (1998) demonstrated that melts at Torfajökull essentially form through PM of hydrated basaltic and silicic crust. The two end members are unlikely to be the sole method of producing silicic rocks at any volcano and variations of both are likely to occur, such as those volcanoes where assimilation fractional crystallisation (AFC) is though to dominate or PM rhyolite/dacite mixing with basalts and subsequent FC of mixed magmas.

Silicic magmatism, and the pale rocks it creates, are taken as strong indicators of shallow level magma chambers and central volcanoes. In the Neogene and Plio-Pleistocene sequences of Iceland the pale silicic rocks indicate ancient central volcanoes that have been exposed by erosion (Walker, 1958). Neogene central volcanoes appear to have erupted onto low angled terrain, devoid of ice allowing central volcanoes to build broad edifices which stood proud of the surrounding rift system but without the steep relief of today's subglacially formed volcanoes (Walker, 1963). No evidence, thus far, indicates the remains of steep strato-volcanoes in the Neogene.

1.1.4 Fissure and Dyke Swarm

Fissure systems in the active rift zones are 2-50 km wide and 10-140km long (Gudmundsson, 2000; Hjartardóttir et al., 2009). They are characterised by series of tension cracks and faults as well as eruptive fissure vents - cone rows (Figure 1.2), fissure swarms may be associated with a central volcano. If a system includes a central volcano, then the swarm is commonly delineated by open fractures and normal faults in the areas distal to the central volcano. But closer to the central volcano it is more commonly delineated by cone rows as well as other types of linear vent systems (e.g. Hjartardóttir et al., 2009). This appears highly dependent upon the system in question. Fissure swarms are the focal point of crustal accretion and rifting, a typical eruption in Iceland is a >1km^3 flood lava eruption on a fissure swarm (Thordarson and Höskuldsson, 2008). At least 75% of magma volume production is along fissure swarms, the rest being accommodated in the central volcano (Hartley and

Figure 1.2: A typical Icelandic eruption – the fissure eruption at Holuhraun, north of Dyngjujökull 2014/15. The eruption took place within a fissure swarm, the magma was sourced through a dyke from the Bárðabunga system, and the whole event included a significant amount of rifting. Photo: R. Askew.

Thordarson, 2013).

Below the surface of active fissure swarms the rifting manifests as normal faulting and dyking. Dyke swarms (Figure 1.3) are visible in the excavated sections of the volcanic strata in Iceland and show that a significant amount of crustal spreading is accommodated by magmatic intrusion into the crust. It's likely that many of these dykes were intruded passively into the crust during crustal extension/faulting, the dykes following fault lines, others will have intruded actively from chamber over-pressurisation though still following lines of weakness. Dyke density is known to increase with depth (Walker, 1958), leading to the assumption that there is a sheeted dyke region of 100% intrusions, though these deep complexes are not exposed in Iceland. Individual dykes can be highly variable in both width and in length, dykes over 18 km in length have been mapped (Gudmundsson, 2002), and widths vary from 10's cms to 10's of metres across. Dykes swarms have been mapped out in Neogene stratigraphy around Iceland, and are commonly associated with exposed central volcanoes. A fissure swarm is often thought to represent the surface expression of a dyke swarm (Gudmundsson, 2000)

1.1.5 System evolution

The evolution of a volcanic system has up to date been viewed as follows: a fissure swarm develops and matures, erupting plateau or flood basalts from fissure eruptions (Figure 1.4). Subsequently, accumulation of basaltic magma in the shallow crust (c. 5-2 km) forms a shallow magma chamber. Magma influx continues into both the swarm and shallow reservoir, the presence of a magma reservoir essentially concentrates volcanism to a confined point above it. Thus a central volcano forms (Figure 1.4). In this theory, the volcano and fissure swarm then "dies" when the magmatic source is cut off as crustal dynamics present in Iceland cause the system to drift away from the rift zone. Mapping in eastern Iceland indicated that thick flood or plateau basalts underlie central volcanoes and thicken towards those volcanic systems, whilst equivalent thick groups are not seen above other central volcanoes (Óskarsson, 2015), suggesting the eruption of these groups before a central volcano evolves. A note on nomenclature should be made here, throughout this thesis, we use the term 'plateau basalt' to

Figure 1.3: Dyke swarm outcrops in Norðurdalur, each dyke represents some degree of rifting, though most do not reach the surface. Arrows show some of the larger dykes, not all dykes are pointed out.

represent the large volume (>1 km^3) basaltic lavas that form most of the crust of the Iceland plateau. The term is often used interchangeably with flood basalt.

However, systems with a fissure swarm and no central volcano, or a central volcano with no fissure swarm, both exist in Iceland. The slow spreading Reykjanes ridge does not contain any central volcanoes, probably due to the ultra-slow spreading rate along the ridge. However, there are geothermal areas on Reykjanes which indicates a relatively high and continuous heat flux beneath the crust. There are up to 10 well-developed (mature) central volcanoes: Snæfellsjökull, Eyjafjallajökull, Katla, Tindfjöll, Torfajökull, Hekla, Kerlingafjöll, Tungnafellsjökull, Þórðarhyrna, and Grímsvötn, without well-developed fissure swarms. This raises serious questions about the general application of the "general consensus" view/model presented above and in Figure 1.4.

Thus the question remains, will a volcano such as Eyjafjallajökull eventually gain a fissure swarm and be taken over by it? Or will a central volcano eventually form on the Reykjanes peninsula? It is entirely plausible that neither will occur, since the crust dynamics such as thickness, proximity to the plume head and other factors are entirely different in both locations. A simple model probably cannot be applied to all volcanic systems in Iceland equally, intimate knowledge of each system is required before an understanding can take place. This study considers the hypothesis presented above and the questions this brings in order to analyse what came first, the central volcano, or the fissure swarm?

Our study draws together our current understanding of active systems to create a parallel with the Neogene system of Breiðdalur. At Breiðdalur both a central volcano and its fissure swarm are exposed, as well as the lavas that eventually buried the volcano. With this cross

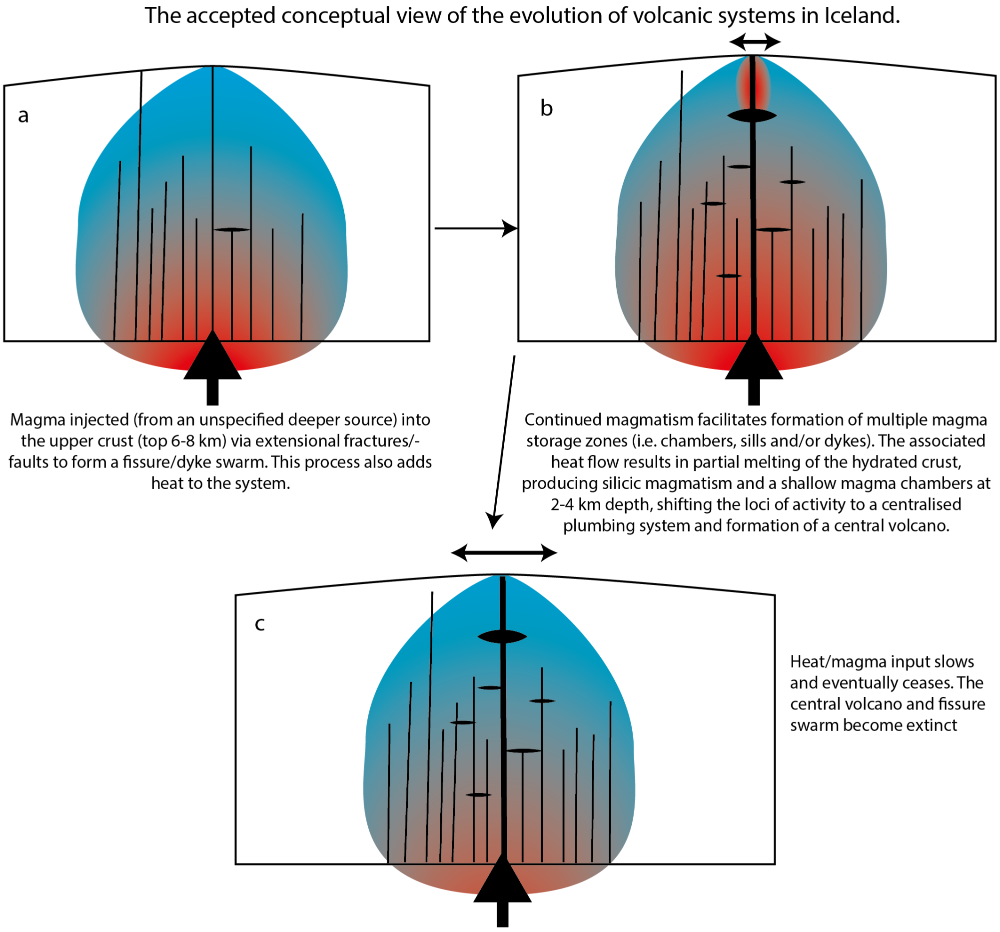

Figure 1.4: Model of hypothesis 1: Fissure Swarm, then Central Volcano. Whereby a volcanic system begins with heat and magmatic input from a mantle or deep crustal reservoir which injects through the colder crust as verticle regional dykes and can erupt as plateau basalts. The continued dyke injection becomes more concentrated into a point source, eventually leading to the creation of shallow crustal magma reservoirs and evolved magmas. The system then 'dies' when there is not continued magmatic or heat input.

sectional view, we will evaluate the temporal evolution of the units throughout the Breiðdalur volcanic system; including the timing between the central volcano, the dyke swarm, and the plateau basalts covering the volcano. Utilising petrological and geochemical tools, we will investigate the magmatic relationship between the volcano and the dyke swarm, and evaluate the interplay between neighbouring volcanic systems.

These investigations will work towards improving our understanding of large scale crustal accretion processes in Iceland, focusing on the role that the East Fjord Neogene volcanic activity played. We hope that the conclusions and data outlined here contributes towards a larger dataset on Icelandic volcano geology, geological mapping, geochronology and geochemistry.

Chapter 2

Geological Background

2.1 Eastern Iceland

The Neogene lava pile in the east of Iceland has a westward dip between 2-12°. This dip is thought to be generated by the excess weight and thickening of the crust along the axial rift via emplacement of volcanic products (Pálmason and Sæmundsson, 1974). This occurrence is currently understood to result in tilting of the crust towards the axial rift causing a westward regional tilt in the Neogene succession of East Iceland (Walker, 1964) and an eastward tilt in the time equivalent succession in Western Iceland. This general westward dip, means that the further to the east one goes, the succession exposed becomes older (Figure 2.1). Also, one of the advantages of this regional tilt is that lavas exposed at sea level are traceable to mountain tops further east. The exposure of deeper volcanic and magmatic edifices at the surface was aided by Plio-Pleistocene glaciations, incising deep fjords in the lava pile. In the south east, estimations from zeolite alteration (Walker, 1960) and magma emplacement depth suggest around 2 km of material was removed through erosion, in the northeast approximately 1 km was removed (Gústafsson, 1992). The difference in erosion rates is due to the proximity to highland areas of the Vatnajökull ice cap, and the thickest ice-age glaciers, which is located in the south east of Iceland due to dominant southwesterly winds and accompanying high precipitation rates. This process also exposes central volcanoes, such as the Breiðdalur volcano (Figure 2.1 and 2.2).

Our current inferences about Icelandic volcanic systems is taken from what is visible in the neo-volcanic zones and our understanding of the tectonic structure of systems in the east fjords of Iceland (Walker, 1958; Carmichael, 1964; Walker, 1974).

2.2 Breiðdalur volcanic system

Breiðdalur is situated west of the town of Breiðdalsvík, and the first exposures of Breiðdalur volcanics, part of the Breiðdalur volcanic system, are found around 18 km along route 1 from the town (Figure 2.3). Due to the roughly east–west trend of valleys and fjords through westward dipping stratigraphy, the same units may be found in valleys and fjords to the north or south. The lowermost central volcano units, found in Berufjörður to the south, are located close to the farm of Gautavík, around 35 km from the town of Djúpivogur or 30 km from Breiðdalsvík. Many of the units in this area are found up valley from the lower exposure. The caldera is exposed at the head of Breiðdalur valley and a small sliver along Selá, Berufjörður. Silicic volcanic rocks are located across the peaks of northern Berufjörður and above Þorgrímsstaðir in Breiðdalur. This thesis details the re-mapping of the Breiðdalur volcano and the age dating of the volcanic system in order to understand the timing of magmatism within a volcanic system. This is coupled with a geochemical campaign that aims to understand the geochemical evolution of the volcanic system through time as well as giving insight into the regional magmatic regimes active during the Neogene.

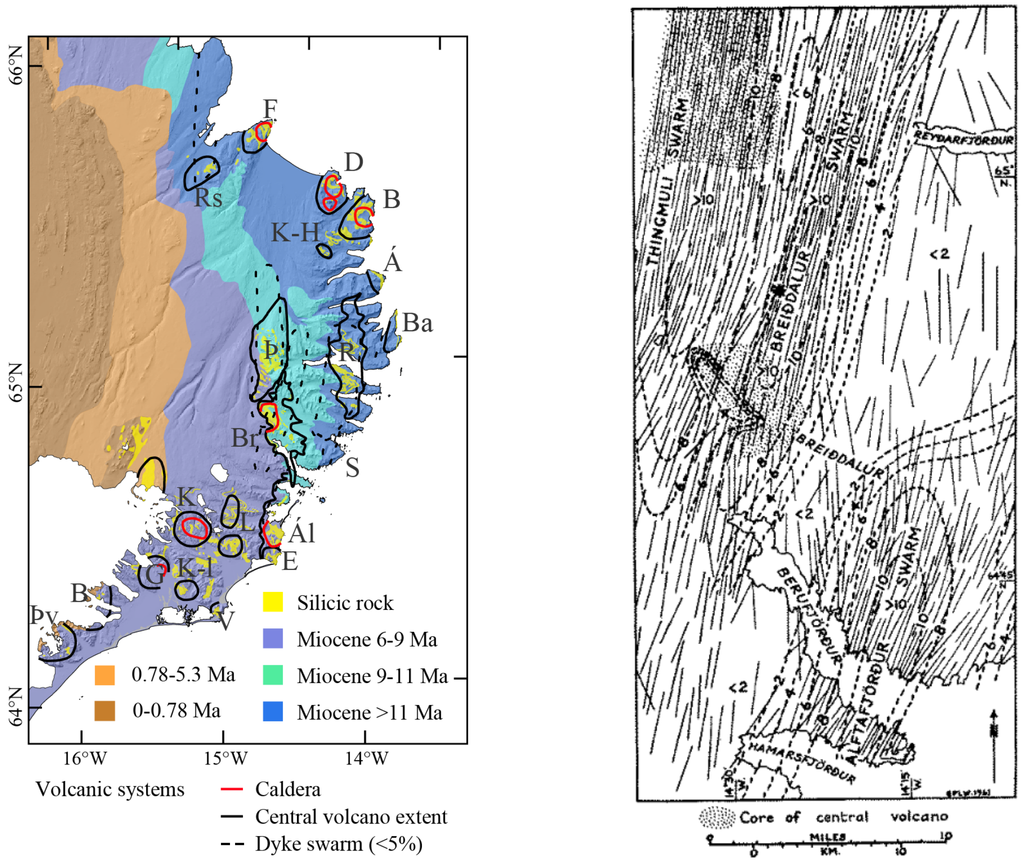

(a) (b)

Figure 2.1: a) East fjord central volcanoes (see table 2.1 for labels). The oldest systems are in the north and the youngest in the south. The central volcanoes of Breiðdalur (Br), Þingmúli (Þ), Álftafjörður (Á) and Reyðarfjörður (R) have their approximate full extents outlined, other volcanoes are outlined as presented by data from Nátturufræðistofunun's geology GIS shapefiles. The extents of dyke swarms were mostly presented by Walker (1963), as show in in (b), and Walker (1958). The Streitishvarf (S) dyke swarm has been added and the Álftafjörður swarm slightly altered from the original mapping which originally suggested it extended up to Barðsnes.

Our study revisits the important work carried out by George Walker in the 1950s and 60's and utilises modern high resolution geochemical analysis to build upon this previous studies, along with a 'fresh pair of eyes' to modify the geological map of the area (Walker, 1963). Further to this, high precision age dating of a volcanic system, as presented in this study has

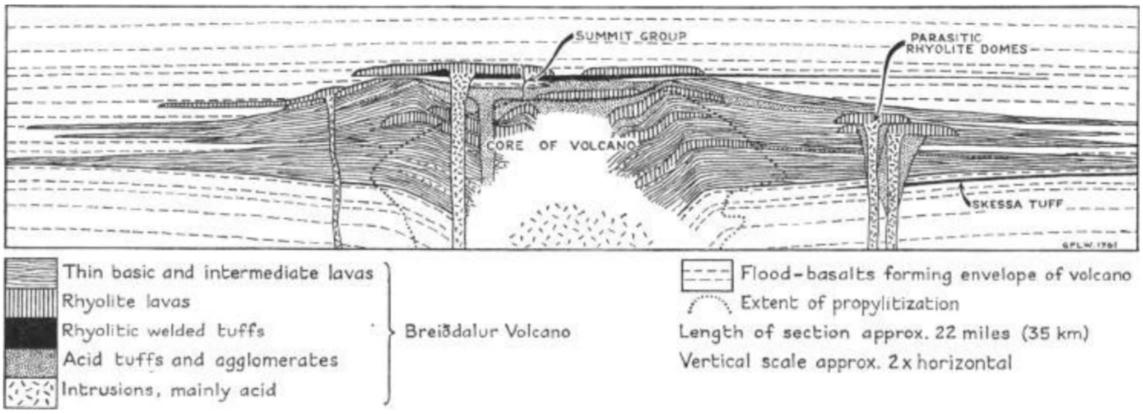

Figure 2.2: From Walker (1963), a schematic cross section of Breiðdalur volcano. Which provides the early basis for ideas on the geology of volcanoes in Iceland.

rarely been done and only a handful modern dating studies are available (e.g. Åberg et al., 1987; Riishuus et al., 2010; Martin et al., 2011; Berg, 2016). As this thesis goes on to show, with improved age dating techniques, current models of crustal evolution need to be updated as the difference between old and new age determinations can be up to +/-1 Ma.

Rhyolite (liparite) was first mapped around Berufjörður and Breiðdalur in the early 1900's by Thoroddsen (1901), the significance of these rocks in the stratigraphy was not fully realised until the work of George Walker and others in the 1950's and 60's. Walker's seminal work on central volcanoes in eastern Iceland, was the first published work to acknowledge that the presence of evolved rocks and evidence of localised geothermal activity pointed to the presence of long lived magma chambers as well as a central volcano (Walker, 1958, 1963). The work also provided a conceptual model of a central volcano (Figure 2.2). Magnetostratigraphy on the rocks of the east fjords (Watkins and Walker, 1977) gave a suggested age of 10 M.y. to Breiðdalur central volcano. K/Ar age dating then adjusted the age of lavas in Reyðarfjörður, located just above Skessa Tuff to 9.2 Ma (Helgason, 1982). Walker (1963) speculated whether the Skessa Tuff was related to the magmatism that formed from the Breiðdalur central volcano and thus represents an embryonic stage. Re-examined geological mapping of the area does not refute the idea but suggests it is unlikely. Recently the Skessa tuff was age dated by $^{40}Ar/^{39}Ar$ technique to 10.2 Ma ±0.2 Ma (Riishuus et al., 2010) a date considered more reliable than the previous 9.2 Ma. This date is coincident with the Streitishvarf composite dyke to the east, which is suggested to have been sourced from Álftafjörður to the south (Martin and Sigmarsson, 2010), though this deduction about its origin is challenged by strike measurements (Askew, 2011), and AMS measurements (Eriksson et al., 2011). A granophyric block in a tuff located in the summit sequence of Breiðdalur was dated to 8.9 ($\pm$0.5) Ma (Gale et al., 1966), more recently a silicic intrusion in Berufjörður, was dated to 9.2 Ma (Martin et al., 2011), suggesting an approximate time-frame of Breiðdalur's activity from around 10 Ma – 9 Ma. Our results build upon this, and by utilising high precision age dating, we display the temporal evolution of a volcanic system in Iceland through time.

The Breiðdalur fissure swarm is dissected and the dyke swarm is well exposed in western Berufjörður and north of Breiðdalur in Norðurdalur. The highest dyke density is in Norðurdalur, where dykes make up around 25% of the stratigraphy over a section of around

100m width (Walker, 1963). The swarm extends northwards for at least 15 km, and southwards the dykes are not exposed at the surface south of Berufjörður (Figure 2.1). Much of the growth by extension is accommodated in these dyke swarms (Helgason and Zentilli, 1985; Gudmundsson, 2000; Urbani et al., 2015).

2.3 The Petrology of Eastern Iceland volcanism

East fjords volcanism is predominantly tholeiitic and basaltic magmatism is rather uniform in composition, only a small amount of rocks could be defined as alkalic (e.g. Gallagher, 2013) and primitive or depleted rocks are surprisingly absent (e.g. Harðarson, 1994; Harðarson et al., 2008). This is in comparison to the breadth of compositions found in the Pleistocene and Holocene basalts from the neovolcanic zones. This difference observed was postulated to be due to the Neogene lavas being formed by large on-axis eruptions fed by a homogenised mantle reservoir. Because of this interpretation, several researchers have suggested that the Neogene basalt stratigraphy outside of the domains of the central volcanoes, gives an insight into temporal variations in mantle plume signatures along an axial rift zone, throughout the Miocene and into the Pliocene (Schilling et al., 1983; O'nions and Pankhurst, 1973; Hardarson and Fitton, 1997; Hanan and Schilling, 1997; Kitagawa et al., 2008). The general consensus from these cited studies, is that there is a distinct pulsing in the plume throughout the Neogene with a general trend towards lowered plume activity, and thus more depleted isotopic signatures along much of the rift system (see also Spice et al. (2016)).

Individual studies of the petrology of volcanic systems in eastern Iceland essentially began with Carmichael (1964), who defined the basaltic to silicic magmas of Þíngmúli as products of fractionation in an underlying magma chamber. This is defined as the typical tholeiite trend by many authors (e.g. Arculus, 2003; Kitagawa et al., 2008), though was recently suggested to actually be formed through two separate methods, one being FC under reduced conditions and the other magma mixing and FC under oxidised conditions (Charreteur et al., 2013). Fagridalur volcano is also suggested to display a typical tholeiite trend (Geirsson, 1993). Vestrahorn and Eystrahorn plutons have also been the subject of petrogenetic studies (e.g. Mattson et al., 1986; Furman et al., 1992a, respectively), leading to the conclusion that these plutons are transitional in character, and sourced from a younger rift relocation/jump around 5-6 Ma (Åberg et al., 1987; Martin et al., 2011). Schnell (1994) completed a thorough study of the silicic magmatism at Breiðdalur, suggesting that the more evolved rocks were produced by fractional crystallisation of the most primitive rocks, or their intrusive counterpart, at the volcano. Such that olivine-tholeiites formed quartz tholeiites > icelandites > rhyolites. Further studies on Neogene central volcanoes are predominantly concerned with mapping (Gibson, 1963; Blake, 1970; Gústafsson et al., 1989; Gústafsson, 1992) and production of silicic magmas (Martin and Sigmarsson, 2010; Charreteur et al., 2013; Charreteur and Tegner, 2013; Berg, 2016).

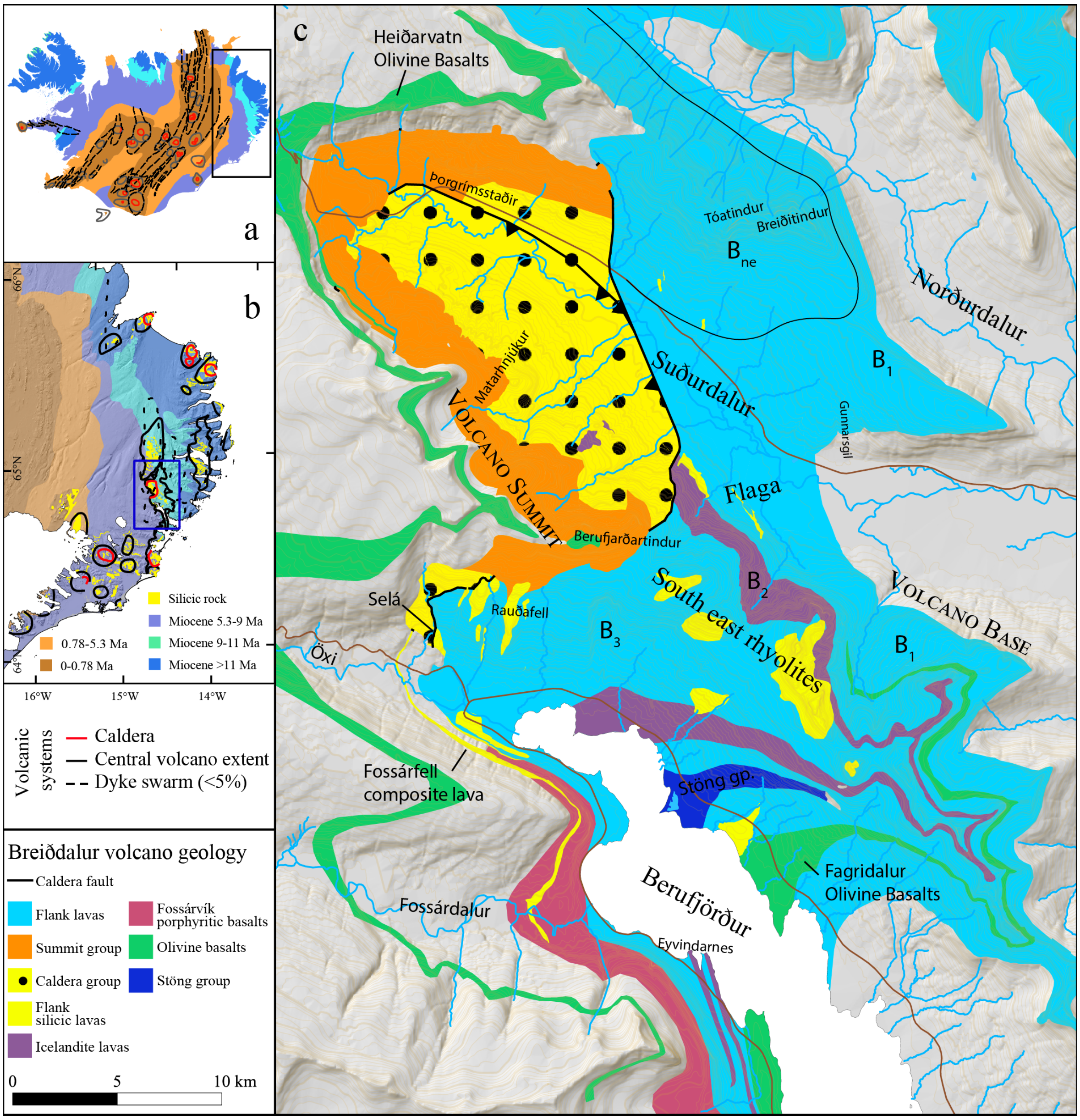

Figure 2.3: The study area. a) Icelandic geology, black box is: b) east fjords volcanic systems (See Figure 2.1 for further details), Breiðdalur shown in in the blue box. c) Breiðdalur volcano geology and localities, B_1: Lower eastern flank sequence, B_2: Icelandite lava sequence, B_3: Upper eastern flank sequence and B_{ne}: North eastern flank sequence. Samples were taken from within the volcano and the plateau basalt envelope around the volcano).

Table 2.1: Ages of central volcanoes in eastern Iceland. Volcanoes are listed from north to south following names and locations by Walker (1974) and Gústafsson (1992).

Volcanic system	Label	Age	Type	Reference
Fagridalur	F	14 - 12 Ma	Central volcano and dyke swarm	Martin et al. (2011)
Refsstaðir	Rs	12 Ma	Small central volcano and dyke swarm	Martin et al. (2011)
Dyrfjöll	D	12 - 13.5 Ma	Large silicic central volcano and dyke swarm	Gústafsson*
Breiðavík	B	12.5 - 13.1 Ma	Large silicic central volcano and dyke swarm	Gústafsson*
Álfavík	Á	13 Ma	Central volcano	Gústafsson*
Kækjuskörð	K-H	12 - 13 Ma	Small central volcano (or parasitic volcano)	No dates
Herfell	K-H	12.4 Ma	Small central volcano (related to Kækjuskörð?)	Gústafsson*
Barðsnes	Ba	13 Ma	Central volcano - mostly eroded	Watkins and Walker (1977)
Reyðarfjörður	R	11 - 12 Ma	Large silicic central volcano and dyke swarm	Martin et al. (2011)
Skrúður		Unknown	Off land	
Þíngmúli	Þ	9 - 10 Ma	Large silicic central volcano and dyke swarm	No specific dates
Breiðdalur	Br	9 - 10 Ma	Large silicic central volcano and dyke swarm	Riishuus et al. (2010); Martin et al. (2011) Askew and Thordarson (In Prep)
Streitishvarf	S	10 Ma	Dyke swarm	Martin et al. (2011)
Álftafjörður	Ál	10 - 11 Ma	Large silicic central volcano and dyke swarm	
Lón	L	Unknown		
Kollumúli	K	Unknown		
Eystrahorn	E	6 - 7 Ma	Pluton	Martin et al. (2011); Padilla et al. (2016)
Vestrahorn	V	3 - 4 Ma	Pluton	Martin et al. (2011)
Ketil-laugarfjall	K-l	Unknown		
Geitafell	G	5 - 6 Ma	Central volcano and dyke swarm	Fridleifsson (1983)
Birnudalstindur	B	4 - 5 Ma ?	Central volcano and dyke swarm	Klausen, NordVulk Report, 1995
Thverartindur	Þv	4 - 5 Ma ?	Central volcano and dyke swarm	Klausen, NordVulk Report, 1995

**Gústafsson presented work and dates to: https://www.breiddalssetur.is/images/Jardfraedi-geology/Fyrirlestrar-presentaions/2014/2014-8-30-Jfr-Austurlands/ludvik.e.gustafsson-erindi_walker_symposium_30_8_2014.pdf.*

Chapter 3

Methodology

3.1 Background

3.1.1 Geochronology

Geochronology is an important tool used throughout Earth Sciences and Life Sciences. There are various methods used to be able to conceive the age of a certain event and these are roughly broken into relative and absolute techniques. The earliest dating methods available to researchers in Iceland, were biostratigraphic markers and a pre-defined notion of accumulation rates of lavas, Holocene eruptions utilise tephra-chronology in order to date lavas and tephra deposits. Watkins and Walker (1977) were some of the earliest to conduct a paleomagnetic study on the lavas of the east fjords of Iceland, which contributed to our understanding of plate spreading and the crustal evolution of Iceland and the North Atlantic. Updating geochemical and geochronological datasets in areas that appear to be well represented is often undervalued despite the fact that these old and now unreliable data often provide the basis for theories, hypotheses and models. It is therefore important to periodically review and reassess older datasets and where required, redo any analysis needed. Geochronology of the east fjord stratigraphy of Iceland is one such dataset, previous campaigns took detailed stratigraphic transects and utilised K-Ar age dating and magnetostratigrahy in order to evaluate crustal 'drift' (e.g. Ross and Mussett, 1976; McDougall et al., 1976a,b; Watkins and Walker, 1977; E. Mussett et al., 1980). These studies provided invaluable information regarding the formation and evolution of the earths crust and the mechanism of plate tectonics at mid ocean ridges. More recently researchers in eastern Iceland focused campaigns on silicic magmatism and understanding the formation and role of silicic magmas in Iceland (e.g. Åberg et al., 1987; Martin and Sigmarsson, 2010; Martin et al., 2011; Berg, 2016). When other studies looked into the ages of the plateau sequences (e.g. Riishuus et al., 2010), the question of the reliability of the previous regional dating studies came about. Further to this, no previous campaigns had tried to fully understand the evolution of a single volcanic system. Most were concerned with the formation of silicic magmatism and the relationship of silicic magma with the surrounding stratigraphy. Since volcanic systems are key to crustal accretion, and understanding both Neogene and modern systems will improve our understanding of crustal formation, volcano and volcanic system evolution and ultimately the evaluation of hazards at volcanic systems, we focus on a single volcanic system, Breiðdalur.

^{40}Ar/^{39}Ar age dating is now a well established technique for dating basaltic rocks and is increasingly used throughout Iceland to date magmatic events. This technique is rapidly reevaluating the relationships between events previously dated through older Ar-Ar and K-Ar techniques. Though ^{40}Ar/^{39}Ar dating is more costly and more time consuming than K-Ar, most recent developments have been to the ^{40}Ar/^{39}Ar technique and most labs currently utilise this method for dating volcanic rocks. ^{40}Ar/^{39}Ar age dating is a relative dating method as it utilises the Ar isotopic ratio of a sample vs a known age standard, assessed through separate methods. It uses the ratio of ^{40}Ar which is derived from the radiogenic decay of ^{40}K against that of ^{39}Ar produced through the transmutation of ^{39}K by particle bombardment in a nuclear reactor.

U-Pb age dating of zircons is another well established and well utilised technique. Again, it is used throughout the east of Icelandic to date silicic magmatic events (e.g. Åberg et al., 1987; Riishuus et al., 2010; Martin et al., 2011; Berg, 2016). U-Pb age dates provide high precision and high accuracy, often with errors of less than around 0.1 My for samples of Neogene age.

3.2 Techniques

During the production of this thesis several methods of analysis were used: Field mapping, GIS map production, XRF major and trace element, major and trace element Inductively Coupled Plasma Optical Emission Spectrometer (ICP-OES), major and trace Inductively Coupled Plasma Mass Spectrometer (ICP-MS), Pb, Hf, Sr and Nd isotopic analysis through Multi Collector Inductively Coupled Plasma Mass Spectrometer (MC-ICP-MS) and Thermal Ionisation Mass Spectrometry (TIMS). The methodology is presented here and the results are presented in the relevant chapters.

3.3 Field mapping and map production

The geological mapping of Breiðdalur presented here, builds upon the previous work of Walker (1963). The lowest stratigraphic unit on the map is marked as the Skessa Tuff; any units below this are outside the mapping area and therefore not shown. The upper delineation of the mapping area is the same as chosen by Walker (1963): representing a clear discontinuity in Berufjörður and Breiðdalur, described further in the text.

Key map units were defined through petrology, geochemistry, facies, or simple grouping of lavas. However, clear differentiation of flank lavas and fissure swarm lavas was not always possible, as a result of extensive erosion, weathering or petrological similarity. In the field, a similar method of identify lavas was used as to Walker (1964), but the terminology used differs, e.g.: Tholeiite was a term used by Walker for apyhric basalts, but here the term is used purely geo-petrologically. Rocks were instead defined by their texture as noted in the field: aphyric basalt, porphyrytic basalt (> 20% phenocrysts), olivine basalts (olivine bearing basalts), icelandites/andesites (fine grained, platy cleavage, shiny surface, > 10 m thickness) and silicic rocks. Groups were often defined if a similarity was noted throughout a sequence, or no time gap was visible between neighbouring lavas. Other lavas may be distinguished if they contained a significant number of phenocrysts or contained the mineral olivine as a phenocryst, which is not commonly found in east fjord lavas. The map is broadly broken up into: flank sequence, caldera sequence (Core Group Walker (1963)), and summit sequence. The South Eastern Rhyolites (SER) group is a term chosen by Schnell (1994) to describe what Walker termed 'flank rhyolites'. Since the updated term is more descriptive of position, we use SER here and describe it closely with the Summit sequence lavas. In this description of units we use the terms 'early' and 'late' Breiðdalur, and the sequences are described according to their age relation: flank units being the earliest and summit sequences being the latest. Intrusions are described within relevant sections except the dyke swarm dykes, which are described separately.

Contacts between units are generally well exposed and easy to trace even on aerial imagery. Contacts, faults, and discontinuities are described as certain, inferred, or uncertain. Certain refers to features that have been traced in the field, were easily traceable on aerial imagery, or were marked as certain in Walker (1963). Inferred features are often obscured by e.g. talus but can be placed with some accuracy (often 10's metres) whereas uncertain contacts were difficult to trace and are inferred with a higher degree of uncertainty (>10's metres). The map is presented in Paper 1 summary and in full in Supplementary Material.

The map was compiled using both ArcGIS and QGIS, aerial imagery and 20 m DEM was courtesy of Landmælingar Íslands (Land Survey of Iceland, lmi.is), 1:600,000 geological maps and shapefiles were courtesy of Nátturufræðistofnun Íslands (Icelandic institute of Natural History, ni.is). The map was exported as a .pdf or other vector file and edited for publication using Adobe Illustrator.

3.4 Age Dating

Most of the samples selected for age determination are mafic but include a small selection of silicic samples, and as such, is representative of the overall petrology of the volcano. Medium to coarse grained samples were required for groundmass plagioclase analysis. Silicic samples were often fine grained to glassy and aphyric and most were not suitable for $^{40}Ar/^{39}Ar$ analysis. However two of the silicic samples were selected for zircon based U/Pb age dating due to their high zirconium content. These are the rhyolitic dyke of Gunn-1 and the dacitic inclined sheet, WP470. They were analysed at the CODES Laser Ablation Inductively Coupled Plasma Mass Spectrometer (LA-ICP-MS) laboratory, School of Earth Sciences, University of Tasmania by J. Thompson following the method in Kosler (2001). Approximately 200–400 g of rock was crushed in a Cr-steel ring mill to a grain size <400 micron. Non magnetic heavy minerals were then separated using a gold pan and a Fe-B-Nd hand magnet. The zircons were hand picked from the heavy mineral concentrate under the microscope in cross-polarised transmitted light. The selected crystals were placed on double sided sticky tape and epoxy glue was then poured into a 2.5 cm diameter mould on top of the zircons. The mount was dried for 12 hours and polished using clean sandpaper and a clean polishing lap. The samples were then washed in distilled water in an ultrasonic bath.

The analyses in this study were performed on an Agilent 7900 quadrupole ICPMS with a 193 nm Ar-F excimer laser and the Resonetics S155 ablation cell at the University of Tasmania in Hobart. The downhole fractionation, instrument drift and mass bias correction factors for Pb/U ratios on zircons were calculated using 2 analyses on the primary (91500 standard of Wiedenbeck et al. (1995)) and checked on 1 analysis on each of the secondary standard zircons (Temora standard of Black et al. (2003); Plesovice zircon of Sláma et al. (2008); Mud Tank zircons of Black and Gulson (1978)) analysed at the beginning of the session and every 15 unknown zircons (roughly every 1/2 hour) using the same spot size and conditions as used on the samples (Standards: Table C.2). The correction factor for the $^{207}Pb/^{206}Pb$ ratio was calculated using large spots of NIST610 analysed every 30 unknowns and corrected using the values recommended by Baker et al. (2004).

Each analysis on the zircons began with a 30 second blank gas measurement followed by a further 30 seconds of analysis time when the laser was switched on. Zircons were sampled on 32 micron spots using the laser at 5 Hz and a density of approximately 2 J/cm2. A flow of He carrier gas at a rate of 0.35 litres/minute carried particles ablated by the laser out of the chamber to be mixed with Ar gas and carried to the plasma torch. Isotopes measured were 49Ti, 56Fe, 90Zr, 178Hf, 202Hg, 204Pb, 206Pb, 207Pb, 208Pb, 232Th, 235U and 238U with each element being measured every 0.17s with longer counting time on the Pb isotopes compared to the other elements. The data reduction used was based on the method outlined in detail in Halpin et al. (2014) and is similar to that outlined in Black et al. (2004) and Paton et al. (2010). Uncertainties were calculated using methods similar to that outlined in Halpin et al. (2014) and Paton et al. (2010).

$^{40}Ar/^{39}Ar$ age dating was undertaken at the University of California Santa Barbara Ar-Ar laboratory, samples were crushed in a tungten carbide jaw crusher and 100 – 250 µm sized chips were separated. Again, chips were cleaned using D.I. water and left in an ultrasonic bath for 1 hour, cleaned with D.I. water and left in the ultrasonic bath for another hour. The clean chips were further cleaned with D.I. water and partially digested using dilute HF. The HF was rinsed off the samples before being left again in a D.I. water ultrasonic bath. They were dried before the groundmass plagioclases were separated by Frantz magnetic separator. Irradiation and Ar–Ar incremental step heating methods follow those given in Faulds et al. (1995).

Sample errors are presented with sample ages.

3.5 Major and Trace Elements

The majority of major and trace element analysis was undertaken through the University of Edinburgh XRF facility. Samples were crushed and milled to homogenisation using a tungsten carbide mill. The homogenous powder was used to create pressed powder pellets for trace element analysis and glass pellets, using the following methodology, for major element analysis. Glass beads were made by firstly heating the sample powders at 1100°C to remove volatiles, the dry sample was reweighed and mixed with LiB flux in order to reduce the melting T of the sample. The samples were then heated to 1100°C and melted. The melt was transferred to a carbon cast and left to cool into glass before being transferred to the analysis instrument. Concise details of the procedure are written in Fitton et al. (1998).

The trace and major elements were analysed on a Panalytical PW2404 wavelength-dispersive sequential X-ray spectrometer with a 3kW Rh-anode, end-window tube by Nick Oddling at the University of Edinburgh (Standards: Table C.3).

3.6 Isotopes

Isotopic analysis was undertaken on a total of 18 samples from the east of Iceland. The samples were collected during field campaigns in 2014 and 2015, the campaign focused on 4 volcanic systems: Álftafjörður, Breiðdalur, Þingmúli and Reyðarfjörður. This ia a pilot study, thus, the samples chosen for analysis represent the lithological range in these volcanic systems, both geographically and petrographically. Compositions from basaltic to silicic were chosen and at least one sample from a flank lava and a regional dyke from each volcano. Analysis was carried out at The University of Iceland Institute of Earth Sciences (IES) (6 samples; Pb, Nd, Hf) and the Pheasant Memorial Lab (PML), University of Okayama in Misasa, Japan (12 samples; Sr, Nd, Pb, Hf, trace elements).

University of Iceland procedure:
6 samples were crushed in a jaw crusher and milled using an agate mill. Around 1 g of powdered samples were weighed out in the clean lab before being washed in a solution of 6M HCl and a drop of HBr, in an ultrasonic bath and finally with MQH_2O. The samples were dissolved in concentrated HF and HNO3 solution, ultrasonicated and heated for a few days. Then the solution was dried and dissolved again in HNO_3 before using HCl in order to destroy all remaining precipitate. The solution was used for sequential ion chromatography of Pb, Hf, Sr and Nd.

Pb was separated on anion columns using amberlite resin. Pb ratios were measured in 1% HNO_3 solution spiked with Tl. Hf, Sr and REE were first separated stepwise in one process on a 30 ml Savillex column using 100–200 mesh cation resin. Then the elements were purified separately.

Hf was purified on 2 ml Triskem columns using LN-spec resin, and the Hf isotope ratio measured in 1% HNO_3 solution. Sr was cleaned up on 100 mg of Eichrom Sr resin and the Sr isotope ratio measured in 1% HNO_3 solution. Nd was separated from other REE elements on 100 mg LN-spec columns, and the Nd ratio measured in 1% HNO_3 solution. All lab work was completed by or done under the supervision of Guðrun Sverisdottir. Analysis was undertaken on Nu-Instruments MC-ICP-MS at the University of Iceland IES. The standard used was JB-3 and returned good reproducibility, a blank was used throughout the procedure (Standards: Table C.5).

Pheasant Memorial Lab procedure:
25 samples were crushed in a jaw crusher and milled in an agate mill, in preparation for trace element and isotope analysis. Several grams of powdered sample was separated into a small sample beaker and taken into the PML clean laboratory. The procedure for trace element analysis by ICP-MS followed Yokoyama et al. (1999) "method 3" except high Mg and Al samples which were digested using a teflon bomb technique (Takei et al., 2001), Sr and Nd analysis by TIMS followed CITE, Pb by TIMS followed Kuritani and Nakamura (2002) and Hf by MC-ICP-MS followed Lu et al. (2007). The wet chemistry was supervised by Technician Chie-so Sakaguchi and Prof. Katsura Kobayashi during a research visit to PML, funded by the Watanabe Trust Fund and PML (Standards: Table C.5 and C.4).

Samples were crushed and milled at PML, milling took place for 1 hour using an agate mill to create homogenous powder. The powder was separated for clean lab use and XRF use.

Clean lab:

Between 600 mg to 1 g of sample was taken into 2 batches as duplicate and original.

Acid leaching was undertaken using 8 ml 6M HCl, the sample-acid mix was ultrasonicated for 2 hours, removed and centrifuged for 5 minutes at 3000 RPM. The acid was removed from the beaker and kept in PP bottle for analysis of elements lost. 8 ml USQ water was added to the sample which was then centrifuged again for 5 minutes, the water was removed and discarded. The addition and removal of water was repeated 2 more times (3 total).

Sample decomposition followed procedure '3' in Yokoyama et al. (1999): The leached sample was decomposed using 1 ml $HClO_4$, 1 ml 2D 30M HF and 0.33 ml HCl. Samples were then ultrasonicated for 6 hours, then placed in incubators overnight, the samples were heated at 110°C for several hours to evaporate HCl, the heat was then increased to 160°C to evaporate HF and finally to 195c to evaporate the last of the $HClO_4$. The dried samples were remixed with $HClO_4$ and the heating step repeated. The dried samples were mixed with 1 ml 6M HCl and placed back into the incubators at 110°C, silicic samples were partially separated at this step and placed into Teflon bombs for HP/HT decomposition at 240°C for 3 days.

Samples for trace element analysis were diluted with HNO_3 after drying overnight, the solution was ultrasonicated for 2 hours to ensure complete dissolution. 0.1 ml of the sample + HNO_3 solution was diluted further with 0.9 ml of HNO_3 in a microtube to create a dilution factor of 2000 for use on the ICP-MS. The 12 samples selected for Sr and Nd isotope analysis were diluted with HCl and ultrasonicated for 20–30 minutes. The samples still contained some particulates, so HCl diluted samples were mixed with 1 ml $HClO_4$ and 1 ml HF and left in the ultrasonic bath overnight. After ultrasonication the samples were placed into incubators to dry.

Sr and Nd: Follows procedure in Yoshikawa and Nakamura (1993). After sample decomposition 1.0 ml of 4.0 M HCl was added and to the sample and the sample placed in an ultrasonic bath for up to 30 minutes. The solution was then poured into a concave beaker and centrifuged for 5 minutes. The columns were prepared with BioRad 50W "X10" resin (1.0 ml) and cleaned using 6 M HCl, MilliQ, second 6M HCl and USQ. The resin was conditioned with 1.0 ml of 4.0 M HCl, when the conditioning acid was drained from the resin the 1.0 ml of the sample solution was loaded onto the column. After loading, the column was washed with a total of 2.5 ml of 2.8 M HCl. Once washed a clean flat bottomed beaker was placed under the column and the washing solution discarded. Rb and Sr were eluted with 4.0 ml of 4.0 M HCl, the flat bottomed beaker was removed and set aside for Rb-Sr separation. A second flat bottomed beaker was placed under the column for elution of Sm and Nd with 6.0 ml of 6.0 M Hcl.

Rb-Sr preparation: 3 drops of 0.015N H3PO4 was added to the elutant and set in an incubator at 70°C overnight until 1 drop remained, in the morning a cap was placed on the beakers (not closed) and T increased to 110°C. Once dry, 1-3 drops of Pyridine were added, this solution was dried up at 60°C for 2-3 hours. Sr was analysed using TIMS.

Pb and Hf: Follows the procedure outlined in Kuritani and Nakamura (2002).

Hf separation:

The samples were centrifuged and the supernate was separated from any precipitates. The separation procedure follows that in Lu et al. (2007), the procedure outlined is a 2 column procedure. The first column uses anion exchange to separate major elements, the second is an extraction resin which purifies Hf from Ti and Zr.

Instruments:

University of Iceland, IES
– Nu-Instruments MC-ICP-MS

Pheasant Memorial Lab (PML)
– Thermo Fisher Scientific, ICAP ICP-MS (Trace)
– Trained in use: Thermo Fisher Scientific, Triton TIMS (Sr, Nd, Pb)
– Trained in use: Thermo Fisher Scientific, Neptune MC-ICP-MS (Hf)

Chapter 4

Summary of Papers

Presented here is a summary of the following papers, plus a reference version of the geological map of Breiðdalur:

Paper 1:
Geological Mapping of Breiðdalur Volcano (In review, Jökull, 2019) *Robert A. Askew[1], Thorvaldur Thordarson[1], Ármann Höskuldsson[1]*

Paper 2:
Temporal and spatial evolution of the Neogene age Breiðdalur central volcano through ^{39}Ar/^{40}Ar and U-Pb age dating (In review JVGR, 2019) *Robert A. Askew[1], Thorvaldur Thordarson[1], Phil Gans[2], Sebastian Meffre[3], Jay Thompson[3]*

Paper 3:
Geochemistry of the Breiðdalur volcanic system (In Prep.) *Robert A. Askew[1], Thorvaldur Thordarson[1]*

Paper 4:
Isotopic geochemistry of Miocene east fjord volcanic systems (Report, 2019) *Robert A. Askew[1], Thorvaldur Thordarson[1], Katsura Kobayashi[4], Hiroshi Kitagawa[4], Chie Sakaguchi[4], Ármann Höskuldsson[1]*

[1]Institute of Earth Sciences, Askja, University of Iceland, Sturlugata 7, 101 Reykjavík, Iceland
[2]Department of Earth Science, 1006 Webb Hall, University of California, Santa Barbara, CA 93106-9630
[3]ARC Centre of Excellence in Ore Deposits (CODES), School of Physical Sciences, University of Tasmania, Private Bag 79, Hobart, Tasmania 7001, Australia
[4]The Pheasant Memorial Laboratory for Geochemistry and Cosmochemistry, Institute for Planetary Materials, Okayama University, Misasa, Tottori, 682-0193, Japan

Personal Contributions

The manuscripts described are all the result of combined efforts by all the authors. My contributions are as follows:
Paper 1: Robert A. Askew: main author, undertook mapping, sampling, GIS. Thorvaldur Thordarson: second author, supervisor, procured funding, scientific knowledge input. Ármann Höskuldsson: third author, supervisor, scientific knowledge input, further funding sources **Paper 2:** Robert A. Askew: main author, undertook mapping, sampling, sample preparation, interpretation. Thorvaldur Thordarson: second author, supervisor, procured funding, scientific knowledge input. Phil Gans: third author, runs Ar-Ar lab in UCSB, supervisor, ran Ar-Ar analysis, knowledge input. Jay Thompson: fourth author, undertook sample prep for U-Pb analysis and wrote methodology on that section. Leonid Danyushevsky: fifth author, lab manager for University of Tasmania U-Pb dating where samples were analysed. **Paper 3:** Robert A. Askew: main author, undertook sampling and lab work. Thorvaldur Thordarson: second author, supervisor, procured funding, scientific knowledge input. Lab work was undertaken in Edinburgh under supervision of lab technician Nic Oddling. **Report 4:** Robert A. Askew: main author, undertook sampling and lab work. Thorvaldur Thordarson: second author, supervisor, procured main project funding, scientific knowledge input. Katsura Kobayashi: Lab manager in Misasa, assisted with procuring funding for the project and was the main Japanese point of contact. Scientific discussion. Hiroshi Kitagawa: Assisted with laboratory work and assisted by running several samples for major and trace elements. Scientific discussion. Chie Sakaguchi: Lab technician in Misasa, demonstrated all lab protocols, techniques and sample analysis. Ármann Höskuldsson: Main point of contact in Iceland for Japanese collaboration, assisted in securing funding

4.1 Paper 1: Geological Mapping of Breiðdalur Volcano

4.1.1 Overview

We present an updated and digitised geological map of Breiðdalur in paper 1. It contains descriptions of lithological sequences and units within the Breiðdalur volcano and the key lithofacies associations. This section provides a basis for the studies in the following papers.

This paper and section of study involved fieldwork in the Breiðdalur area, that resulted in the revision of the previous study by Walker (1963). This includes new information regarding re-interpretation of the core-group as a caldera group bounded by caldera faults as well as the size of the caldera, its extent and its relative timing. Further to this we provide new divisions of the flank group which clarifies the growth and extent of this group and its relation to the rest of the volcano. This provides a stage-by-stage reconstruction of the volcano's growth and evolution which is underpinned by age dates in paper 2 and geochemistry in paper 3.

Collectively these observations provide updated information on and a new insight into evolution and growth of Neogene central volcanoes and their linkage to the associated dyke swarm.

4.1.2 Summary of results

The map is digitised and presented in this thesis (preview Figure 4.1). Our mapping shows that the Breiðdalur central volcano began as a series of lavas erupted over relatively quick succession upon a basement of plateau basalt lavas. Our mapping defines the flank group as 5 separate sub-units, shown in Figure 4.1:

- B_1: The oldest eastern flank lavas mapped as the entire basal structure that is exposed above the Grænavatn Porphyrytic Group (GPG) and below the Flaga andesite group (B_2) or lavas co-eval with it (B_{ne})
- Stöng group: A small group within B_1, represents a distinct localised unit on the Breiðdalur volcano east flank.
- B_2: the eastern flank Flaga Icelandite lavas.
- B_3: the eastern flank youngest lavas, situated above B_2.
- B_{ne}: the north eastern flank mafic to intermediate lavas, approximately co-eval to B_2 – B_3 but does not feature a conspicuous group of icelandite lavas.

The first eruptions (B_1, Lower flank sequence) were probably associated with a rise in topography of the local area. This suggestion is based on the change in thickness from the underlying plateau basalt groups e.g. the GPG (generally >5m) to the first Breiðdalur volcano lavas of <5 m, suggesting they erupted onto a sloping landscape. Alternatively the lavas erupted at the central volcano during B_1 stage may be of lower viscosity than the plateau basalts below due to volatile contents (As suggested by Gibson (1963)), erupted at higher effusion rates or were superheated on eruption. This is beyond the scope of this study and probably cannot be answered without a detailed study on this aspect. One of the most stark observations is the colour change from grey plateau basalts, to the black central volcano lavas (Figure 4.2), which most likely is due to higher degree of alteration/metamorphism induced by higher porosity within the clinker of the thin dark lavas compared to the underlying and thicker, grey pahoehoe lavas. A key factor is the relative thickness of the coherent lava core and the highly porous clinker zones at the bases and tops of these a´a lavas. The B_1 sequence is around 400 m thick (Figure 4.2 and 4.7). As the growth of the volcano continues, more evolved and thicker (>15 m) lavas of basaltic icelandite to icelandite composition, representing the Middle Flank Sequence (B_2), covered the B_1 sequence. The B_2 icelandite lava sequence is 400 m thick and is distinct from the thin basaltic lavas, as thick ($>$15 m) lavas (Figure 4.2). The Upper Flank sequence (B_3), is marked by a change from these thicker icelandites back into thinner, black a'a basaltic ($<$ 5m) lavas similar in form to the lower eastern flank lavas. The youngest lavas exposed on Breiðdalur's flank, are silicic lava flows of the South Eastern Rhyolites (Figure 4.3), along with silicic tuffs and composite flows which are described with the Summit Group. On the north eastern flank (B_{ne}) of Breiðdalur volcano is a sequence similar to the B_2, but is not solely built up of icelandite lavas, because it includes thin basalt lavas intercalated with the thicker icelandite lavas. This sequence appears to be stratigraphically coeval to B_2 and into B_3. This sequence is mapped as flank basalts B_{ne} (located near the mountains of Tóatindur and Breiðitindur). At the head of Breiðdalur valley itself there is an area, 5 km in diameter and up to 500 m thick, exposing pumice breccia or lapilli tuff (We use pumice breccia or lapilli tuff here to describe what Walker (1963) called agglomerate; Figure 4.4), tephra sediments, breccias and lake deposits, all cross cut by various intrusions. It was previously called the 'core group', and suggested to have been an area of subsidence into a magma chamber:

> The variable direction of dip in the core must be the result of very irregular subsidence, greater at some points than at others. A form of cauldron-subsidence into the inferred underlying magma-chamber is probably involved, ... It is significant that no sign of ring- dykes or ring-fractures has been discerned; subsidence of a different type is involved at Breiddalur. (Walker, 1963)

We now redefine this as the 'caldera group', and suggest that the main caldera may have formed through a large explosive eruption, the products of which were deposited into the caldera depression (Figure 4.4). The emptying of the magma chamber allowed the caldera to subside, no ring dykes are seen because these, if present, would be at a deeper level than is currently exposed. However, we interpret the sharp, though irregular, contact between the flank and the caldera group, as the caldera fault (Figures 4.4 and 4.7). The caldera complex (Cole et al., 2005) is measured as around 10 km in diameter, with only a third to half of the caldera exposed. Post-caldera collapse, the area had further subsidence events which allowed caldera lakes to form within areas of subsidence, producing laminated siltstones such as exposed in Hesthálsá (Figure 4.4(e)). These siltstones are then further tilted, indicating a new area of subsidence. This subsidence is most likely eruption related, since the fine layers of siltstone (e.g. in Hesthálsá) are overlain by more pumice breccia and tuff.

Magmas of andesitic composition are relatively common, though not voluminous, within the caldera as dykes, or shallow intrusions and occasional lavas. An andesite, exposed as Ketilhnjúkur appears to be a dome-like structure with lavas spreading from it, adding further evidence to a 'multiple collapse' caldera complex. Silicic volcanism, of rhyolitic composition, is most evident towards the end stages of the volcano. The caldera was formed through a large silicic eruption and the volcano's summit group lavas are thick, broad rhyolitic lavas. These, along with a sequence of tuffs and basalt lavas, overlie the caldera sequences and flank lavas, the best exposures of these lavas form the summits of mountain to the north of Berufjörður (Figure 4.5). Many of the silicic lavas are significant in size, the Berufjarðartindur rhyolite lava flow is around 1.4 km^3 in volume and probably formed a high and significant mountain-top to the volcano (Figure 4.3). Rhyolitic magmatism is also evident as dykes and intrusions within the caldera and flank lavas, further to this, mixed magmas are evident as composite lavas and intrusions found in the caldera and summit sequences (Map (Appendix) and Figure 4.5). Mixed magmas appear to be a late stage product, only occurring in the summit group, post caldera collapse The most significant of these is the Berufjörður or Fossárdalur composite lava on the southern flank of Breiðdalur. This lava is thought to have erupted from a plug exposed as the mountain of Rauðafell in Berufjörður (Figure 4.3), it displays a bimodal mixing and mingling relationship between a basal mixed mafic-intermediate section and a rhyolitic upper section of the flow, both sections contain mafic enclaves. Late stage composite lavas, together with rhyolitic lavas intercalated with basaltic lavas demonstrates that mafic magmas are still being generated and feeding eruptions at Breiðdalur even towards the end of the volcano's life. This late stage silicic magmatism at Breiðdalur is at odds with the suggestion by (Walker, 1963) and by other studies throughout the British Palaeogene Igneous Province (BPIP), where it is understood that silicic magmatism preceded mafic magmatism (Kerr et al., 1999; O'Driscoll, 2006; Meade et al., 2014). These differences could be accounted for due to the difference in crust, BPIP volcanoes formed in the less dense continental crust of metasediments (e.g. Le Bas, 1966; Meyer et al., 2009; Meade et al., 2014) whereas Icelandic crust is predominantly basaltic.

This field mapping indicates that mafic magmatism occurs for the duration of the volcano's life, from birth, throughout the flank sequence, as mixed magmas in the caldera and summit group as well as mafic lavas in the summit group. Furthermore, that silicic magmatism appears to be confined to the youngest (later) stages of the volcano's life. The volcano was subsequently buried by plateau basalts erupting along the Breiðdalur fissure swarm, and presumably from nearby or neighbouring fissures swarms. We also demonstrate that the Breiðdalur caldera was formed during a large eruptive event, though it may not have been catastrophic, the eruption will certainly have had local, regional and possibly even farther afield consequences. The caldera was a focal point for explosive silicic and mafic activity, lavas, tuffs and ignimbrites of the summit group also appear to have erupted within and upon the caldera complex, though the degree of subsidence decreases as does the degree of geothermal activity at the surface. These findings can be related to active calderas such as the nearby Askja volcano (e.g. Hartley and Thordarson, 2012), which displays many similarities to those demonstrated here at Breiðdalur.

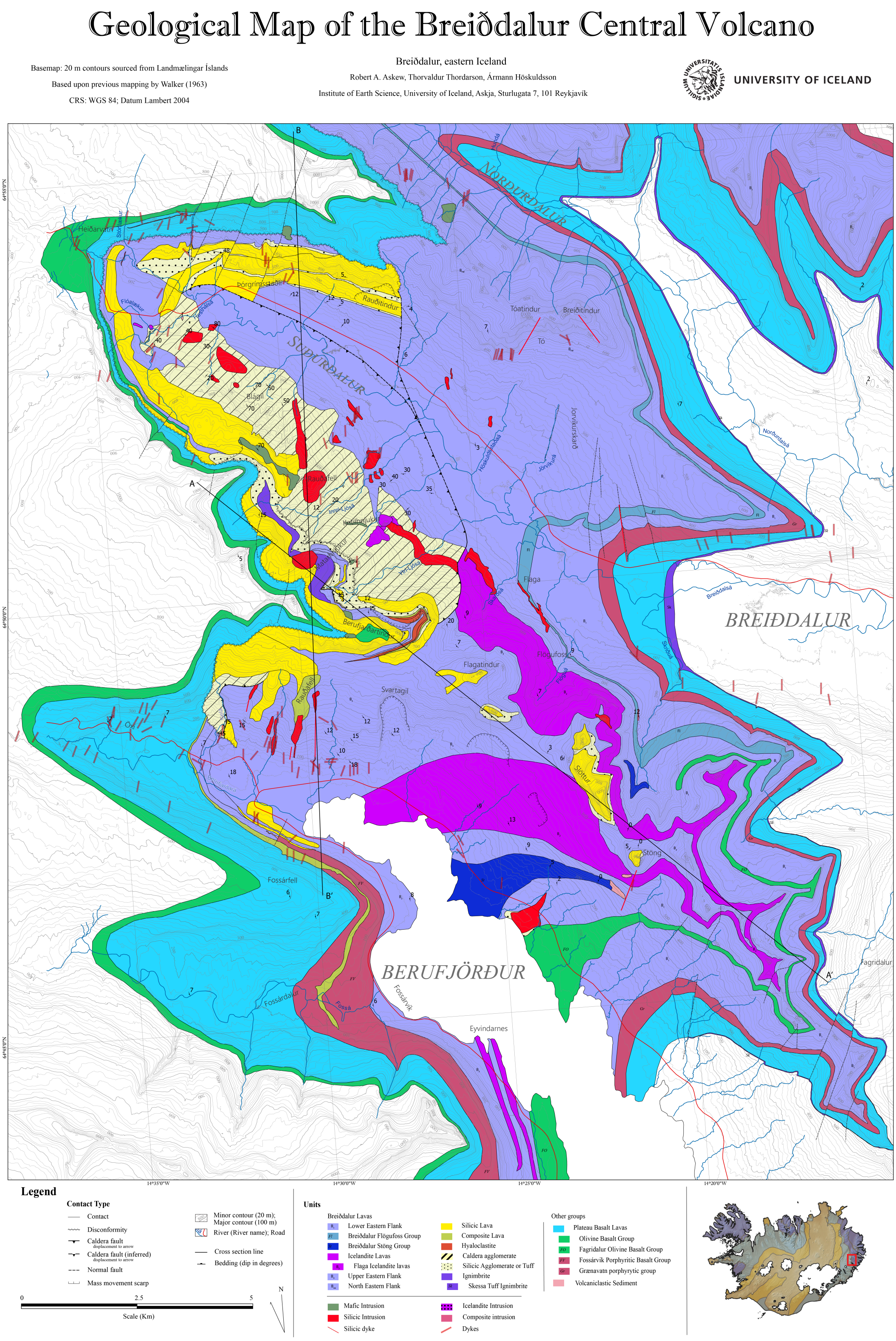

Figure 4.1: Geological map of Breiðdalur volcano, reference figure. Full scale figure in Appendix.

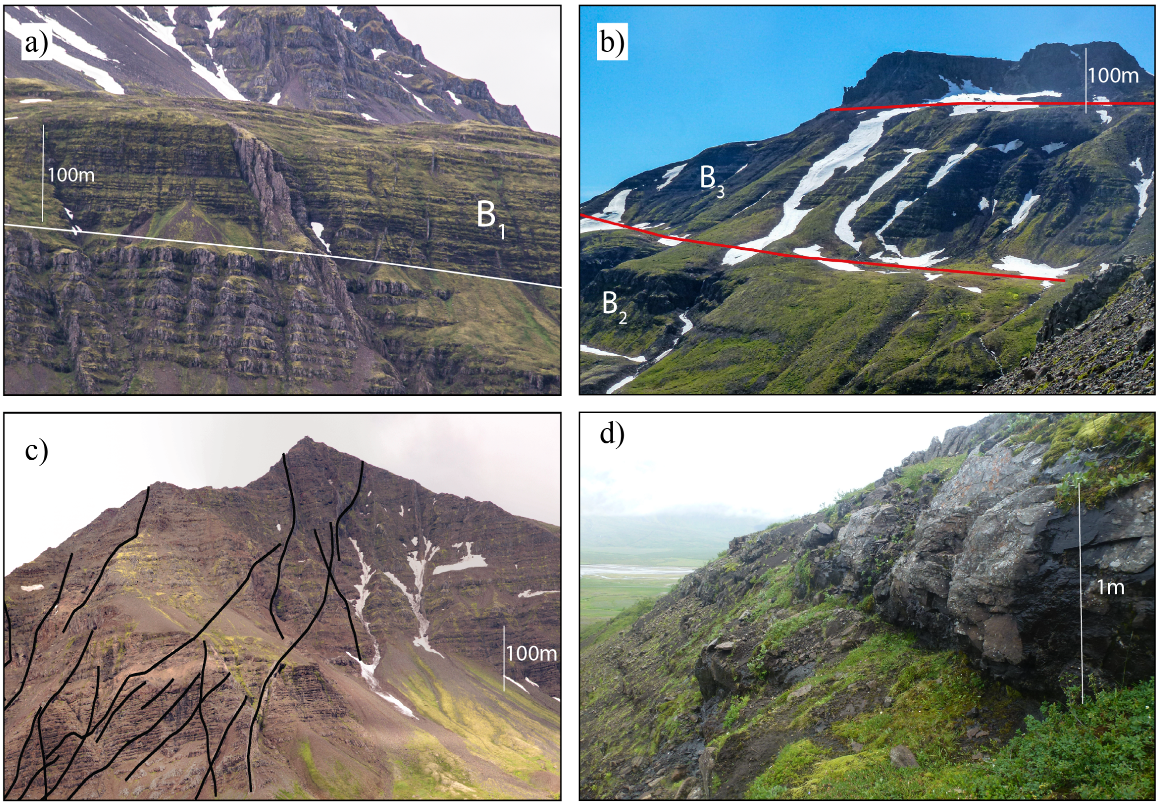

Figure 4.2: The flanks of Breiðdalur volcano. a) Shows the difference between the grey and relatively thicker 'plateau basalts' which include the Grænavatn porphyrytic group, below Breiðdalur, and the distinct change to the thin and dark basalts of the B_1 Breiðdalur flank lavas. The white line indicates the exact point where the morphology of the lavas changes. Several dykes cross cut the sequences at this locality. b) The B_2 and B_3 flank groups, the youngest mafic flank group displays similar lava morphologies as seen in the oldest B_1 group, the B_2 is characterised by thicker andesite lavas, intercalated with basaltic lavas. Rhyolite lavas appear during the B_3 phase, in this image is Flögutindur rhyolite part of the SER. c) Flank lavas of the B_{ne}, black lines show the cone sheet swarm well exposed in this locality. d) Typical field outcrops of the Breiðdalur flank mafic lavas, the lavas are thin and their vesicular base and tops are often weathered away leaving grassy slopes.

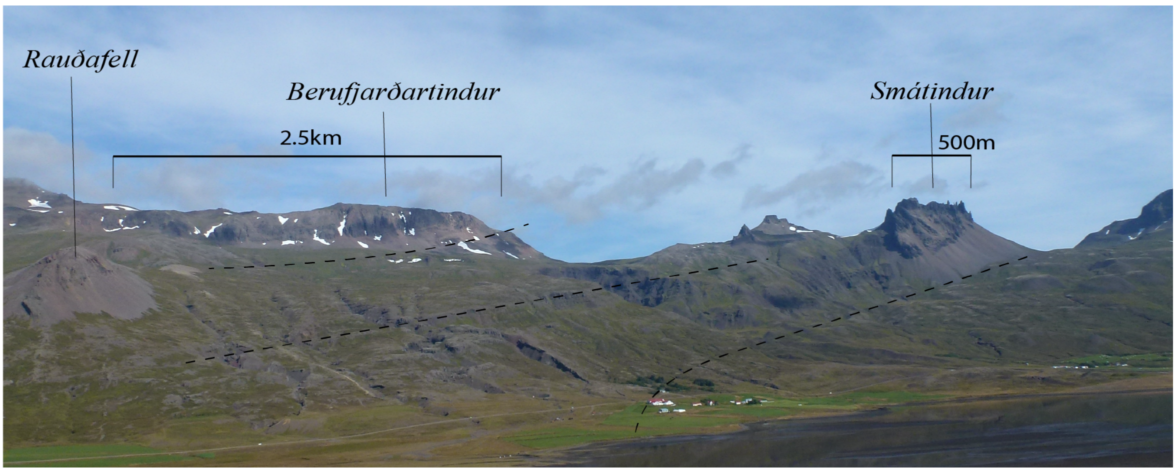

Figure 4.3: Photo direction: South.The Berufjarðartindur rhyolite lava, in relation to the western-most SER lavas. Smátindur is shown, the peak just left of this is Flögutindur. Dotted lines show approximate stratigraphy for reference.

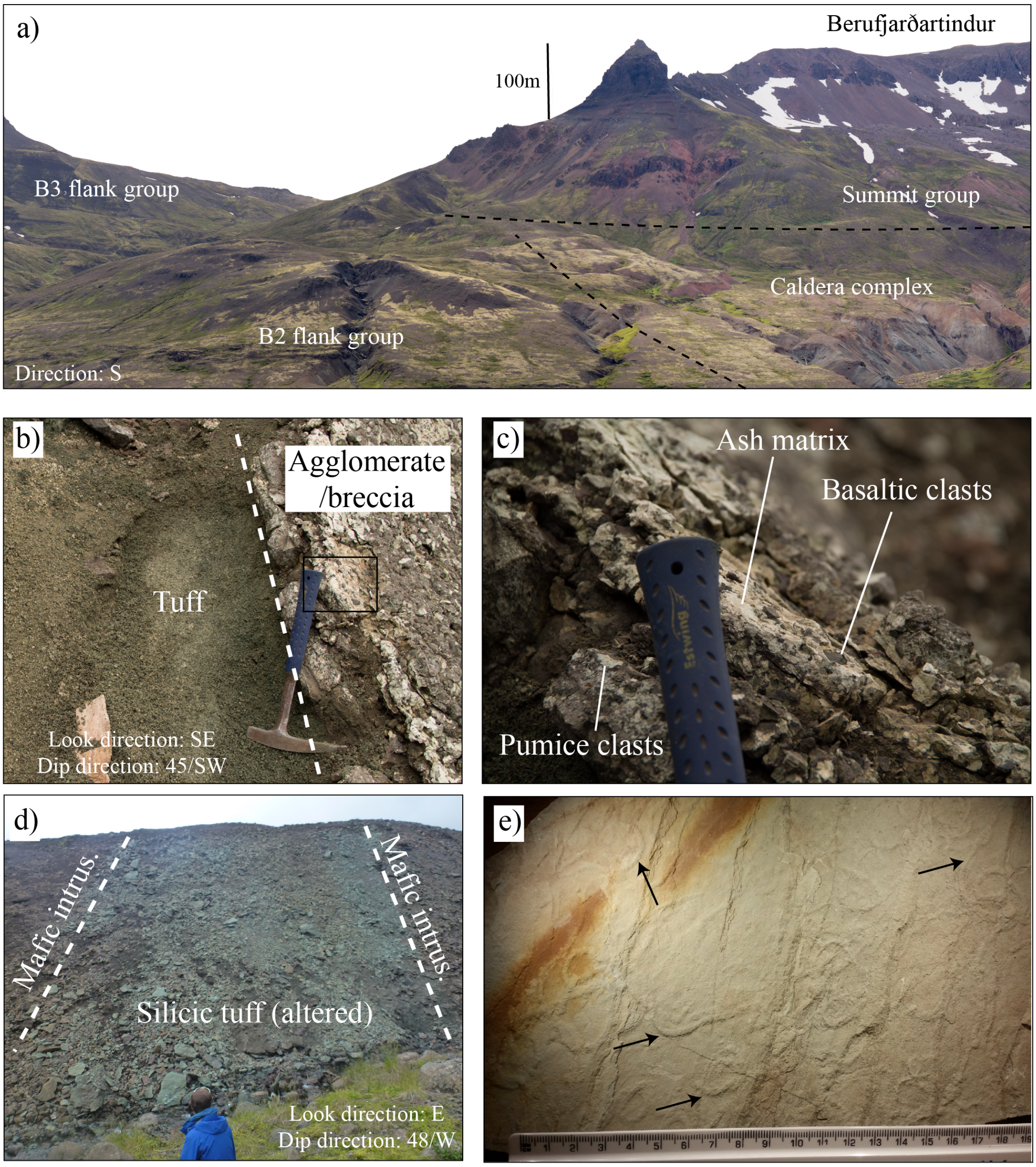

Figure 4.4: Central volcano unit relationships and the caldera complex group. a) Relationship between the caldera complex, the overlying summit group, and the B2/3 flank units. b) Caldera complex units, altered tuff (green alteration) overlain by agglomerate: basaltic lithics, rhyolitic pumice clasts in an ash matrix. c) close up of the agglomerate, hammer for scale. d) Outcrop of silicic tuff in Hesthálsá, within the caldera complex. The tuff displays greenish chlorite alteration and is intruded by mafic bodies. The outcrop weathering is typical throughout the caldera complex. e) Image of Hesthálsá siltstone, trace fossil remains (Repichnea) can be seen on the bedding surface (arrows indicate the shapes of the traces).

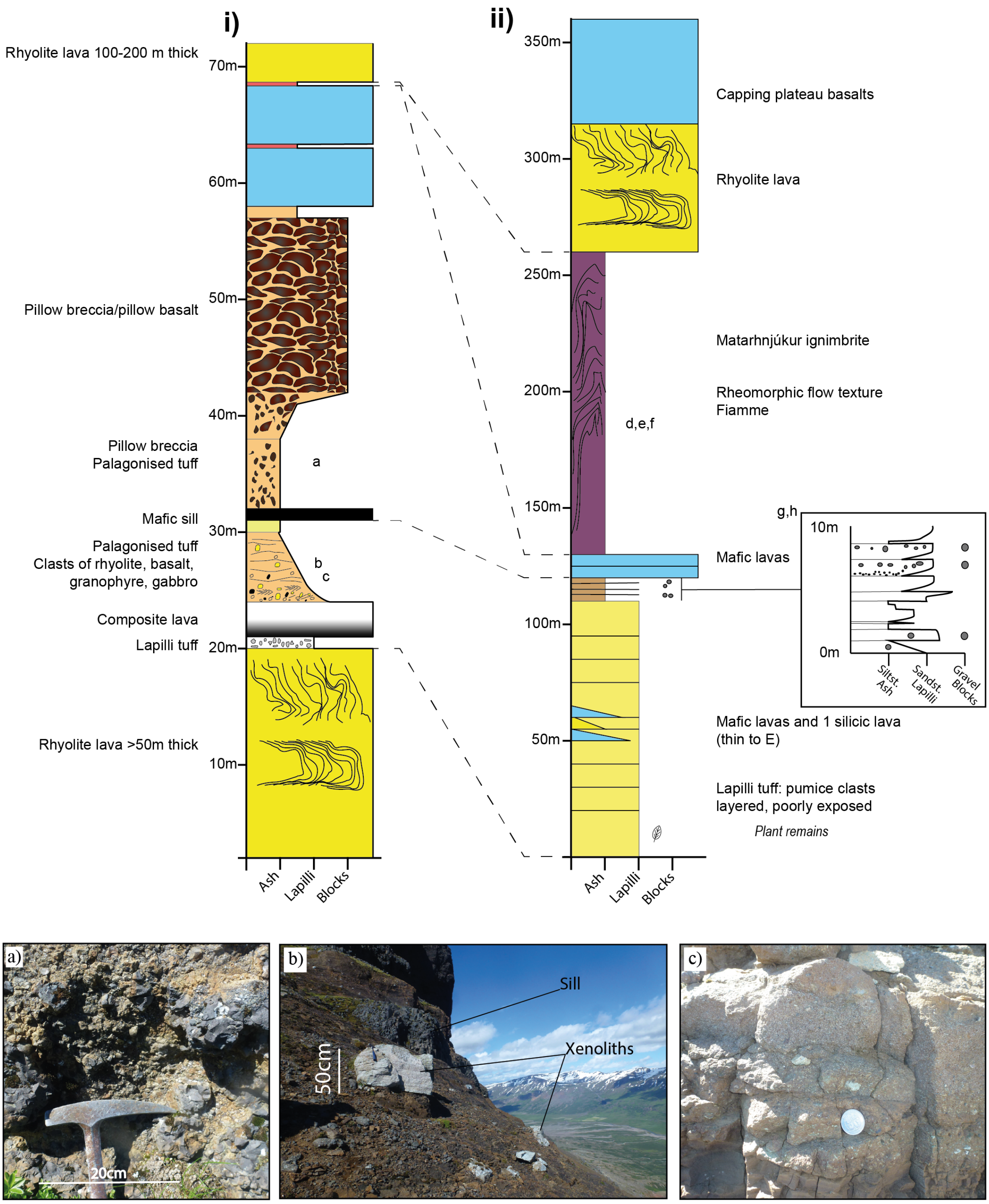

Figure 4.5: Logs of the central and eastern summit group. i) Eastern summit group by Berufjarðartindur. ii) Central summit group from Ýtri Ljósá to Matarhnjúkur. Colours relate to map except: red = red beds, sediments and tuffs with a distinctive red colour in the field; orange: palagonised tuff, with a distinct brown-orange colour in the field; brown: sediment. Composite lava is shown as white and black. Small letters on the logs indicate approximate locations of images a-h (this figure and next figure). a) Palagonised tuff matrix with brecciated basalt clasts, the remains of pillows. b) Palagonised tuff from an explosive eruption which brought clasts of wall rock to the surface. c) some of the sedimentary style structures found within the tuff of (b).

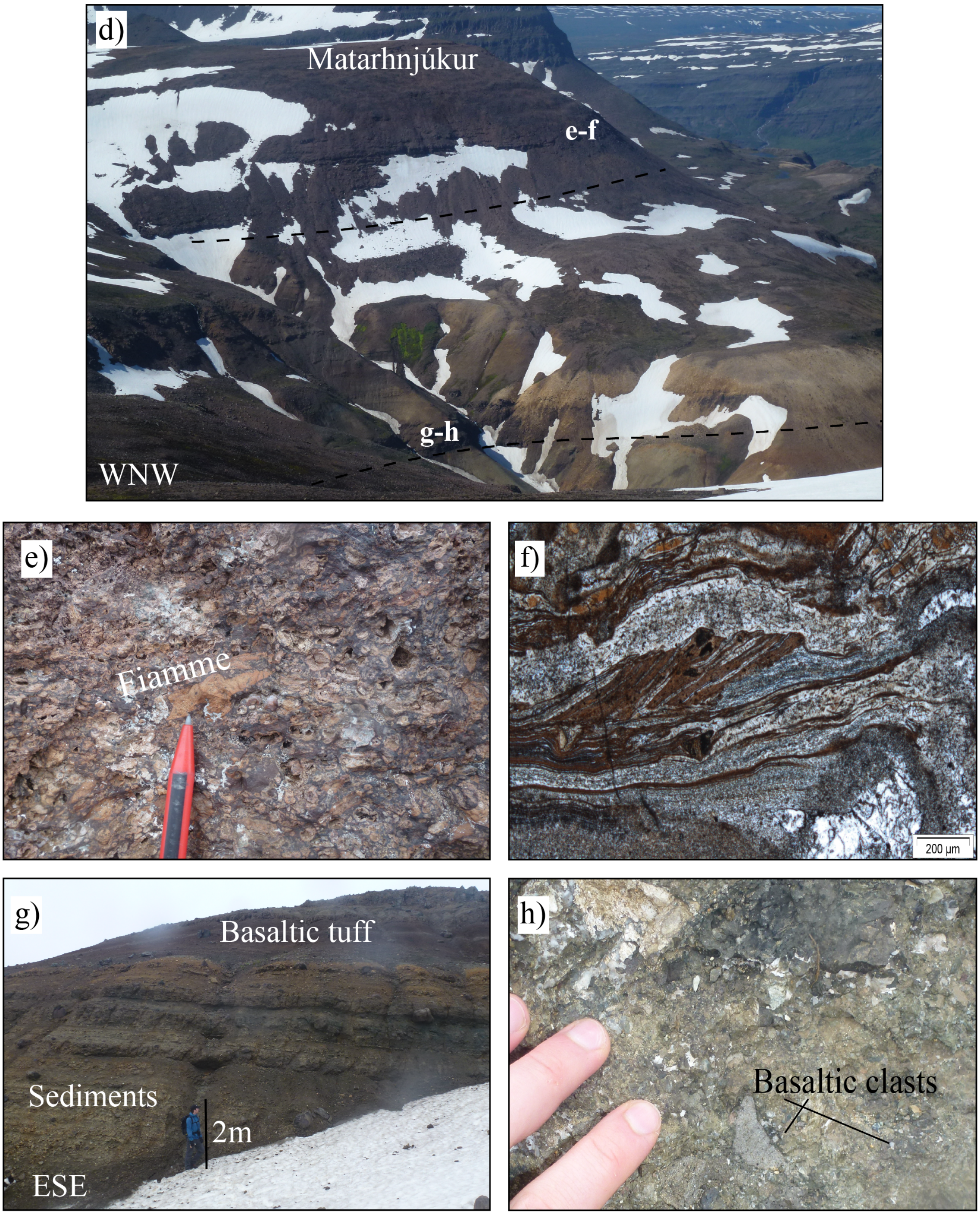

Figure 4.6: Continued from previous figure. d) View WNW of Matarhnjúkur from Berufjarðartindur, dotted lines show stratigraphy for reference. e) The lava-like rheomorphic ignimbrite of Matarhnjúkur in the field. The ignimbrite has a distinctive red-pink colour, fiamme is shown with pencil for scale. f) Rheomorphic structure within the ignimbrite in thin section, the ignimbrite consists of an ash matrix and spherulitic texture is common, vesicles are variable in size from sub cm to around 10 cm, often elongate with the flow structures. g) Sedimentary sequence below matarhnjúkur. h) Sandstone of the sequence in (g), clasts of gravel to boulders are seen, though the larger boulders are infrequent (not shown).

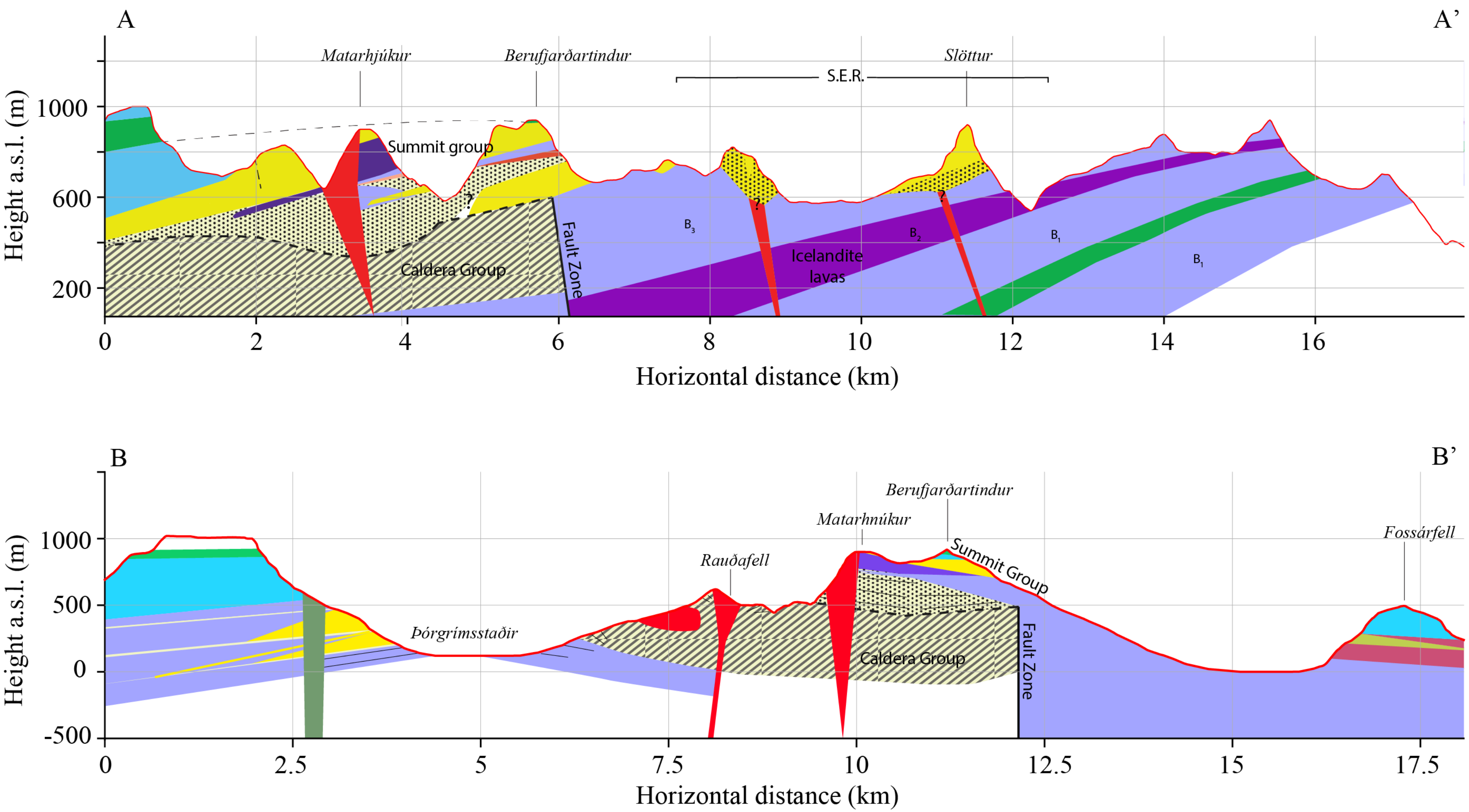

Figure 4.7: Geological cross sections of Breiðdalur volcano, see Map in Appendix for Legend and Cross Section trace. Upper cross section from west (left) to east (right), lower cross section from north (left) to south (right). The sections outline the caldera and summit sequences and their relations to each other and the flank sequence.

4.2 Paper 2: Temporal and spatial evolution of the Neogene age Breiðdalur central volcano through $^{39}Ar/^{40}Ar$ and U-Pb age dating

4.2.1 Overview

Age dating of the volcanism and magmatism at the Neogene Breiðdalur volcano is the focus of Paper 2. This is achieved through high resolution age dating of the volcanic succession that makes up the central volcano, including the immediate formations below and above the volcano. Previous age dating studies concentrated on the plateau basalt stratigraphy and magnetostratigraphy (Watkins and Walker, 1977; Helgason, 1982, 1983; Duncan and Helgason, 1998; Helgason and Duncan, 2014) or on the silicic magmatism associated with central volcanoes (Åberg et al., 1987; Martin and Sigmarsson, 2010; Martin et al., 2011; Berg, 2016). In order to fully understand volcano geology and the evolution of magmatic systems we need to combine geological observations with high precision age dating. Our study quantifies the relationship between a volcano and the fissure system associated with it as well as the lifespan of the central volcano itself. An age dating campaign was undertaken from 2012 to 2015. The samples span the stratigraphy from Streitishvarf to the upper Breiðdalur area. The campaign produced results that required revision of the geochronological model for the southern east fjords volcanic systems of Iceland, as well as a detailed age evolution model of a single volcanic system, the Breiðdalur volcano.

4.2.2 Summary of results

Our results shown in Table 4.1 and Figure 4.8 show that Breiðdalur volcano´s lifespan was around 1 My. During which time the volcano's activity produced over 600 km^3 of material, spreading over 1000 km^2 and probably creating a 1-2 km high edifice. Most of the activity was mafic, with around 10-15 % being more evolved magmatism. Early activity at the volcano occurred at around 10.1 Ma (Lower eastern flank sequence B_1, Figure 4.8). The activity progressed quickly, with the 1000 m thick flank sequence being fully formed, and probably forming a broad cone, by around 9.5 – 9.6 Ma (Figure 4.9).

A silicic magma chamber was active from 9.58 My to 9.1 My, before regional and local mafic activity overtook the system and subsequently buried the volcano. A caldera forming event occurred at 9.5 – 9.6 Ma (Figure 4.9), the caldera was infilled by the material from the eruption. The caldera experienced further, smaller explosive silicic events before 9.3 Ma. A depleted silicic magma reservoir and continuing mafic activity at the volcano, may be responsible for creating mixed or composite lavas, with high basalt to rhyolite ratios, the Fossárdalur composite flow (9.5 Ma), formed just after the suggested age of the caldera event, when the silicic reservoir would be depleted or recharging.

Effusive silicic volcanism typifies the later stages of the volcano's lifespan, seen in the summit group and SER, from around 9.3 – 9.1 Ma, mafic volcanism is still present. After 9.1 Ma, the volcano stops building its edifice and plateau basalts from the surrounding fissure swarms bury the volcano. A plateau lava overlying the highest lava from the volcano is also dated to 9.1 Ma (figure 4.8 and 4.9), though the error of 0.2 Ma essentially means, even if the volcano is 1000 m high an eruption 10 m thick every 2000 years could bury the volcano within the error period.

The Breiðdalur dyke swarm long outlives the central volcano which ceases activity around 9.1 Ma, dyke activity is continuous from 9.8 Ma to 7.8 Ma. Eruptions from the dyke swarm will have occurred outside of the volcano, or on the flanks, and slowly buried the volcano along with lavas from other volcanic systems (Table 4.1 and Figure 4.8). Due to accuracy of modern $^{40}Ar/^{39}Ar$ age dating dating and the relatively short timescale of the volcano's lifespan little further information would be gained from more sampling.

Our study has also re-evaluated age dates around Hamarsfjörður and Álftafjörður, suggesting that Álftafjörður volcano is around 10 – 9 My old (Figure 4.10). This has implications for regional temporal studies of the east fjords plateau basalts.

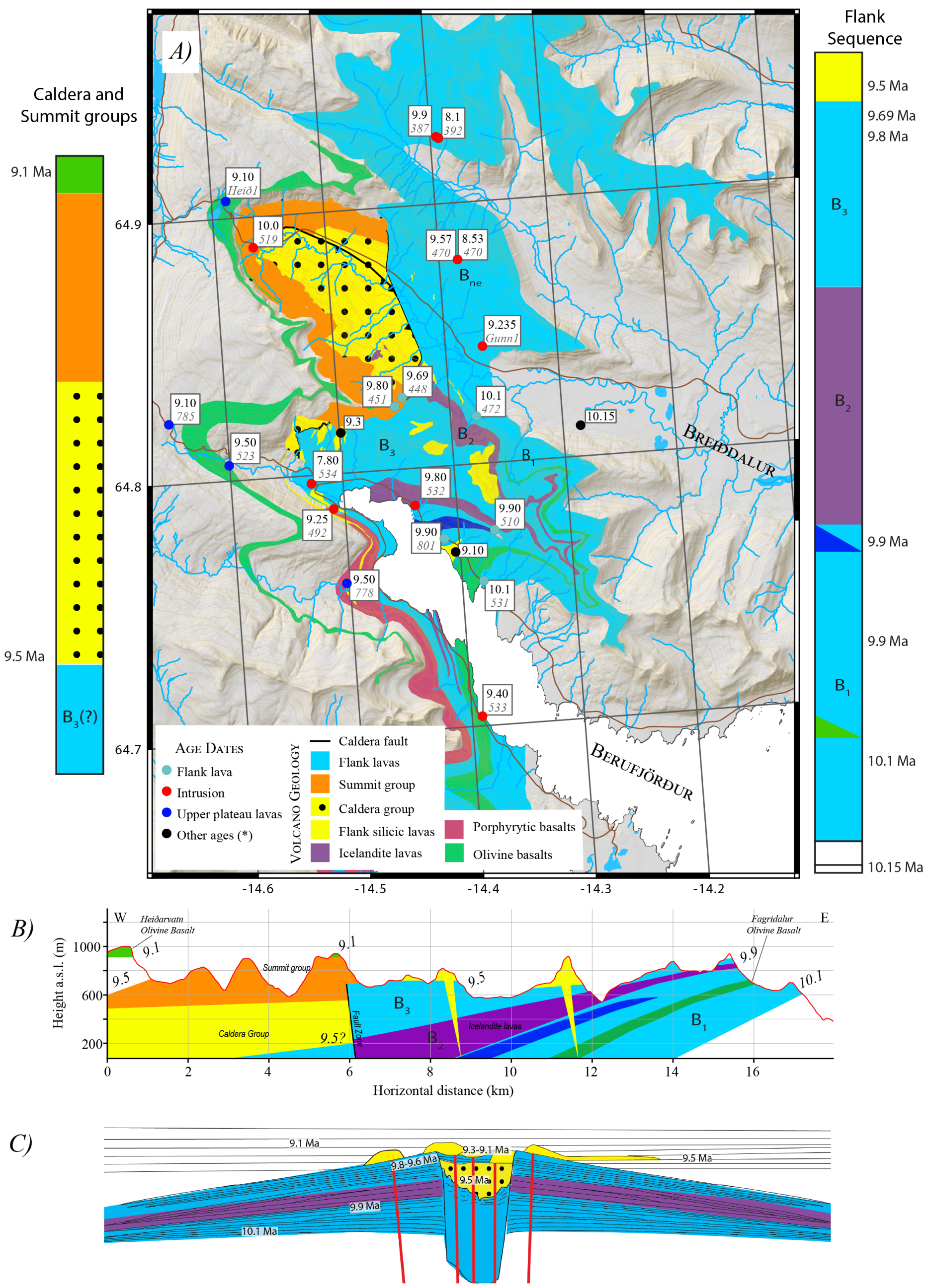

Figure 4.8: A) Age dates (errors in Table 4.1) from throughout the Breiðdalur volcanic system on a simplified geological map of Breiðdalur (Localities shown in Figure 2.3). B_1: Lower eastern flank sequence, B_2: Icelandite lava sequence, B_3: Upper eastern flank sequence and B_{ne}: North eastern flank sequence, the dark blue sequence within the B_1 is the Stöng group (9.9 Ma). To the left of A) is a simplified stratigraphic log of the Caldera and summit group with approximate ages of the caldera event (9.5) and the capping olivine basalt group (9.1). To the right is a simplified log of the eastern flank sequence. B) A simplified geological cross section of the Breiðdalur area with ages for reference. C) A simplified sketch of the Breiðdalur volcano with the age of each sequence.

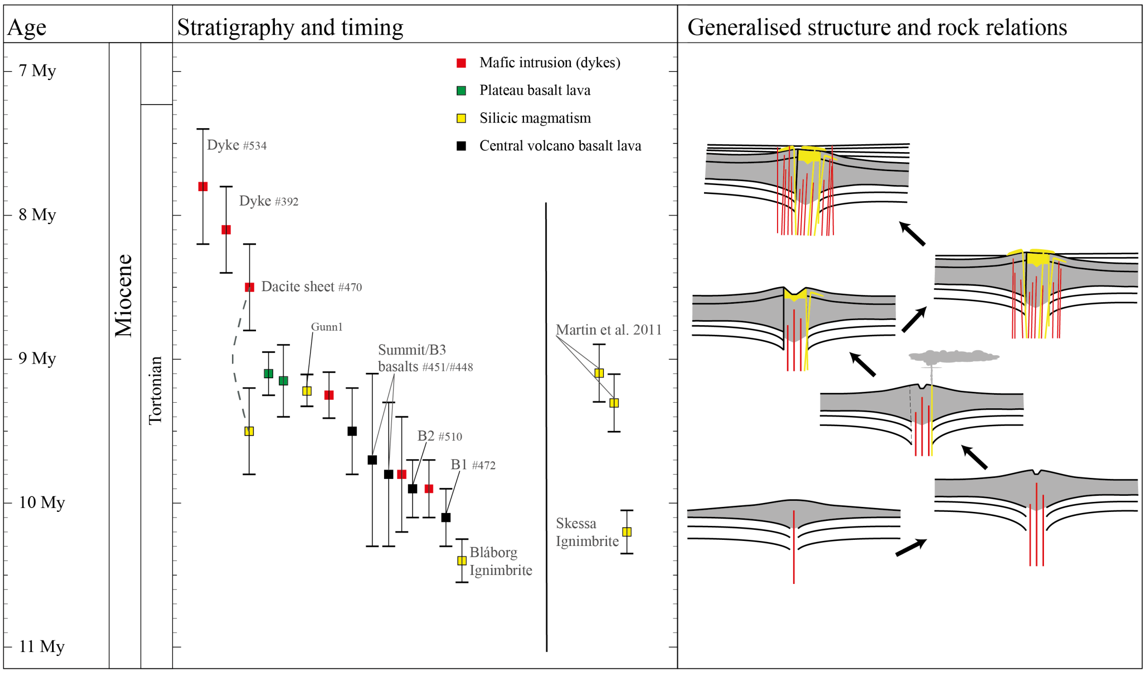

Figure 4.9: Stratigraphic representation of the age progression through Breiðdalur, dotted line links 2 ages from one sample. On the right is a generalised rock relation diagram of central volcano magmatism throughout time. Central volcano magmatism effectively ceases at around 9.1 Ma, younger dykes are found, so dyke/fissure swarm activity continues. Dates presented in the central partition are cited from Martin et al. (2011) and Skessa Ignimbrite age from Riishuus et al. (2010), all other dates are from this study.

Table 4.1: Age dates from the Breiðdalur volcanic system

Sample #	Analysis	Sequence	Lat.	Long.	Sample details	$^{40}Ar/^{39}Ar$	U-Pb	Error
Skessa[1]	GM				Skessa Tuff Ignimbrite[1]	10.15		± 0.1
472	GM	F	64.818147	-14.376627	Lower eastern flank lava	10.1		± 0.2
510	GM	F	64.774337	-14.367796	Mid-eastern flank lava	9.9		± 0.2
801	GM	F	64.772455	-14.413190	Mid-eastern flank lava	9.9		± 0.2
451	GM	S	64.824026	-14.449095	Summit sequence basalt lava	9.8		± 0.5
448	GM	S	64.827269	-14.441849	Summit sequence basalt lava	9.7		± 0.6
778	GM	U	64.757996	-14.502869	Plateau basalt (Fossárvík porphyrytic group) lava	9.5		± 0.3
Rauðf1[2]	GM	S			Rauðafell rhyolite lava[2]	9.3		± 0.2
785	GM	U	64.823157	-14.651802	Plateau basalt lava, Öxi	9.1		± 0.15
Heið1	GM	U			Plateau basalt lava, Heiðárvatn	9.1		± 0.15
519	GM	I	64.888376	-14.565322	Mafic sill in caldera	10		± 0.2
387	GM	I	64.925673	-14.394553	Dyke	9.9		± 0.2
532	GM	I			Dyke	9.8		± 0.4
470	U-Pb Zircon	I	64.827005	-14.440187	Dacitic Inclined Sheet **(01)		9.57	± 0.39
533	GM	I			Dyke	9.4		± 0.2
492	GM	I	64.786648	-14.509945	Dyke	9.25		± 0.16
Gunn1	U-Pb Zircon	I	64.844650	-14.366633	Rhyolitic dyke		9.235	± 0.15
Beruf1[3]	GM	S			Berufjörður rhyolite intrusion[3]	9.1		± 0.2
470	U-Pb Zircon	I	64.827005	-14.440187	Dacitic Inclined Sheet **(02)		8.53	± 0.39
392	GM	I	64.925075	-14.392401	Dyke	8.1		± 0.3
534	GM	I			Dyke	7.8		± 0.2

*Age dates from lavas and dykes in the Breiðdalur system, upper section is lavas, lower section is intrusions. GM: Groundmass plagioclase $^{40}Ar/^{39}Ar$ analysis. F = Flank sequence; S = Summit sequence; U = Upper sequence lavas - not defined, lavas thought not to be sourced from the Breiðdalur volcano seen to be on-lapping onto the late stage volcano lavas; I = Intrusions. [1]Riishuus et al. (2010); [2]Martin and Sigmarsson (2010); [3]Martin et al. (2011) (Kelduskogar). **(#) Zircons from Sample 470 split into 2 populations 01 and 02, see text for details.*

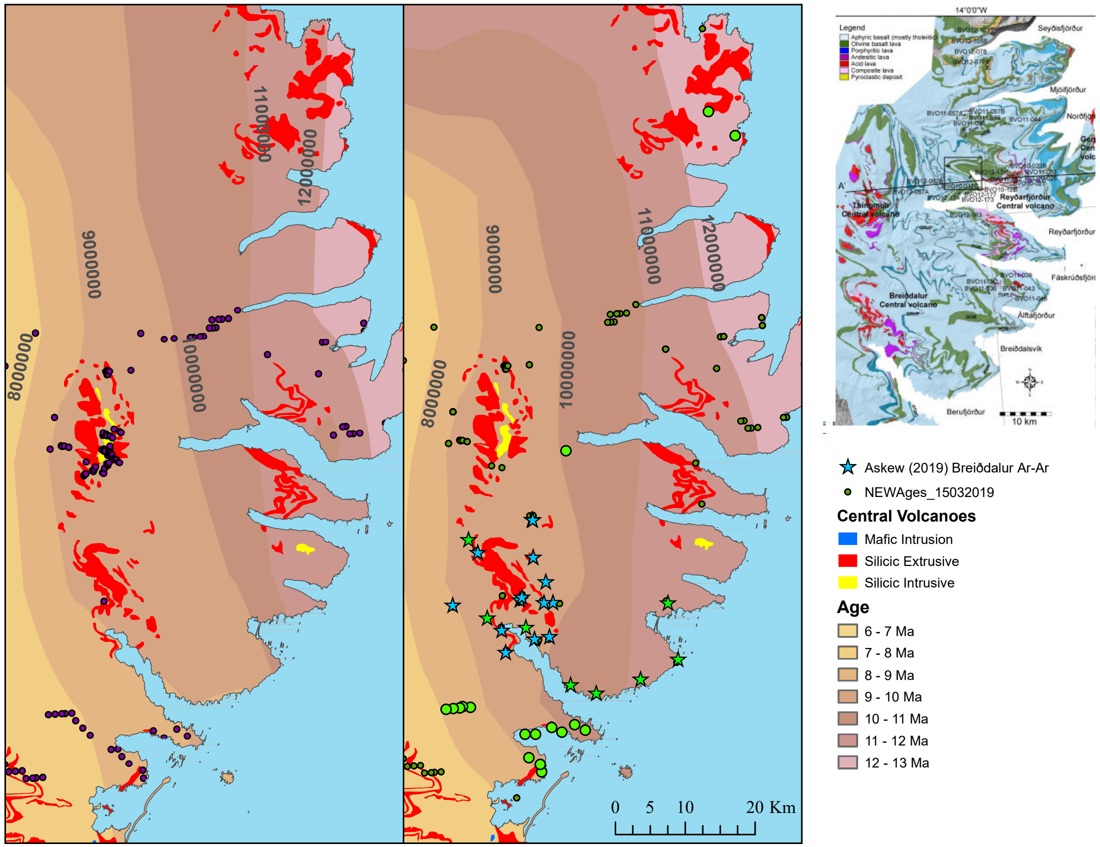

Figure 4.10: Age estimates of the eastern Iceland lava pile, compiled raster images utilising (a) Age dates prior to the year 2000 in eastern Iceland and (b) age dates post-2000, from this study and old dates reevaluated or erased through stratigraphic relation. Small points are age dates complied by Kitagawa et al. (2008) using data from McDougall et al. (1976a,b); Ross and Mussett (1976); Watkins and Walker (1977); E. Mussett et al. (1980). Blue stars are age dates from this study (Table 4.1), green stars are from this study taken by Gans, green circles are reevaluated ages. Inset, geological map (Óskarsson and Riishuus, 2013), showing the general stratigraphic structure of the east fjords which the age raster tries to best fit.

4.3 Paper 3: Geochemistry of the Breiðdalur volcanic system.

4.3.1 Overview

In this investigation, we analyse samples taken from over 70 location throughout the Breiðdalur volcano, and couple this with previous geochemical and petrological date acquired by other authors e.g Walker, 1963; Schnell, 1994, along with previous field mapping and age dates taken in the same campaign. The samples provide a concise overview of the geochemistry of a single volcanic system, the basement lavas beneath this volcano and the lava envelope surrounding it, as well as providing a stratigraphical framework for understanding any variations in lava geochemistry throughout the life of the system.

We also delve further into the question of the formation of silicic magmas at this volcano. Two separate publications brought separate conclusions through different analysis methods: Schnell (1994) suggested that evolved melts were produce through Assimilation Fractional Crystallisation (AFC), with fractional crystallisation being dominant and assimilation of the wall rock providing the slight variations shown in the data. Martin et al. (2011) suggested that Breiðdalur silicic lavas were produced purely by partial melting, through O isotopes, and trace element analysis. Rhyolite-MELTS (Gualda et al., 2012) is used to investigate, among other processes,fractional crystallisation pathways in magmatic systems. Charreteur et al. (2013) utilised MELTS to suggest 2 methods of forming evolved melts at Þingmúli central volcano (located 20 km north of Breiðdalur, Figure 2.1): Fractional crystallisation of basalt in a reduced environment and secondly, mixing of mafic and silicic melt and subsequent fractional crystallisation under more oxidised conditions. Our investigation will also test the 2 hypotheses of magmatic evolution and formation of silicic magmas, partial melting vs fractional crystallisation, through MELTS modelling, Sr isotope ratios and field geology investigations.

4.3.2 Summary of results

The results of geochemical analysis are presented in Appendix Table C.1, these samples are also presented in the TAS diagram and immobile element discrimination diagram (Figure 4.11). Þingmúli (Carmichael, 1964; Charreteur et al., 2013) and Álftafjörður (Gallagher, 2013) volcanic systems neighbour the Breiðdalur system, these 3 volcanic systems all display similar geochemistries, being broadly tholeiitic, with elevated incompatible element ratios compared to modern day axial rift tholeiites (Figures 4.11a, 4.11b and 4.12). Rocks with low Nb/Y or Zr/Y ratios and of primitive composition are absent from this sample dataset, the data we are comparing with, and the east fjords in general (e.g. Harðarson et al., 2008). This suggests that Breiðdalur system is probably typical within the east fjords but may not be entirely comparable to the closest axial rift, the NVZ (see also Figure 4.12). Samples from Þingmúli have, in general, a higher ratio of Nb/Y than the other two systems (Figure 4.11b), with Breiðdalur showing the lowest ratio. This may be a factor of clinopyroxene crystallisation differences between the systems since Y is relatively more compatible in clinopyroxene than Nb. The two systems' samples are also presented in Figure 4.13, where Þingmúli shows a higher range of MgO and Zr than the other two volcanic systems, but the data lack geological constraints e.g. where the samples came from in the system. Similarly Álftafjörður

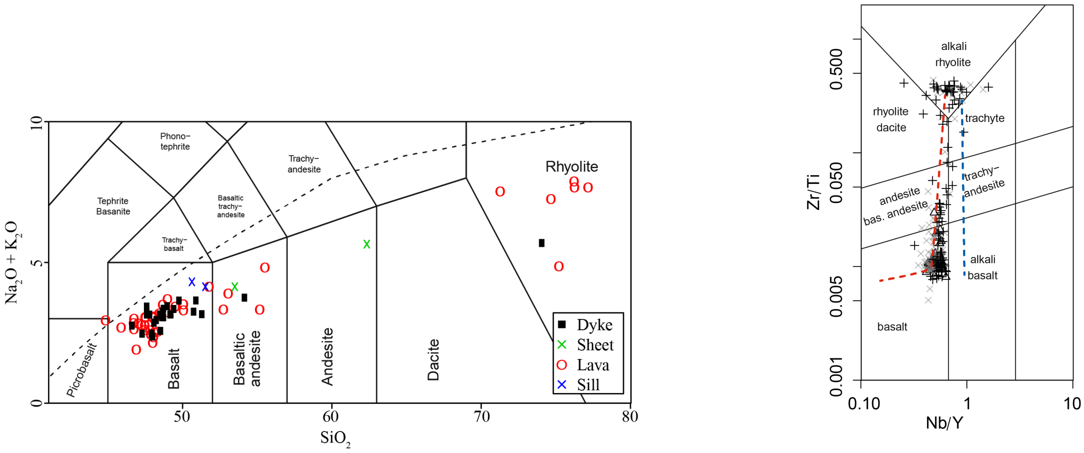

(a) TAS diagram (Le Bas et al., 1986) displaying geochemical data from Breiðdalur volcanic system. Alkali elements may be subject to some alteration post-emplacement, but the same results are found in alternative classification diagrams.

(b) Immobile trace element diagram, to compare Neogene volcanic systems. From Winchester and Floyd (1977) modified by Pearce (1996).

Figure 4.11: Discrimination diagrams, Breiðdalur and comparison to immobile elements. Figure (b): X = Breiðdalur; + = Þingmúli; Δ = Álftafjörður dykes. Red line = Typical tholeiite trend (NVZ/WVZ). Blue line = Alkaline trend (Hekla). This indicates that, though alteration can cause mobility of alkaline elements, this does not affect the rocks to a notable extent in discriminating samples. Þingmúli data from Carmichael (1964); O'Nions et al. (1977); Wood (1978); Charreteur et al. (2013), Álftafjörður data from Gallagher (2013). Breiðdalur samples plotting in the ´alkalic' section of (b) are data from Schnell (1994), thus it is difficult to comment on these individual samples and their uncertainties.

system is only represented here by the dyke swarm, which does show a greater compositional range than the Breiðdalur dyke swarm with dykes of much more evolved MgO.

Basaltic lavas from the Breiðdalur volcano plot within a relatively confined geochemical range most notable when compared with data from surrounding flood basalts and basaltic dykes of the entire system (Figure 4.14). The average composition of Breiðdalur dykes is slightly enriched in incompatible elements compared to Breiðdalur volcano lavas.

Major and trace element data is concurrent with field and petrographical assessments (e.g. Figure 4.15) of the Breiðdalur volcanic system: evolved magmatism occurred late in the volcano's lifespan and intermediate magmas are a minor, though significant, portion of the stratigraphy (Figure 4.16). The earliest magmas (B_1) from the Breiðdalur volcano are relatively evolved basalts (MgO 5 – 6 wt. %), these appear to progress (Figure 4.14 and 4.13) into more evolved basalts – basaltic icelandites in the upper B_1 before the B_2 sequence of icelandites. Above B_2, the B $_3$ lavas display a slightly larger range of compositions compared to the B_1 lavas (e.g. MgO 4 – 7 wt. %), interestingly, these are slightly more primitive (or less evolved) than the earlier lavas. Basaltic dyke compositions are confined to a rather small range (Figure 4.14). MgO ranges from 4 – 7 wt.%, similar to the compositions of the basaltic central volcano lavas. This trend is similar in other elements shown, though TiO_2 ranges slightly higher in the dyke samples, and Y slightly lower, this does not appear to be a significant difference. Central volcano lavas and dyke swarm dykes appear to show very slightly more confined ranges in compositions compared to plateau basalt lavas, the

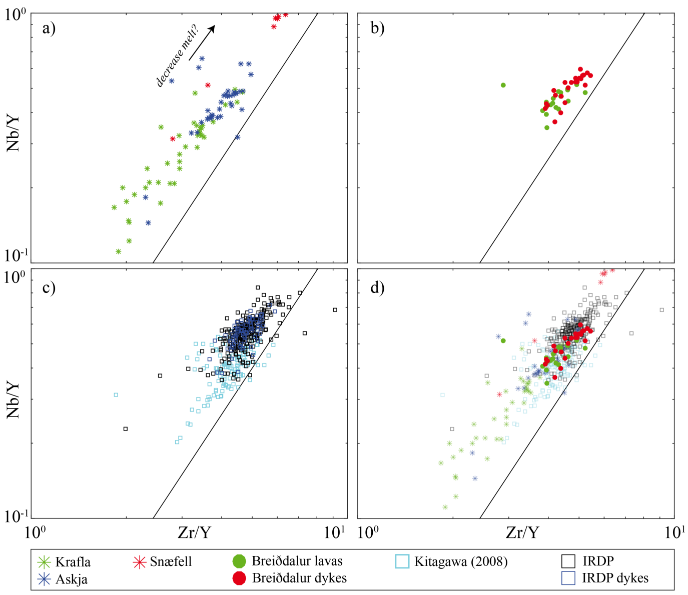

Figure 4.12: Nb/Y vs Zr/Y ratios for Breiðdalur samples. a) Krafla, Askja and Snæfell volcanic system samples, these systems were chosen due to their proximity to the current location of Breiðdalur volcanic system. b) Breiðdalur basaltic lavas and dykes, a single outlier is evident. c) East fjord lavas and dykes, samples from Kitagawa (2006) and Flower et al. (1982) (IRDP). d) The Breiðdalur volcano is slightly enriched by comparison to the systems of the NVZ though appears typical of east fjord geochemistries. Dyke samples often appear to display more enriched ratios than lavas from the same area.

incompatible trace element (in basaltic melts) Zr (Figure 4.14 and 4.13) shows lower concentrations in rocks above the central volcano, this trend is seen, though less discernibly, in MgO (Figure 4.13).

Our MELTS modelling results did not provide a clear answer or distinction between the two methods of forming evolved melts at Breiðdalur: fractional crystallisation or partial melting. Figure 4.16 shows some of the MELTS lines predicted by the model, which appears to fit the data well, and those that do not fit can be estimated by mixing from the least evolved compositions. However, our field studies indicate that there is still a significant Daly Gap (Daly, 1925). Icelandites (Figure 4.15b) form an important part of the volcano stratigraphy, but volumetrically are not significant. Dacites are almost completely missing from the stratigraphy bar a few intrusions, one of which is certainly a mixed magma (sample 370). Rhyolites (e.g. Figure 4.15f) are, however, volumetrically significant, representing about 15% of the stratigraphy. This amount of melt would require a rather large amount of primary basaltic melt that forms silicic magma through fractional crystallisation, and presumably dacites and icelandites would representing a more significant portion of the stratigraphy, with rhyolites being least significant. Thus the two results do not appear to match well. Further to this, running a partial melting model in MELTS can produce the same composition rhyolite from plateau basalt compositions. Therefore, we suggest that partial melting of hydrated basalt crust is the dominant process in forming silicic melts at Breiðdalur.

With regard to the evolved basalts and rocks up to icelandite composition, the trends seen in the volcano stratigraphy (Figure 4.14) and in trace element variations (Figure 4.16) up to basaltic icelandite or even icelandite composition can fit well into a fractional crystallisation model. The earliest Breiðdalur lavas are some of the least evolved, suggesting they have spent less time in the crust than later mafic lavas. Lavas steadily become more evolved with time until icelandites are produced, this could indicate a magma reservoir fractionating melts to icelandite composition beneath Breiðdalur, a process which takes 200 Ka. The heat input would also melt the crust surrounding this reservoir, our age dates indicate this takes at least 500 Ka (Section 4.2). Rocks of compositions lying between evolved basalt to rhyolite can be produced by mixing of the two magmas, which would form the same trends shown in Figure 4.16.

The restricted range in compositions of basaltic lavas from the central volcano is suggestive of a confined magmatic plumbing system which allows basalts to mix and become an 'average' of the source compositions (Figure 4.16). The slightly greater range in plateau basalt compositions presumably means these magmas are residing in the crust for less time and mixing less, this is however, juxtaposed with the dyke swarm magmas which display an even more restricted range (Figure 4.16 and 4.14). This suggests either the plateau basalts after the volcano are not related to the dykes, or, more likely, some of the plateau basalts are related and other are from other dyke swarms/sources. The slightly less evolved nature of the plateau basalts after the central volcano is an interesting note, geological mapping has shown that olivine basalt lavas (lavas containing olivine in groundmass or phenocryst phase) appear to occur above central volcanoes in several cases (e.g. Walker, 1963; Óskarsson, 2015, Paper 1: this thesis). Olivine bearing dykes (Figure 4.15e) in Berufjörður also cross cut the sequence of plateau basalts covering the volcano, indicating these dykes are younger than the volcano (backed up by age dates, Paper 2). This appears to back up this notion, and suggests that more primitive (i.e. less evolved) mafic magmas appear later in the system's life cycle.

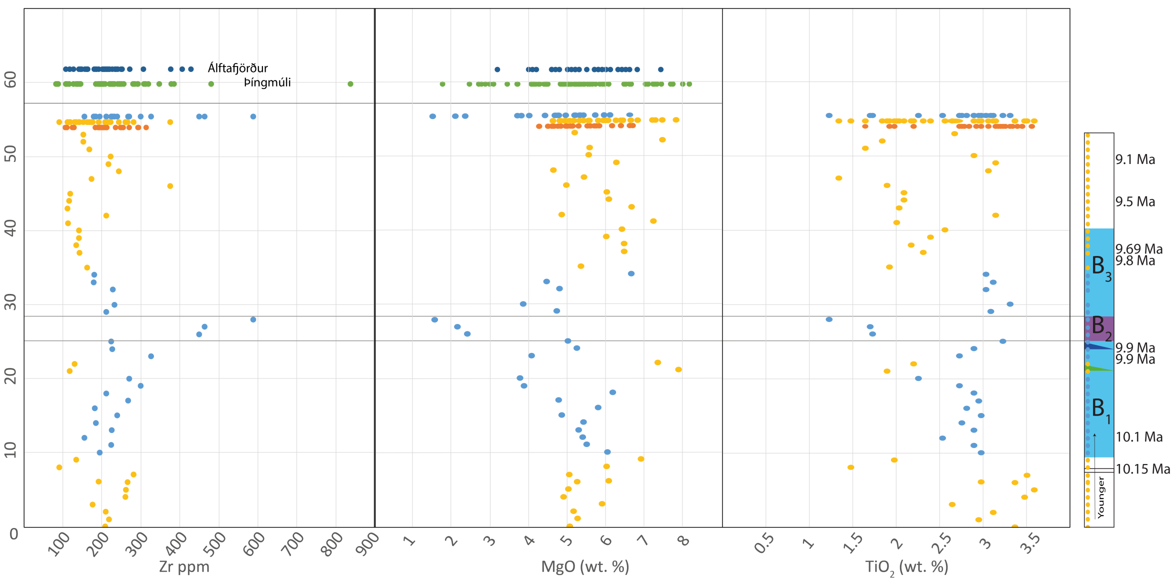

Figure 4.13: Figure key as in Figure 4.14. Zr, MgO and TiO$_2$against stratigraphy (arbitrary numbering) in order to compare magmatic evolution up to icelandite through the volcano's stratigraphy. Álftafjörður (Gallagher, 2013) and Þingmúli Charreteur et al. (2013) (blue and green respectively) data is also shown for comparison with other volcanic systems compositional range (for rocks up to icelandite composition, data cited in Figure 4.11). The horizontal lines indicate the icelandite lavas of B$_2$ group. The blue points, central volcano lavas, appear to become more evolved up to the icelandite group at around 9.9 My. After this group the compositions of the blue points and plateau lavas (yellow points) thought to be part of the late succession of the volcano (yellow overlapping with B$_3$), show relatively more primitive compositions. Lower Ti in upper plateau basalts may indicate early fractionation of TiFe oxides during magma ascent.

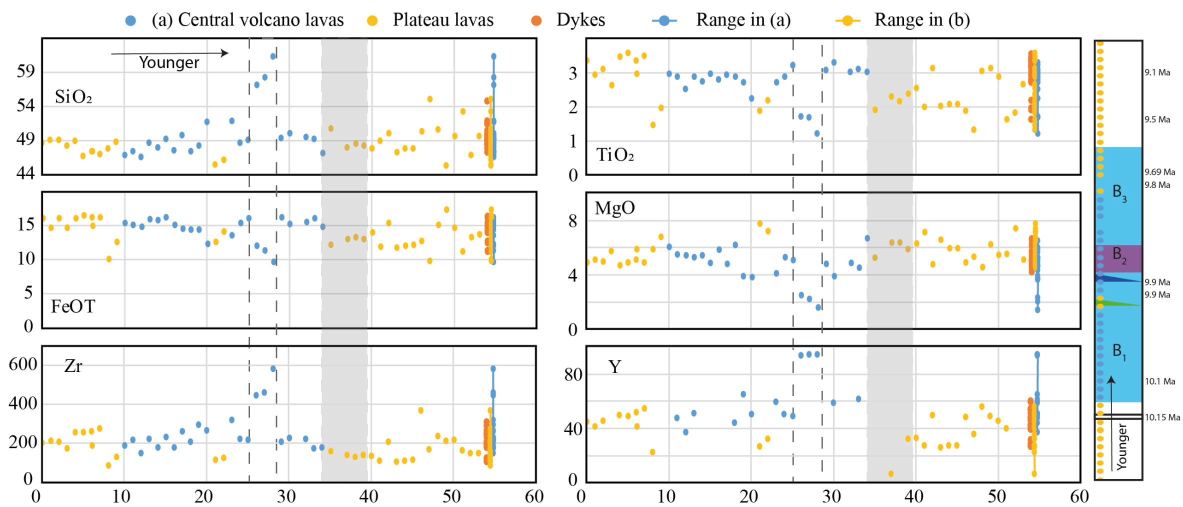

Figure 4.14: Selected major and trace elements in basaltic to intermediate samples from the Breiðdalur area against stratigraphic height (samples over 64 wt.% SiO$_2$ not shown). 0: Oldest sample below the central volcano, 53: Youngest sample. Dyke sample geochemical ranges are shown on the right. Dashed line box: Flaga andesites (B$_2$), grey box: Summit sequence lavas on Berufjarðartindur. To the right, simplified stratigraphic log of the eastern flank sequence, note, the sequences are adjusted to relate to the graphs and do not represent true stratigraphic thickness.

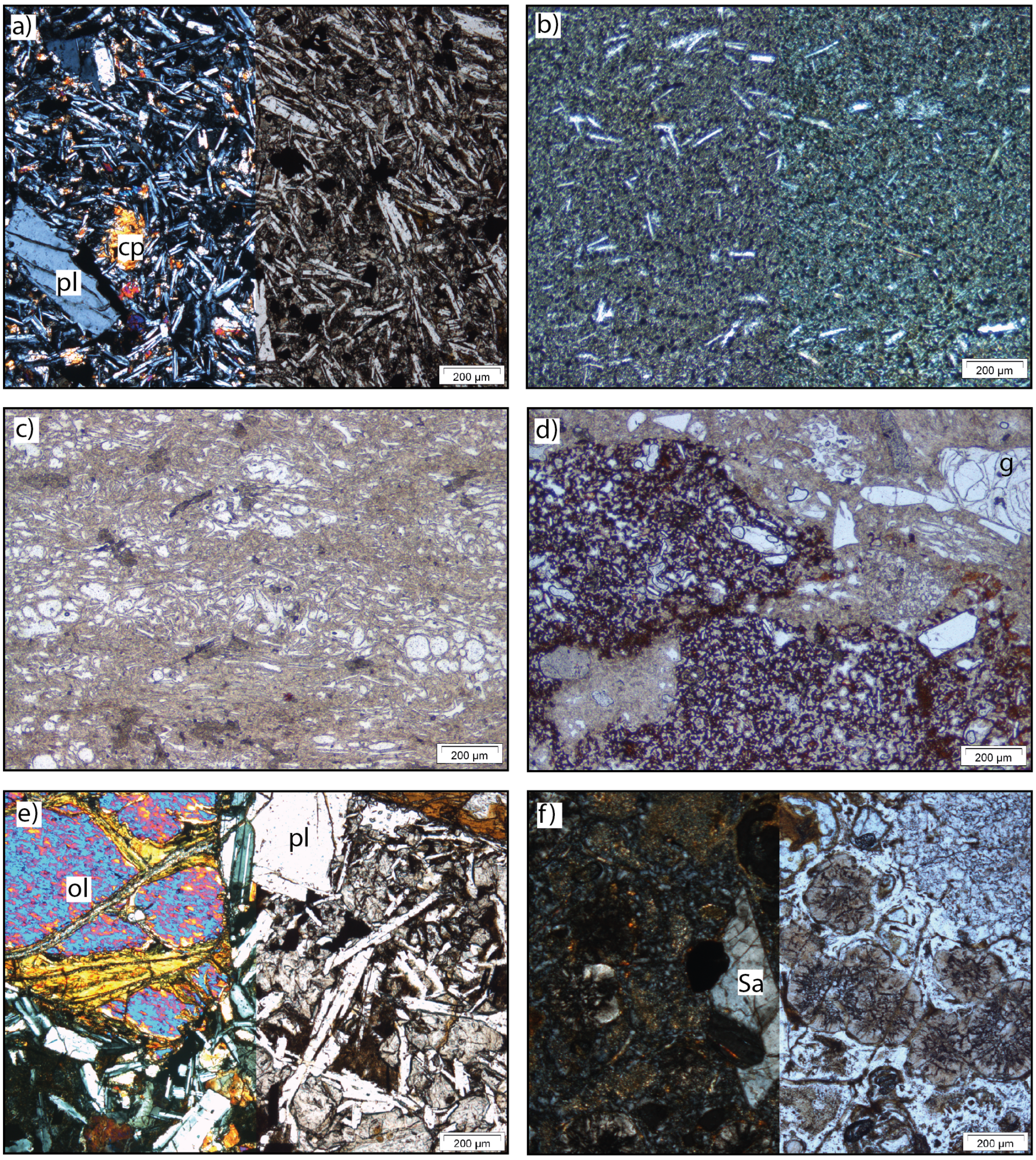

Figure 4.15: Photomicrographs of Breiðdalur volcanic system units. pl: plagioclase; cp: clinopyroxene; g: glass; ol: olivine; Sa: sanidine. a) Sample 801, upper B_1 group, 9.9 +/-0.2 Ma. This lava displays a medium grained groundmass of plagioclase, clinopyroxene and oxides. Irregularly shaped phenocrysts of plagioclase and clinopyroxene up to 5mm in size are present. b) Sample of a B_2 Icelandite lava. The groundmass is very fine grained, consisting of plagioclase, clinopyroxene and oxides. Phenocrysts are plagioclase, of up to 200um (long axis). c) and d) are samples from the Berufjarðartindur tuff. The sample consists of a glassy and vesicular matrix of pumice and ash, containing shards of unaltered glass (g), feldspars and basaltic tephra (d) black sections). e) Dyke sample 496, the sample is coarse grained basalt to dolerite with a groundmass of plagioclase, clinopyroxene and oxides. Phenocrysts of olivine and plagioclase of 1cm in size, iddingsite alteration is seen on the olivine phenocrysts. f) Sample 405, a rhyolite lava displaying very fine grained quartz and feldspar groundmass with spherulitic texture. Secondary mineralisation is prevalent throughout, small phenocrysts of sanidine are infrequent (<5%).

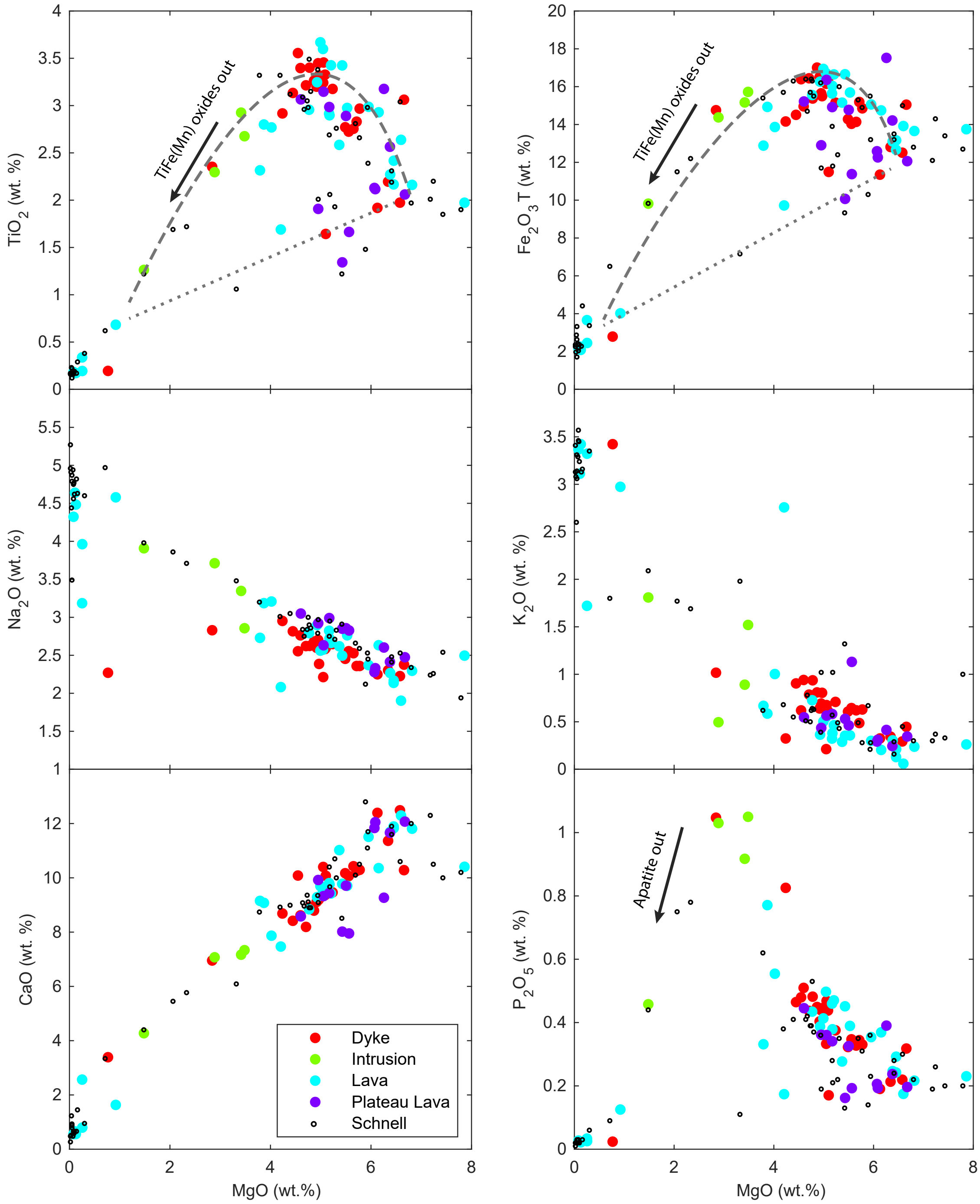

Figure 4.16: Selected major elements against MgO for Breiðdalur rocks from this study and a complementary study by Schnell (1994). Dashed lines in TiO_2 and Fe_2O_3T graphs show fractional crystallisation trends approximated by MELTS from a basaltic magma; dotted lines show mixing trends if the magmas were to mix between the most primitive magma and most silicic magma. The Breiðdalur rocks are divided into lavas, dykes and intrusions (sills or sheets). Arrows indicate various phases likely to be lost from the melt as fractionating phases if fractional crystallisation was dominant.

4.4 Paper 4: Isotopic geochemistry of Miocene east fjord volcanic systems

4.4.1 Overview

(Presented as a report, to be prepared for publication)

The focus of paper 4 is a study of isotopic variation in eastern Iceland volcanic systems and Breiðdalur volcanic system. Being able to effectively suggest the provenance of lavas, dykes and sills is valuable for geological mapping and models of crustal accretion processes. Previous isotopic studies had focused on the Neogene basalt sequences (Kitagawa, 2006; Kitagawa et al., 2008) or silicic magmatism (Schnell, 1994; Martin and Sigmarsson, 2007, 2010; Berg, 2016). If, as is suggested by many studies (e.g. Sigmarsson et al., 2008) magmatism in Iceland may be controlled by the interaction of plume magma with MORB, it should be possible to use isotopic variation to map the volcanic systems and their relationship with the plume head (e.g. Kokfelt et al., 2006; Halldorsson et al., 2008; Maclennan, 2008; Shorttle and Maclennan, 2011; Shorttle et al., 2013, 2014; Sigmarsson and Halldórsson, 2015).

Our study sampled lavas, dykes and intrusions from the volcanic systems of Breiðdalur, Þingmúli, Reyðarfjörður and Álftafjörður. The objective was to characterise the magmatic signature of the volcanic systems by sampling units from each area. If the isotopic compositions are characteristic for the magma source of each system then sampling dykes known to be from Þingmúli and from Breiðdalur should allow us to characterise the magmatic signature for each dyke swarm and allow for mapping of overlapping dyke swarms. Consequently, their interaction could be better understood. Similarly with the lavas of central volcanoes and plateau basalts, if there are distinctive geochemical traits or trends in lavas, then there is the potential to improve geological mapping of the plateau basalt stratigraphy of the Neogene sequences.

4.4.2 Summary of results

The results are shown in Figures 4.17 and Table 4.2. Figure 4.17 displays combined data fields from Welke et al. (1968); Schilling (1973); Sigvaldason (1974); Sun and Jahn (1975); Jakobsson (1979b); Condomines et al. (1983); Kurz et al. (1985); Furman et al. (1992a); Hardarson et al. (1997); Chauvel and Hémond (2000); Kempton et al. (2000); Maclennan et al. (2001); Prestvik et al. (2001); Breddam (2002); Fitton et al. (2003); Thirlwall et al. (2004); Kokfelt et al. (2006); Halldorsson et al. (2008); Peate et al. (2010); Kuritani et al. (2011); Shorttle et al. (2013); Manning and Thirlwall (2014). The volcanoes of this study are consistently closely spaced in isotope space, and Álftafjörður volcano displays the highest radiogenic Pb values of any of these volcanoes. Our study attempted to find a method of distinguishing volcanic systems, there appears to be some merit in this but a more detailed study would be required. Samples from neighbouring volcanoes, such as Þingmúli and Breiðdalur appear to have shared a similar magma source region, because the magmas produced at these volcanoes are almost identical in terms of their Pb isotope values (Figure 4.17).

The volcanic systems in this study are relatively enriched in radiogenic isotopes, most samples from Breiðdalur, Reyðarfjörður and Þingmúli volcanoes are closely spaced in isotope variation diagrams (e.g. Figure 4.17). This close spacing means they cannot be distinguished by isotopic composition alone, but this implies that their magma source zones must have been similar. Þingmúli and Breiðdalur are neighbouring systems both active at the same time (Figure 4.10), thus their magma source zone could feasibly be similar or connected. Álftafjörður volcano is more enriched than the other systems in this study (Figure 4.17) and this is due to a spatial variation in the magma source composition, not a temporal variation as has been suggested previously (Kitagawa, 2006; Harðarson et al., 2008, Figure 4.18 and 4.19). The temporal variation argument requires that the lavas of the east fjords all come from the same source zone/area, however, this cannot be the case, as highlighted by mapping of the plateau basalts Óskarsson (2015); Óskarsson et al. (2017) and from our revised age map of the east fjords in Figure 4.10. Plateau basalt lavas can spread over great distances, but the majority of the stratigraphy is built by lavas from nearby fissure systems, thus lavas in the south east are from a volcanic system in the south east.

Álftafjörður neighbours Breiðdalur and Þingmúli, according to field relations (Blake, 1970, Figure 4.10) its active lifespan also overlaps with them. The distinct isotopic ratios of Álftafjörður by comparison to the other two, implies that the mantle source zone for its magmas is not related or connected to the northern neighbours.

The volcanic systems in this study overlap somewhat in composition with enriched NVZ systems (Figure 4.17 and 4.18) and lavas from the RVB, though it is unlikely that we can draw a tectonic analogue comparing east fjord systems with RVB systems. The systems were probably part of a rift zone or belt with a moderate degree of mixing between a slightly enriched (EMI and EMII) mantle source and a depleted source (Álftafjörður being even more enriched). Magmas produced in the central volcanoes produced more evolved magmas through a combination of partial melting and/or fractional crystallisation.

A further result and conclusion of this study is that Streitishvarf dyke swarm is not related to Álftafjörður, it is at least 1 My older and geochemically distinct, this implies that there is a volcanic system off shore from the Streitishvarf area.

Sample	Location	$^{146}Nd/^{148}Nd$	Error(2sm)	$^{86}Sr/^{87}Sr$	Error(2sm)	$^{206}Pb/^{204}Pb$	Error(2sm)
669	Alftafjordur					18.5559	0.0009
673	Alftafjordur	0.513000	0.000006	0.703476	0.000006	18.6538	0.0045
674	Alftafjordur	0.513005	0.000005	0.703414	0.000006	18.4827	0.0021
675	Alftafjordur					18.5548	0.0011
392	Breiddalur					18.5461	0.0030
446	Breiddalur					18.5546	0.0011
469	Breiddalur	0.513037	0.000008	0.703357	0.000007	18.5519	0.0044
472	Breiddalur					18.4937	0.0013
678	Breiddalur					18.5308	0.0017
778	Breiddalur	0.513013	0.000007	0.703329	0.000006	18.6139	0.0059
788	Breiddalur	0.513021	0.000008	0.703376	0.000007	18.4684	0.0059
791	Breiddalur	0.513026	0.000007	0.703380	0.000006	18.5174	0.0052
801	Breiddalur	0.513011	0.000007	0.703412	0.000007	18.5274	0.0021
697	Reydarfjordur	0.513041	0.000007	0.703352	0.000007	18.5032	0.0046
800	Reydarfjordur	0.513025	0.000008	0.703426	0.000006	18.3910	0.0046
682	Streitishvarf	0.513029	0.000007	0.703367	0.000007	18.5174	0.0050
689	Thingmuli	0.513028	0.000008	0.703369	0.000006	18.5242	0.0043
690	Thingmuli	0.513028	0.000007	0.703384	0.000007	18.4970	0.0031

Sample	Location	$^{207}Pb/^{204}Pb$	Error(2sm)	$^{208}Pb/^{204}Pb$	Error(2sm)	$^{176}Hf/^{177}Hf$	Error(2sm)
669	Alftafjordur	15.5120	0.0011	38.4009	0.0043	0.283196	0.0000053
673	Alftafjordur	15.5063	0.0012	38.3878	0.0017	0.283185	0.0000065
674	Alftafjordur	15.4924	0.0007	38.2344	0.0009	0.283148	0.0000044
675	Alftafjordur	15.5016	0.0015	38.3169	0.0052	0.283221	0.0000047
392	Breiddalur	15.4835	0.0032	38.2753	0.0079	0.283213	0.0000052
446	Breiddalur	15.4826	0.0011	38.2541	0.0026	0.283183	0.0000057
469	Breiddalur	15.4884	0.0017	38.2605	0.0031	0.283169	0.0000041
472	Breiddalur	15.4827	0.0014	38.2027	0.0030	0.283256	0.0000057
678	Breiddalur	15.4923	0.0008	38.2478	0.0030	0.283198	0.0000045
778	Breiddalur	15.4833	0.0012	38.2759	0.0008	0.283168	0.0000101
788	Breiddalur	15.4842	0.0011	38.2148	0.0009	0.283200	0.0000243
791	Breiddalur	15.4846	0.0012	38.2374	0.0010	0.283196	0.0000050
801	Breiddalur	15.4931	0.0007	38.2850	0.0012	0.283152	0.0000067
697	Reydarfjordur	15.4779	0.0009	38.2134	0.0009	0.283182	0.0000134
800	Reydarfjordur	15.4815	0.0012	38.1607	0.0009	0.283196	0.0000044
682	Streitishvarf	15.4806	0.0012	38.2255	0.0015	0.283177	0.0000073
689	Thingmuli	15.4819	0.0012	38.2051	0.0017	0.283173	0.0000041
690	Thingmuli	15.4837	0.0009	38.2111	0.0009	0.283158	0.0000039

Table 4.2: Isotopic ratios for samples in this study with individual 2 sigma errors. Sample numbers can be related to Table C.1.

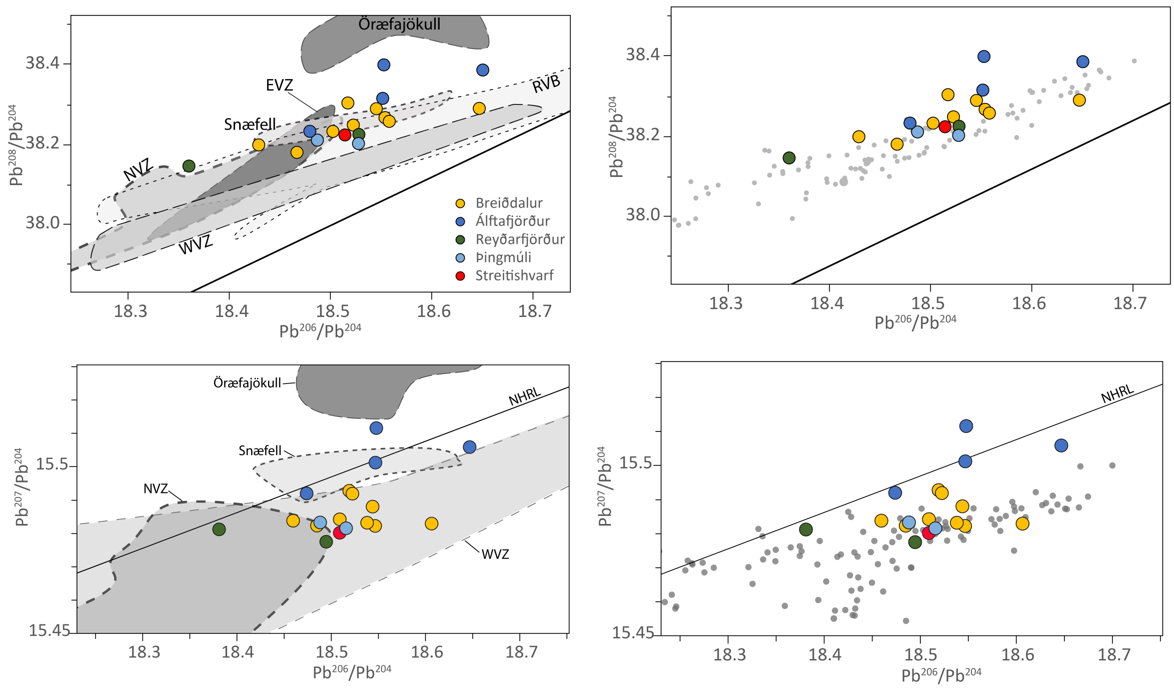

Figure 4.17: Figure key in top left graph. Top left: ^{208}Pb/^{204}Pb isotopic variability in samples from this study in relation to the geochemistry of active volcanic zones in Iceland. Top right: Samples from this study against the comprehensive dataset of plateau basalt lavas in the east fjords of Kitagawa (2006) (grey points). Of interest is the ^{208}Pb enrichment displayed by Álftafjörður (blue) and some samples from Breiðdalur.
Bottom left: ^{207}Pb/^{204}Pb isotopic variability in samples from this study in relation to the geochemistry of active volcanic zones in Iceland. Bottom right: the same sample set against the dataset of Kitagawa (2006), again the same samples show enrichment in ^{207}Pb even against east fjord plateau lavas. Errors are presented in Table 4.2 though mostly are represented by the point size. Figure data fields are a combined geochemical dataset compiled using the GeoRoc database, see text for references.

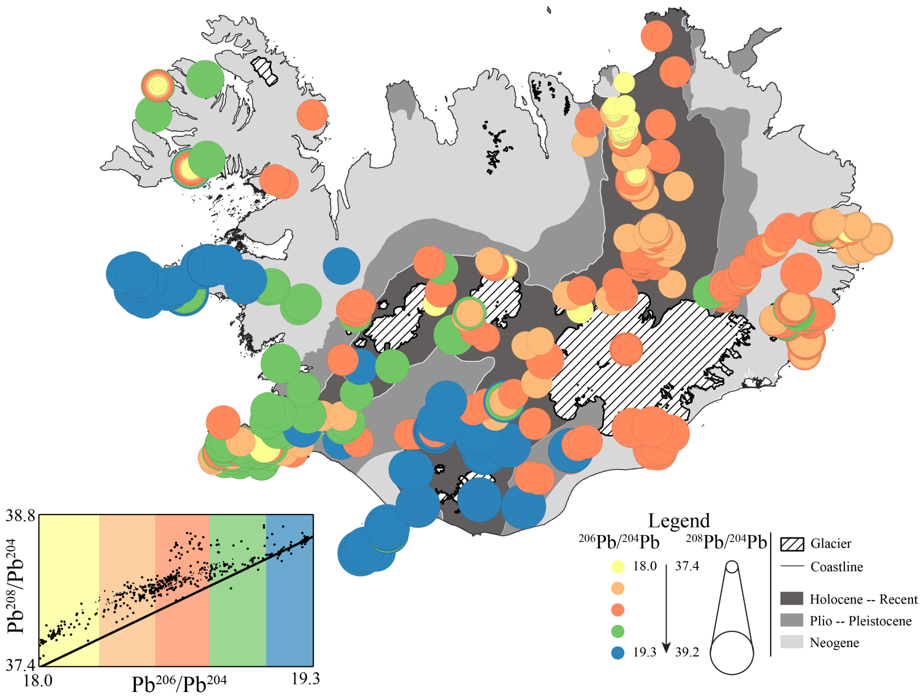

Figure 4.18: Pb isotopic variability map, Iceland for basaltic samples. The colours and symbol sizes indicate relative ratios (as shown bottom left), which gives a simple visualisation of mantle properties. Notably eastern Iceland is most isotopically similar to the NVZ and northern EVZ. Graph in bottom left refers to Figure 4.17.

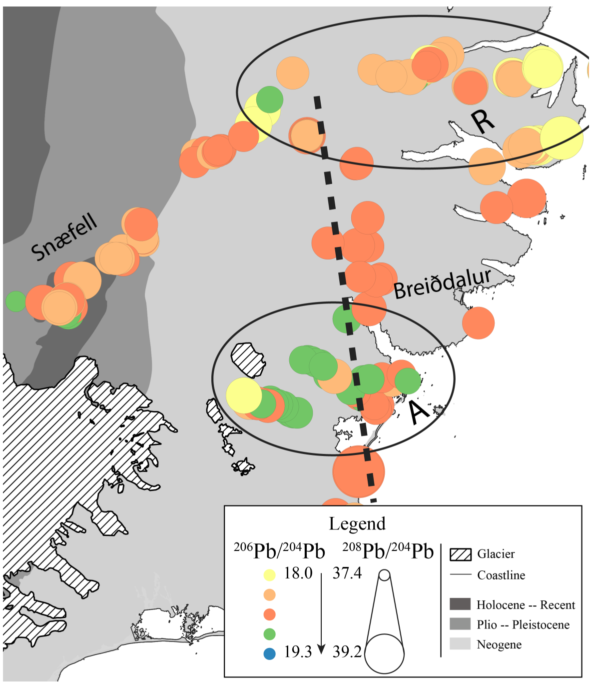

Figure 4.19: Pb isotopic variability map, the East Fjords. Discussion is in the text. The map indicated an increase in ^{206}Pb ratio to the south east, closer to the plume head. Dashed line: Extinct volcanic belt containing Þingmúli, Breiðdalur and Álftafjörður. Ellipses: upper = zone of more depleted lavas, there appears to be a temporal variation from more depleted, to less depleted and back with time (younging to the left - west). lower = more enriched in ^{206}Pb, ^{208}Pb and ^{207}Pb as shown in figures above. R= Reyðarfjörður, A= Álftafjörður

4.5 Non-first author papers

1. Pedersen, G.B.M., et al., Lava field evolution and emplacement dynamics of the 2014–2015 basaltic fissure eruption at Holuhraun, Iceland, J. Volcanol. Geotherm. Res. (2017)

   Role: Part of the IES eruption and hazard monitoring team. Role was predominantly field based, taking samples and acquiring data for use in hazard monitoring and study.

2. Pfeffer, M.A., et al., Ground-based measurements of the 2014-2015 Holuhraun volcanic cloud (Iceland). Geosciences (2018)

   Role: Part of the IES eruption and hazard monitoring team in association with the Icelandic Meterological Office. Assisting in collecting gas samples (multi-collector) and Fourier Transform Infra-Red (FTIR) spectroscopy data collection and analysis.

3. Halldórsson, S.A., et al., Petrology and geochemistry of the 2014–2015 Holuhraun eruption, central Iceland: compositional and mineralogical characteristics, temporal variability and magma storage, Contributions to Mineralogy and Petrology, (2018)

   Role: Part of the IES eruption and hazard monitoring team. Role was predominantly field based, taking samples and acquiring data for use in hazard monitoring and study.

Chapter 5

Conclusion

Mapping and sampling of the Breiðdalur volcanic system was undertaken, lavas, dykes and intrusions were age dated and geochemically analysed, which has yielded valuable information on the timescales of a Neogene volcanic system, and its dynamics of growth.

In all, the Breiðdalur volcanic system was active for 2.3 Ma (10.1 – 7.8 Ma), the central volcano for 1 Ma (10.1 – 9.1 Ma) and the exposed dyke swarm for 2 Ma (9.8 – 7.8 Ma). Suggesting that the Breiðdalur central volcano began building its edifice some 200 – 300 Ky before the exposed dyke swarm was active (Figure 5.1). This is the first detailed chronological scenario developed for a volcanic system in Iceland, as we have been guessing from a small range of age dates and geological mapping up until now. This gives us a more detailed understanding of how a volcanic system evolves and the timescales involved. From a curiosity driven science perspective, this allows us to better fit models of central volcano and volcanic system magmatic evolution into a real timescale. From a social perspective, this can alter how we view both resources (such as geothermal energy or water), and hazards (e.g. what style of activity can we assume will come ´next' at a system), when we understand the timescales of such systems.

Over the 2.3 Ma lifespan, the 100 m thick Breiðdalur volcanic cone was built first, in around 0.5 Ma, following a pattern of: evolved basalts - andesites - evolved basalts - rhyolite. This detailed mapping and more accurate timescale of growth has implications for models of magmatic evolution at volcanoes in Iceland. The general trend in magmatism throughout the volcano is from basalt > rhyolite over time, however, mafic magmatism is continuous throughout, notable from basaltic lavas which are seen throughout the flank sequence, and into the summit sequence, sandwiched between rhyolitic lavas. The mafic dyke swarm is continuous throughout from 9.8 Ma, the swarm and any eruptions from the dykes became the dominant feature of the system after 9.1 Ma. The basaltic lavas erupted from these dykes buried the volcano. This implies that there is a decoupled magmatic plumbing system, one providing mafic magma that intrudes or erupts with relatively shorter crustal residence times than magma feeding a shallower magmatic reservoir system which resides for longer times in the shallow crust.

Our study also analysed any relationship in the geology and geochemistry of neighbouring Neogene volcanoes. These volcanoes, Breiðdalur and Þíngmúli, have very similar geochemistries, they are broadly tholeiitic with slightly enriched incompatible trace element ratios and even their isotopic ratios are indistinct. This implies that the mantle source zone for the magmas feeding these volcanoes was similar and that geochemistry cannot effectively unravel the two volcanic systems. Thus geological mapping is key for marking the extents of central volcanoes and their dyke swarms. The isotopic ratios of the Neogene volcanoes in this study are rather distinct from many Holocene volcanic systems, indicating that there is a temporal variation in the mantle source zone from 10 Ma to present. Álftafjörður volcano is a tholeiitic volcano, with some alkalic magmatism, the isotopic ratios for Álftafjörður are distinct from the other volcanoes in this study, with a higher EMII mantle source. Álftafjörður must have been sourced from a mantle which has similar isotopic ratios to the ÖVB, though with higher degrees of melting or shallower melt depths leading to more tholeiitic magma geochemistry.

As has been shown in other projects, east fjord plateau basalts are not regional-rift events that are sourced from the same place. They are more localised, sourced from specific fissure swarms and flowing into certain areas. This is important when understanding plume-pulse or variation models, since one cannot compare lavas in the south of the east fjords with lavas to the north of the east fjords since their chemistry will vary due to a spatial variation, rather than temporal.

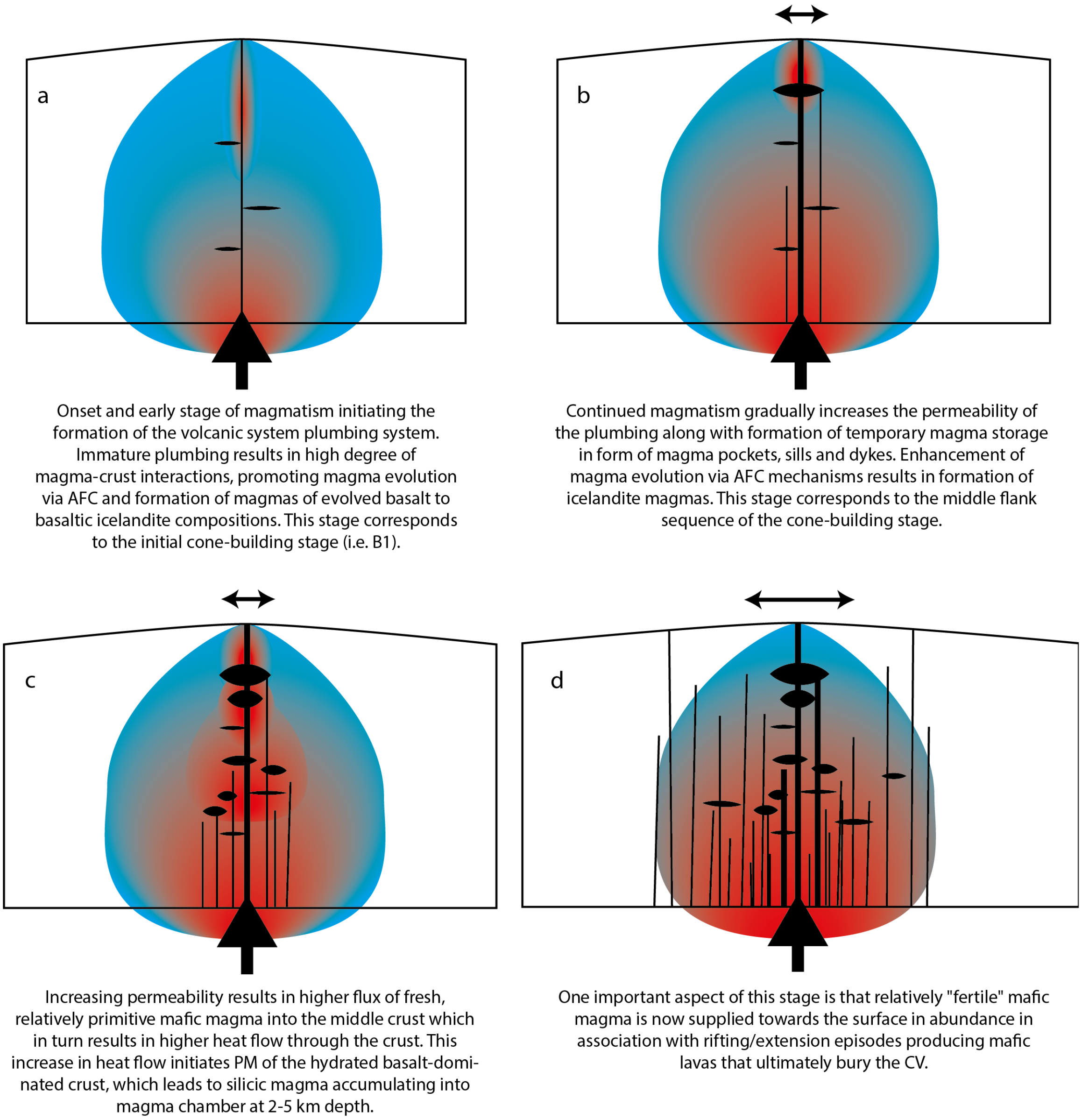

Figure 5.1: Conceptual model of volcanic system evolution: Central Volcano, then Fissure Swarm.

5.1 Future Work

The Neogene sequences of Iceland are still a poorly studied area, despite their window into volcanic and magmatic processes affecting the active volcanoes of Iceland. The central volcanoes of Iceland provide individual cross sections, each appears to be slightly different from the next, displaying the highly variable nature of volcanism. Several authors use different techniques to unravel the mode of formation of silicic magmas, however, many studies land upon entirely opposing conclusions, even when studying the same magmas by different techniques. As techniques, accuracy and understanding improves we need to continuously reevaluate older findings, further studies on silicic magma genesis in Iceland are warranted. Further to this, geochemistry of volcanoes and plateau basalts needs to be improved. Our dataset brings forth more questions than answers, and a more detailed and explicit study on isotopic systematics of central volcanoes in Iceland is needed as well as continued higher detail geological mapping of volcanic systems and regional geology.

Bibliography

Arculus, R. J. (2003). Use and abuse of the terms calcalkaline and calcalkalic. *Journal of Petrology*, 44(5):929–935.

Árnadóttir, T., Hreinsdóttir, S., Gudmundsson, G., Einarsson, P., Heinert, M., and Völksen, C. (2001). Crustal deformation measured by gps in the south iceland seismic zone due to two large earthquakes in june 2000. *Geophysical research letters*, 28(21):4031–4033.

Baker, J., Peate, D., Waight, T., and Meyzen, C. (2004). Pb isotopic analysis of standards and samples using a 207pb–204pb double spike and thallium to correct for mass bias with a double-focusing mc-icp-ms. *Chemical Geology*, 211(3-4):275–303.

Åberg, G., Bollmark, B., and Macintyre, R. M. (1987). Age of the austurhorn intrusion; a net-veined complex in southeastern iceland. *GFF*, 109(4):291–293.

Berg, S., Troll, V., Riishuus, M., Burchardt, S., and Krumbholz, M. (2014). Silicic magma genesis in neogene central volcanoes in northeast iceland. In *EGU General Assembly Conference Abstracts*, volume 14, page 10678.

Berg, S. E. (2016). *Silicic Magma Genesis in Basalt-dominated Oceanic Settings : Examples from Iceland and the Canary Islands*. Doctoral thesis, comprehensive summary, Department of Earth Sciences.

Black, L. and Gulson, B. (1978). The age of the mud tank carbonatite, strangways range, northern territory. *J. Aust. Geol. Geophys.*, 3:227–232.

Black, L. P., Kamo, S. L., Allen, C. M., Aleinikoff, J. N., Davis, D. W., Korsch, R. J., and Foudoulis, C. (2003). Temora 1: a new zircon standard for phanerozoic u–pb geochronology. *Chemical geology*, 200(1-2):155–170.

Black, L. P., Kamo, S. L., Allen, C. M., Davis, D. W., Aleinikoff, J. N., Valley, J. W., Mundil, R., Campbell, I. H., Korsch, R. J., Williams, I. S., et al. (2004). Improved 206pb/238u microprobe geochronology by the monitoring of a trace-element-related matrix effect; shrimp, id–tims, ela–icp–ms and oxygen isotope documentation for a series of zircon standards. *Chemical Geology*, 205(1-2):115–140.

Blake, D. (1966). The net-veined complex of the austurhorn intrusion, southeastern iceland. *The Journal of Geology*, pages 891–907.

Blake, D. (1970). Geology of alftafjordur volcano, a tertiary volcanic centre in south-eastern iceland. *Scientia Islandica*, 2:43–63.

Bodvarsson, G. (1970). An estimate of the natural heat resources in a thermal area in iceland. *Geothermics*, 2:1289–1293.

Breddam, K. (2002). Kistufell: Primitive melt from the iceland mantle plume. *Journal of Petrology*, 43(2):345–373.

Carmichael, I. S. E. (1964). The petrology of thingmuli, a tertiary volcano in eastern iceland. *Journal of Petrology*, 5(3):435–460.

Charreteur, G. and Tegner, C. (2013). Magmatic emulsion texture formed by mixing during extrusion, rauðafell composite complex, breiðdalur volcano, eastern iceland. *Bulletin of volcanology*, 75(6):1–17.

Charreteur, G., Tegner, C., and Haase, K. (2013). Multiple ways of producing intermediate and silicic rocks within thingmúli and other icelandic volcanoes. *Contributions to Mineralogy and Petrology*, 166(2):471–490.

Chauvel, C. and Hémond, C. (2000). Melting of a complete section of recycled oceanic crust: Trace element and pb isotopic evidence from iceland. *Geochemistry, Geophysics, Geosystems*, 1(2):n/a–n/a.

Clifton, A. E. and Kattenhorn, S. A. (2006). Structural architecture of a highly oblique divergent plate boundary segment. *Tectonophysics*, 419(1-4):27–40.

Clifton, A. E., Pagli, C., Jónsdóttir, J. F., Eythorsdóttir, K., and Vogfjörð, K. (2003). Surface effects of triggered fault slip on reykjanes peninsula, sw iceland. *Tectonophysics*, 369(3-4):145–154.

Cole, J., Milner, D., and Spinks, K. (2005). Calderas and caldera structures: a review. *Earth-Science Reviews*, 69(1):1 – 26.

Condomines, M., Grönvold, K., Hooker, P., Muehlenbachs, K., o'Nions, R., Oskarsson, N., and Oxburgh, E. (1983). Helium, oxygen, strontium and neodymium isotopic relationships in icelandic volcanics. *Earth and Planetary Science Letters*, 66:125–136.

Daly, R. A. (1925). The geology of ascension island. In *Proceedings of the American Academy of Arts and Sciences*, volume 60, pages 3–80. JSTOR.

Darbyshire, F. A., White, R. S., and Priestley, K. F. (2000). Structure of the crust and uppermost mantle of iceland from a combined seismic and gravity study. *Earth and Planetary Science Letters*, 181(3):409–428.

Duncan, R. A. and Helgason, J. (1998). Precise dating of the holmatindur cooling event in eastern iceland: Evidence for mid-miocene bipolar glaciation. *Journal of Geophysical Research: Solid Earth (1978–2012)*, 103(B6):12397–12404.

E. Mussett, A., G. ROSS, J., and L. Gibson, I. (1980). ^{40}ar/^{39}ar dates of eastern iceland lavas. *Geophysical Journal of the Royal Astronomical Society*, 60:37 – 52.

Eason, D. E., Sinton, J. M., Grönvold, K., and Kurz, M. D. (2015). Effects of deglaciation on the petrology and eruptive history of the western volcanic zone, iceland. *Bulletin of Volcanology*, 77(6):47.

Einarsson, P. (1978). S-wave shadows in the krafla caldera in ne-iceland, evidence for a magma chamber in the crust. *Bulletin Volcanologique*, 41(3):187–195.

Einarsson, P. (2008). Plate boundaries, rifts and transforms in iceland. *Jökull*, 58(12):35–58.

Einarsson, P., Björnsson, S., Foulger, G., Stefánsson, R., and Skaftadóttir, T. (1981). Seismicity pattern in the south iceland seismic zone. *Earthquake Prediction: An International Review*, 4:141–151.

Einarsson, P. and Eiríksson, J. (1982). Earthquake fractures in the districts land and rangárvellir in the south iceland seismic zone. *Jökull*, 32:113–120.

Einarsson, P., Hjartardóttir, Á. R., Hreinsdóttir, S., and Imsland, P. (2018). The structure of seismogenic strike-slip faults in the eastern part of the reykjanes peninsula oblique rift, sw iceland. *Journal of Volcanology and Geothermal Research*.

Eriksson, P. I., Riishuus, M. S., Sigmundsson, F., and Elming, S.-A. (2011). Magma flow directions inferred from field evidence and magnetic fabric studies of the streitishvarf composite dike in east iceland. *Journal of Volcanology and Geothermal Research*, 206(1):30–45.

Faulds, J. E., Feuerbach, D. L., Reagan, M. K., Metcalf, R. V., Gans, P., and Walker, J. D. (1995). The mount perkins block, northwestern arizona: An exposed cross section of an evolving, preextensional to synextensional magmatic system. *Journal of Geophysical Research: Solid Earth*, 100(B8):15249–15266.

Fitton, J., Saunders, A., Larsen, L., Hardarson, B., and Norry, M. (1998). Volcanic rocks from the southeast greenland margin at 63°n: composition, petrogenesis, and mantle sources. *In Saunders, A.D., Larsen, H.C., and Wise, S.W., Jr. (Eds.), Proc. ODP, Sci. Results, 152: College Station, TX (Ocean Drilling Program)*, page 331–350.

Fitton, J., Saunders, A., Norry, M., Hardarson, B., and Taylor, R. (1997). Thermal and chemical structure of the iceland plume. *Earth and Planetary Science Letters*, 153(3):197–208.

Fitton, J. G. (2007). The oib paradox. *Geological Society of America Special Papers*, 430:387–412.

Fitton, J. G., Saunders, A. D., Kempton, P. D., and Hardarson, B. S. (2003). Does depleted mantle form an intrinsic part of the iceland plume? *Geochemistry, Geophysics, Geosystems*, 4(3).

Flower, M., Pritchard, R., Brem, G., Cann, J., Delaney, J., Emmerman, R., Gibson, I., Oakley, P., Robinson, P., and Schmincke, H.-U. (1982). Chemical stratigraphy, iceland research drilling project, reydarfjordur, eastern iceland. *Journal of Geophysical Research: Solid Earth*, 87(B8):6489–6510.

Fridleifsson, G. O. (1983). *Geology and the alteration history of the Geitafell central volcano, southeast Iceland.* PhD thesis, Earth Sciences.

Furman, T., Frey, F. A., and Meyer, P. S. (1992a). Petrogenesis of evolved basalts and rhyolites at austurhorn, southeastern iceland: the role of fractional crystallization. *Journal of Petrology*, 33(6):1405–1445.

Furman, T., Meyer, P. S., and Frey, F. (1992b). Evolution of icelandic central volcanoes: evidence from the austurhorn intrusion, southeastern iceland. *Bulletin of volcanology*, 55(1-2):45–62.

Gale, N., Moorbath, S., Simons, J., and Walker, G. (1966). K ar ages of acid intrusive rocks from iceland. *Earth and Planetary Science Letters*, 1(5):284–288.

Gallagher, C. (2013). Álftafjörður dyke swarm, petrology, geochemistry and structure. Thesis, School of Earth Sciences, The University of Edinburgh.

Geirsson, K. (1993). Pétrologie d'une série tholéiitique complete: le volcan central de fagridalur, nord-est de l'islande.

Gibson, I. L. (1963). *The Reydarfjordur acid volcanic centre of Eastern Iceland*. PhD thesis, Imperial College London.

Gústafsson, L. E. (1992). *Geology and petrography of the Dyrfjöll Central Volcano, eastern Iceland*, volume 138. Selbstverlag Fachbereich Geowissenschaften, FU Berlin.

Gualda, G. A., Ghiorso, M. S., Lemons, R. V., and Carley, T. L. (2012). Rhyolite-melts: a modified calibration of melts optimized for silica-rich, fluid-bearing magmatic systems. *Journal of Petrology*, 53(5):875–890.

Gudmundsson, A. (1995). Ocean-ridge discontinuities in iceland. *Journal of the Geological Society*, 152(6):1011–1015.

Gudmundsson, A. (2000). Dynamics of volcanic systems in iceland: Example of tectonism and volcanism at juxtaposed hot spot and mid-ocean ridge systems. *Annual Review of Earth and Planetary Sciences*, 28(1):107–140.

Gudmundsson, A. (2002). Emplacement and arrest of sheets and dykes in central volcanoes. *Journal of Volcanology and Geothermal Research*, 116(3):279–298.

Gunnarsson, B., Marsh, B. D., and Taylor Jr, H. P. (1998). Generation of icelandic rhyolites: silicic lavas from the torfajökull central volcano. *Journal of Volcanology and Geothermal Research*, 83(1-2):1–45.

Gústafsson, L. E., Lapp, B., Thomas, L., and Lapp, M. (1989). Tertiary silicic rocks in the area of the kaekjuskörð rhyolitic volcano, eastern iceland. *Jökull*, 39:75–89.

Halldorsson, S. A., Oskarsson, N., Gronvold, K., Sigurdsson, G., Sverrisdottir, G., and Steinthorsson, S. (2008). Isotopic-heterogeneity of the thjorsa lava—implications for mantle sources and crustal processes within the eastern rift zone, iceland. *Chemical Geology*, 255(3):305–316.

Halpin, J. A., Jensen, T., McGoldrick, P., Meffre, S., Berry, R. F., Everard, J. L., Calver, C. R., Thompson, J., Goemann, K., and Whittaker, J. M. (2014). Authigenic monazite and detrital zircon dating from the proterozoic rocky cape group, tasmania: Links to the belt-purcell supergroup, north america. *Precambrian Research*, 250:50–67.

Hanan, B. B. and Schilling, J.-G. (1997). The dynamic evolution of the iceland mantle plume: the lead isotope perspective. *Earth and Planetary Science Letters*, 151(1):43 – 60.

Harðarson, B. (1994). Geochemical variation in the tertiary basalts of iceland. *Mineralogical Magazine*, 58:372–373.

Harðarson, B. S. (1993). *Alkalic rocks in Iceland with special reference to the Snaefellsjökull volcanic system*. University of Edinburgh.

Harðarson, B. S., Fitton, J. G., and Hjartarson, Á. (2008). Tertiary volcanism in iceland. *Jökull*, 58:161–178.

Hardarson, B., Fitton, J., Ellam, R., and Pringle, M. (1997). Rift relocation—a geochemical and geochronological investigation of a palaeo-rift in northwest iceland. *Earth and Planetary Science Letters*, 153(3-4):181–196.

Hardarson, B. S. and Fitton, J. G. (1997). Mechanisms of crustal accretion in iceland. *Geology*, 25(11):1043–1046.

Hards, V. L., Kempton, P., Thompson, R., and Greenwood, P. (2000). The magmatic evolution of the snaefell volcanic centre; an example of volcanism during incipient rifting in iceland. *Journal of Volcanology and Geothermal Research*, 99(1-4):97–121.

Hartley, M. and Thordarson, T. (2012). Formation of öskjuvatn caldera at askja, north iceland: Mechanism of caldera collapse and implications for the lateral flow hypothesis. *Journal of Volcanology and Geothermal Research*, 227:85–101.

Hartley, M. E. and Thordarson, T. (2013). The 1874–1876 volcano-tectonic episode at askja, north iceland: Lateral flow revisited. *Geochemistry, Geophysics, Geosystems*, 14(7):2286–2309.

Helgason, J. (1982). Magnetostratigrahy of the exposed lava section east of the irdp drill hole in reydarfjordur, eastern iceland. *Journal of Geophysical Research: Solid Earth*, 87(B8):6396–6404.

Helgason, J. (1983). *Structural relationships and magnetostratigraphy of the volcanic succession and the Breiddalur dyke swarm in Reydarfjordur, eastern Iceland*. Dalhousie University.

Helgason, J. (1984). Frequent shifts of the volcanic zone in iceland. *Geology*, 12(4):212–216.

Helgason, J. (1985). Shifts of the plate boundary in iceland: some aspects of tertiary volcanism. *Journal of Geophysical Research: Solid Earth (1978–2012)*, 90(B12):10084–10092.

Helgason, J. and Duncan, R. A. (2014). Magnetostratigraphy, k-ar dating and erosion history of the hafrafell volcanics, se–iceland. *JOKULL*, 64:41–60.

Helgason, J. and Zentilli, M. (1985). Field characteristics of laterally emplaced dikes: Anatomy of an exhumed miocene dike swarm in reydarfjördur, eastern iceland. *Tectonophysics*, 115(3):247–274.

Hjartardóttir, Á. R., Einarsson, P., and Björgvinsdóttir, S. G. (2016). Fissure swarms and fracture systems within the western volcanic zone, iceland – effects of spreading rates. *Journal of Structural Geology*, 91:39 – 53.

Hjartardóttir, Á. R., Einarsson, P., and Sigurdsson, H. (2009). The fissure swarm of the askja volcanic system along the divergent plate boundary of n iceland. *Bulletin of Volcanology*, 71(9):961.

Jakobsson, S. (1974). *Eldgos við Eldeyjarboða*. Museum of Natural History, Department of Geology and Geography.

Jakobsson, S. P. (1979a). *Outline of the Petrology of Iceland*. Museum of Natural History, Department of Geology and Geography.

Jakobsson, S. P. (1979b). Petrology of recent basalts of the eastern volcanic zone, iceland. *Acta Naturalia Islandica*.

Jakobsson, S. P., Jónasson, K., and Sigurdsson, I. A. (2008). The three igneous rock series of iceland. *Jökull*, 58:117–138.

Jakobsson, S. P., Jónsson, J., and Shido, F. (1978). Petrology of the western reykjanes peninsula, iceland. *Journal of Petrology*, 19(4):669–705.

Jóhannesson, H. (1980). Jardlagaskipun og thróun rekbelta á vesturlandi (english summary: Evolution of rift zones in western iceland). *Náttúrufrædingurinn*, 50:13–31.

Jóhannesson, H. (2nd edition 2014). Geological map of iceland. bedrock geology. 1:600,000.

Jóhannesson, H. and Sæmundsson, K. (1998, revised 2009). Geological map of iceland. 1: 600,000. tectonics. *Icelandic Institute of Natural History*.

Kempton, P., Fitton, J., Saunders, A., Nowell, G., Taylor, R., Hardarson, B., and Pearson, G. (2000). The iceland plume in space and time: a sr–nd–pb–hf study of the north atlantic rifted margin. *Earth and Planetary Science Letters*, 177(3-4):255–271.

Kerr, A. C., Kent, R. W., Thomson, B. A., Seedhouse, J. K., and Donaldson, C. H. (1999). Geochemical evolution of the tertiary mull volcano, western scotland. *Journal of Petrology*, 40(6):873–908.

Kitagawa, H. (2006). *Petrological and geochemical study of the Icelandic Tertiary lavas: Implications for the evolution of Iceland mantle plume*. PhD thesis, Department of Earth and Planetary Sciences.

Kitagawa, H., Kobayashi, K., Makishima, A., and Nakamura, E. (2008). Multiple pulses of the mantle plume: evidence from tertiary icelandic lavas. *Journal of Petrology*, 49(7):1365–1396.

Kokfelt, T. F., Hoernle, K., Hauff, F., Fiebig, J., Werner, R., and Garbe-Schoenberg, D. (2006). Combined trace element and pb-nd–sr-o isotope evidence for recycled oceanic crust (upper and lower) in the iceland mantle plume. *Journal of Petrology*, 47(9):1705–1749.

Kosler, J. (2001). Laser-ablation icpms study of metamorphic minerals and processes. *Laser-ablation-ICPMS in the Earth Sciences; Principles and Applications Mineralogical Association of Canada Short Course Handbook*, 29:185–202.

Kuritani, T. and Nakamura, E. (2002). Precise isotope analysis of nanogram-level pb for natural rock samples without use of double spikes. *Chemical Geology*, 186(1):31 – 43.

Kuritani, T., Yokoyama, T., Kitagawa, H., Kobayashi, K., and Nakamura, E. (2011). Geochemical evolution of historical lavas from askja volcano, iceland: implications for mechanisms and timescales of magmatic differentiation. *Geochimica et Cosmochimica Acta*, 75(2):570–587.

Kurz, M. D., Meyer, P. S., and Sigurdsson, H. (1985). Helium isotopic systematics within the neovolcanic zones of iceland. *Earth and Planetary Science Letters*, 74(4):291–305.

LaFemina, P. C., Dixon, T. H., Malservisi, R., Árnadóttir, T., Sturkell, E., Sigmundsson, F., and Einarsson, P. (2005). Geodetic gps measurements in south iceland: Strain accumulation and partitioning in a propagating ridge system. *Journal of Geophysical Research: Solid Earth*, 110(B11).

Le Bas, M., Le Maitre, R., Streckeisen, A., Zanettin, B., and Rocks, I. S. o. t. S. o. I. (1986). A chemical classification of volcanic rocks based on the total alkali-silica diagram. *Journal of petrology*, 27(3):745–750.

Le Bas, M. J. (1966). On the origin of the tertiary granophyres of the carlingford complex, ireland. In *Proceedings of the Royal Irish Academy. Section B: Biological, Geological, and Chemical Science*, pages 325–338. JSTOR.

Loughlin, S. C. (1995). *The evolution of the Eyjafjoll volcanic system, southern Iceland.* PhD thesis, Durham University.

Lu, Y., Makishima, A., and Nakamura, E. (2007). Purification of hf in silicate materials using extraction chromatographic resin, and its application to precise determination of 176hf/ 177hf by mc-icp-ms with 179hf spike. *Journal of Analytical Atomic Spectrometry*, 22(1):69–76.

MacDonald, R., McGarvie, D., Pinkerton, H., Smith, R., and Palacz, A. (1990). Petrogenetic evolution of the torfajökull volcanic complex, iceland i. relationship between the magma types. *Journal of Petrology*, 31(2):429–459.

Maclennan, J. (2008). Lead isotope variability in olivine-hosted melt inclusions from iceland. *Geochimica et Cosmochimica Acta*, 72(16):4159–4176.

Maclennan, J., Mkenzie, D., Gronvöld, K., and Slater, L. (2001). Crustal accretion under northern iceland. *Earth and Planetary Science Letters*, 191(3–4):295–310.

Manning, C. J. and Thirlwall, M. F. (2014). Isotopic evidence for interaction between öræfajökull mantle and the eastern rift zone, iceland. *Contributions to Mineralogy and Petrology*, 167(1):959.

Martin, E., Paquette, J. L., Bosse, V., Ruffet, G., Tiepolo, M., and Sigmarsson, O. (2011). Geodynamics of rift–plume interaction in iceland as constrained by new 40ar/39ar and in situ u–pb zircon ages. *Earth and Planetary Science Letters*, 311(1):28–38.

Martin, E. and Sigmarsson, O. (2007). Crustal thermal state and origin of silicic magma in iceland: the case of torfajökull, ljósufjöll and snæfellsjökull volcanoes. *Contributions to Mineralogy and Petrology*, 153(5):593–605.

Martin, E. and Sigmarsson, O. (2010). Thirteen million years of silicic magma production in iceland: links between petrogenesis and tectonic settings. *Lithos*, 116(1):129–144.

Mattson, S. R., Vogel, T. A., and Wilband, J. T. (1986). Petrochemistry of the silicic-mafic complexes at vesturhorn and austurhorn, iceland: evidence for zoned/stratified magma. *Journal of Volcanology and Geothermal Research*, 28(3–4):197–223.

McDougall, I., Watkins, N. D., and Kristjansson, L. (1976a). Geochronology and paleomagnetism of a miocene-pliocene lava sequence at bessastadaa, eastern iceland. *American Journal of Science*, 276(9):1078–1095.

McDougall, I., Watkins, N. D., Walker, G. P. L., and Kristjansson, L. (1976b). Potassium-argon and paleomagnetic analysis of icelandic lava flows: Limits on the age of anomaly 5. *Journal of Geophysical Research (1896-1977)*, 81(8):1505–1512.

Meade, F., Troll, V., Ellam, R., Freda, C., Font, L., Donaldson, C., and Klonowska, I. (2014). Bimodal magmatism produced by progressively inhibited crustal assimilation. *Nature communications*, 5:4199.

Meyer, R., Nicoll, G. R., Hertogen, J., Troll, V. R., Ellam, R. M., and Emeleus, C. H. (2009). Trace element and isotope constraints on crustal anatexis by upwelling mantle melts in the north atlantic igneous province: an example from the isle of rum, nw scotland. *Geological Magazine*, 146(3):382–399.

Morgan, W. J. (1971). Convection plumes in the lower mantle. *Nature*, 230(5288):42.

Nichols, A., Carroll, M., and Höskuldsson, A. (2002). Is the iceland hot spot also wet? evidence from the water contents of undegassed submarine and subglacial pillow basalts. *Earth and Planetary Science Letters*, 202(1):77–87.

Nicholson, H., Condomines, M., Fitton, J. G., Fallick, A. E., Gronvold, K., and Rogers, G. (1991). Geochemical and isotopic evidence for crustal assimilation beneath krafla, iceland. *Journal of Petrology*, 32(5):1005–1020.

O'Driscoll, B. (2006). Magmatic layering and magnetic fabrics in the palaeogene carlingford later gabbros, co. louth, ireland. *Irish Journal of Earth Sciences*, 24:37.

O'Nions, R., Hamilton, P., and Evensen, N. (1977). Variations in143nd/144nd and87sr/86sr ratios in oceanic basalts. *Earth and Planetary Science Letters*, 34(1):13–22.

O'nions, R. and Pankhurst, R. (1973). Secular variation in the sr-isotope composition of icelandic volcanic rocks. *Earth and Planetary Science Letters*, 21(1):13–21.

Óskarsson, B. V. (2015). *Volcanological studies of Neogene flood basalt groups in eastern Iceland.* Thesis, Department of Earth Sciences.

Óskarsson, B. V., Andersen, C. B., Riishuus, M. S., Sorensen, E. V., and Tegner, C. (2017). The mode of emplacement of neogene flood basalts in eastern iceland: The plagioclase ultraphyric basalts in the grænavatn group. *Journal of Volcanology and Geothermal Research*, 332:26–50.

Óskarsson, B. V. and Riishuus, M. S. (2013). The mode of emplacement of neogene flood basalts in eastern iceland: Facies architecture and structure of the hólmar and grjótá olivine basalt groups. *Journal of Volcanology and Geothermal Research*, 267:92–118.

Oskarsson, N., E. Sigvaldason, G., and Steinþórsson, S. (1982). A dynamic model of rift zone petrogenesis and the regional petrology of iceland. *Journal of Petrology*, 23.

Oskarsson, N., Steinthorsson, S., and Sigvaldason, G. (1985). Iceland geochemical anomaly: origin, volcanotectonics, chemical fractionation and isotope evolution of the crust. *Journal of Geophysical Research: Solid Earth*, 90(B12):10011–10025.

Padilla, A., Miller, C., Carley, T., Economos, R., Schmitt, A., Coble, M., Wooden, J., Fisher, C., Vervoort, J., and Hanchar, J. (2016). Elucidating the magmatic history of the austurhorn silicic intrusive complex (southeast iceland) using zircon elemental and isotopic geochemistry and geochronology. *Contributions to Mineralogy and Petrology*, 171(8-9):69.

Pálmason, G. and Sæmundsson, K. (1974). Iceland in relation to the mid-atlantic ridge. *Annual review of earth and planetary sciences*, 2:25.

Paton, C., Woodhead, J. D., Hellstrom, J. C., Hergt, J. M., Greig, A., and Maas, R. (2010). Improved laser ablation u-pb zircon geochronology through robust downhole fractionation correction. *Geochemistry, Geophysics, Geosystems*, 11(3).

Pearce, J. A. (1996). A user's guide to basalt discrimination diagrams. *Trace element geochemistry of volcanic rocks: applications for massive sulphide exploration. Geological Association of Canada, Short Course Notes*, 12:79–113.

Peate, D. W., Breddam, K., Baker, J. A., Kurz, M. D., Barker, A. K., Prestvik, T., Grassineau, N., and Skovgaard, A. C. (2010). Compositional characteristics and spatial distribution of enriched icelandic mantle components. *Journal of Petrology*, 51(7):1447–1475.

Prestvik, T. (1979). *Geology of the Oraefi district, southeastern Iceland.* University of Iceland.

Prestvik, T. (1985). *Petrology of Quaternary Volcanic Rocks from Örœfi, Southeast Iceland.* University of Trondheim, the Norwegian Institute of Technology.

Prestvik, T., Goldberg, S., Karlsson, H., and Grönvold, K. (2001). Anomalous strontium and lead isotope signatures in the off-rift Öræfajökull central volcano in south-east iceland: Evidence for enriched endmember(s) of the iceland mantle plume? *Earth and Planetary Science Letters*, 190(3):211 – 220.

Riishuus, M., Miggins, D., Koppers, A., and Duncan, R. (2010). 40ar/39ar incremental heating experiments on celadonite from the skessa tuff, eastern iceland: Thermochronology of low-temperature alteration of a flood basalt pile during burial metamorphism. In *AGU Fall Meeting Abstracts*, volume 1, page 4873.

Ross, J. and Mussett, A. (1976). 40ar/39ar dates for spreading rates in eastern iceland. *Nature*, 259(5538):36.

Sæmundsson, K. (1974). Evolution of the axial rifting zone in northern iceland and the tjornes fracture zone. *Geological Society of America Bulletin*, 85(4):495–504.

Saemundsson, K. (1978). Fissure swarms and central volcanoes of the neovolcanic zones of iceland. *Geol. J. Spec*, 10:415–432.

Saemundsson, K. (1979). Outline of the geology of iceland. *Jökull*, 29:7–28.

Sæmundsson, K. (1991). Jardfrædi kröflukerfisins. *Náttúra Myvatns. Hid íslenska Náttúrufrædifélag, Reykjavík*, pages 24–95.

Saemundsson, K. and Jóhannesson, H. (1994). Jarðlög upp af síðu og fljótshverfi, aldur og myndunarsaga (build up and age of the rock sequence of the síða-fljótshverfi highland). *Geoscience Society of Iceland Spring Meeting*.

Saunders, A., Fitton, J., Kerr, A. C., Norry, M., and Kent, R. (1997). The north atlantic igneous province. *Geophysical Monograph-American Geophysical Union*, 100:45–94.

Schilling, J., Meyer, P., and Kingsley, R. (1983). Rare earth geochemistry of iceland basalts: spatial and temporal variations. In *Structure and Development of the Greenland-Scotland Ridge*, pages 319–342. Springer.

Schilling, J.-G. (1973). Iceland mantle plume: geochemical study of reykjanes ridge. *Nature*, 242:565–571.

Schnell, T. (1994). *Breiðdalur central volcano, eastern Iceland: genesis of the evolved rocks*. Thesis, Department of Earth Sciences.

Shorttle, O. and Maclennan, J. (2011). Compositional trends of icelandic basalts: Implications for short–length scale lithological heterogeneity in mantle plumes. *Geochemistry, Geophysics, Geosystems*, 12(11):n/a–n/a.

Shorttle, O., Maclennan, J., and Lambart, S. (2014). Quantifying lithological variability in the mantle. *Earth and Planetary Science Letters*, 395:24–40.

Shorttle, O., Maclennan, J., and Piotrowski, A. M. (2013). Geochemical provincialism in the iceland plume. *Geochimica et Cosmochimica Acta*, 122:363–397.

Sigmarsson, O. and Halldórsson, S. A. (2015). Delimiting bárðarbunga and askja volcanic systems with sr-and nd-isotope ratios. *Jökull*, 65:17–27.

Sigmarsson, O., Hémond, C., Condomines, M., Fourcade, S., and Oskarsson, N. (1991). Origin of silicic magma in iceland revealed by th isotopes. *Geology*, 19(6):621–624.

Sigmarsson, O., Maclennan, J., and Carpentier, M. (2008). Geochemistry of igneous rocks in iceland: a review. *Jökull*, 58:139–160.

Sigvaldason, G. E. (1974). Basalts from the centre of the assumed icelandic mantle plume. *Journal of Petrology*, 15(3):497–524.

Sinton, J., Grönvold, K., and Sæmundsson, K. (2005). Postglacial eruptive history of the western volcanic zone, iceland. *Geochemistry, Geophysics, Geosystems*, 6(12).

Sláma, J., Košler, J., Condon, D. J., Crowley, J. L., Gerdes, A., Hanchar, J. M., Horstwood, M. S., Morris, G. A., Nasdala, L., Norberg, N., et al. (2008). Plešovice zircon—a new natural reference material for u–pb and hf isotopic microanalysis. *Chemical Geology*, 249(1-2):1–35.

Spice, H. E., Fitton, J. G., and Kirstein, L. A. (2016). Temperature fluctuation of the iceland mantle plume through time. *Geochemistry, Geophysics, Geosystems*, 17(2):243–254.

Stefánsson, R., Böđvarsson, R., Slunga, R., Einarsson, P., Jakobsdóttir, S., Bungum, H., Gregersen, S., Havskov, J., Hjelme, J., and Korhonen, H. (1993). Earthquake prediction research in the south iceland seismic zone and the sil project. *Bulletin of the Seismological Society of America*, 83(3):696–716.

Steinþórsson, S. (1981). Ísland og flekakenningin. *Náttúra Íslands (2nd ed., pp. 29–63). Reykjavík: Almenna bókafélagið.*

Sun, S.-S. and Jahn, B.-m. (1975). Lead and strontium isotopes in post-glacial basalts from iceland. *Nature*, 255(5509):527.

Takei, H., Yokoyama, T., Makishima, A., and Nakamura, E. (2001). Formation and suppression of alf₃ during hf digestion of rock samples in teflon bomb for precise trace element analyses by icp-ms and id-tims. *Proceedings of the Japan Academy, Series B*, 77(1):13–17.

Thirlwall, M. (1995). Generation of the pb isotopic characteristics of the iceland plume. *Journal of the Geological Society*, 152(6):991–996.

Thirlwall, M., Gee, M., Taylor, R., and Murton, B. (2004). Mantle components in iceland and adjacent ridges investigated using double-spike pb isotope ratios. *Geochimica et Cosmochimica Acta*, 68(2):361–386.

Thorarinsson, S. (1958). The oraefajôkull eruption of 1362: Acta naturalia islandica, v.

Thorarinsson, S., Sæmundsson, K., and Williams, R. S. (1973). Erts-1 image of vatnajökull: analysis of glaciological, structural, and volcanic features. *Jökull*.

Thorarinsson, S. B. and Tegner, C. (2009). Magma chamber processes in central volcanic systems of iceland: constraints from layered gabbro of the austurhorn intrusive complex. *Contributions to Mineralogy and Petrology*, 158(2):223–244.

Thordarson, T. and Höskuldsson, A. (2008). Postglacial volcanism in iceland. *Jökull*, 58(198):e228.

Thordarson, T. and Larsen, G. (2007). Volcanism in iceland in historical time: Volcano types, eruption styles and eruptive history. *Journal of Geodynamics*, 43(1):118–152.

Thoroddsen, T. (1901). *Das Erdbeben in Island im Jahre 1896*. N/A.

Torsvik, T., Amundsen, H., Trønnes, R., Doubrovine, P., Gaina, C., Kusznir, N., Steinberger, B., Corfu, F., Ashwal, L., Griffin, W., Werner, S., and Jamtveit, B. (2015). Continental crust beneath southeast iceland. *Proceedings of the National Academy of Sciences of the United States of America*, 112(15):E1818–E1827.

Urbani, S., Trippanera, D., Porreca, M., Kissel, C., and Acocella, V. (2015). Anatomy of an extinct magmatic system along a divergent plate boundary: Alftafjordur, iceland. *Geophysical Research Letters*, 42(15):6306–6313.

Vink, G. E. (1984). A hotspot model for iceland and the vøring plateau. *Journal of Geophysical Research: Solid Earth (1978–2012)*, 89(B12):9949–9959.

Walker, G. P. (1958). Geology of the reydarfjördur area, eastern iceland. *Quarterly Journal of the Geological Society*, 114(1-4):367–391.

Walker, G. P. (1960). Zeolite zones and dike distribution in relation to the structure of the basalts of eastern iceland. *The Journal of Geology*, 68(5):515–528.

Walker, G. P. (1963). The breiddalur central volcano, eastern iceland. *Quarterly Journal of the Geological Society*, 119(1-4):29–63.

Walker, G. P. (1964). Geological investigations in eastern iceland. *Bulletin Volcanologique*, 27(1):351–363.

Walker, G. P. (1975). Excess spreading axes and spreading rate in iceland. *Nature*, 255(5508):468.

Walker, G. P. L. (1974). The structure of eastern iceland. In Kristjansson, L., editor, *Geodynamics of Iceland and the North Atlantic Area*, pages 177–188, Dordrecht. Springer Netherlands.

Ward, P. L. (1971). New interpretation of the geology of iceland. *Geological Society of America Bulletin*, 82(11):2991–3012.

Watkins, N. and Walker, G. (1977). Magnetostratigraphy of eastern iceland. *American Journal of Science*, 277(5):513–584.

Welke, H., Moorbath, S., Cumming, G., and Sigurdsson, H. (1968). Lead isotope studies on igneous rocks from iceland. *Earth and Planetary Science Letters*, 4(3):221–231.

Wiedenbeck, M., Alle, P., Corfu, F., Griffin, W., Meier, M., Oberli, F., Quadt, A. v., Roddick, J., and Spiegel, W. (1995). Three natural zircon standards for u-th-pb, lu-hf, trace element and ree analyses. *Geostandards newsletter*, 19(1):1–23.

Winchester, J. A. and Floyd, P. A. (1977). Geochemical discrimination of different magma series and their differentiation products using immobile elements. *Chemical geology*, 20:325–343.

Wolfe, C. J., Bjarnason, I. T., VanDecar, J. C., and Solomon, S. C. (1997). Seismic structure of the iceland mantle plume. *Nature*, 385(6613):245.

Wood, D. A. (1978). Major and trace element variations in the tertiary lavas of eastern iceland and their significance with respect to the iceland geochemical anomaly. *Journal of Petrology*, 19(3):393–436.

Yokoyama, T., Makishima, A., and Nakamura, E. (1999). Evaluation of the coprecipitation of incompatible trace elements with fluoride during silicate rock dissolution by acid digestion. *Chemical Geology*, 157(3):175 – 187.

Yoshikawa, M. and Nakamura, E. (1993). Precise isotope determination of trace amounts of sr in magnesium-rich samples. *Journal of Mineralogy, Petrology and Economic Geology*, 88(12):548–561.

Appendix A

Manuscripts

A.1 Paper 1: Geological Mapping of Breiðdalur volcano

Geological Mapping of Breiðdalur Volcano

Robert A. Askew*[1], Thorvaldur Thordarson[1] and Ármann Höskuldsson[1]

[1]Institute of Earth Sciences, University of Iceland, Sturlugata 7, 101, Reykjavik
*corresponding email: robert@ni.is

Abstract

Geological mapping is an important tool in understanding volcanic structures and hazards. Here we present the geological map and volcanic structure of Breiðdalur volcano in eastern Iceland. Breiðdalur is a caldera central volcano, consisting of mafic to intermediate flank sequences, a 10–12 km wide caldera with 10–15 km^3 of pumice breccia infill and silicic summit lavas erupted during late stage activity. This paper compiles and updates previous geological mapping in the area more in line with modern understanding of volcanic systems in Iceland and presents a 1:40,000 geological map of the volcano. The volcano is predominantly tholeiitic basalt and around 25 % of the mapped area consists of more evolved rocks. The flanks of the volcano consist of 4 sub-units, lower mafic lavas, eastern flank icelandite lavas, eastern flank upper lavas and north eastern flank lavas. Silicic rocks are concentrated in the later stages of the volcano's life, both within the caldera complex—delineated by an inferred caldera fault—and the South-Eastern Rhyolites erupted onto the flanks of the volcano. The volcano is enveloped by mafic plateau basalts sourced from surrounding fissure systems including Breiðdalur's own system. A dyke swarm cross cuts much of the area and is related to the Breiðdalur volcanic system.

1 Introduction

Breiðdalur volcanic system, located in eastern Iceland (Figure 1), comprises a caldera volcano and extensive fissure swarm residing within a glacially incised fjord landscape (Figure 2). Rhyolitic peaks of Berufjörður are the most obvious indication of the presence of an area of evolved magmatism, termed a central volcano. Geological mapping of the lava sequences in the area shows a transition from the basaltic plateau lava stratigraphy, seen across much of eastern Ice- land, to more evolved volcanic sequences (Óskarsson, 2015; Walker, 1963). The volcanic system itself spans 350 km^2 of land, but the main edifice is more localised (throughout Berufjörður and the Breiðdalur) covering approximately 40 km^2 and comprises an approximately 10 km wide caldera. The total volume of the volcano is estimated at around 400 km^3, with around 80-85% of this volume being mafic lavas. Activity has been characterised by both abundant explosive and effusive, mafic to silicic volcanism, in addition to significant paleo-geothermal activity. The sequence has been subject to secondary, low-grade zeolite metamorphism, which occurred during burial, the highest peaks have been subjected to the

*Present address: Icelandic Institute of Natural Sciences, Urriðaholtsstræti 6-8, 210 Garðabær, Iceland

lowest grade, or no, regional zeolite alteration (Walker, 1960). The zeolite alteration probably occurred at least 1 My post-emplacement (Riishuus et al., 2010).

Breiðdalur volcanic system contains a central volcano and a dyke swarm, the dyke swarm trends NNE—SSW from the southwest of Berufjörður up to Reyðarfjörður further north (Figure 1). The two highest density areas are in Norðurdalur and Berufjörður (Öxi) (see main geological map for location names). There is a low density of regional (>1 km long, north—south) dykes in the Breiðdalur caldera. The area displays a high number of localised intrusions, but these are probably related to smaller scale central volcano magmatism rather than the regional rifting regime. Dykes that do cross the caldera are thick (>1 m) and long (>5 km) basaltic intrusions which are clearly much younger than the volcano and, in some cases, even younger than the lavas covering the volcano.

The discovery of the Breiðdalur central volcano, and the presence of central volcanoes in eastern Iceland, is attributed to the work of George Walker in the 1960's, with a seminal paper (Walker, 1963) describing and mapping out Breiðdalur volcano. The volcano is well exposed across much of the landscape and is consequently easily accessible by main roads and tracks. Hence, it provides a perfect natural laboratory for the study of volcanological and magmatic processes in Iceland. This paper presents an updated geological map of Breiðdalur and a description of the volcano and its units as well as a new evaluation on what they reveal about the sequence events key volcanological events during its construction. As such this paper forms the foundation of additional research into the evolution of Breiðdalur volcano through geochronology and geochemistry.

The east fjords of Iceland are mountainous, with peaks up to 1200 m and deeply incised fjords (Figure 2). Exposures are often good, though valleys are filled with alluvium and steep mountainsides are often littered with landslide debris. The map area consists of the main valley of Breiðdalur, split into 2 valleys to the west, Norður- and Suður-dalur, Berufjörður fjord is located south of this valley. The map accompanying this manuscript is available as Supplementary Material.

2 Field mapping and map production

The geological mapping of Breiðdalur presented here, builds upon the previous work of Walker (1963). The lowest stratigraphic unit on the map is marked as the Skessa Tuff; any units below this are outside the mapping area and therefore not included. The upper delineation of the mapping area is the same as chosen by Walker (1963): representing a clear discontinuity in Berufjörður and Breiðdalur (see text below for further details).

Key map units were defined through petrology, geochemistry, facies, or simple grouping of lavas. However, differentiation of flank lavas and fissure swarm lavas was sometimes challenging because of extensive erosion, weathering or petrological similarity. In the field, a similar method of identify lavas was used as to Walker (1964), but the terminology used differs, e.g.: Tholeiite was a term used by Walker for fine grained apyhric basalts, but here the term is used purely

Name	Field description	Petrology
Tholeiitic basalt	Grey to black, very fine to fine grained, usually aphyric (<5%).	*Groundmass*: Plagioclase, Clinopyroxene, Magnetite/Ilmenite usually no olivine
Olivine basalt	Dark grey to black with rounded weathered surface, usually medium to coarse grained, olivine may be visible. May or may not contain phenocrysts.	*Groundmass*: Plagioclase, clinopyroxene, oxides, +/- olivine *Phenocrysts*: +/-olivine, clinopyroxene, plagioclase
Porphyrytic basalt	Grey to black weathering, fine to coarse grained, >20% plagioclase phenocrysts	*Groundmass*: plagioclase, clinopyroxene, oxides *Phenocrysts*: plagioclase, clinopyroxene (often seen together as rounded glomerocrysts)

Table 1: Field descriptions and typical petrology of the main types of basaltic rocks differentiated in the field.

geo-petrologically (basalts that falls on the tholeiitic magma suite, as defined by Jakobsson et al. (1979) or Jakobsson et al. (2008)), depending whether the latter provides a full definition of the tholeiite magma suite). Other lavas may be distinguished if they contained a significant number of phenocrysts or contained the mineral olivine (termed 'Olivine Basalts' by Walker (1964); Table 1). Groups, are here defined as a sequence of petrologically similar lavas that are distinct from the lavas below and above the sequence. Groups can include lavas separated by sedimentary interbeds, hence can be made up of products of a single eruption (no interbeds) or multiple events (contains interbeds). One such example is the Flaga group, a group of pāhoehoe lavas with no visible soil or sediment horizon between each lobe or flow.

The map is broadly broken up into: the flank sequence, caldera sequence (Core Group Walker (1963)), and summit sequence. The South Eastern Rhyolites (SER), Schnell (1994), or the 'flank rhyolites', Walker (1963). Since the SER is more descriptive of position, we elected to use it here and describe it closely with the Summit sequence lavas. The flank sequence itself is broken up into 4 units, described in detail below. The sequences are described roughly in their age relation: flank units being the earliest and summit sequences being the latest. Intrusions are described within relevant sections.

Contacts between units are generally well exposed and easy to trace even on aerial imagery. Contacts between rock units are denoted as a single line, mainly for clarity on the map, but also because exposures are very good and only a few places are inferred across, these are mainly within the caldera and summit sequence where large land movement debris fields and alluvium cover significant amounts of the land. Nonetheless, no distinction is made on the map. Contacts, where they were not traced in the field, were traced on aerial imagery and using the older geological map.

3 Map Units

3.1 Basement

Much of the Miocene stratigraphy in Iceland is characterised by layers of regional scale plateau lava succession which provided the basement upon which Breiðdalur succession was emplaced. These lavas are most commonly tholeiitic in nature although mildly alkaline lavas are present as a minor component. The most common basalt lava is uniformly fine grained and aphyric, and typically make up over 80% of the lava sequence. However, regional groups (as defined by Walker (1964)) that differ from the "norm", such as porphyritic or olivine-bearing basalts (Table 1), along with widespread ignimbrites are used as marker horizons for correlation and mapping the flood lava sequence in the east fjords. The oldest marker horizon of concern is the at 10.2 (±0.2) Ma, Skessa Tuff, which is a silicic ignimbrite and tuff horizon whose origin has been associated with the Breiðdalur central volcano (Walker, 1962, 1963; Riishuus et al., 2010). The Grænavatn Porphyrytic Group (GPG), sitting just above the Skessa Tuff, is a conspicuous formation due to its high concentration of rounded plagioclase macrocrysts (Gibson et al., 1966; Helgason, 1982; Walker, 1958). This thick sequence of lavas was defined by Walker (1963) as the basement to the Breiðdalur central volcano, the suggestion being, that the Skessa Tuff was an eruption from an early Breiðdalur volcano and Grænavatn was erupted just above this, before mafic lavas forming the early volcano edifice erupted onto this basement. The GPG does not represent an early eruption from the central volcano as the morphology of the flows does not fit the type of eruptions that occur from a central volcano, rather the morphology is typical of plateau or flood basalt volcanism occurring along a fissure swarm. The high density of plagioclase phenocrysts are entrained from a magma reservoir located beneath a fissure segment to the north west of the Breiðdalur system (Óskarsson, 2015).

3.2 Early Breiðdalur: Flank Sequences

The base of the Breiðdalur central volcano is marked as a distinct shift from thick (5—20 m), grey, plateau basalts (e.g. the pāhoehoe of the GPG) to thin (<5 m), to a sequence of black a'a lavas (Figure 3), inferred from dated lavas above and below to be emplaced around 10 (±0.2) Ma (inferred date). Due to the westward dip of the lava pile in eastern Iceland, and the east-west valley morphology, only the eastern flanks of Breiðdalur are well exposed. It can be assumed that the volcano was roughly symmetrical, since the Neogene Icelandic topography was relatively low relief and any topography was normally caused by volcanism or rifting. The flank sequences are mapped, for the most part, as a single undifferentiated unit, similar to the mapping by Walker (1963). It is broken up into 4 separate sub-units to aid description:

- B_1: The oldest eastern flank lavas mapped as the entire basal structure that is exposed above the GPG and below the Flaga andesite group (B_2) or where B_2 does not extend to lavas co-eval with it (B_{ne})
- B_2: the eastern flank Flaga Icelandite lavas.
- B_3: the eastern flank youngest lavas, mapped above B_2.
- B_{ne}: the north eastern flank mafic to intermediate lavas, approximately co-eval to B_2 – B_3 but does not contain a conspicuous group of icelandite lavas.

The entire eastern flank sequence is up to 1000 m metres thick close to the head of the volcano, comprised of lavas ranging from mafic to intermediate in composition. The top of the flank sequence is essentially denoted as the lavas below the SER of Röndulfur, Smátindur, Slöttur and Stöng, though lavas are inferred to be above these.

Most of the B_1 sequence is comprised of a'a lavas and their thickness (<5 m) is relatively consistent throughout, above which is B_2, the Flaga icelandite lavas which are on the order of 15 – 30 m thick. The group is around 400 m thick in total. The final sequence B_3 returns to <5 m thick mafic lavas. B_{ne} consists of both thin mafic lavas and thicker icelandites, this sequence is delineated around the mountains of Breiðatindur and Tóatindur, above the B_1 sequence. Most of the central volcano lavas are lobate, with individual lobes visible on the scale of tens of metres across; while sheet-like units extending laterally for tens to hundreds of metres in an outcrop are present but relatively rare. The B_1 sequence can be traced from the northern flanks of Berufjörður, northwards toward Reyðarfjörður, stratigraphically overlying the volcano of Reyðarfjörður and approximately coeval with Þingmúli central volcano.

One of the oldest mapped groups is the "Flögufoss group" (Map unit: Fl) within B_1. This group is within the lower flank sequences, passes by the farm of Flaga, where a silicic sill cross cuts the group. The group, which is best exposed by the Flögufoss, is a compound pāhoehoe lava, here comprised of around six stacked lobes at the waterfall locality. Each lobe has a coherent base with fine vesicles, and the vesicle size increases upwards until around 15 cm from the base of the lobe. The cores of the lobes are vesicle poor, with any vesicles present stretched in the flow direction or retained in pipes, and cooling joints are irregular. The upper crust is vesicular and coherent, suggesting true pāhoehoe. This group is separated due to its excellent exposure and is a "type locality" for pāhoehoe lavas sourced from the Breiðdalur volcano.

The Fagridalur olivine basalt group (Map unit: green, within B_1) is exposed along the south eastern flank of Breiðdalur. The group thickens to the south, towards Álftafjörður, the lavas within this group contain olivine as a phenocryst phase. A thin, 50 cm, silicic tuff is seen between 2 lavas in the group on the northern shore of Berufjörður (not shown on map).

The Stöng group (Map unit: St) within B_1, on the north side of Berufjörður, stratigraphically below the earliest icelandite lavas. This group is identified by its 'abnormal' structure, compared to the surrounding flank lavas. This structure is most obvious from the southern side of the fjord, where the group of lavas terminates at around 400 m a.s.l. at a coarse, poorly sorted breccia. The group shows the 'normal' regional dip at fjord level (around 10° east), the dip is then reduced to 0° at 400 m, where the surrounding lavas dip around 8-6° at this level. This group coincides with the mapped area of icelandite lavas by Walker (1963), new geochemistry shows these lavas are olivine normative basalts (Askew et. al. In Prep.). Consequently, the adequate adjustments were made to the distribution of B_2.

Red sediment interbeds are commonly present between lavas. These beds vary in thickness, from 1–2 cm to 10's of cm's. Their presence suggests a time gap for wind-blown sediment to accumulate, essentially a gap between eruptions. In certain areas thicker sediment horizons are visible in the flank sequences, these include a 2 m dark grey sandstone above the GPG in Skriðuá, the sediment is layered, each layer being around 2–3 cm thick and variable in grainsize from fine sandstone to fine gravel. In the B_3 sequence, close to Rauðafell in Berufjörður, a very confined sediment is exposed. The unit is around 5 m thick and around 15 m wide forming a channel shape within the lavas, the lowest section is a white, fine grained silicic tuff, containing black glassy fragments and grey basaltic fragments. The tuff appears to have been remobilised into the channel, it is finely layered, fissile and many of the clasts are sub-rounded to sub-angular suggesting some degree of transportation. Above the white tuff is a blue sediment with red clasts within it, the true colour of the clasts is grey, and the rock seems to have been altered by jasper mineralisation. The blue, fine grained matrix was presumably white though no true colour remains, the rock is clast supported, the clasts are sub-rounded to sub-angular and on average around 1cm in size.

The morphology of the lower flank lavas indicates that the volcanism was accompanied by a localised rise in topography, forming volcanic edifice with a shallow slope. Without this rise, the lower thin lavas would presumably start off thicker and become thinner as the edifice built up.

3.2.1 Intermediate rock formations within the flank sequence

Some of the earliest icelanditic lavas are located 200 metres above the farm of Flaga or about 300 m a.s.l. (Figure 3). A sequence of flows, predominantly of icelandite to basaltic icelandite in composition, around 400 m thick can be traced from above Flaga eastwards. The group thins to the east reflecting a decrease in number of intermediate lavas away from the centre of the volcano, the same group is seen in Berufjörður. There are intermediate composition flows present on Tóatindur (Walker, 1963) though they do not form a single thick sequence as is seen south of Breiðdalur. Intermediate flows are also visible at Eyvindarnes, Berufjörður. The presence of intermediate rocks in the flank sequences, suggests that there is a persistent heat source beneath the volcano which allows the formation of more evolved rocks. Silicic tuffs appear infrequently and often in thin layers or confined areas in the flank sequences, which would suggest these are coming from further afield than the Breiðdalur central volcano, though it cannot be effectively ruled out.

3.3 A More Mature Volcano: Caldera Sequences

Possibly the starkest feature of the Breiðdalur volcano is that most of the valley head is comprised of the pumice breccia and sediments that once infilled a large depression in the centre of the volcanic edifice. This sequence has also been subjected to extensive geothermal alteration. Walker (1963) named this sequence "the core group" because he did not identify the existence of the caldera. Herein we define it as the caldera group, because the evidence (see below) strongly indicates that the volcano features a caldera. We present the caldera group as a single sequence comprised of several extrusive and intrusive igneous as well as sedimentary formations. These include the important 'Agglomerate formation'; silicic lavas; mafic lavas; intrusions.

The presence of a caldera, now partially exposed at the head of Breiðdalur, is borne from several layers of evidence:

1. There is an abrupt change from the layered lava sequence of the flanks, to the complex structure of the pumice breccia or agglomerate.

2. Point 1 leads to the inference of a caldera fault zone, marked on the map leading northward from Berufjarðartindur. An abrupt disconformity can only be feasibly caused by a fault.

3. Cone sheets with a westwards dip of 30 – 45°, mainly exposed across the southern faces of the mountains Tóatindur and Breiðitindur, indicate a shallow magma chamber to the west of these exposures (Figure 4). This in itself does not confirm a caldera was present, but it highlights the presence of the shallow magma reservoir, which intermittently became over-pressured, beneath the western end of Breiðdalur.

4. Within the caldera sequence there are multiple areas of evidence for the presence of surface water and one good example of standing water. Along the bank of Hesthálsá is a sequence of siltstones dipping around 45°SW. These finely laminated siltstones must have formed in an area of standing water (i.e. a caldera lake) and in one area there are trace fossils (of type *Repichnea*) within the siltstones. In other areas of the caldera, interbedded with the massive pumice breccias, are fine grained siltstones or tuffs which display bedding from fine laminations to 10's cm thick layers and occasional cross-bedding style structures. Their appearance suggests they were tuffs that were remobilised within the depression and subsequently tilted. It is difficult to discern if these were remobilised by water or by wind since the exposures of each section are confined to rather narrow gullies.

5. Geothermal activity resulted in alteration that is confined to the caldera area, where the highest temperature geothermal area (with epidote as an alteration phase indicating upper Greenschist stage of metamorphism, >200°) is centred around the Blágil area (Figure 8). Calcite and pyrite also occur as veins and alteration minerals within the caldera sequences, a concentrated high temperature area must have been present at a shallow level below the head of Breiðdalur.

6. Any bedding that is present within the caldera generally has steep dips, up to 70°, most of the recorded dips are to the south west. The maximum thickness of the caldera fill is around 500 m, close to Matarhnjúkur, and below the 'summit sequence' of tuffs, agglomerates and lavas. This scale of subsidence is not surprising because larger scale subsidence is common at caldera volcanoes.

The exact timing of formation of the caldera is not possible to deduce at this stage, but cross cutting relationships between the flank sequence, the caldera agglomerate and the upper bracket of the summit sequence, show that it took place during the later stages of Breiðdalur's lifespan– after the flank sequence lavas had formed. The delineation of the caldera group is marked on its eastern side by a distinct disconformity, most visible on the southern side of the Breiðdalur. This contact is marked on the map as the main caldera fault zone between the flank sequence lavas and the agglomerate. It is convoluted and complex, with stepped faulting visible in places. The fault boundary is intruded by dykes, sills and sheets, and much of it reveals enhanced alteration. In Berufjörður by Selá, a small sliver of felsic material is wedged between flood basalts capping the volcano, the rhyolite of Berufjarðatindur (BFT), and the B_3 flank sequence

(Figure 5). This sequence consists of a pitchstone lava, green to yellow coloured lapilli tuff and other undifferentiated silicic rocks, has a sharp vertical contact with the upper flank sequence and is taken here to represent a section of the caldera sequence. The Selá sequences also dip by around 45 – 50° to the south west, which is much greater than the regional dip and for that matter dip of any other sequence, outwith the caldera, within the volcano edifice (Appendix Map). On the northern side of Suðurdalur, by Þórgrímsstaðir no obvious caldera sequence occurs, instead a succession of lavas and tuffs with dips closer to regional values (<12°) occurs, though there is some pervasive hydrothermal alteration within the sequence. This leads to the interpretation that a disconformity could occur through the Breiðdalur valley, or simply be buried beneath this sequence. There is a discontinuity between the B_{ne} flank sequence, and the rhyolite lavas exposed at Rauðitindur, this appears to be sharp, leading to the mapping of the fault to the east of Rauðitindur. This area is a talus and debris filled valley obscuring the more complex relationships.

3.3.1 Mafic Lavas

The lowermost sections of the caldera sequence is comprised of strongly geothermally altered mafic lavas, that are predominantly basaltic. Where it is possible to measure their dip, the lavas dip up to 40° with no apparent main strike direction (See Appendix Map). These lavas, best exposed on the southern side of Suðurdalur, between Hesthálsá and Skarðsá, may be equivalent to lavas in the flank sequence that collapsed into the caldera.

3.3.2 Agglomerate

An excellent view into the caldera sequence can be seen up the small gully of Ytri Ljósá Gil; the strongly altered sequence of pumice breccia and intrusions is bright white to yellow in colour, hence the name of the river, Ljósá — "The Light Coloured River". Moving up sequence, the bulk of the extrusives are agglomerates, comprised of white to grey pumice fragments and lithic clasts sitting in an ash matrix. The lithic clasts are coarse sand sized to gravel sized (<10 cm) fragments. The lithics are variable in type and colour, most obvious are the darkest clasts which clearly stand out from the lighter coloured ash matrix and pumice. The agglomerate commonly features localised bedded or layered horizons, which may indicate primary volcaniclastic deposition by laterally moving currents or post-emplacement remobilisation of parts of the agglomerate. Bedding varies in dip from 70 to 40° are observed often variable over short distances of 10's to 100's of metres, dip direction is also changeable though the dominant exposed dip directions are south to south-westerly. The dip direction may be a factor of exposure, since the western side of the caldera does not appear to be exposed which would presumably have dominant dips to the east assuming that the dips were a factor of subsidence. The degree of dip noticeably decreases up sequence, and exposures of the upper caldera sequence more closely follow the regional dip of Breiðdalur if slightly increased, to 15 degrees west to south west.

There is significant evidence for the presence of water within the caldera. The extent and nature of alteration within the caldera fill sequence indicates that a vigorous geothermal system was present within the volcano post caldera collapse. There is also evidence for running and standing water present in the caldera at times. Sedimentary structures such as cross-bedding and size grading, are visible within the pumice breccia, indicating remobilisation by running water. In addition, the presence of sequences comprised of finely laminated silt and mudstones strongly indicate that some form of a caldera lake was present at times throughout the volcano's life. Two examples of lithologies indicating the presence of standing water on the volcano are well exposed in the sequence: Hesthálsá sediments are fine siltstones dipping steeply to the south west with abundant trace fossils (*Repichnia*), the siltstone sequence is exposed over about 20 metres but the true thickness is not obtainable due to insufficient extent of the exposure. The second is exposed at BFT in the summit sequence (see 'Summit Sequence' below), which comprises lavas, tuffs, agglomerate and a hyaloclastite. The hyaloclastite formed as lava flowed into standing water, forming pillows, which subsequently broke up into a hyaloclastite "delta".

3.3.3 Silicic Lavas

Thick silicic rock formations are present within the caldera sequence and the greatest challenge is to distinguish intrusive and extrusive formations within the highly disrupted and often heavily altered caldera sequence. The distinction between intrusions and lavas in the field is most commonly obtained through grainsize, the presence of a rubbly surface or clear cross cutting relationships. Within the Breiðdalur caldera sequence, the intrusions were emplaced at very shallow levels, thus were exposed to high cooling rates and consequently are fine grained. Furthermore, the contacts are commonly obscured by extensive talus slopes.

3.3.4 Mafic Caldera Intrusions

Intrusions are present throughout the entire caldera sequence, they vary in composition from basaltic (described here) to intermediate and to silicic (described below). Structurally mafic intrusions within the caldera do not exhibit a distinguishable pattern (disregarding regional dykes). Inclined sheets outside of the caldera, however, do exhibit a dip towards an area below the centre of the caldera. Post-caldera intrusions are emplaced within the clastic sequences of the caldera fill; some are very fine-grained to glassy and feature hackly jointing as if quenched upon contact with external water. Intrusions close to the inferred caldera fault zone are aligned with the fault direction, presumably because it is a structural weakness and therefore a preferred magma pathway (Browning and Gudmundsson, 2015).

Mafic intrusions close to the top of the caldera fill sequence are coarser grained than those sitting lower in the sequence. The groundmass crystals in the upper intrusions are typically between 1-2 mm, while in those lower down in diameter the crystal size is <1mm. A good example is a 20 m thick and 100 m wide doleritic sill west of Rauðafell in Suðurdalur and above Blágil (see Appendix Map). The intrusion sits at the boundary between the caldera group and the sub-horizontal summit group. The sill's intrusive position may be related to the structural/rheological boundary between sub horizontal summit sequence lavas and the upper caldera agglomerates.

3.3.5 Intermediate Rocks

Intermediate magmas are present throughout the caldera sequence. For example, the knoll of Ketilhnúkur in the main valley is a dome-like edifice, with the lava thinning away out from the dome (Figure 6 and 8). A large, roughly spherical intermediate intrusion is placed close to Hesthálsá in Suðurdalur. It is a dark grey andesite, weathering to a red colour, it is fine grained with no discernable phenocrysts.

3.3.6 Silicic Caldera Intrusions

Silicic intrusions within the caldera fill sequence are often highly altered and eroded and exhibit an obvious cross cutting relationship with the surrounding agglomerate group. Within the agglomerate, these silicic intrusions are variable in shape and size, due to the 'malleable' nature of the agglomerate substrate. The caldera fault zone is commonly utilised as a pathway for silicic intrusions.

3.4 The Summit Sequence and the South Eastern Rhyolites

3.4.1 Summit Sequence

The majority of extrusive rhyolites at Breiðdalur stratigraphically sit above the flank sequence or the caldera sequence (Figure 7). These are grouped together as silicic lavas on the geological map, though separate formations are referred to by their position on the volcano: The South Eastern Rhyolites (SER) of Flagatindur, Röndulfur, Slöttur, and Stöng; The Summit group rhyolites of Berufjarðartindur, Fossárfell, Hestháls, and Þorgrimsstaðir. This is purely based on their stratigraphic position in the volcano, which may be broadly related to the timing of their formation, but not intended to indicate anything about their magmatic or petrographic differences and evolution. Most of the lavas are aphyric rhyolites, except the lava of Flögufell (Schnell, 1994). As all of the silicic lavas and other extrusives are located high in the volcano's stratigraphy it is generally thought that much of the rhyolitic magmatism took place over a short period late in the volcano's life. Where the overlying stratigraphy is not eroded away, they are covered by plateau basalt lavas.

The summit group is demarcated by both, an unconformity between the steeply dipping caldera group agglomerates and the sub horizontal lavas, breccias and sediments of the lower summit group (Figure 6 and 7) and/or a lack of localised geothermal alteration. Lavas found within the 'summit group', display a regional dip, coherent with the surrounding plateau basalts, and overlying agglomerate. The lower summit group is relatively well exposed close to the mountain Matarhnjúkur (Figure 6) and the top of the Ljósá. The group begins as a series of tuffs, block-loaded agglomerates and mafic lavas, at between 600 – 700 m a.s.l. in Suðurdalur. Above this, the Matarhnjúkur ignimbrite is exposed on the mountain of the same name. The ignimbrite appears to lay relatively conformably on the underlying tuff. The ignimbrite a conspicuous pink rhyolitic rock, containing elongate cavities and finely welded fiamme in a fine tuff matrix. Its maximum thickness is around 95 m, rapidly thinning and tapering out to the southeast over a distance of 1000-1500 m. It is still 70 m thick at Dýristindur, 3 km to northwest, but appears to taper out shortly thereafter. Walker (1962) claims that the tuff is exposed on the northern side of Suðurdalur, though we found no indication of this and this was not marked on the final geological map. Nonetheless, this is a significant ignimbrite and appears to be filling in a topographic depression. A minimum estimate of its total volume is around 0.6 km^3. The Matarhnjúkur ignimbrite may be related to the BFT rhyolite, and as it probably filled topographic lows it created a relatively flat topography within the caldera.

Another portion of the summit group is best described through the exposures across BFT (Figure 7 and 8). This sequence begins above an obvious pink rhyolite lava. Conformable above this is a white rhyolitic tuff breccia, with well-preserved pumice fragments. The breccia is comprised of a fine-grained tuff matrix, varying from white to light-brown and black in colour. The clasts within are highly variable, and pumice fragments are found through much of the sequence, though they appear concentrated in the lowest section. Lithic clasts are variable both in composition and in size, ranging from mm to 0.5 m sized clasts with the smaller size ranges being the most common. Compositionally they range from (in approx. abundance order): rhyolite, pitchstone, basalt, granophyre, and gabbro. Above this layer is a composite lava or "emulsion rock" that is poorly preserved. The rock is clearly composite in nature with contrasting rhyolite and mafic sections similar to other composite rocks found at this stratigraphic level.

Above the composite rock is a thin, light brown laminated siltstone of 50 cm thickness, over this is a brown rock comprised of dark glassy coarse sand-sized grains, a palagonised tuff. Within this sits larger blocks of vesicular basalt with occasional glassy rims. The size and abundance of the clasts increase higher in the outcrop and the clasts become more coherent after 10 m, clearly showing pillow basalt structure though with some degree of damage to pillows. The lower section formed through the breakup of pillows and glassy basalt in water, as indicated by the abundance of pillow fragments within the tuff. The degree of break-up decreases upwards, hence the increasing size of clasts and better preservation of pillows. The pillow breccia and tuff forms a sheer cliff on the north-eastern face. This is where it appears thickest, and the bed then thins to the south and to the west and is ultimately obscured by talus. The localisation of the pillow breccia suggests it was formed via eruption into a body of standing water, e.g. a caldera lake. The tuff below may also have been deposited into the lake and settled on the lakebed and the emulsion rock may have been more pervasively weathered and affected by emplacement into standing water.

Above the hyaloclastite is a sequence of basalts, mapped as flank lavas, part of the later sequence of B_3. This package of lavas, at BFT, are predominantly aphyric basalts. A single lava bearing macrocrysts of plagioclase and clinopyroxene in a coarse plagioclase, clinopyroxene and glass matrix lies on top of the pillow breccia tuff. It weathers to a dark black colour, though appears to contain no olivine, this may be the 'olivine basalt' mapped in this area by (Walker, 1963). Above the basalts a thin "wedge" of agglomerate bearing large silicic and basaltic clasts is overlain by the thick, red rhyolite lava of BFT rhyolite. The BFT rhyolite has a volume of 1.4 – 2 km^3

and a thickness of 200 m, it displays conspicuous flow banding. Walker (1962, 1963) inferred that the Matarhnjúkur ignimbrite (above) and the BFT rhyolite may be from the same intrusive plug, located on the north western side of Matarhnjúkur. However, a fault mapped in the silicic lava to the south of the plug is not mapped in the plug, suggesting the plug is younger than the lava. The BFT rhyolite formed the summit rhyolite, probably forming the highest point in the Breiðdalur volcano and was probably the last or one of the last gasps of the central volcano. The BFT rhyolite is subsequently covered by plateau basalts including the Heiðarvatn olivine basalt group (Not shown in map. 9.1 My (±0.15 My) Gans. Pers. Comm.). Summit group rhyolites' mapped definition is inferred from their position: un-deformed above caldera agglomerate and overlain by basaltic lavas.

3.4.2 South Eastern Rhyolites

The SER sit atop the basaltic lavas of the Breiðdalur flank sequence, the eruptions appear to be forceful, breaking the lavas below and show signs of post-eruptive subsidence. The SER and upper Breiðdalur flank lavas show lesser degrees of dip than those lower down, an expected consequence of less load stress on the higher stratigraphic lavas (Walker, 1960). The rhyolite lava of Slöttur and Stöng forms 2 distinct peaks, each with cliffs of 200 m and 150 m high respectively. The Stöng lava is a continuation of the Slöttur, with the former peak also showing what is believed to be the agglomerate from the eruption vent. The rhyolite is well jointed and completely aphyric, it has a spherulitic texture (spherulites around 1mm in diameter). Flögutindur rhyolite is a plagioclase phyric lava with strong cleavage and flow structure. The rhyolite rests directly atop an agglomerate, the lava may be a continuation of the lava at Röndulfur or may have a separate, now eroded vent. Smátindur rhyolite is a large rhyolite flow or dome erupted effusively after an initial explosive event created a layer of agglomerate below the lava. The rhyolite is glassy and aphyric with a spherulitic texture. The lava's contact zone with the agglomerate is often chilled pitchstone, the agglomerate and blocks of rhyolite suggest the initial phase of the eruption event was explosive and an effusive lava phase proceeded it.

3.5 The size of Breiðdalur volcano

The entire flank sequence is around 1000 m thick, though there may be some lavas that erupted on the fissure swarm and onlapped the volcano's flank, the edifice probably stood around 1 km above the surrounding plateau lavas. In the latest stage of the volcano, the summit sequence lavas, especially the prominent BFT rhyolite flow, would have formed the highest point of the volcano area. The entire volume of the volcano is calculated as approximately 600 km^3, the footprint area of the volcano was around 1000 km^2 based on the current extent of the eastern flank. This approximate volume is a large but not far above average for Icelandic central volcanoes.

3.6 Burial of the Breiðdalur Volcano: Regional Plateau Basalt Volcanism

A discontinuity is visible in the lavas and volcano sequences leading down from BFT to the valley, as seen from the valley at the head of Berufjörður, looking westwards (e.g. Figure 5). This discontinuity is also visible, though less starkly, in Breiðdalur (Figure 6 and 8). The lavas are banking up against the central volcano, essentially burying it.

3.7 Localised geothermal regime: A Mature Volcano and Persistent Shallow Magma

High temperature, localised, hydrothermal alteration is confined to the caldera sequences. Highly porous agglomerate rocks and a high geothermal gradient from a shallow magma reservoir below the caldera, resulted in a geothermal system with visible alteration up to epidote facies. Furthermore, veins of calcite crosscut the caldera sequence, of which one exposed vein is large enough to have been of economic value. Pyrite and chalcopyrite are visible throughout the sequence to varying degrees, though some of the highest density areas are around large intrusions within the sequence. The most notable of which is found below the Rauðafell rhyolite.

4 Conclusions

Breiðdalur volcano began its formation around 10.0 Ma. Thin lava packages built a broad sided volcano upon the plateau basalt terrane typical of the east fjords. Linking the Skessa Tuff ignimbrite to the formation of Breiðdalur is difficult, but cannot be ruled out effectively, though it is preferable to suggest the volcano built a mafic edifice which digressed into mafic and intermediate volcanism. Sometime during the formation of the volcano, a caldera collapse event occurred. The ejecta from this event effectively infilled the caldera but could be remobilised and deformed by subsequent events. Any tephra ejected further from the volcano has not been traced, but this could be a factor of preservation or of exposure. Silicic magmatism appears to be confined to later stages. All silicic lavas sit high on the volcano edifice and many silicic intrusions cut through the flanks and caldera sequences. Assuming a large caldera collapse event, any material within the area of the caldera would be destroyed or hidden, but the significant amount of silicic volcanism at high stratigraphic levels (relatively young age) and the known absolute age dates all confined to 9.3 — 9.1 My gives a strong indication this magmatism occurred late.

The Breiðdalur dyke swarm was active throughout the volcano's lifespan and the dyking continued after the ligfespan of the central volcano ended. Some of these dykes may feed fissure eruptions on the Breiðdalur fissure swarm, which ultimately interfinger with the Breiðdalur volcano. It is likely that other rift systems were active at the time and also interfingered with lavas from Breiðdalur; this interfingering can be best seen on the flanks of Fossárfell but is present through the whole flank sequence.

References

Browning, J., Gudmundsson, A., 2015. Caldera faults capture and deflect inclined sheets: an alternative mechanism of ring dike formation. Bulletin of Volcanology 77 (1), 1–13.

Jakobsson, S. P., Jónasson, K., Sigurdsson, I. A., 2008. The three igneous rock series of Iceland. Jökull 58, 117–138.

Jakobsson, S. P., et al., 1979. Petrology of recent basalts of the eastern volcanic zone, Iceland. Acta Naturalia Islandica.

Óskarsson, B. V., 2015. Volcanological studies of Neogene flood basalt groups in eastern Iceland. Thesis, Department of Earth Sciences. URL http://hdl.handle.net/1946/22929

Riishuus, M., Miggins, D., Koppers, A., Duncan, R., 2010. 40ar/39ar incremental heating experiments on celadonite from the skessa tuff, eastern Iceland: Thermochronology of low-temperature alteration of a flood basalt pile during burial metamorphism. In: AGU Fall Meeting Abstracts. Vol. 1. p. 4873.

Schnell, T., 1994. Breiðdalur central volcano, eastern Iceland: genesis of the evolved rocks. Thesis, Department of Earth Sciences.

Walker, G. P., 1960. Zeolite zones and dike distribution in relation to the structure of the basalts of eastern Iceland. The Journal of Geology 68 (5), 515–528.
URL http://www.journals.uchicago.edu/doi/abs/10.1086/626685

Walker, G. P., 1962. Tertiary welded tuffs in eastern Iceland. Quarterly Journal of the Geological Society 118 (1-4), 275–290.

Walker, G. P., 1963. The Breiðdalur central volcano, eastern Iceland. Quarterly Journal of the Geological Society 119 (1-4), 29–63.

Walker, G. P., 1964. Geological investigations in eastern Iceland. Bulletin Volcanologique 27 (1), 351–363.
URL http://dx.doi.org/10.1007/BF02597532

Figure Captions

Figure 1: Generalised geological maps, a) Iceland's crustal structure and current volcanic systems. b) East fjord crustal structure, map area in black box, neighbouring volcanoes are indicated. c) Generalised Breiðdalur volcano, only the eastern flanks of the volcano are exposed. Geological data (for a and b) from The Icelandic Institute of Natural History (https://www.ni.is/), note dyke swarm information is incomplete for northernmost volcanoes and volcanoes shown in the south western extent of the map.

Figure 2: Breiðdalur valley looking westward. On either side of the valley Neogene lavas are exposed; at the head of the valley, Breiðdalur's caldera or core group agglomerates are exposed. The prominent peaks to the left of the image are the rhyolite capped peaks of (from left to right) Röndulfur, Flögufell, and Berufjarðartindur.

Figure 3: The flanks of Breiðdalur volcano. Notably, this image shows the difference between the grey and relatively thicker 'plateau basalts' which include the Grænavatn porphyritic group, below Breiðdalur, and the distinct change to the thin and dark basalts of the B_1 Breiðdalur flank lavas. The white line indicates the exact point where the morphology of the lavas changes. The black line indicates another distinct change and a small plateau above the B_1 sequence, above this line are relatively thicker (than the Breiðdalur mafic lavas below) grey, intermediate composition lavas (B_2 or Breiðdalur Flaga Icelandites). Several dykes crosscut the sequences at this locality.

Figure 4: The mountain of Tóatindur, where the Breiðdalur sheet and dyke swarms are both well exposed, cross cutting Breiðdalur flank lavas of around 9.4–9.5 Ma. Sheets dip around 40 degrees west to south west, occasional intrusive bodies are present (grey shapes) where sheets or dykes appear to have stagnated in the crust. Sheets vary in chemical composition, most are basaltic but range up to rhyolite in composition.

Figure 5: Selá caldera and flank contact, pink rhyolite and agglomerate crops out to the west (left), westward dipping lavas stop abruptly at the river gorge and direct contacts are not visible. The lowermost outcrop of the caldera group is a silicic body, against which an overthickened basaltic plateau lava abuts. Within the agglomerate sequence, steeply dipping (40 degrees west) beds are visible, alternating basaltic, rhyolitic, pitchstone and tuffs.

Figure 6: The caldera and summit sequence of Breiðdalur, viewing direction South. the caldera group (CG) consisting predominantly of pumice breccia or agglomerate tuff and lavas, outlined within the CG is Ketilhnjúkur icelandite lava (K). The black line denotes the approximate location of the unconformity between the CG and the Summit Group (SG), the SG is thickest at this location. The peak (936 M a.s.l.) of Matarhnjúkur (M), a pink, layered, silicic ignimbrite (inset top right (M.a) image, pencil for scale) is a major part of the SG. Inset bottom right (SG.a), person for scale, is a section of the SG found just above the unconformity; tuffs, lavas and sediments show consistent layering (white lines). Plateau basalts (PB) younger than the volcano lie above this area.

Figure 7: Berufjarðartindur north east summit group section, log shown to the left, 20 m intervals between scale bars. A landslide obscures contacts to the right of the image. The caldera group forms the base of this section (caldera fault is just off image to the left). A pink-red rhyolite overlies the caldera group, above this is the sequence of pumice breccia, composite rock and a thin (0.5 m) siltstone. The siltstone is then overlain by the pillow breccia tuff and pillow basalts, which forms the steep nose of the north eastern knoll. 3 basalt lava flows overlie this, and finally the Berufjarðartindur rhyolite lava at the summit of the

mountain.

Figure 8: Map of the caldera and summit sequences of Breiðdalur with inset images of some key features, localities are explained in the text. Legend as in the main map. HeO: Hæðarvatn olivine basalt group.

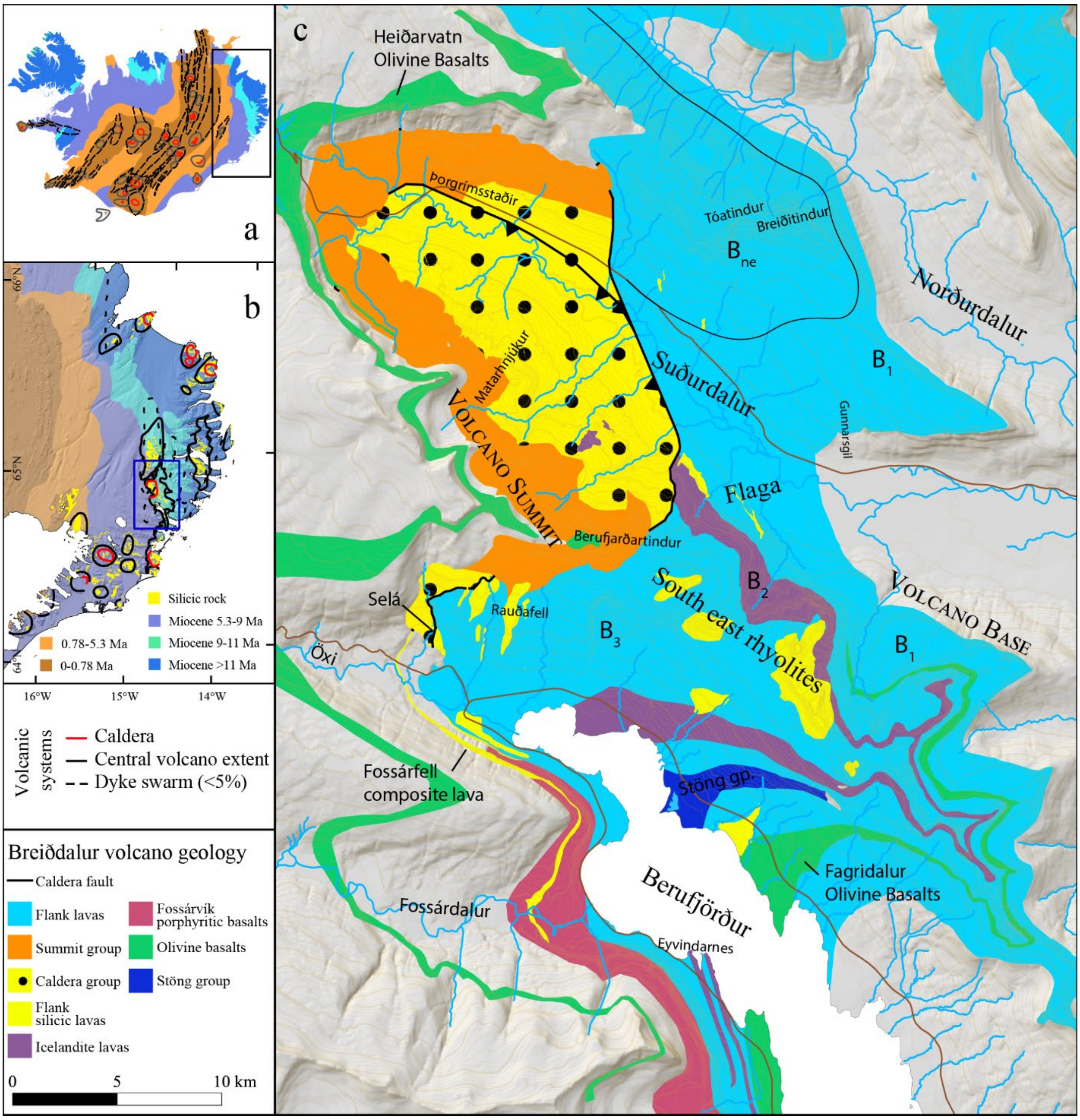

Figure 1

Figure 2

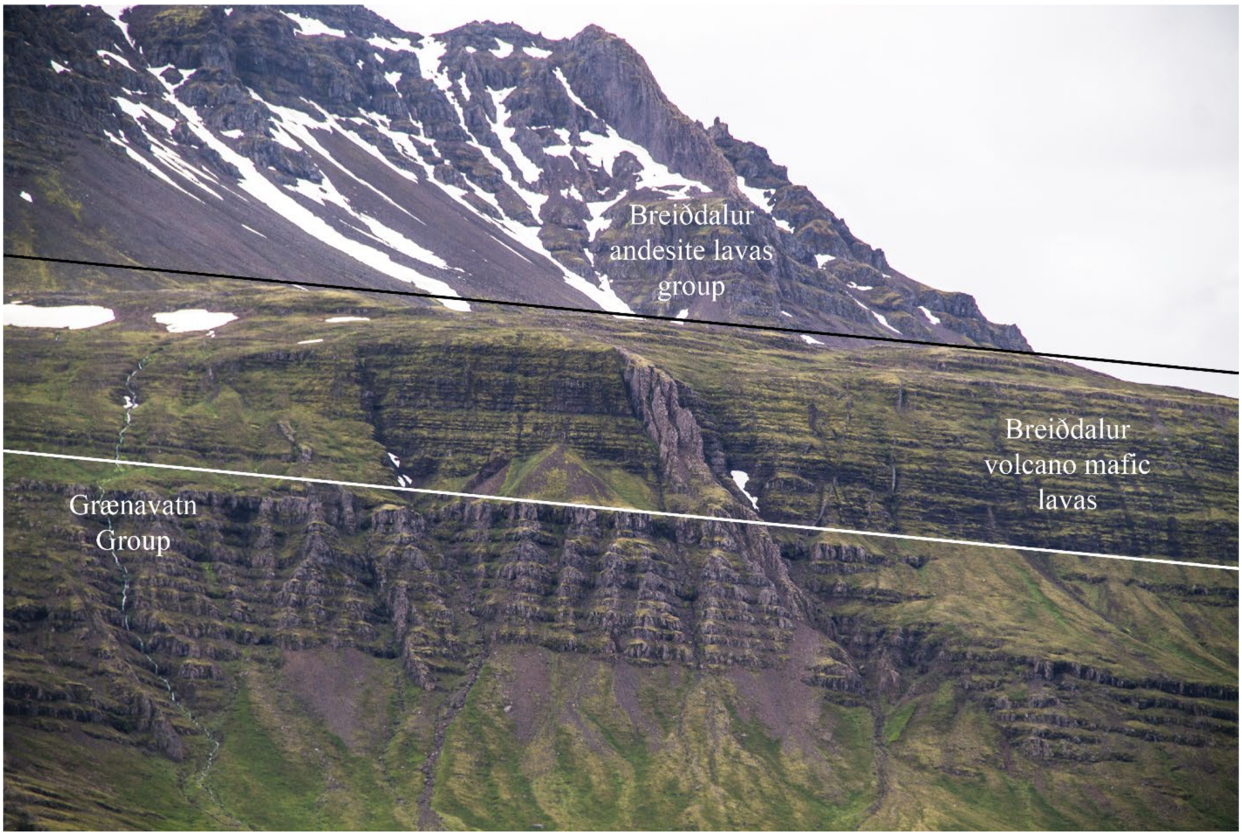

Figure 3

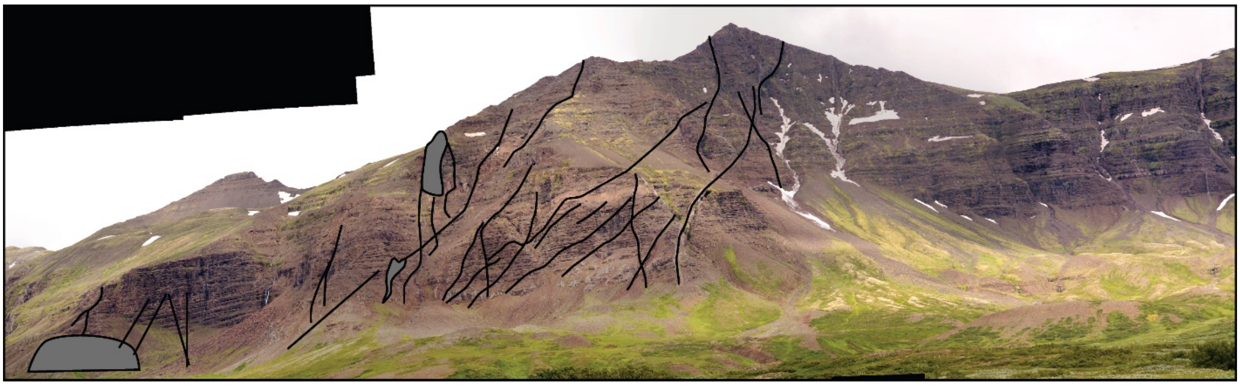
Figure 4

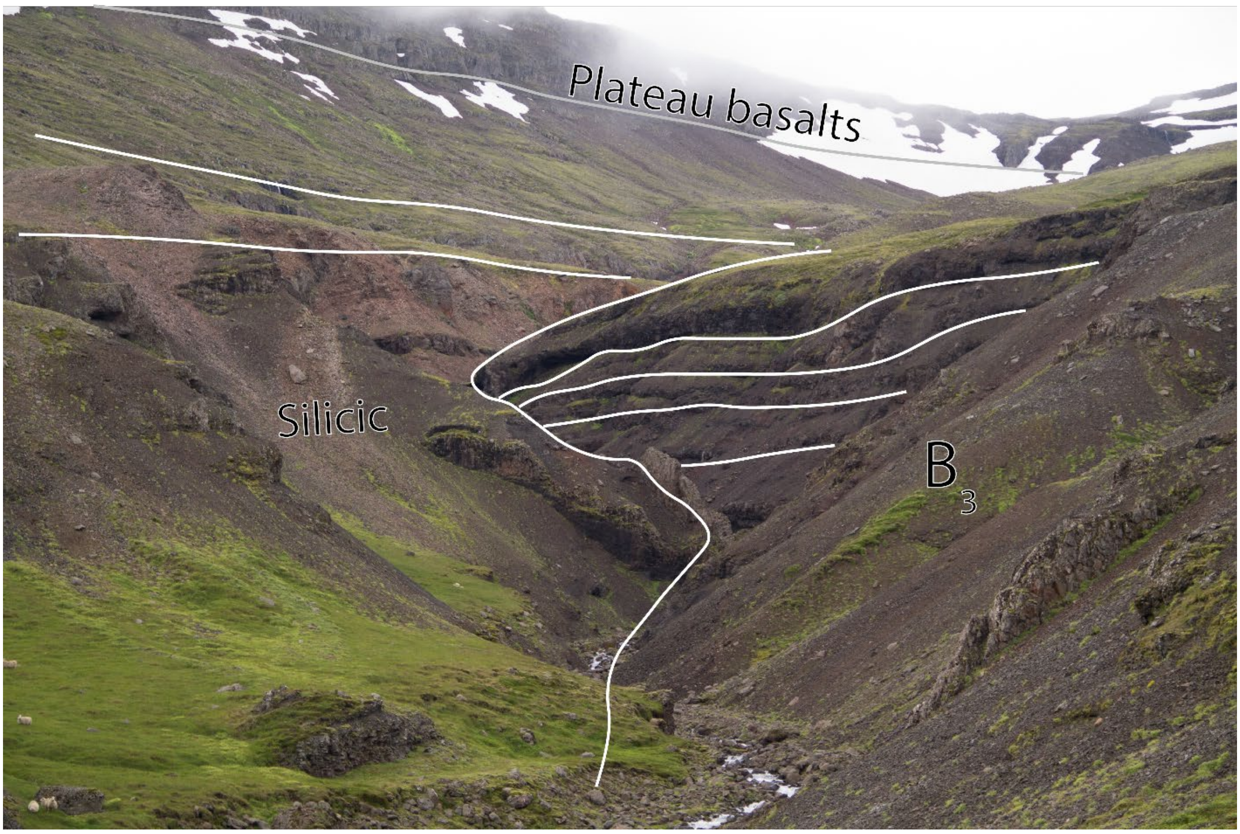

Figure 5

Figure 6

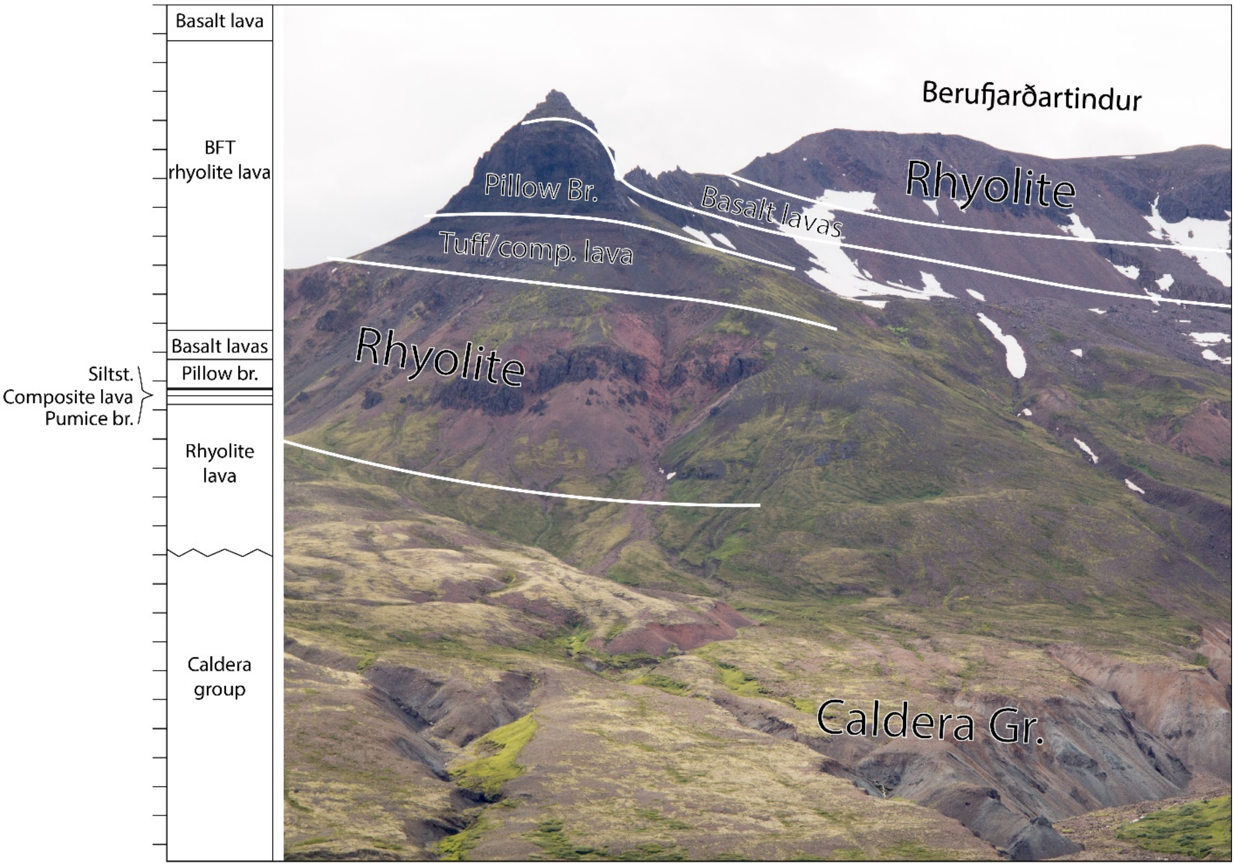

Figure 7

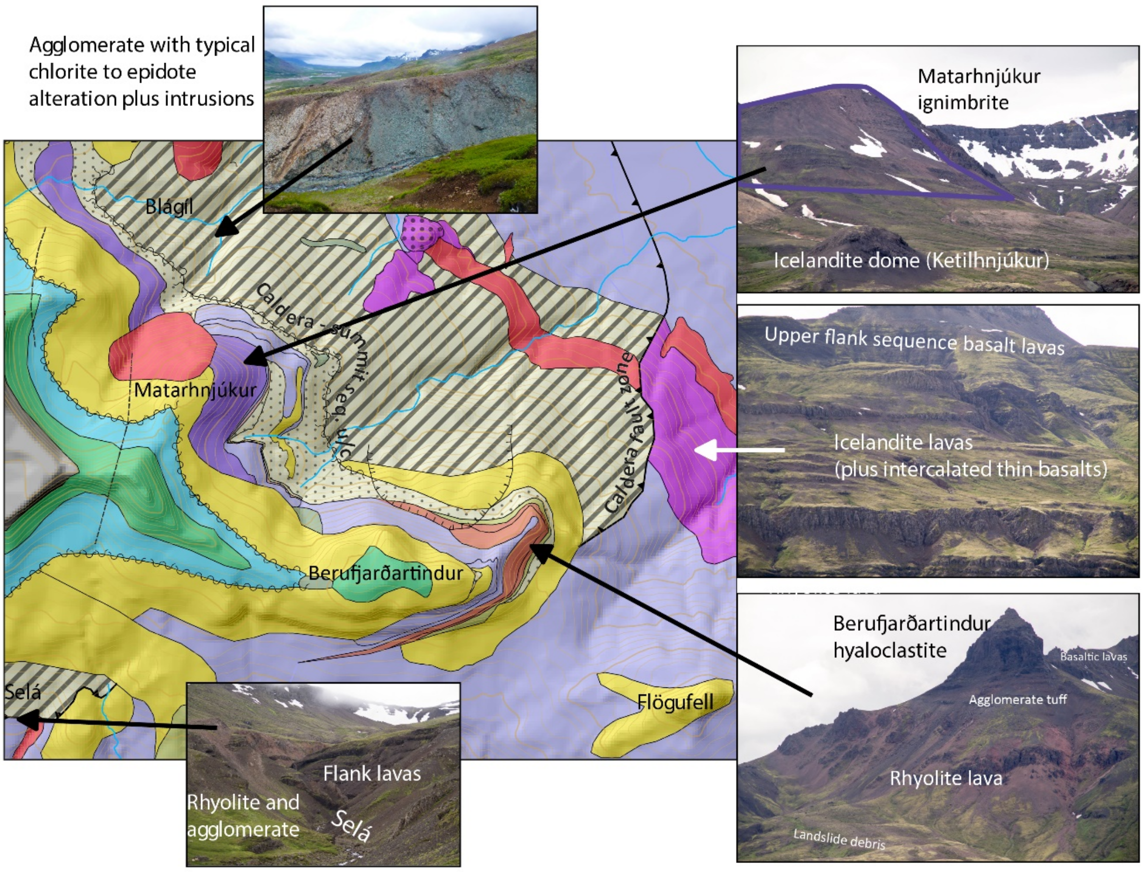

Figure 8

A.2 Paper 2: Temporal and spatial evolution of the Neogene age Breiðdalur central volcano through $^{39}Ar/^{40}Ar$ and U-Pb age dating

Temporal and spatial evolution of the Neogene age Breiðdalur central volcano through $^{39}Ar/^{40}Ar$ and U-Pb age dating

Robert A. Askew[a,1,*], Thorvaldur Thordarson[a], Phil Gans[b], Jay Thompson[c], Leonid Danyushevsky[c]

[a]*Institute of Earth Sciences, University of Iceland, Sturlugata 7, 101, Reykjavik*

[b]*Department of Earth Science, 1006 Webb Hall, University of California, Santa Barbara, CA 93106-9630*

[c]*Centre for Ore Deposits and Earth Sciences (CODES) University of Tasmania Private Bag 79, Hobart, Tasmania 7001, Australia*

Abstract

The volcanic sequences in eastern Iceland provide a cross section of magmatic activity from the Iceland rift system throughout the Miocene. This study focuses a high precision age dating campaign on a single Miocene volcanic system, the Breiðdalur system, in order to quantify the evolution of the central volcano and the associated dyke swarm. The central volcano consists of a lower flank of mafic lavas erupted onto a basement of plateau basalts, an upper flank of intermediate and mafic lavas, an 8-10 km wide caldera and a summit sequence comprised predominantly of thick silicic lavas. This study indicates that the central volcano has a lifespan of 1 My, from 10.1 – 9.1 Ma, intermediate magmatism began around 9.9 Ma and the caldera formed between 9.8 – 9.5 Ma, evolving through multiple nested-caldera forming events. Effusive silicic magmatism is predominantly in the youngest sequences between 9.5 and 9.1 My, after 9.1 My the central volcano activity effectively ceases and the volcano becomes buried by plateau basalts. The dyke swarm is known to be active at 9.9 Ma, and continues to be active until 7.8 My, 1.3 My after the central volcano.

Keywords: Volcano geology, Volcano stratigraphy, Geochronology, Iceland

---

1. Introduction

The current view is that the neovolcanic zones are delineated by a series of discrete volcanic system that are typified by conspicuous volcano-tectonic architecture, featuring a fissure (dyke) swarm or a central volcano or both (Figure 1). Furthermore, these systems are thought to be active for up to 1.5 million years. The fissure (dyke) swarms are taken to be elongate structures, 5 to 20 km-wide and 50 to 200 km-long, that are aligned sub-parallel to the axis of the hosting volcanic zone (i.e. almost perpendicular active spreading). When present the central volcano is considered to be the focal point of eruptive activity and the largest edifice within each system. Hitherto the understanding has been that a volcanic system initially develops as a fissure swarm where the dominating eruption activity is monogenetic fissure-fed basaltic eruptions. Later the plumbing for the volcanic system develops a shallow magma chamber and constructs central volcano typified by eruptions of intermediate to rhyolite magmas (e.g. Saemundsson, 1979; Gudmundsson, 1995, 2000). In this understanding the presence of a central volcano is a measure of maturity of the system (e.g. Thordarson and Larsen, 2007). However, this time sequence as well as the association between the fissure swarm and the central volcano is far

*Corresponding author
Email address: `robert@ni.is` (Robert A. Askew)
[1]Present address: Icelandic Institute of Natural History, Urriðaholtsstræti 6-8, 210 Garðabær, Iceland.

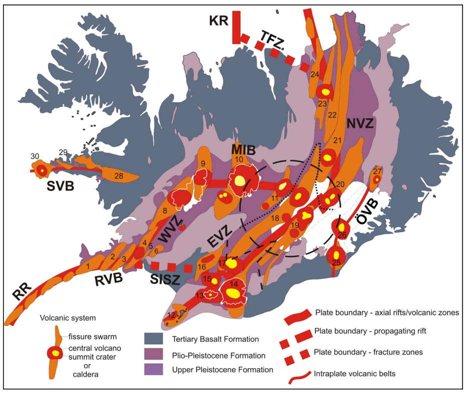

(a) Volcanic systems of the Neo-volcanic zones, from Thordarson and Larsen (2007), systems contain a central volcano, a fissure swarm or both.

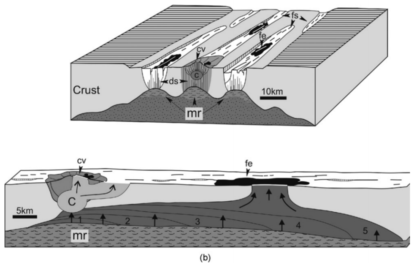

(b) One of the current views on the structure of volcanic systems in Iceland. mr: Mantle reservoir, cv: central volcano, fs: fissure swarm, fe: fissure eruption, C: shallow magma chamber.

Figure 1

from certain. It is noteworthy, that nine volcanic systems feature only a central volcano, four systems a central volcano and an immature fissure swarm and 11 systems contain only geothermal system or an embryonic central volcano (Table 1 in Thordarson and Larsen, 2007). This information clearly demonstrates that there is no universal rule controlling the evolution of volcanic systems in Iceland. In this context it is interesting to note that all of the systems that feature both a central volcano and a well-developed fissure swarm are all located in the axial rift in the interior of Iceland where the crust is thickest, while those that lack central volcanoes tend to be located at the coastal ends of the axial rifts where the crust is thinnest. Furthermore, those systems that only feature central volcanoes tend to be located within the propagating part of the East Volcanic Zone and in the intraplate volcanic belts where the crust is relatively thick (Figure 1). Hence, it cannot be ruled out that in some and perhaps in majority of the cases that central volcanoes are the first major structure to form on a volcanic system. Is it possible that such cases represent the initiation and embryonic growth of a volcanic system, that is the stage when deeper-sourced magma is establishing migration through the thick Icelandic crust through a confined path? Several geological observations give support to this notion. Firstly, of the four most active volcanic systems in Iceland, three (i.e. Grímsvötn, Katla and Hekla) feature a mature central volcano but an immature fissure swarm and the fourth (i.e. Bárðarbunga-Veiðivötn) features a developed but apparently very young swarm (Thordarson and Larsen, 2007). Secondly, the Krafla fissure swarm in North Iceland cuts through the corresponding central volcano and is physically splitting its caldera into two halves (e.g. Saemundsson, 1991; Hjartardóttir et al., 2012). At the Askja system the fissure swarm appears to be encroaching on the central volcano (e.g. Hartley and Thordarson, 2013). Thirdly, the extinct Tertiary central volcanoes are buried by the basaltic lavas produced by the nearby fissure eruptions, indicating that the activity on the systems fissure swarms continued well beyond the lifetime of the central volcano (e.g. Walker, 1963). In this study we aim to evaluate these two opposing ideas on the potential evolutionary path of volcanic systems in Iceland via age dating, underpinned by geological mapping, of a well exposed Neogene Breiðdalur central volcano and associated dyke swarm in eastern Iceland.

Currently, no previous studies have tried to fully evaluate the age span and the age-dependent evolution of a volcanic system in Iceland. At Breiðdalur volcano it is possible to mark the 'beginning' and 'end' of the central volcano, as well as the relation between volcano and the dyke swarm within this system, and thus it is possible to evaluate the sequences temporally and spatially. The emphasis of this project was upon the relationship between the volcano and the dyke swarm, as well as the age relationship with the plateau lavas covering the volcano.

Volcanic system	Label	Age	Type	Reference
Fagridalur	F	14 - 12 Ma	Central volcano and dyke swarm	Martin et. al.
Refsstaðir	Rs	12 Ma	Small central volcano	Martin et. al.
Dyrfjöll	D	12 - 13.5 Ma	Large silicic central volcano and dyke swarm	Gústafsson*
Breiðavík	B	12.5 - 13.1 Ma	Large silicic central volcano and dyke swarm	Gústafsson*
Álfavík	Á	13 Ma	Central volcano	Gústafsson*
Kækjuskörð	K-H	12 - 13 Ma	Small central volcano (or parasitic volcano)	No dates
Herfell	K-H	12.4 Ma	Small central volcano (related to Kækjuskörð?)	Gústafsson*
Barðsnes	Ba	13 Ma	Central volcano - mostly eroded	Watkins and Walker
Reyðarfjörður	R	11 - 12 Ma	Large silicic central volcano and dyke swarm	Martin et. al.
Skrúður		Unknown	Off land	
Þíngmúli	Þ	9 - 10 Ma	Large silicic central volcano and dyke swarm	No specific dates
Breiðdalur	Br	9 - 10 Ma	Large silicic central volcano and dyke swarm	Martin et al. (2011); Riishuus et al. (2010) Askew and Thordarson (In Prep)
Streitishvarf	S	10 Ma	Dyke swarm	Martin et al. (2011)
Álftafjörður	Ál	10 - 11 Ma	Large silicic central volcano and dyke swarm	
Lón	L	Unknown		
Kollumúli	K	Unknown		
Eystrahorn	E	6 - 7 Ma	Pluton	Martin et al. (2011); Padilla et al. (2016)
Vestrahorn	V	3 - 4 Ma	Pluton	Martin et al. (2011)
Ketil-laugarfjall	K-l	Unknown		
Geitafell	G	5 - 6 Ma	Central volcano and dyke swarm	Fridleifsson (1983)
Birnudalstindur	B	4 - 5 Ma ?	Central volcano and dyke swarm	Klausen, NordVulk Report, 1995
Thverartindur	Þv	4 - 5 Ma ?	Central volcano and dyke swarm	Klausen, NordVulk Report, 1995

Table 1: Ages of central volcanoes in eastern Iceland. Volcanoes are listed from north to south following names and locations by Walker (1974) and Gústafsson (1992). *Gústafsson presented work and dates to: `https://www.breiddalssetur.is/images/Jardfraedi-geology/Fyrirlestrar-presentaions/2014/2014-8-30-Jfr-Austurlands/ludvik.e.gustafsson-erindi_walker_symposium_30_8_2014.pdf`.

An additional task in this study is to review existing geochronological datasets in the east of Iceland. These previous campaigns are based on detailed stratigraphic transects and utilised Ar-Ar and K-Ar age dating and magnetostratigraphy and aimed at evaluating crustal 'drift' (e.g. Watkins and Walker, 1977; McDougall et al., 1976a; Moorbath et al., 1968; E. Mussett et al., 1980). More recent studies have focused on age dating and petrological studies on silicic magmatism in order to improve the understanding of silicic magmatism in Iceland (e.g. Berg, 2016; Martin et al., 2011; Martin and Sigmarsson, 2010; Åberg et al., 1987; Padilla et al., 2016). A few recent studies have had another look at some of the ages of the plateau sequences (e.g. Riishuus et al., 2010), and in doing so, raised some concerns about the reliability of previously acquired ages. The Skessa Tuff ignimbrite, located beneath the basal lavas of Breiðdalur volcano, is dated to around 10.15 Ma ($\pm$0.15 My Riishuus et al. (2010)), contrary to a date from McDougall et al. (1976a) (and similar dates from Albertsson et al., 1982) who gave an age for the lava above the Skessa Tuff of 9.05 My old ($\pm$0.26 My).

2. Geological Setting

Around 22 separate volcanic systems have been identified within eastern Iceland, consisting of central volcanoes, central volcanoes with dyke swarms, or only dyke swarms. Table 1 lists the currently

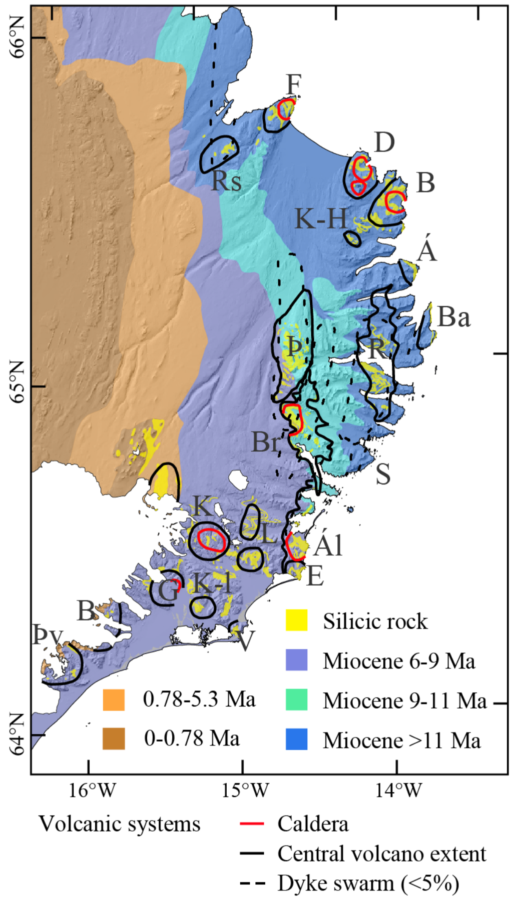

Figure 2: East fjord central volcanoes, Labels referenced in Table 1, Breiðdalur volcano (this study), is label 'Br'. The oldest systems are in the north and the youngest in the south. The central volcanoes of Breiðdalur, Þingmúli, Álftafjörður and Reyðarfjörður have their approximate full extents outlined, other volcanoes are outlined as presented by data from Náttúrufræðistofunun's geology GIS shapefiles. The extents of dyke swarms were mostly presented by Walker (1964), the Streitishvarf dyke swarm has been added and the Álftafjörður swarm slightly altered from the original mapping which originally suggested it extended up to Barðsnes.

known systems, their approximate ages and what the systems contain, their locations are shown in Figure 3. The oldest volcanic systems are found in the northernmost areas of eastern Iceland, the large silicic caldera- volcanoes of Dyrfjöll, Breiðavík and their dyke swarms as well as smaller but similar age volcanoes nearby are all around 13 – 14 My old. The systems generally young to the south, Breiðdalur, Þíngmúli and Álftafjörður were all active at similar times between 11 - 9 My. The youngest volcanic systems are located in the south east, exposed along the glacial valleys close to Vatnajökull: Geitafell, Birnudalstindur and Þverártindur between 4 – 6 Ma. Vestrahorn and Eystrahorn Plutons were intruded into older crust, presumably erupting lavas on the surface as central volcanoes, these form the youngest rocks of the east fjords related to a rift relocation event c. 7 Ma (Furman et al., 1992; Martin et al., 2011; Åberg et al., 1987).

Breiðdalur volcanic system, located in eastern Iceland, comprises a caldera volcano and extensive fissure (dyke) swarm residing within a glacially incised fjord landscape (Figure 2 and 3). The discovery of the Breiðdalur central volcano, and the presence of central volcanoes in eastern Iceland, is attributed to the work of George Walker in the 1960's, with a seminal paper (Walker, 1963) describing and mapping out Breiðdalur volcano. The volcanic system itself spans over 400 km^2 of land from Álftafjörður to Reyðarfjörður, the caldera and central point of the volcano is located in Suðurdalur, Breiðdalur. Activity was typified by mafic to silicic volcanism featuring both effusive and explosive eruptions, a caldera collapse and sustained geothermal activity, at least, in post caldera collapse period. The volcano is well exposed across much of the landscape and is consequently easily accessible by main roads and tracks. Hence, it provides an ideal natural laboratory to study chronological evolution of a Neogene volcanic system and its central volcano.

2.1. Geology of the Breiðdalur Volcanic System

The extent of the Breiðdalur volcanic system is outlined in Figure 2 (Br), the central volcano extends from southernmost outcrops near Djúpivogur to northernmost outcrops to the west of Reyðarfjörður. The volcano spans around 350 km^2, the Breiðdalur dyke swarm extends several km further north, in total the swarm is 50 km long from north to south and 10 - 15 km wide. The dyke swarm mostly comprises of basaltic dykes which can be several metres thick, a single dyke may be traced many km's to at least 15 km (Gudmundsson, 2002). The central volcano was, during its mature stage, a broad sided edifice, with a height of up to 1 – 1.5 km above the surrounding plateau basalt terrane.

The volcano is split into units descriptive of their location (Figure 3). These units are termed: flank sequences, caldera sequences, summit sequences, the South Eastern Rhyolites (SER) group and the dyke swarm. The base of the volcano is suggested to be the point at which grey >5 m thick plateau lavas are overlain by thin < 5 m, black basaltic lavas, these thin lavas sit atop a plagioclase phyric plateau basalt group, the Grænavatn Porphyrytic Group (GPG) which themselves overlie the 10.15 My old Skessa Tuff ignimbrite (Walker, 1962; Riishuus et al., 2010, Askew and Thordarson, In Review). The plateau basalts and regional ignimbrites or tuffs form the basement of the volcano.

The *flank sequence* unit is a 1000 m thick sequence of predominantly basaltic lavas source from the central volcano. These lavas formed a broad shield-like edifice which spanned many 10's of kilometres, the breadth of the volcano was in part due to the relatively low relief landscape surrounding these volcanoes during the Neogene. The base of the flank sequence is the base of the Breiðdalur volcano (Figure 3), where there is a distinct morphology change in lavas as described above. Due to the westward dip of the lava pile in eastern Iceland, and the east-west valley morphology, only the eastern flanks of Breiðdalur are well exposed.

Intermediate lavas are exposed within the flank sequences, though they represent a relatively minor amount of the stratigraphy. They are thick (10 - 25 m) lavas exposed in several areas throughout the flank sequence lavas, though a significant group, up to 400 m thick, of icelandite lavas is exposed on the eastern flank (Figure 3, Askew and Thordarson, In Review).

Caldera sequence unit: Possibly the starkest feature of the Breiðdalur volcano is that most of the valley

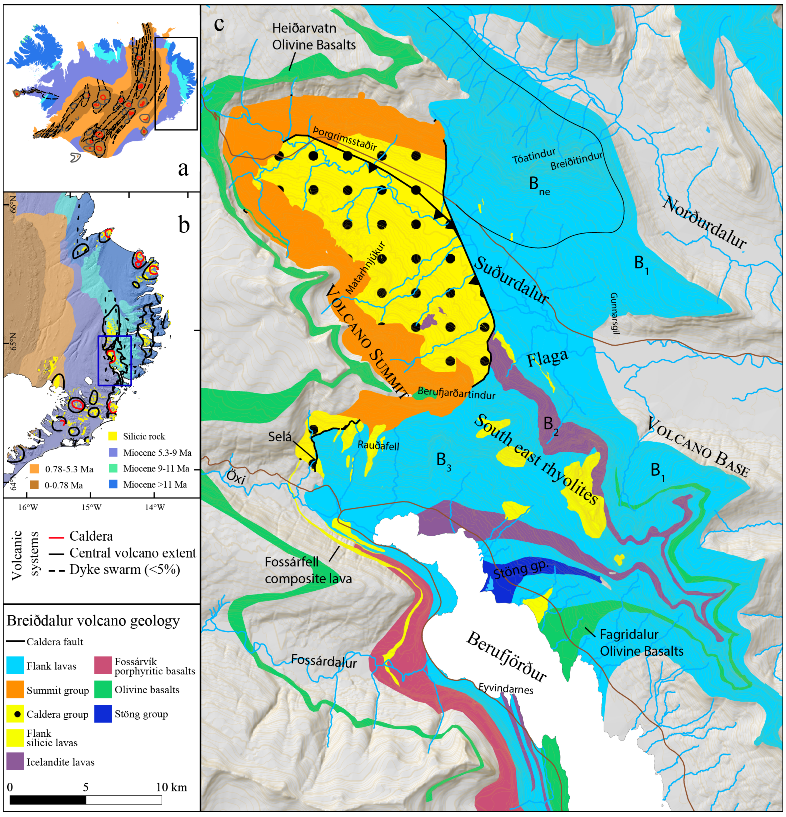

Figure 3: The study area. a) Icelandic geology, black box is: b) east fjords, see Figure 2 for further details. c) Breiðdalur volcano geology and localities, B_1: Lower eastern flank sequence, B_2: Icelandite lava sequence, B_3: Upper eastern flank sequence and B_{ne}: North eastern flank sequence. Sample locations presented in Figure 4.

head is comprised of the altered pumice breccia and sediments that once infilled a large depression in the centre of the volcanic edifice (yellow with dots, Figure 3). There is evidence for smaller, nested, calderas within the main edifice: variable dips up to 70°; remobilised tuff and pumices; siltstones, trace fossils and hyaloclastites, indicating water filled depressions; the Matarhnjúkur ignimbrite also sits within a depression (possibly self formed). The caldera group is mapped a single sequence comprising of several rock formation groups: the significant Agglomerate group (which includes sediments and breccias); silicic lavas; mafic lavas and mafic to silicic intrusions. The caldera group is bounded to the east and south by a caldera fault where a sharp boundary between the agglomerate and flank sequence lavas is visible. There is significant geothermal alteration throughout the caldera sequence.

The final unit of the central volcano itself is defined as 2 separate sub-units, the *Summit group* and the *South Eastern Rhyolites*. The terminology difference is due to their location though their stratigraphic level is similar. In some cases flows can be inferred or directly linked to source vents (Walker, 1963; Schnell, 1994, Askew and Thordarson, In Review). Silicic lava flows in Breiðdalur are of a significant and sometimes remarkable size. A flow-banded rhyolite lava exposed across Berufjarðartindur is up to 200 m thick (140 m average) and exposed for 2-3 km with an inferred area of around 14 km^2, field relations suggest the entire volume of lava could be around 2 km^3 (Schnell, 1994). The total exposed area of silicic magmatism at Breiðdalur is 31.6 km^2, total exposed mafic and intermediate magmatism by area (central volcano only) is 190.5 km^2 meaning that silicic magmatism accounts for 17% of the exposed rock at Breiðdalur.

In the late stages of the volcano's life, rifting to the west of the Breiðdalur system and subsequent loading of the crust by lavas from the rift zones caused a slight tilting of Breiðdalur volcano. The volcano was buried by plateau basalts and a west dipping disconformity is visible between volcano sequences and plateau basalts burying it.

Throughout the lifespan of the Breiðdalur system, a fissure swarm was active to the north and south of the central volcano, erupting lavas onto the northern and southern flanks of the volcano. This is exposed today as the Breiðdalur dyke swarm, the swarm stretches 40—50 km trending NNE—SSW. In the north, there is some cross over with the Þíngmúli dyke swarm and to the south with Álftafjörður's. At the highest density, the dyke swarm comprises at least 20 % of the stratigraphy in a traverse of around 100 m east–west. The dykes vary in thickness from 10's centimetres to metres in width and many show evidence of multiple intrusions. There is a significant gap in dyke density around the Breiðdalur caldera, either due to older dykes being destroyed during caldera collapse or a change in stress field from N-S trending to a radial stress field around the magma reservoir of Breiðdalur volcano.

3. Methods

3.1. Sampling

Samples for $^{40}Ar/^{39}Ar$ dating were collected systematically throughout the succession of the volcanic system. The map in Figure 4 shows sample locations.

3.2. Age dating

Most of the samples selected for age determination are mafic but include a small selection of silicic samples, and as such, is representative of the overall petrology of the volcano. Medium to coarse grained samples were required for groundmass plagioclase analysis. Silicic samples were often fine grained to glassy and aphyric and were not suitable for $^{40}Ar/^{39}Ar$ analysis. However, two of the silicic samples were selected for zircon based U-Pb age dating due to their high zirconium content. These are the rhyolitic dyke of Gunn-1 and the dacitic inclined sheet, WP470. They were analysed at the CODES analytical laboratory, School of Earth Sciences, University of Tasmania by J. Thompson following the method in Kosler (2001). Approximately 200–400 g of rock was crushed in a Cr-steel ring mill to a grain size <400 micron. Non-magnetic heavy minerals were then separated using a gold pan and a Fe-B-Nd hand magnet. The zircons were hand-picked from the heavy mineral concentrate under the microscope in cross-polarised transmitted light. The selected crystals were placed on double sided sticky tape and epoxy glue was then poured into a 2.5 cm diameter mould on top of the zircons. The mount was dried for 12 hours and polished using clean sandpaper and a clean polishing lap. The samples were then washed in distilled water in an ultrasonic bath.

The analyses in this study were performed on a Resolution S155 laser ablation system that houses a Coherent Compex Pro 110 Ar-F excimer laser that outputs a 193nm wavelength beam with a 20ns pulse width. The laser was coupled to an Agilent 7900 quadrupole ICPMS and the analytical equipment was housed at the University of Tasmania in Hobart, Australia. Zircons ablated using a 32-micron diameter spot at 5 Hz and an energy density of approximately 2 J/cm^2. Ablations were performed in pure He gas flowing at a rate of 0.35 litres/minute and carried aerosol ablated by the laser away from the ablation site and immediately mixed with Ar gas (flowing at a rate of 1.05 litres / min) in the funnel and carried to the plasma torch. Nitrogen gas, flowing at 0.015 litres / min, was added to the Ar gas to improve ICP-MS sensitivity. Isotopes measured were ^{49}Ti, ^{56}Fe, ^{90}Zr, ^{178}Hf, ^{202}Hg, ^{204}Pb, ^{206}Pb, ^{207}Pb, ^{208}Pb, ^{232}Th, ^{235}U and ^{238}U with each element being measured every 0.18 s with longer counting time on the Pb isotopes compared to the other elements. Each analysis on the zircons began with 5 laser shots with no data collection to clean the surface of any contamination, next a 30 second blank gas measurement followed by a further 30 seconds of analysis time when the laser was switched on.

The downhole fractionation, instrument drift and mass bias correction factors for Pb/U ratios on zircons were calibrated using the 91500 zircon (Wiedenbeck et al., 1995) that were analysed in duplicate throughout the analytical session to correct for any instrument drift in the Pb/U ratios. The NIST610 glass was used for calibration of the ^{207}Pb/^{206}Pb ratios using values from Baker et al. (2004) and was analysed along with the 91500 zircon throughout the run to correct for instrument drift. The NIST610 glass was also used to calibrate trace element concentrations in the zircon using reference values from Jochum et al. (2011) and with ^{91}Zr as the internal standard element assuming stoichiometric proportions in zircon. The data reduction and uncertainty propagation used was based on the method outlined in detail in Thompson et al. (2018) and is similar to that outlined in Halpin et al. (2014) and Paton et al. (2010).

Accuracy of the Pb/U ages was checked using several secondary reference zircons of varying age and U contents: Temora (Black et al., 2003), Plesovice (Sláma et al., 2008), Mudtank (Black and Gulson, 1978), AusZ-2 and AusZ-5 (Kennedy et al., 2014), Monastery (Zartman et al., 1999), and Penglai (Li et al., 2010). These secondary reference zircons were analysed throughout the session using the same spot size and conditions as used on the samples and were treated as unknowns.

^{40}Ar/^{39}Ar age dating was undertaken at the University of California Santa Barbara Ar-Ar laboratory, samples were crushed in a tungsten carbide jaw crusher and 100 – 250 µm sized chips were separated. Again, chips were cleaned using D.I. water and left in an ultrasonic bath for 1 hour, cleaned with D.I. water and left in the ultrasonic bath for another hour. The clean chips were further cleaned with D.I. water and partially digested using dilute HF. The HF was rinsed off the samples before being left again in a D.I. water ultrasonic bath. They were dried before the groundmass plagioclases were separated by Frantz magnetic separator. Irradiation and Ar–Ar incremental step heating methods follow those given in Faulds et al. (1995).

4. Results

A full table of age dates for Breiðdalur is shown in Table 2, the sample locations in Breiðdalur are shown in Figure 4 and an age progression is shown in Figure 5. All ^{40}Ar/^{39}Ar errors are reported in Table 2, generally samples gave reliable age plateaus though 2 samples with high error values had low Ca and K plagioclases. Errors presented in the table are 2σ, ranges are variable, with a minimum error of $\pm$0.1 My (Ar-Ar) and $\pm$0.1 My (U-Pb), for these age dates and most show an expected (from stratigraphic relations) age progression.

The oldest Breiðdalur lava is sample 470 from the lower eastern flank sequence situated 50 m above the base of Breiðdalur volcano (Figure 4). The results give an age of 10.1 (±0.2) Ma; suggesting Breiðdalur volcano's earliest lavas erupted between 10.1 (±0.2) and 10.15 (±0.15) Ma (Table 2). Next in the succession are two separate samples of 9.9 ±0.2 Ma, which lie around 1-200 m stratigraphically above the previous sample and just below the earliest known Icelandite lavas (Figure 4). The next sampled age progressions are samples 451 and 448, basaltic lavas exposed on Berufjarðartindur, dated respectively to 9.8 ±0.5 Ma and 9.7 ±0.6 Ma. The large errors on the samples are due to low Ca and K in the samples.

The oldest dated silicic magmatism from Breiðdalur is found in sample WP 470, a dacitic sheet containing zircons. The zircon yield was low in this sample and gave 2 populations of zircons (Figure 7a): one population gave the oldest currently dated silicic zircons from Breiðdalur at 9.57 ±0.39 My old, the other at 8.53 ±0.39 My old. The two populations suggests that one set, the older, is inherited into a younger magma and the younger are from a separate magma source or the magma was hot enough to reset the U-Pb ratio. This campaign's next oldest silicic magma age is 9.235 ±0.15 My old (Gunn1, Figure 7b), published age dates of other silicic magmatism in the Breiðdalur area give age dates of 9.3 ±0.2 Ma (Age for sample "Rauðf1, lava and dyke", from Rauðafell in Berufjörður; Martin and Sigmarsson (2010)) and 9.1 ±0.2 Ma or 9.2 ±0.2 Ma (Ar/Ar dates given for "Beruf1", a silicic intrusion on the northern coast of Berufjörður, U-Pb date 9.2 ±0.3; Martin et al. (2011)). Known dates for silicic magmatism fall into the bracket of 9.57 to 9.1 Ma, with an outlier of 8.53 ±0.37 Ma. Mafic magmatism continues throughout as is evident from the mixed and mingled rocks found as composite lavas and intrusions and more well mixed andesites.

Regional plateau basalts above the Breiðdalur central volcano, lap onto younger volcanics creating a structural discontinuity evident in the field. The stratigraphic structure does not appear to be a significant (outwith error) time disconformity, but is clearly an important structural marker. Sample 778, is a porphyritic basaltic lava flow which overlies the Fossárdalur composite lava flow Gibson and Walker (1963) and yields a date of 9.5 ±0.3 My old. Fossárdalur composite lava is suggested to link with Rauðafell intrusion on the north side of Berufjörður (Charreteur and Tegner, 2013; Gibson and Walker, 1963), this intrusion is dated to 9.3 ±0.2 Ma (see above Martin and Sigmarsson, 2010). The youngest lavas dated in the Breiðdalur area are sample 785 from Öxi, Berufjörður and a sample from Heiðarvatn olivine basalt group (Gans, personal comm.). Both samples yield dates of 9.1 ±0.15 Ma, and both lavas lap onto Breiðdalur central volcano and their contacts to the volcano are structurally discontinuous. These lavas are sourced from the west of Breiðdalur, but their origins are currently unknown.

Regional dyke activity progresses throughout the life of the central volcano, the oldest dykes are limited to the current erosion level. Sample 387, a dyke sampled from the high-density dyke area in Norðurdalur, Breiðdalur, is the oldest dyke analysed, giving a date of 9.9 ±0.2 Ma. A dyke dated in Berufjörður, Sample 532 (Gans, personal comm. and unpublished data), gives an age date of 9.8 ±0.4 My old. Another dyke, Sample 533 (Gans, unpublished data), was dated to 9.4 ±0.2 My old, this sample is from the southern side of Berufjörður and still thought to be part of the Breiðdalur system. Sample 492, a dyke sampled from western Berufjorður, gives a date of 9.25 ±0.2 My old. This dyke cross cuts plateau basalts and the Fossárdalur composite lava. The youngest regional dyke ages in this study are found at opposite sides of the Breiðdalur central volcano. Sample 392 is found in Norðurdalur and gave an intrusion date of 8.1 ±0.2 Ma. This sample is found just 10's of metres from the oldest dyke date from the Breiðdalur swarm and in the highest density dyke intrusion area of the swarm. Sample 534 (Gans, unpublished data), gives a date of 7.8 ±0.4 Ma, the dyke is found in Berufjörður, cross cutting a basaltic lava of 9.1 My old. These dates show the spread of dyke swarm activity in the Breiðdalur area is from 9.9 Ma to 7.8 Ma.

A single sample is currently regarded as being anomalous, with respect to the geology and a significant number of other dates. The sample age (sample 519) is shown in Table 2, the sample is currently interpreted as an intrusion in the upper caldera sequence or lower summit sequence, it is difficult to

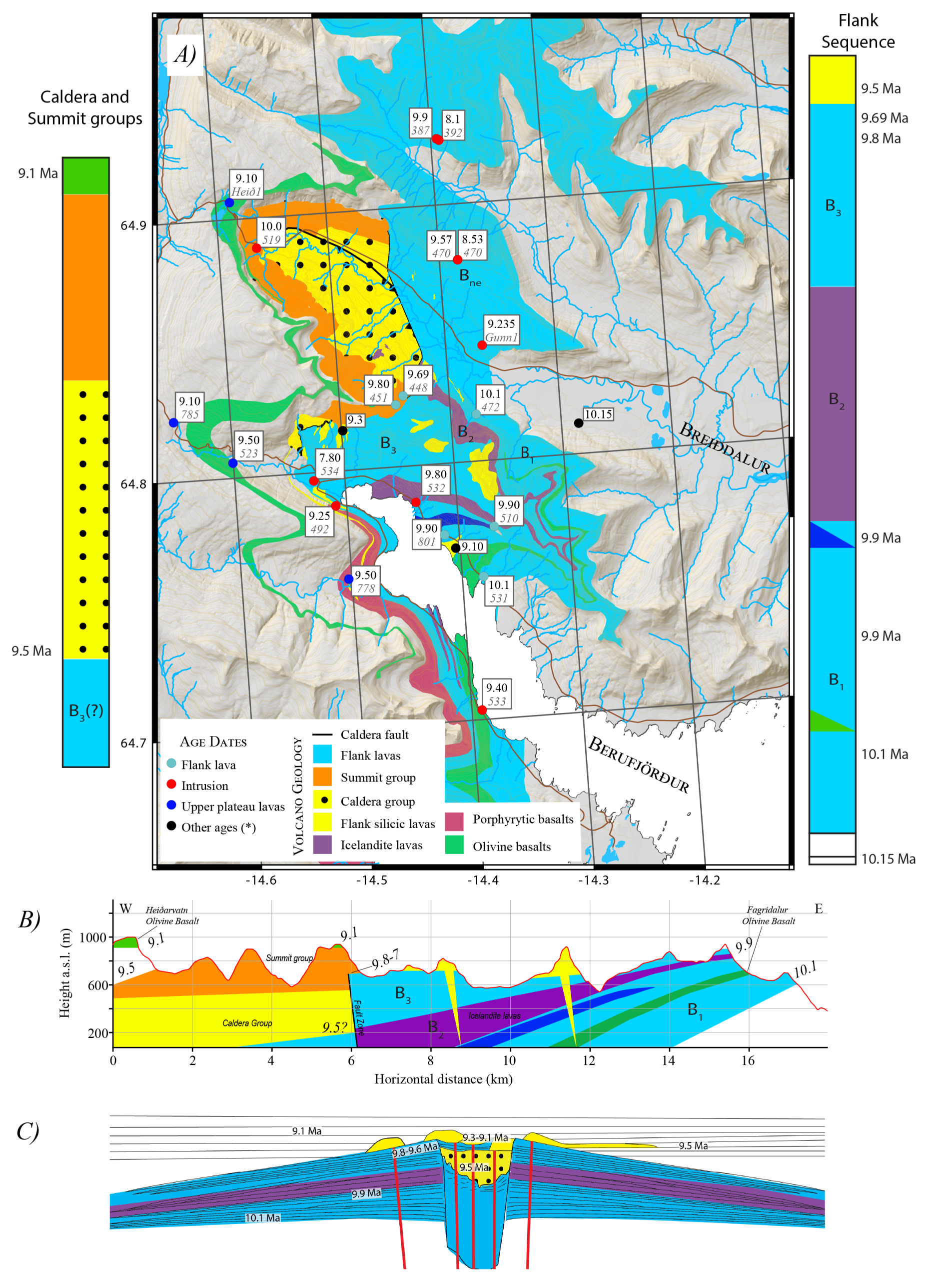

Figure 4: A) Age dates displayed in Table 2 shown on a simplified geological map of Breiðdalur volcano (Figure 3). *Other ages: 10.15 Riishuus et al. (2010), 9.3 and 9.1 Martin et al. (2011). B) Simplified cross section of the eastern flank, caldera and summit sequences

interpret this sample within the stratigraphy and with regards to a significant number of other dates. However, the sample is shown in order that it could offer information or reinterpretation in the event of further evaluation of the geology and geochronology of the area.

5. Discussion

5.1. Breiðdalur evolution

5.1.1. Early build-up of the central volcano

Our age dating campaign is one of the most concise studies undertaken in recent years on a specific central volcano sequence in Iceland. The availability of high precision $^{40}Ar/^{39}Ar$ dates has allowed us to visualise the progression of the volcanic terrane in time. Geological mapping undertaken previously suggests that the Breiðdalur volcano started with a sequence of mafic, tholeiitic lavas erupted onto plateau basalts. The activity began between 10.15 (Skessa Tuff) – 10.1 Ma (472) and appears to have progressed until around 9.7 Ma, when silicic lavas begin to erupt on the flanks of Breiðdalur. Activity and volcanic edifice build-up appears to progress quickly, through the 9.9 Ma Stöng group basaltic lavas, above which a 400 m thick sequence of andesites, basaltic andesites and basalts occurs, finally progressing into the rhyolite lavas of the SER and the summit sequences.

5.1.2. Caldera formation (explosive silicic)

It is thought that the caldera at the head of Breiðdalur formed in a large explosive eruption, this probably occurred between 9.8 – 9.5 Ma (Figure 5). The large age bracket is due to the high analytical uncertainty from 2 lavas (451 and 448 - summit group lavas) which were emplaced within the caldera and onto the flanks of the volcano. The lavas overlie a hyaloclastite, which emplaced into a small caldera lake and lie beneath a 100 m thick silicic lava of Berufjarðatindur and the ignimbrite of Matarhnjúkur. The large, explosive, caldera forming eruption mechanism is suggested due to the large amount of silicic pumice and remobilised silicic material (max. 500 m thick) continuous in the stratigraphy of Breiðdalur caldera sequence. There is evidence that the caldera had repeated 'nesting' events, forming smaller calderas within the main 8 – 10 km one (see Geological Background and Askew and Thordarsson (2019) In Prep.).

An estimate of the volume of the caldera sequences, gives an approximate value of 15 km^3. This is calculated assuming an average depth of the caldera to be around 300 m (maximum is 500 but tapers to the sides) and a minimum diameter of 8 km^2. The volume of material erupted from a single main-caldera forming event may be lower than this, as it does not calculate the 'dense rock equivalent' of the pumices and other tuff products or remove the volume of material from other events within the caldera.

5.1.3. Effusive and intrusive evolved volcanism

The oldest evolved magmatism in Breiðdalur began around 9.9 Ma, with the Flaga andesite lavas (above sample 510, Figure 4). Indicating the presence of a magma chamber which was fractionating primitive basalt magma or assimilating older crust. One of the oldest silicic age dates is from a remobilised magmatic zircon found in a mixed magma dacite sheet, this was dated to 9.57 (± 0.31) Ma. Silicic activity is shown to have progressed until 9.1 (± 0.2) Ma, after this time central volcano activity appears to effectively cease and some of the structurally highest central volcano lavas are buried by plateau basalts (Heið1, Figure 4, Table 2). Separate studies indicate 2 methods of producing silicic magmas at Breiðdalur: Schnell (1994); Charreteur and Tegner (2013) suggest fractional crystallisation of basaltic magma into silicic magma over the 3-400 Ky between the first andesites and the earliest silicic dates, whereas Martin and Sigmarsson (2010) suggest the continued heat input may have lead to large scale partial melting of basaltic crust beneath the volcano. Our study suggests both mechanisms probably occurred at the volcano, where earlier andesites were formed through fractional crystallisation, since little-to-no silicic magmatism occurs before this time. However, to produce the volume of silicic magmatism at Breiðdalur would require a huge amount of basaltic parent magma to fractionate, so

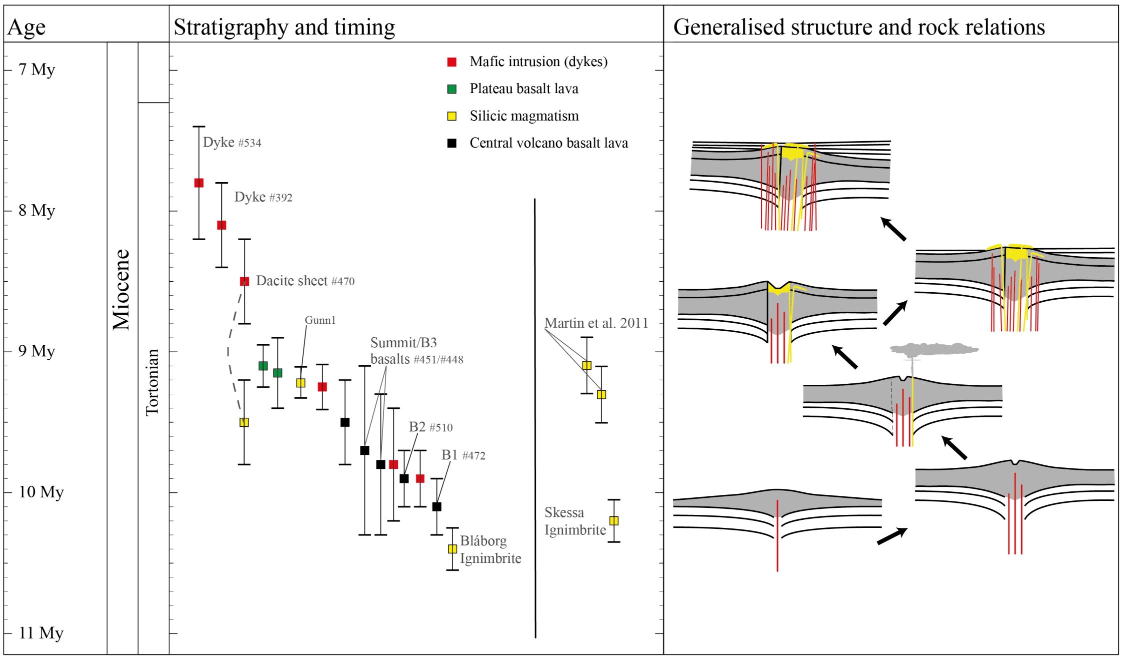

Figure 5: Stratigraphic representation of the age progression through Breiðdalur, dotted line links 2 ages from one sample. On the right is a generalised rock relation diagram of central volcano magmatism throughout time. Central volcano magmatism effectively ceases at around 9.1 Ma, younger dykes are found, so dyke/fissure swarm activity continues. Dates presented in the central partition are cited from Martin et al. (2011) and Skessa Ignimbrite age from Riishuus et al. (2010), all other dates are from this study.

much of the silicic magma probably formed from crustal partial melting. Magma mixing becomes an important and visible process within some magmas of the caldera sequence, but is most obvious in the composite lavas and dykes of the older volcano sequences e.g. Fossárdalur composite lava 9.3 Ma (see below).

5.1.4. Central volcano progression

It is thus suggested that the volcano of Breiðdalur was active for around 1 (± 0.2) My, where magmatic activity was concentrated in a central point now located at the head of the Suðdalur valley (Breiðdalur). The volcano began with mafic activity at around 10.1 Ma which progressed into more evolved effusive activity after 200 Ka, as a magma storage zone beneath the volcano fractionated. Continued heat flow to the volcano melted the basement crust forming silicic magmas and caused a caldera forming eruption between 9.8 and 9.5 Ma. The caldera had several smaller eruption events within it, creating a nested and deformed caldera area. Activity then shifts into a series of effusive silicic eruption, some of these probably erupted whilst the caldera was still active. Mafic and silicic lavas and tuffs of the 'summit group' sequence erupted onto the deformed caldera group sequence between 9.7 and 9.5 Ma. The overlap in caldera formation and caldera cessation (summit group) ages is due to high uncertainty in key samples. The summit sequence fills in much of the depressed topography of the caldera area, one of the final eruptions was the 2 km^3 Berufjarðartindur rhyolite lava, which may be associated with a thick ignimbrite on Matarhnjúkur. The progression appears to indicate that the intensity of silicic eruptions decreased with time: from a earlier explosive activity, to later more effusive activity which caps the volcano with silicic lavas. This may be caused by a change in volatile abundance within the magma storage zone through time.

This general stratigraphic progression is concurrent with other work on Icelandic Neogene volcanoes

(Berg, 2016; Furman et al., 1992) and with specific studies on silicic magma genesis at Breiðdalur (Schnell, 1994; Martin and Sigmarsson, 2010).

5.1.5. Plateau basalts above the volcano

The complex relationship between plateau basalts above Breiðdalur volcano and the central volcano itself is evident from geological mapping of the area. The structural discontinuity to the west of the volcano suggests that, whilst the volcano was still active, voluminous volcanism was occurring to the west of the Breiðdalur rift system after around 9.5 Ma. This volcanism appears to have caused the volcano to tilt to the west, meaning on-lapping lavas appear to bank up against the central volcano sequences. This relationship is not entirely clear-cut, since it may be that some of the youngest volcanic activity at the volcano was occurring coevally to the plateau basalts' eruption.

5.2. Dyke swarm relationship

The dykes in this project are found to the north and south of Breiðdalur, dykes to the south were sampled at an attitude between 0-150 m a.s.l. whereas more northerly dykes are well exposed at an altitude of around 500 m. 'Old' and 'young' dykes are found in both locations, southern dykes exposed at the head of Berufjörður are exposed in stratigraphically high lavas. Results of this age dating campaign (Table 2) show that the dyke swarm was active throughout much of the life of the central volcano, from the oldest dated dyke at 9.9 My (Sample 387), and continued long past much of the central volcano activity (10.1 – 9.1 Ma) to the youngest Breiðdalur dyke of 7.8 My (Sample 534). The 2 oldest dated dykes, 9.9 and 9.8 Ma, occur 2-300 Ka after the onset of central volcano volcanism, and approximately the same time as the upper flank lava sequence (Stöng and Flaga andesites) and summit sequences. The younger dykes ($<$9.4 Ma) all post-date the caldera collapse (9.8 – 9.5 Ma), and samples 392 and 534 post-date the youngest magmatism at the central volcano (9.1 Ma) by $>$1 My.

5.3. Mingled magmas

Mixed and mingled magmas of contrasting compositions are a significant aspect of Icelandic central volcanoes (Gibson and Walker, 1963), the interplay between two contrasting magmas can destabilise a system and cause magma movement (e.g. Blake, 1984, 1966; McGarvie, 1984; Sigurdsson and Sparks, 1981; Sparks and Marshall, 1986; Sparks et al., 1977). Gibson and Walker (1963) examined eastern Iceland composite features, they suggested that most rhyolite-basalt mixed and mingled magmas occurred during the latest stages of the central volcano. Their evidence for this comes from composite lavas, most remarkably the Fossárdalur composite lava in Berufjörður, which is in the very top sequence of the Breiðdalur volcano. This lava flow erupted between 9.3 – 9.5 Ma, post-dating the caldera event. The composite lavas and dykes are rhyolitic, containing basaltic enclaves, often displaying basaltic lava flow bases, or basaltic margins to intrusions.

A dacite sheet, found on the mountain Tóatindur in Breiðdalur, contains two populations of zircons, firstly from 9.57 Ma and a second population from 8.53 Ma. These two separate age dates in a single intrusion suggests 2 magmas of different ages became intermingled. Since most silicic magmatism is confined to ages younger than 9.1 My, it appears that the oldest population is related to a batch of magma from the silicic phase of the central volcano. The youngest zircons are not related to this activity and significantly post-dates the proposed central volcano end-date. This discrepancy may be caused by a magma intruding another older and partially solidified magma reservoir and picking up older zircons. If the later intruding magma body was mafic, the temperature difference may have overcome the closure T of the zircons and 'reset' some of them. This sample yielded only a handful of zircons, so re-sampling and analysing more zircons would be the only way to unravel this sample's history.

Mixed magmas of contrasting compositions are a significant hazard at central volcanoes, basaltic magma intruding a silicic body can mobilise the viscous silicic magma. This can lead to eruptions, many cases will cause explosive eruptions. This study suggests that, if sample 470's two zircon populations are caused by mingling of mafic and silicic magma, then magmas can be mobilised a significant time after silicic activity is thought to have ceased.

5.4. Regional Aspects

Breiðdalur is located along a rift system active from at least 13 Ma until around 8 – 7 Ma before a rift relocation shifted the axis (Helgason, 1984). The east fjords rift system includes the volcanoes shown in Figure 3 and those further north (shown in Hjartarson and Saemundsson (2014) for details). Exposed volcanoes generally young to the south, the volcano of Breiðavík in the north east of Iceland is around 13 My old and the volcanoes of Breiðdalur, Þingmúli and Álftafjörður are the youngest. Even younger exposed volcanoes to the south are thought to be due to the rift relocation around 6 – 7 Ma (Helgason, 1984). Our study has re-evaluated previous age dates of the volcanic stratigraphy in the southern part of eastern Iceland. Older K-Ar, Ar-Ar and paleomagnetic age dating (e.g. McDougall et al., 1976a,b; Ross and Mussett, 1976; Watkins and Walker, 1977; E. Mussett et al., 1980) can now be updated with more modern Ar-Ar age dates, in many cases the newer age dates show around 1 My difference to the older ages. Some of this discrepancy is shown in Figure 6, where the older dates do not fit the stratigraphy when related to other age dates even those of a similar analysis age. The re-evaluated age dates serve to provide a better fit to stratigraphy but the modelling still utilises older age dates where younger dates are not available, this suggests that there are many areas in need of revision. Some of the most significant adjustment of ages, are those near to Álftafjörður volcano. The dated lavas previously held ages of around 9 – 8 Ma, however, these do not correlate with the stratigraphic position of ages from Breiðdalur e.g. Bláberg ignimbrite at 10.4 Ma (Gans, pers. comm.), Skessa ignimbrite at 10.15 Ma (Riishuus et al., 2010) and age dates from this study (including a sample from above the Fossárvík Porphyritic group which on-laps the youngest part of Álftafjörður volcano (Blake, 1970). This reassessment suggests Álftafjörður was active around 10 – 9 Ma, though modern age dates would be required from the area to understand this completely. The volcanoes of (from north to south) Þingmúli, Breiðdalur and Álftafjörður are of the same age, all active during the same time period. Further to this, when taken at face value the diagram appears to show a general progression of volcanism toward the south west, with an 'over'-thickening toward the Vatnajökull ice cap. A challenge to this suggestion is that perhaps there are differential erosion rates which have exposed older stratigraphy to the north. However, the erosion rate would need to be higher in the north for this to be the case. In reality the erosion rate is highest to the south east around the Vatnajökull ice cap and most likely this has been the case for much of the Pliocene and Pleistocene. Zeolite zoning in the lava pile also agrees with the suggestion of a south west progression of activity and a lesser degree of burial of volcanics in the north east: lavas to the north east show fewer zeolites and lower temperature zeolites than found in lavas at an equivalent height above sea level to the south.

5.4.1. Central volcano model

Figure 5 outlines a schematic progression of the Breiðdalur central volcano:

A) At 10.1 Ma: The central volcano erupts mafic lavas onto a basement of plateau basalts, the central volcano lavas are thinner, presumably erupting onto slightly greater relief landscape than the thicker plateau basalts.

B) The central volcano built up a broad sided, shield-volcano for around 300 Ka. At 9.9 Ma a magma reservoir had formed beneath the volcano and fractionated mafic magma into andesites (Icelandite). The andesitic magmas erupted onto the flanks, continuing the build up of the central volcano edifice.

C) Between 9.8 and 9.5 Ma: A caldera forming event drastically changes the shape of the volcano, from that of a broad shield-volcano, to a caldera volcano. The caldera infilled with pumice breccia formed by the eruption. Subsequent activity within the caldera causes subsidence and smaller caldera events, these smaller depressions infilled with sediments, pumice, ash and lithic clasts, from the central volcano. Intrusions also occurred within the caldera post-formation, along with geothermal activity caused by heat from the magma bodies below.

D) Post-caldera collapse: Large volume silicic magmas erupt onto the caldera group, the summit sequence, and the flanks of the volcano, the SER. These are accompanied by composite magmatism, basaltic lavas and silicic tuffs. The thick silicic lavas would have formed a high 'cap' or summit to the volcano, with the impressive 200 m thick Berufjarðartindur rhyolite lava probably being one of the highest points in the area.

E) After 9.1 Ma: Silicic magmatism ceases at the central volcano at around 9.1 Ma. The central volcano does not continue to build an edifice and plateau basalt lavas become dominant. The plateau lavas bury the volcano relatively quickly, the Berufjarðartindur rhyolite lava is overlain by an olivine basalt group of lavas, dated to 9.1 Ma. The central volcano activity may have waned from 9.3 – 9.1 allowing plateau basalt activity to 'catch up' with the central volcano, or the errors within samples (±0.2 My) is more significant than the time taken for the burial of the volcano.

F) Dyke and rifting activity continues on the Breiðdalur volcanic system until 7.8 Ma, meaning the system is active for a total of 2.3 My.

5.5. Conclusion

A suite of samples from the Breiðdalur volcano were analysed for age dates using $^{40}Ar/^{39}Ar$ and U-Pb dating techniques. The results brought the following conclusions:

- Breiðdalur central volcano´s lifespan was around 1 My, from 10.1 – 9.1 Ma, the volcano's activity produced over 300 km^3 of erupted product.
- The Breiðdalur dyke swarm long outlives the central volcano which ceases activity around 9.1 Ma, dyke activity is continuous from 9.8 – 7.8 Ma.
- Thus, the Breiðdalur volcanic system was continuously active from 10.1 – 7.8 Ma, a total of 2.3 My.
- A fractionating magma reservoir was present beneath Breiðdalur from 9.9 Ma. The heat input from this magmatism allowed silicic magma to form through PM, which was contained in a storage zone beneath the volcano from 9.5 My, the magma body became significant enough to create an 8 – 10 km diameter caldera in a single event, and continued until 9.1 My. Mafic activity overtook the Breiðdalur system and subsequently buried the volcano.
- Furthermore, our study has re-evaluated age dates around Hamarsfjörður and Álftafjörður, suggesting that Álftafjörður volcano is around 11 – 9.5 My old. This has implications for regional temporal studies of the east fjords plateau basalts.

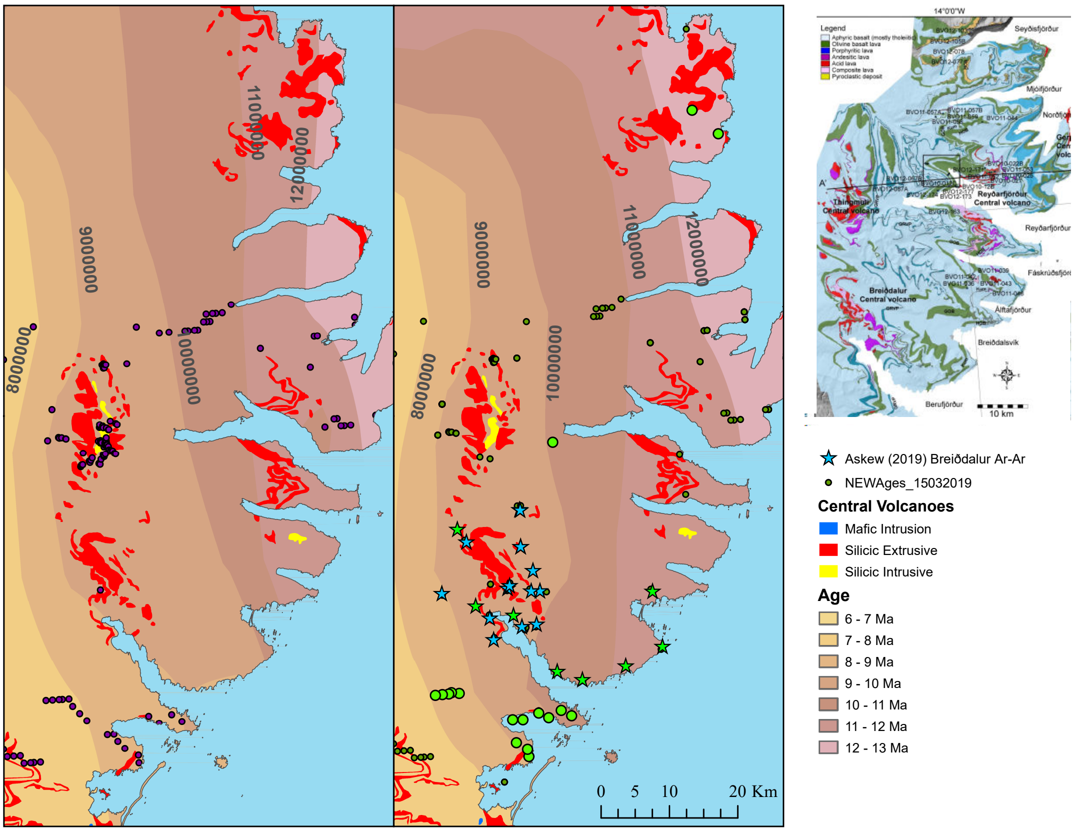

Figure 6: Geochronology of Eastern Iceland. Left) Older data points, ages compiled by Kitagawa (2006) using references therein, note the wide 9–10 My band and the non-fit to stratigraphy shown inset. Right) Reanalysed raster map using more modern age dates from this study (blue stars), P. Gans (unpublished dataset; green stars), Martin et al. (2011), Berg (2016) (from volcanoes to the north not shown in the data extent) and re-evaluated dates (green circles). Silicic lavas and intrusions are displayed to highlight central volcanoes.

Sample #	Analysis	Sequence	Lat.	Long.	Sample details	$^{40}Ar/^{39}Ar$	U-Pb	Error
Skessa[1]	GM				Skessa Tuff Ignimbrite[1]	10.15		± 0.1
472	GM	F	64.818147	-14.376627	Lower eastern flank lava	10.1		± 0.2
510	GM	F	64.774337	-14.367796	Mid-eastern flank lava	9.9		± 0.2
801	GM	F	64.772455	-14.413190	Mid-eastern flank lava	9.9		± 0.2
451	GM	S	64.824026	-14.449095	Summit sequence basalt lava	9.8		± 0.5
448	GM	S	64.827269	-14.441849	Summit sequence basalt lava	9.7		± 0.6
778	GM	U	64.757996	-14.502869	Plateau basalt (Fossárvík porphyrytic group) lava	9.5		± 0.3
Rauðf1[2]	GM	S			Rauðafell rhyolite lava[2]	9.3		± 0.2
785	GM	U	64.823157	-14.651802	Plateau basalt lava, Öxi	9.1		± 0.15
Heið1	GM	U			Plateau basalt lava, Heiðárvatn	9.1		± 0.15
519	GM	I	64.888376	-14.565322	Mafic sill in caldera	10		± 0.2
387	GM	I	64.925673	-14.394553	Dyke	9.9		± 0.2
532	GM	I			Dyke	9.8		± 0.4
470	U-Pb Zircon	I	64.827005	-14.440187	Dacitic Inclined Sheet **(01)		9.57	± 0.37
533	GM	I			Dyke	9.4		± 0.2
492	GM	I	64.786648	-14.509945	Dyke	9.25		± 0.16
Gunn1	U-Pb Zircon	I	64.844650	-14.366633	Rhyolitic dyke		9.235	± 0.15
Berufl[3]	GM	S			Berufjörður rhyolite intrusion[3]	9.1		± 0.2
470	U-Pb Zircon	I	64.827005	-14.440187	Dacitic Inclined Sheet **(02)		8.53	± 0.39
392	GM	I	64.925075	-14.392401	Dyke	8.1		± 0.3
534	GM	I			Dyke	7.8		± 0.2

Table 2: Age dates from lavas and dykes in the Breiðdalur system, upper section is lavas, lower section is intrusions. GM: Groundmass plagioclase $^{40}Ar/^{39}Ar$ analysis. F = Flank sequence; S = Summit sequence; U = Upper sequence lavas - not defined, lavas thought not to be sourced from the Breiðdalur volcano seen to be on-lapping onto the late stage volcano lavas; I = Intrusions. [1]Riishuus et al. (2010); [2]Martin and Sigmarsson (2010); [3]Martin et al. (2011) (Kelduskogar). **(#) Zircons from Sample 470 split into 2 populations 01 and 02, see text for details.

6. Acknowledgements

We acknowledge the support of the Research Fund of the University of Iceland granted to Thorvaldur Thordarson, as well as everyone that assisted with fieldwork and lab work throughout this project.

7. References

References

Albertsson, K., Hooker, P., Miller, J., 1982. A brief k-ar age study of the irdp borehole, reydarfjördur, eastern iceland. Journal of Geophysical Research: Solid Earth 87, 6566–6568.

Baker, J., Peate, D., Waight, T., Meyzen, C., 2004. Pb isotopic analysis of standards and samples using a 207pb–204pb double spike and thallium to correct for mass bias with a double-focusing mc-icp-ms. Chemical Geology 211, 275–303.

Åberg, G., Bollmark, B., Macintyre, R.M., 1987. Age of the austurhorn intrusion; a net-veined complex in southeastern iceland. GFF 109, 291–293.

Berg, S.E., 2016. Silicic Magma Genesis in Basalt-dominated Oceanic Settings : Examples from Iceland and the Canary Islands. Doctoral thesis, comprehensive summary. Department of Earth Sciences. URL: http://urn.kb.se/resolve?urn=urn:nbn:se:uu:diva-272318, doi:http://uu.diva-portal.org/smash/get/diva2:893923/PREVIEW01.jpg.

Black, L., Gulson, B., 1978. The age of the mud tank carbonatite, strangways range, northern territory. J. Aust. Geol. Geophys. 3, 227–232.

Black, L.P., Kamo, S.L., Allen, C.M., Aleinikoff, J.N., Davis, D.W., Korsch, R.J., Foudoulis, C., 2003. Temora 1: a new zircon standard for phanerozoic u–pb geochronology. Chemical geology 200, 155–170.

Blake, D., 1966. The net-veined complex of the austurhorn intrusion, southeastern iceland. The Journal of Geology , 891–907.

Blake, D., 1970. Geology of alftafjordur volcano, a tertiary volcanic centre in south-eastern iceland. Scientia Islandica 2, 43–63.

Blake, S., 1984. Magma mixing and hybridization processes at the alkalic, silicic, torfajökull central volcano triggered by tholeiitic veidivötn fissuring, south iceland. Journal of volcanology and geothermal research 22, 1–31.

Charreteur, G., Tegner, C., 2013. Magmatic emulsion texture formed by mixing during extrusion, rauðafell composite complex, breiðdalur volcano, eastern iceland. Bulletin of volcanology 75, 1–17.

E. Mussett, A., G. Ross, J., L. Gibson, I., 1980. ^{40}ar/^{39}ar dates of eastern iceland lavas. Geophysical Journal of the Royal Astronomical Society 60, 37 – 52. doi:10.1111/j.1365-246X.1980.tb02579.x.

Faulds, J.E., Feuerbach, D.L., Reagan, M.K., Metcalf, R.V., Gans, P., Walker, J.D., 1995. The mount perkins block, northwestern arizona: An exposed cross section of an evolving, preextensional to synextensional magmatic system. Journal of Geophysical Research: Solid Earth 100, 15249–15266.

Fridleifsson, G.O., 1983. Geology and the alteration history of the Geitafell central volcano, southeast Iceland. Ph.D. thesis. Earth Sciences.

Furman, T., Meyer, P.S., Frey, F., 1992. Evolution of icelandic central volcanoes: evidence from the austurhorn intrusion, southeastern iceland. Bulletin of volcanology 55, 45–62.

Gibson, I., Walker, G.P., 1963. Some composite rhyolite/basalt lavas and related composite dykes in eastern iceland. Proceedings of the Geologists' Association 74, 301–303.

Gústafsson, L.E., 1992. Geology and petrography of the Dyrfjöll Central Volcano, eastern Iceland. volume 138. Selbstverlag Fachbereich Geowissenschaften, FU Berlin.

Gudmundsson, A., 1995. Infrastructure and mechanics of volcanic systems in iceland. Journal of Volcanology and Geothermal Research 64, 1–22.

Gudmundsson, A., 2000. Dynamics of volcanic systems in iceland: Example of tectonism and volcanism at juxtaposed hot spot and mid-ocean ridge systems. Annual Review of Earth and Planetary Sciences 28, 107–140. URL: http://www.annualreviews.org/doi/abs/10.1146/annurev.earth.28.1.107, doi:doi:10.1146/annurev.earth.28.1.107.

Gudmundsson, A., 2002. Emplacement and arrest of sheets and dykes in central volcanoes. Journal of Volcanology and Geothermal Research 116, 279–298. URL: http://www.sciencedirect.com/science/article/pii/S0377027302002263, doi:https://doi.org/10.1016/S0377-0273(02)00226-3.

Halpin, J.A., Jensen, T., McGoldrick, P., Meffre, S., Berry, R.F., Everard, J.L., Calver, C.R., Thompson, J., Goemann, K., Whittaker, J.M., 2014. Authigenic monazite and detrital zircon dating from the proterozoic rocky cape group, tasmania: Links to the belt-purcell supergroup, north america. Precambrian Research 250, 50–67.

Hartley, M.E., Thordarson, T., 2013. The 1874–1876 volcano-tectonic episode at askja, north iceland: Lateral flow revisited. Geochemistry, Geophysics, Geosystems 14, 2286–2309.

Helgason, J., 1984. Frequent shifts of the volcanic zone in iceland. Geology 12, 212–216.

Hjartardóttir, Á.R., Einarsson, P., Bramham, E., Wright, T.J., 2012. The krafla fissure swarm, iceland, and its formation by rifting events. Bulletin of Volcanology 74, 2139–2153.

Hjartarson, A., Saemundsson, K., 2014. Geological map of iceland, bedrock. 1: 600,000. Iceland GeoSurvey, Reykjavík .

Jochum, K.P., Weis, U., Stoll, B., Kuzmin, D., Yang, Q., Raczek, I., Jacob, D.E., Stracke, A., Birbaum, K., Frick, D.A., et al., 2011. Determination of reference values for nist srm 610–617 glasses following iso guidelines. Geostandards and Geoanalytical Research 35, 397–429.

Kennedy, A.K., Wotzlaw, J.F., Schaltegger, U., Crowley, J.L., Schmitz, M., 2014. Eocene zircon reference material for microanalysis of u-th-pb isotopes and trace elements. The Canadian Mineralogist 52, 409–421.

Kitagawa, H., 2006. Petrological and geochemical study of the Icelandic Tertiary lavas: Implications for the evolution of Iceland mantle plume. Ph.D. thesis. Department of Earth and Planetary Sciences.

Kosler, J., 2001. Laser-ablation icpms study of metamorphic minerals and processes. Laser-ablation-ICPMS in the Earth Sciences; Principles and Applications Mineralogical Association of Canada Short Course Handbook 29, 185–202.

Li, X.H., Long, W.G., Li, Q.L., Liu, Y., Zheng, Y.F., Yang, Y.H., Chamberlain, K.R., Wan, D.F., Guo, C.H., Wang, X.C., et al., 2010. Penglai zircon megacrysts: a potential new working reference material for microbeam determination of hf–o isotopes and u–pb age. Geostandards and Geoanalytical Research 34, 117–134.

Martin, E., Paquette, J.L., Bosse, V., Ruffet, G., Tiepolo, M., Sigmarsson, O., 2011. Geodynamics of rift–plume interaction in iceland as constrained by new 40ar/39ar and in situ u–pb zircon ages. Earth and Planetary Science Letters 311, 28–38. URL: http://www.sciencedirect.com/science/article/pii/S0012821X11005000, doi:https://doi.org/10.1016/j.epsl.2011.08.036.

Martin, E., Sigmarsson, O., 2010. Thirteen million years of silicic magma production in iceland: links between petrogenesis and tectonic settings. Lithos 116, 129–144.

McDougall, I., Watkins, N.D., Kristjansson, L., 1976a. Geochronology and paleomagnetism of a miocene-pliocene lava sequence at bessastadaa, eastern iceland. American Journal of Science 276, 1078–1095. URL: http://www.ajsonline.org/content/276/9/1078.short, doi:10.2475/ajs.276.9.1078, arXiv:http://www.ajsonline.org/content/276/9/1078.full.pdf+html.

McDougall, I., Watkins, N.D., Walker, G.P.L., Kristjansson, L., 1976b. Potassium-argon and paleomagnetic analysis of icelandic lava flows: Limits on the age of anomaly 5. Journal of Geophysical Research (1896-1977) 81, 1505–1512. URL: https://agupubs.onlinelibrary.wiley.com/doi/abs/10.1029/JB081i008p01505, doi:10.1029/JB081i008p01505, arXiv:https://agupubs.onlinelibrary.wiley.com/doi/pdf/10.1029/JB081i008p01505.

McGarvie, D.W., 1984. Torfajokull: A volcano dominated by magma mixing. Geology 12, 685–688.

Moorbath, S., Sigurdsson, H., Goodwin, R., 1968. K/ar ages of the oldest exposed rocks in iceland. Earth and Planetary Science Letters 4, 197 – 205. URL: http://www.sciencedirect.com/science/article/pii/0012821X68900356, doi:https://doi.org/10.1016/0012-821X(68)90035-6.

Padilla, A., Miller, C., Carley, T., Economos, R., Schmitt, A., Coble, M., Wooden, J., Fisher, C., Vervoort, J., Hanchar, J., 2016. Elucidating the magmatic history of the austurhorn silicic intrusive complex (southeast iceland) using zircon elemental and isotopic geochemistry and geochronology. Contributions to Mineralogy and Petrology 171, 69.

Paton, C., Woodhead, J.D., Hellstrom, J.C., Hergt, J.M., Greig, A., Maas, R., 2010. Improved laser ablation u-pb zircon geochronology through robust downhole fractionation correction. Geochemistry, Geophysics, Geosystems 11.

Riishuus, M., Miggins, D., Koppers, A., Duncan, R., 2010. 40ar/39ar incremental heating experiments on celadonite from the skessa tuff, eastern iceland: Thermochronology of low-temperature alteration of a flood basalt pile during burial metamorphism, in: AGU Fall Meeting Abstracts, p. 4873.

Ross, J., Mussett, A., 1976. 40ar/39ar dates for spreading rates in eastern iceland. Nature 259, 36.

Saemundsson, K., 1979. Outline of the geology of iceland. Jökull 29, 7–28.

Saemundsson, K., 1991. Geology of the Krafla area. Icelandic Natural Sci. Soc., Reykjavík. volume 29. journal article 2. pp. 24–95.

Schnell, T., 1994. Breiðdalur central volcano, eastern Iceland: genesis of the evolved rocks. Thesis. Department of Earth Sciences.

Sigurdsson, H., Sparks, R., 1981. Petrology of rhyolitic and mixed magma ejecta from the 1875 eruption of askja, iceland. Journal of Petrology 22, 41–84.

Sláma, J., Košler, J., Condon, D.J., Crowley, J.L., Gerdes, A., Hanchar, J.M., Horstwood, M.S., Morris, G.A., Nasdala, L., Norberg, N., et al., 2008. Plešovice zircon—a new natural reference material for u–pb and hf isotopic microanalysis. Chemical Geology 249, 1–35.

Sparks, R.S.J., Marshall, L.A., 1986. Thermal and mechanical constraints on mixing between mafic and silicic magmas. Journal of Volcanology and Geothermal Research 29, 99–124. URL: http://www.sciencedirect.com/science/article/pii/0377027386900417, doi:http://dx.doi.org/10.1016/0377-0273(86)90041-7.

Sparks, S.R., Sigurdsson, H., Wilson, L., 1977. Magma mixing: a mechanism for triggering acid explosive eruptions. Nature 267, 315.

Thompson, J.M., Meffre, S., Danyushevsky, L., 2018. Impact of air, laser pulse width and fluence on u–pb dating of zircons by la-icpms. Journal of Analytical Atomic Spectrometry 33, 221–230.

Thordarson, T., Larsen, G., 2007. Volcanism in iceland in historical time: Volcano types, eruption styles and eruptive history. Journal of Geodynamics 43, 118–152.

Walker, G.P., 1962. Tertiary welded tuffs in eastern iceland. Quarterly Journal of the Geological Society 118, 275–290.

Walker, G.P., 1963. The breiddalur central volcano, eastern iceland. Quarterly Journal of the Geological Society 119, 29–63.

Walker, G.P., 1964. Geological investigations in eastern iceland. Bulletin Volcanologique 27, 351–363. URL: http://dx.doi.org/10.1007/BF02597532, doi:10.1007/bf02597532.

Walker, G.P.L., 1974. The structure of eastern iceland, in: Kristjansson, L. (Ed.), Geodynamics of Iceland and the North Atlantic Area, Springer Netherlands, Dordrecht. pp. 177–188.

Watkins, N., Walker, G., 1977. Magnetostratigraphy of eastern iceland. American Journal of Science 277, 513–584.

Wiedenbeck, M., Alle, P., Corfu, F., Griffin, W., Meier, M., Oberli, F., Quadt, A.v., Roddick, J., Spiegel, W., 1995. Three natural zircon standards for u-th-pb, lu-hf, trace element and ree analyses. Geostandards newsletter 19, 1–23.

Zartman, S., Richardson, S., Gurney, J., Moore, R., 1999. in: Proceedings of the 7th International Kimberlite Conference: (J.B. Dawson volume). Authors A-K, Red Roof Design.

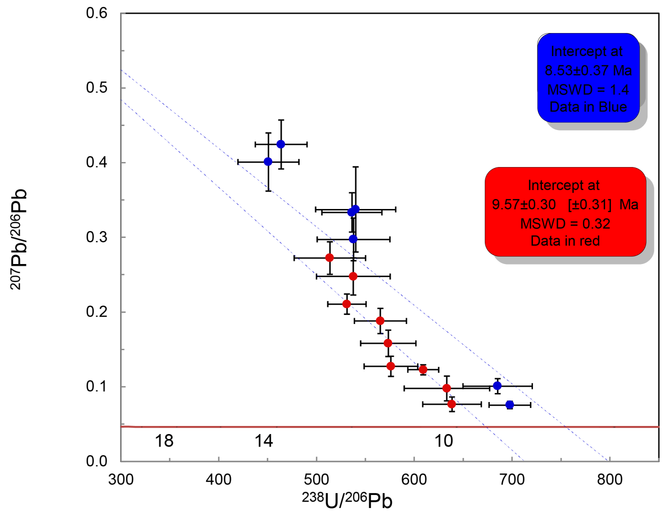

(a) Sample 470

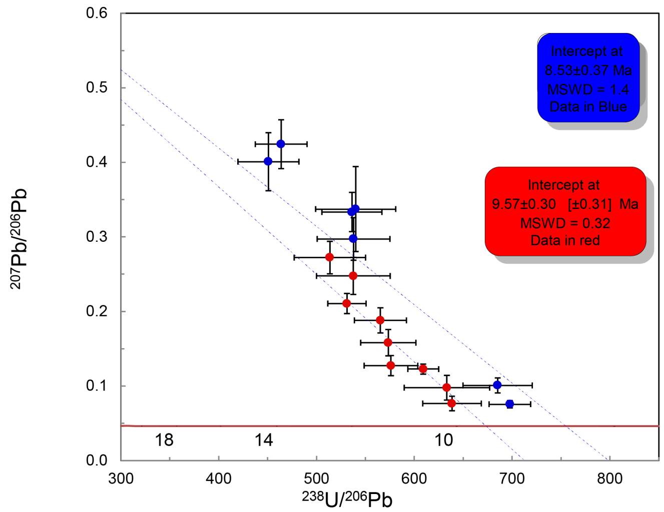

(b) Sample Gunn1

Figure 7: Conchordia diagrams for samples Gunn1 and 470.

A.3 Paper 3: Geochemistry of the Breiðdalur volcanic system

Geochemistry of the Breiðdalur volcanic system

Robert A. Askew[1a], Thorvaldur Thordarson[a]

[a]Institute of Earth Sciences, University of Iceland, Sturlugata 7, 101, Reykjavik

Abstract

This study provides a concise overview of geochemical evolution throughout the volcanic life of the Breiðdalur central volcano and the associated dyke swarm. The study is coupled with age dates taken during a study alongside this, and detailed geological mapping, to fit the geochemical data into a stratigraphic and temporal framework. The Breiðdalur volcano is a tholeiitic to slightly transitional volcano, comprised of a flank of tholeiitic basaltic lavas and icelandite lavas that covers around 350 km^2. The icelandite lavas appear to be related to the basaltic lavas through fractional crystallisation. An 8 – 10 km wide caldera sits at the head of Breiðdalur, filled with up to 500 m of silicic pumice breccia, silicic lavas cap the caldera sequence as well as the flank sequences. The silicic magmas at Breiðdalur are voluminous and generally occur later in the volcano's life. The magma volume alone suggests these were formed through a predominant partial melting of basaltic crust, this also appear to be backed up by new Sr isotope data. Any magmatic trends seen can be attributed to mixing of basaltic to intermediate magmas with silicic magmas, rather than fractional crystallisation, though both play a role.

1. Introduction

The Breiðdalur volcano and volcanic system, is a well exposed Miocene age central volcano and dyke swarm (Walker, 1963, Askew and Thordarson, Submitted). The exposures in the incised, fjord landscape, gives an almost complete picture of the volcanic evolution of this volcano throughout its 1 My life. Previous geological mapping and age dating provides a stratigraphic framework allowing for a precise history of the volcano, which further geochemical analysis fits into.

In this investigation, we analyse samples taken from over 70 location throughout the Breiðdalur volcano, and couple this with previous geochemical and petrological data acquired by other authors e.g Walker, 1963; Schnell, 1994, along with previous field mapping and age dates taken in the same campaign (Askew and Thordarson, Submitted; Askew et. al., Submitted). The samples provide a concise overview of the geochemistry of a single volcanic system, the basement lavas beneath this volcano and the lava envelope surrounding it, as well as providing a framework for understanding any variations in lava geochemistry throughout the life of the system. We delve further into the question of the formation of silicic magmas at this volcano, since 2 separate publications brought 2 separate conclusions through different analysis methods. The first study by Schnell (1994) suggested that the rhyolites of Breiðdalur volcano were formed through a process of fractional crystallisation with a minimal amount of assimilation of surrounding country rock. This was concluded after analysis of mineral scale geochemistry and Sr isotope results from a suite of basaltic - icelanditic - rhyolitic rock throughout Breiðdalur. A later study by Martin and Sigmarsson (2010) deduced that rhyolites at Breiðdalur must be produced by partial melting of plateau basalts, their deduction was based on results of O and Nd isotope analyses on rhyolites along with trace and Th concentrations in those rocks. Notably however, their suggestion that partial melting of hydrated basaltic crust causes rhyolites to have δ18O ratios of less than 5‰, directly contradicts the result of one of the Breiðdalur rhyolites' $\delta^{18}O$ of over 5‰. Charreteur et al. (2013) utilised MELTS (Gualda et al., 2012) to suggest 2 methods of forming

[1]Present address: Icelandic Institute of Natural History, Urriðaholtsstræti 6-8, 210 Garðabær, Iceland.

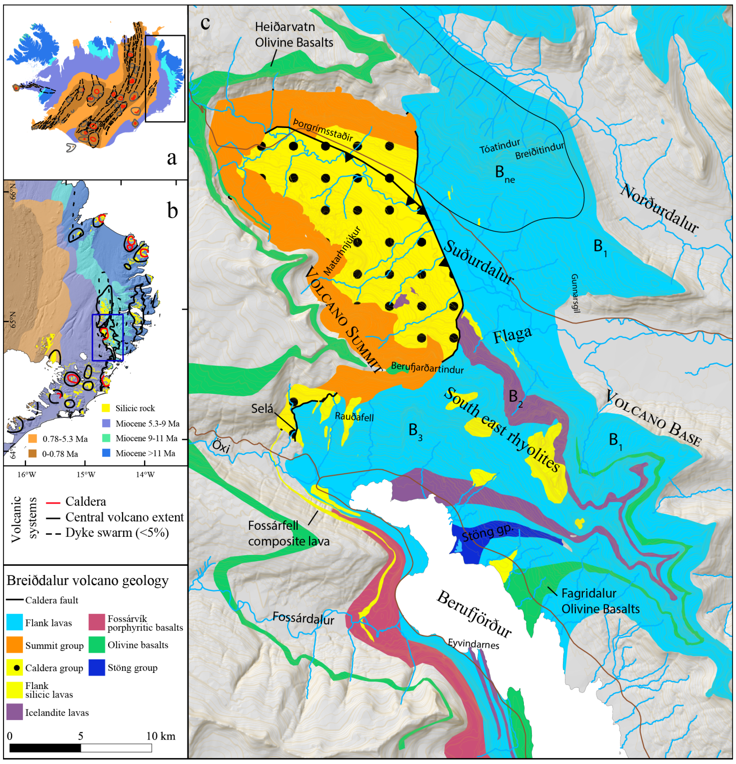

Figure 1: The study area. a) Icelandic geology, black box is: b) east fjords volcanic systems, Breiðdalur shown in in the blue box. c) Breiðdalur volcano geology and localities, B_1: Lower eastern flank sequence, B_2: Icelandite lava sequence, B_3: Upper eastern flank sequence and B_{ne}: North eastern flank sequence. Samples were taken from within the volcano and the plateau basalt envelope around the volcano.

evolved rocks at Þingmúli central volcano, located 20 km north of Breiðdalur (Figure 1). Their study indicated that evolved rocks at Þingmúli may be produced by fractional crystallisation in two environments at the central volcano, a reduced or more closed system, and a reduced system open to hydrothermal fluids. Rhyolite-MELTS is used to investigate, among other processes, fractional crystallisation pathways in magmatic systems. Our investigation will also test the 2 hypotheses of magmatic evolution and formation of silicic magmas through MELTS modelling, Sr isotope ratios and field geology investigations.

Breiðdalur volcano is known to be broadly tholeiitic (Walker, 1963; Schnell, 1994), Þingmúli volcano is also tholeiitic. The basalt to rhyolitic rocks at Þingmúli are often referred to as the 'classic' tholeiite fractional crystallisation trend (e.g. Arculus, 2003; Kitagawa et al., 2008), though this was readdressed by Charreteur et al. (2013) as discussed above.

2. Geological Setting

Breiðdalur volcanic system, located in eastern Iceland (Figure 1), comprises a caldera volcano and extensive fissure swarm residing within a glacially incised fjord landscape. Geological mapping of the lava sequences in the area shows a transition from the basaltic plateau lava stratigraphy, seen across much of eastern Iceland, to the pale coloured rocks of more evolved volcanic sequences. The volcanic system itself spans 350 km^2 of land, but the main edifice is more localised (throughout Berufjörður and the Breiðdalur) covering approximately 40 km^2 and comprises a 10 km wide caldera. Activity has been characterised by both abundant explosive and effusive, mafic-silicic volcanism, in addition to significant paleo-geothermal activity. The discovery of the Breiðdalur central volcano, and the presence of central volcanoes in eastern Iceland, is attributed to the work of George Walker in the 1960's, with a seminal paper (Walker, 1963) describing and mapping out Breiðdalur volcano. The volcano is well exposed across much of the landscape and is consequently easily accessible by main roads and tracks. Hence, it provides a perfect natural laboratory for the study of volcanological and magmatic processes in Iceland.

The Breiðdalur system lies within the east fjords chain of volcanoes, where around 22 volcanic systems are exposed bracketing ages from 13 – 5 Ma.

2.1. Geology of the Breiðdalur Volcanic System

The extent of the Breiðdalur volcanic system is outlined in Figure 1, the central volcano extends from southernmost outcrops near Djúpivogur to northernmost outcrops to the west of Reyðarfjörður. The volcano spans around 350 km^2, the Breiðdalur dyke swarm extends several km further north, in total the swarm is 50 km long from north to south and 10 - 15 km wide. The dyke swarm mostly comprises of basaltic dykes which can be several metres thick, a single dyke may be traced many km's to at least 15 km (Gudmundsson, 2002). The central volcano was, during its mature stage, a broad sided edifice, with a height of up to 1 – 1.5 km above the surrounding plateau basalt terrane (Askew and Thordarson, Sumitted).

The volcano is split into units descriptive of their location (Figure 1). These units are termed: flank sequences, caldera sequences, summit sequences, the South Eastern Rhyolites (SER) group and the dyke swarm. The base of the volcano is suggested to be the point at which grey >5 m thick plateau lavas are overlain by thin < 5 m, black basaltic lavas, these thin lavas sit atop a basaltic, plagioclase phyric, plateau lava group, the Grænavatn Porphyrytic Group (GPG). This again overlies the 10.15 My old Skessa Tuff ignimbrite (Walker, 1962; Riishuus et al., 2010, Askew and Thordarson, Submitted). The plateau lavas are sourced from fissure swarm eruptions on volcanic systems generally outwith the central volcano area, they are almost entirely basaltic in composition. These plateau lavas are the main country rock forming the basement of the volcano.

The *flank sequence* unit is a 1000 m thick sequence of predominantly basaltic lavas sourced from the central volcano. These lavas formed a broad shield-like edifice which spanned many 10's of kilometres, the breadth of the volcano was in part due to the relatively low relief landscape surrounding these volcanoes during the Neogene. The base of the flank sequence is the base of the Breiðdalur volcano (Figure 1), where there is a distinct morphology change in lavas as described above. Due to the westward dip of the lava pile in eastern Iceland, and the east-west valley morphology, only the eastern flanks of Breiðdalur are well exposed. The flank sequence is broken down into 4 component sequences:

- B_1: Lower (oldest) east flank basaltic lavas 10.1 – 9.9 Ma.
- B_2: Mid-east flank 'Flaga' icelandite lavas 9.9 – 9.8 Ma.
- B_3: Upper east flank basaltic lavas >9.8 Ma.
- B_{ne}: Northeast flank mafic to intermediate lavas.

Intermediate lavas are exposed within the flank sequences, though they represent a relatively minor amount of the stratigraphy. They form thick (10 - 25 m) lavas and in the B_2 sequence, form a significant group, up to a total of 400 m thick (Askew and Thordarson, Sumitted). In the north east of Breiðdalur (B_{ne}) basaltic icelandite to icelandite lavas crop out though do not form a single thick sequence.

Caldera sequence unit: Possibly the starkest feature of the Breiðdalur volcano is that most of the valley head is comprised of the altered pumice breccia and sediments that once infilled a large depression in the centre of the volcanic edifice (yellow with dots, Figure 1). There is evidence for smaller, nested, calderas within the main edifice: variable dips up to 70°; remobilised tuff and pumices; siltstones, trace fossils and hyaloclastites, indicating water filled depressions; the Matarhnjúkur ignimbrite also sits within a depression (possibly self formed). The caldera group is mapped a single sequence comprising of several rock formation groups: the significant Agglomerate group (which includes sediments and breccias); silicic lavas; mafic lavas and mafic to silicic intrusions. The caldera group is bounded to the east and south by a caldera fault where a sharp boundary between the agglomerate and flank sequence lavas is visible. There is significant geothermal alteration throughout the caldera sequence.

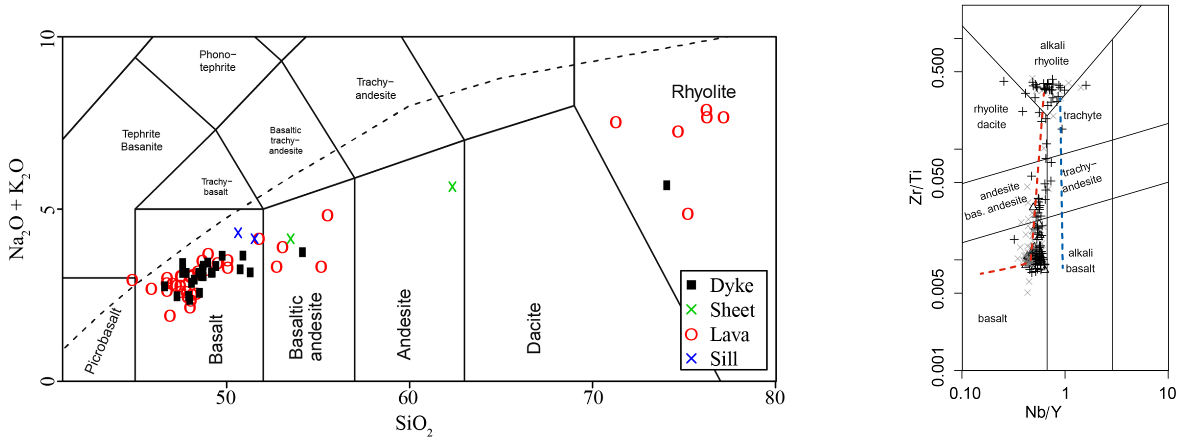

(a) (b)

Figure 2: Discrimination diagrams, Breiðdalur and comparison to immobile elements. Figure (b): X = Breiðdalur; + = Þingmúli; Δ = Álftafjörður dykes. Red line = Typical tholeiite trend (NVZ/WVZ). Blue line = Alkaline trend (Hekla). This indicates that, though alteration can cause mobility of alkaline elements, this does not affect the rocks to a notable extent in discriminating samples. Þingmúli data from Carmichael (1964); Charreteur et al. (2013); Wood (1978); O'nions et al. (1977), Álftafjörður data from Gallagher (2013). (a) TAS diagram (Le Bas et al., 1986) displaying geochemical data from Breiðdalur volcanic system. Alkali elements may be subject to some alteration post-emplacement, but the same results are found in alternative classification diagrams. (b) Immobile trace element diagram, to compare Neogene volcanic systems. From Winchester and Floyd (1977) modified by Pearce (1996).

The final unit of the central volcano itself is defined as 2 separate sub-units, the *Summit group* and the *South Eastern Rhyolites*. The terminology difference is due to their location though their stratigraphic level is similar. In some cases flows can be inferred or directly linked to source vents (Walker, 1963; Schnell, 1994, Askew and Thordarson, In Review). Silicic lava flows in Breiðdalur are of a significant and sometimes remarkable size. A flow-banded rhyolite lava exposed across Berufjarðartindur is up to 200 m thick (140 m average) and exposed for 2-3 km with an inferred area of around 14 km^2, field relations suggest the entire volume of lava could be around 2 km^3 (Schnell, 1994). The total exposed area of silicic magmatism at Breiðdalur is 31.6 km^2, total exposed mafic and intermediate magmatism by area (central volcano only) is 190.5 km^2 meaning that silicic magmatism accounts for 17% of the exposed rock at Breiðdalur.

In the late stages of the volcano's life, rifting to the west of the Breiðdalur system and subsequent loading of the crust by lavas from the rift zones caused a slight tilting of Breiðdalur volcano. The volcano was buried by plateau basalts and a west dipping disconformity is visible between volcano sequences and plateau basalts burying it.

Throughout the lifespan of the Breiðdalur system, a fissure swarm was active to the north and south of the central volcano, erupting lavas onto the northern and southern flanks of the volcano. This is exposed today as the Breiðdalur dyke swarm, the swarm stretches 40—50 km trending NNE—SSW. In the north, there is some cross over with the Þingmúli dyke swarm and to the south with Álftafjörður's. At the highest density, the dyke swarm comprises at least 20 % of the stratigraphy in a traverse of around 100 m east–west. The dykes vary in thickness from 10's centimetres to metres in width and many show evidence of multiple intrusions. There is a significant gap in dyke density around the Breiðdalur caldera, either due to older dykes being destroyed during caldera collapse or a change in stress field from N-S trending to a radial stress field around the magma reservoir of Breiðdalur volcano.

2.2. Sampling

Samples were collected throughout the stratigraphy of the volcanic system, the greatest effort was on dykes of the dyke swarm and lavas of the central volcano. Plateau basalts were also sampled below the volcano in order to provide an overview of the sequence pre-volcano, and likewise for plateau basalts post-volcano.

Intrusions within the caldera, within the flank sequences and intrusions of the sheet swarm were also sampled. The emphasis of this project was upon the relationship between the volcano and the dyke swarm, thus most of the samples are representative of the basaltic lavas and dykes

3. Methods

3.1. Major and Trace Elements

The majority of major and trace element analysis was undertaken through the University of Edinburgh XRF facility according to methods outlined in Fitton et al. (1998). Samples were crushed and milled to homogenisation using a tungsten carbide mill. The homogenous powder was used to create pressed powder pellets for trace element analysis and glass pellets, using the following methodology, for major element analysis. Glass beads were made by firstly heating the sample powders at 1100°C to remove volatiles, the dry sample was reweighed and mixed with LiB flux in order to reduce the melting T of the sample. The samples were then heated to 1100°C and melted. The melt was transferred to a carbon cast and left to cool into glass. The trace elements and majors were analysed on a Panalytical PW2404 wavelength-dispersive sequential X-ray spectrometer with a 3kW Rh-anode, end-window tube by Nick Oddling at the University of Edinburgh (Standards: Table 1).

3.2. Sr Isotopes

Sr isotopes were analysed on a handful of samples at the Pheasant Memorial Lab, Misasa, Japan.

Acid leaching was undertaken using 8 ml 6M HCl, the sample-acid mix was ultrasonicated for 2 hours, removed and centrifuged for 5 minutes at 3000 RPM. The acid was removed from the beaker and kept in PP bottle for analysis of elements lost. 8 ml USQ water was added to the sample which was then centrifuged again for 5 minutes, the water was removed and discarded. The addition and removal of water was repeated 2 more times (3 total). Sample decomposition followed procedure '3' in Yokoyama et al. (1999).

After sample decomposition 1.0 ml of 4.0 M HCl was added and to the sample and the sample placed in an ultrasonic bath for up to 30 minutes. The solution was then poured into a concave beaker and centrifuged for 5 minutes. The columns were prepared with BioRad 50W "X10" resin (1.0 ml) and cleaned using 6 M HCl, MilliQ, second 6M HCl and USQ. The resin was conditioned with 1.0 ml of 4.0 M HCl, when the conditioning acid was drained from the resin the 1.0 ml of the sample solution was loaded onto the column. After loading, the column was washed with a total of 2.5 ml of 2.8 M HCl. Once washed a clean flat bottomed beaker was placed under the column and the washing solution discarded. Rb and Sr were eluted with 4.0 ml of 4.0 M HCl, the flat bottomed beaker was removed and set aside for Rb-Sr separation.

Rb-Sr preparation: 3 drops of 0.015N H_3PO_4 was added to the elutant and set in an incubator at 70°C overnight until 1 drop remained, in the morning a cap was placed on the beakers (not closed) and T increased to 110°C. Once dry, 1-3 drops of Pyridine were added, this solution was dried up at 60°C for 2-3 hours.

The purified sample was placed onto a Tungsten filament and analysed on the Thermo Fisher TIMS alongside blanks and standard sample JB-2. Standard errors are displayed in Table 2

4. Results

4.1. Whole Rock Compositions: Breiðdalur system

Major and trace element compositions for 70 samples are shown in Supplementary Material and TAS is presented in Figure 2. Whole rock chemistry suggests that Breiðdalur is an enriched tholeiitic volcano with elevated alkali and incompatible element ratios compared to the conventional tholeiite trend (Carmichael, 1964). The samples are all from eastern Iceland volcanic sequences from 9 — 10 My old, most of the samples are from Breiðdalur Central Volcano. They represent lavas, dykes and intrusions in the Neogene sequences

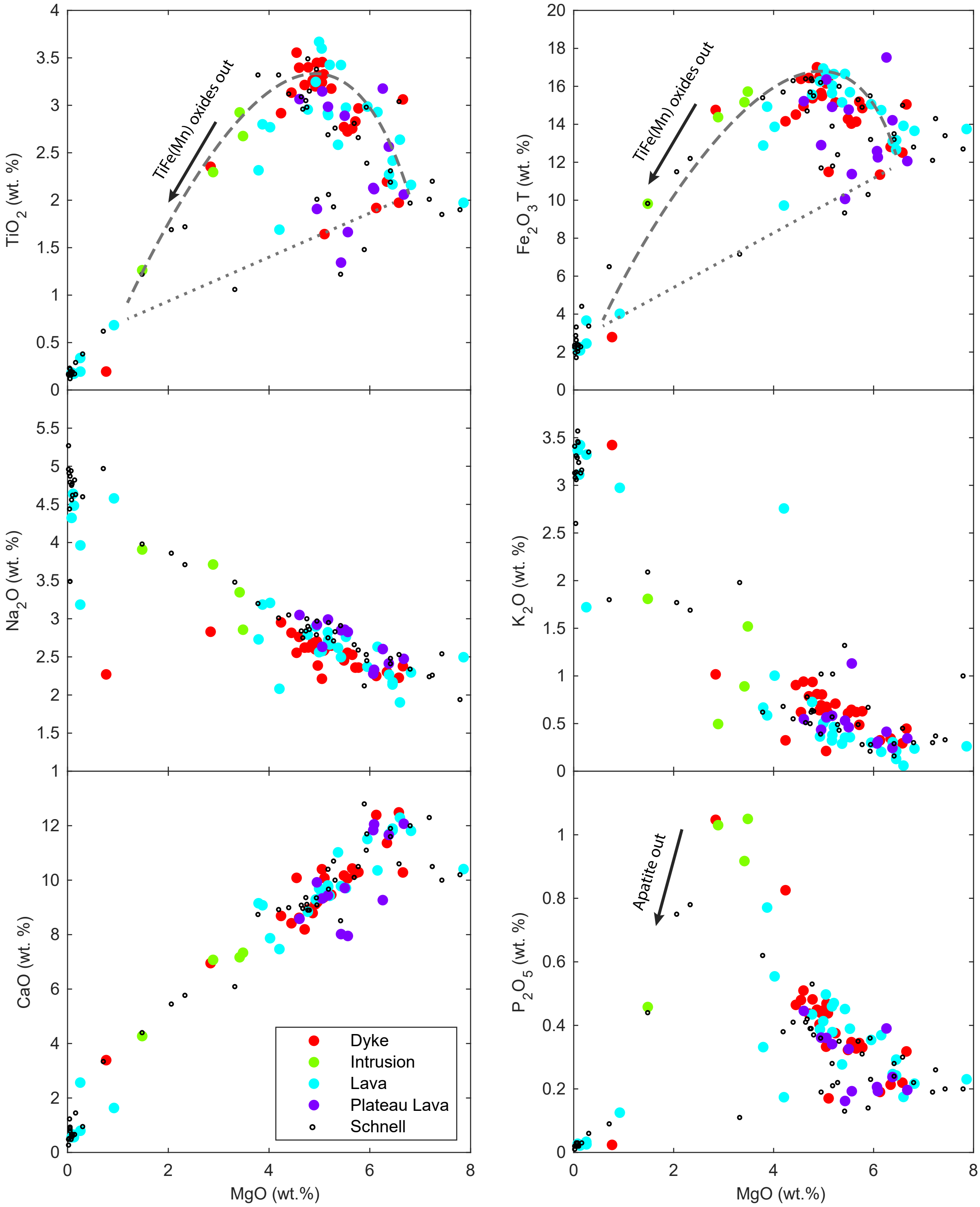

Figure 3: Selected major elements against MgO or SiO_2 for Breiðdalur rocks from this study and a complementary study by Schnell (1994). Dashed lines in TiO_2 and Fe_2O_3T graphs show fractional crystallisation trends approximated by MELTS from a basaltic magma; dotted lines show mixing trends if the magmas were to mix between the most primitive magma and most silicic magma. The Breiðdalur rocks are divided into lavas, dykes and intrusions (sills or sheets). Arrows indicate the major crystallising phases that take up those elements.

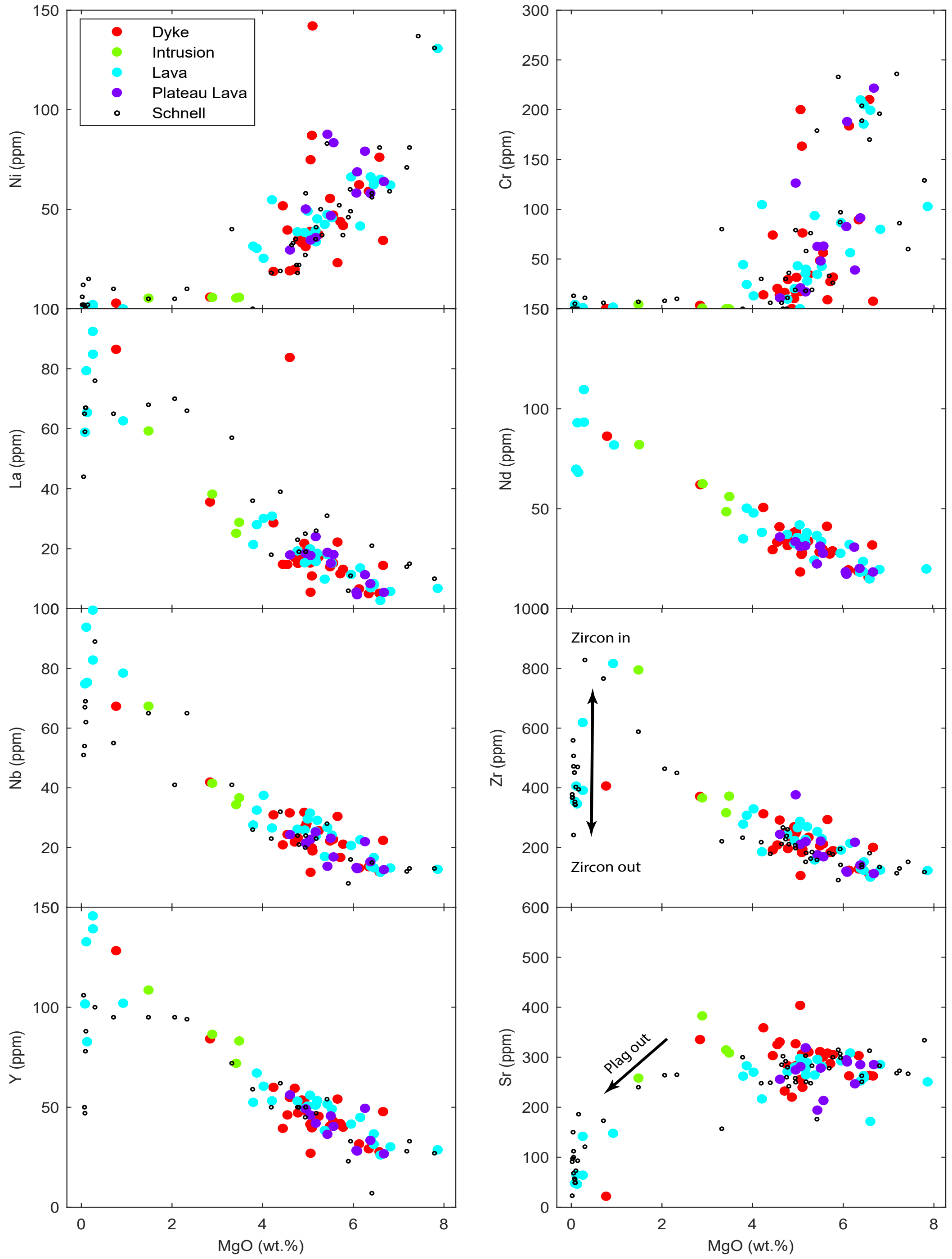

Figure 4: Selected trace elements against MgO for Breiðdalur rocks from this study and Schnell (1994).

both related to the central volcano as well as flood basalts that surround and interfinger with the volcano. Basalts from the Breiðdalur central volcano or dyke swarm are relatively evolved quartz-tholeiite basalts. All basalts display MgO contents of <7 wt. %, with the majority of samples <5 wt. % the range of MgO is 4.1 – 6.82 wt. %. FeO_T (Fe_2O_3 – FeO ratio 0.8998) values for basalts vary from 12.6 -– 18.5 wt. %, intermediate rocks 10.8 -– 16.0 wt % and silicic rocks 2.3 -– 9.3 wt. %. Mg# calculated from the ratio of FeO to MgO is no greater than Mg 82 in basaltic samples and decreases as low as Mg 14 in silicic samples. TiO_2 varies from 1.6 – 3.6 wt. % in the basalts, 1.2 -– 2.9 wt. % in the intermediate rocks and 0.1 — 0.8 wt. % in silicic. Ca, Sr and Ba can be used as proxies to plagioclase crystallisation, though all are low-T hydrothermally mobile, in the basalts Sr varies from 232 – 403 ppm, intermediate rocks from 216 – 382 ppm and silicic rocks from 21 – 226 ppm. Plagioclase, clinopyroxene and olivine are the major crystallising phases, olivine is often missing from the lavas of the central volcano and is uncommon in the dykes but can be found in a small number as both a phenocryst and groundmass phase. A small degree of plateau basalts are olivine bearing.

Major and trace elements are compared for samples of different volcanic system units, dykes, intrusions, lavas and silicic lavas (Figure 3 and 4). There is no discernible stratigraphic trend in the composition throughout the Breiðdalur central volcano flank sequence lavas, aside from the most evolved rocks only being present in the youngest parts of the volcano. When comparing the basaltic rock chemistries, including an extra dataset from the thesis of Schnell (1994), we find a higher degree of variability in the composition of plateau basalt lavas and basaltic dykes compared to the range of basaltic central volcano flank sequence lava compositions (Figure 5). Basaltic dykes from the dyke swarm are shown to be slightly more evolved basalts than the central volcano lavas and they also display a greater geochemical range than these lavas (Figure 2).

4.2. Petrology and chemistry: Flank Sequence

The flank sequence consists of a 1000 m thick sequence of lava flows, mostly sourced from Breiðdalur volcano (Figure 1). Much of the flank sequence is comprised of thin basaltic lava flows, these are often fine grained, apyhric plagioclase-clinopyroxene-oxide basalts. Their morphology is variable from pahoehoe to a'a, several units within the sequence are compound lava flows 10's metres thick consisting of several lobe layers. A portion of the flank sequence is comprised of thicker, aphyric, flow banded with platey cleavage, andesitic lavas, these occur from around 9.9 Ma (Askew et. al. Sumitted), 200 m above the valley floor in Breiðdalur (Figure 1: B_2). This sequence is, itself around 400 m thick, predominantly of andesites, before returning to thin basaltic lavas (B_3) though interspaced with intermediate lavas.

Geochemically the sampled lavas, including a comparative dataset by Schnell (1994), vary from SiO_2 45.5 – 61.5 wt. %, AlO_3 12.9 – 15.7 wt. %, TiO_2 1.22 – 3.32 wt. %, FeO 8.85 – 18.2, MgO 1.48 – 7.79. Throughout the eastern flank sequence, there is a progression through the lower flank lavas (B_1) towards more evolved lavas (B_2), then a shift back to mafic lavas above this (B_3, Figures 5 and 6). This same pattern may be representative of the general volcano evolution, though the north eastern flank (B_{ne}) does not show the same thick group of icelandite lavas as seen in B_2. Icelandite lavas are present (Walker, 1963) at a similar stratigraphic height and age.

4.3. Petrology and chemistry: Plateau basalts

Plateau basalt lavas envelope the Breiðdalur volcano (Figure 1). They are the basement of the central volcano and also bury the volcano. Their petrologies are variable, though the most common petrology is grey, >5 m thick, plagioclase-clinopyroxene-oxide aphyric to <10% plagioclase phyric basalts. Plagioclase is the most common macrocryst phase in plateau basalts, when macrocrysts are present. Several groups within the Breiðdalur area contain >20% plagioclase macrocrysts, such groups are termed porhyrytic groups or porphyry lavas. Notable groups in the sample area include the Grænavatn porphyrytic group (Walker, 1963) and the Fossárvík porphyritic group (stratigraphic numbers 40 – 45, Figures 1 and 5) which onlaps onto the Breiðdalur flank lavas. Basalt lavas containing olivine as a groundmass often weather to a black, rounded rock (Walker, 1964). A minor amount of plateau basalts display olivine as a significant macrocryst phase, notable groups include the Fagridalur olivine basalt group (stratigraphic number 21 and 22), exposed on the eastern flank and the Heiðarvatn olivine basalt group which caps, or covers, the summit group of Breiðdalur (Figure 1).

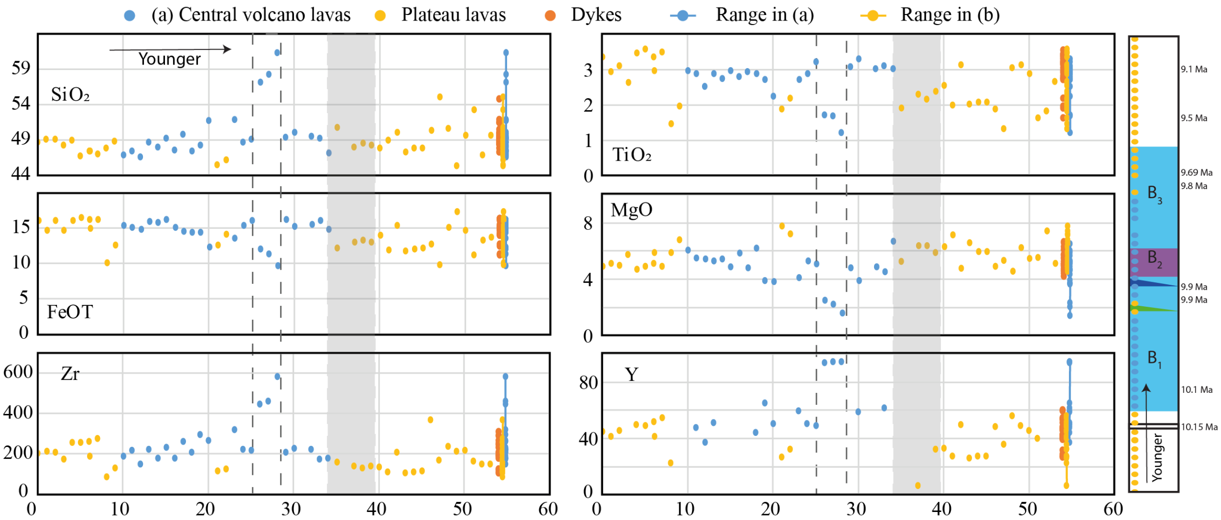

Figure 5: Selected major and trace elements in basaltic to intermediate samples from the Breiðdalur area against stratigraphic height (samples over 64 wt.% SiO_2 not shown. 0: Oldest sample below the central volcano, 53: Youngest sample. Dyke sample geochemical ranges are shown on the right. Dashed line box: Flaga andesites (B_2), grey box: Summit sequence lavas on Berufjarðartindur. To the right, simplified stratigraphic log of the eastern flank sequence, note, the sequences are adjusted to relate to the graphs and do not represent true stratigraphic thickness.

The lavas vary from SiO_2 45.5 – 55.14 wt. %, Al_2O_3 12.51 – 16.4 wt. %, TiO_2 1.33 – 3.61 wt. %, FeO 9.0 – 15.7 wt. %, MgO 4.80 – 7.79 wt. %. The range in compositions is greater in the sampled plateau basalts than the sampled flank sequence lavas (Figure 5). Several lavas are more evolved (up to 55 wt. % SiO_2) than might be expected of a widespread plateau basalt lava, however, the abundance of plagioclase as a macrocryst within plateau basalts could cause an increase in SiO_2, Al, and trace elements Ba or Sr contents. Sample 781, is a porphyritic lava flow sampled from above the volcano and contains 55 wt.% SiO_2.

4.4. Petrology and chemistry: Dyke Swarm

Petrologically the dykes are predominantly plagioclase-clinopyroxene ± olivine basalts of grainsizes from fine to doleritic, phenocrysts, when present are plagioclases up to 1 cm in size (most commonly <5 mm), clinopyroxene phenocrysts are present in a small number of dykes and olivine is a rare, but present, phenocryst phase.

The dykes show a broad range in tholeiitic basaltic chemistries, they vary from SiO_2 47.3 – 54.9 wt. %, Al_2O_3 12.7 – 16.7 wt. %, TiO_2 1.6 – 3.6 wt. %, FeO 10.2 – 14.8 wt. %, MgO 2.8 – 6.7 wt. %. Similar to plateau basalts, the range in dyke chemistries is greater than the range of central volcano basaltic lavas. Dykes appear to plot in many cases, as more enriched in incompatible elements than central volcano lavas and plateau basalts. Comparatively, dykes show the lowest MgO value compared to the lowest MgO of any plateau basalt, and some plateau basalt samples display higher MgO than the highest MgO values in dykes.

4.5. Petrology and chemistry: Intermediate and Silicic magmas

Silicic rocks are present within the caldera of Breiðdalur, as well as in the summit and SER sequences, which overlie the caldera and flank sequences, and as intrusions throughout the flank sequences. They are >71 wt % SiO_2, aphyric rhyolites (Figure 2). Feldspar bearing rhyolites are present but not a significant aspect of the volcano, notably the rhyolite flow of Flögutindur which is found in the SER is feldspar bearing.

The sampleset presented here was heavily based on studying the basaltic lavas and dykes of Breiðdalur, thus there is a representative set of intermediate samples missing. Those that are present are complemented with some from the Schnell (1994) study in order to create a more complete dataset. Intermediate samples are

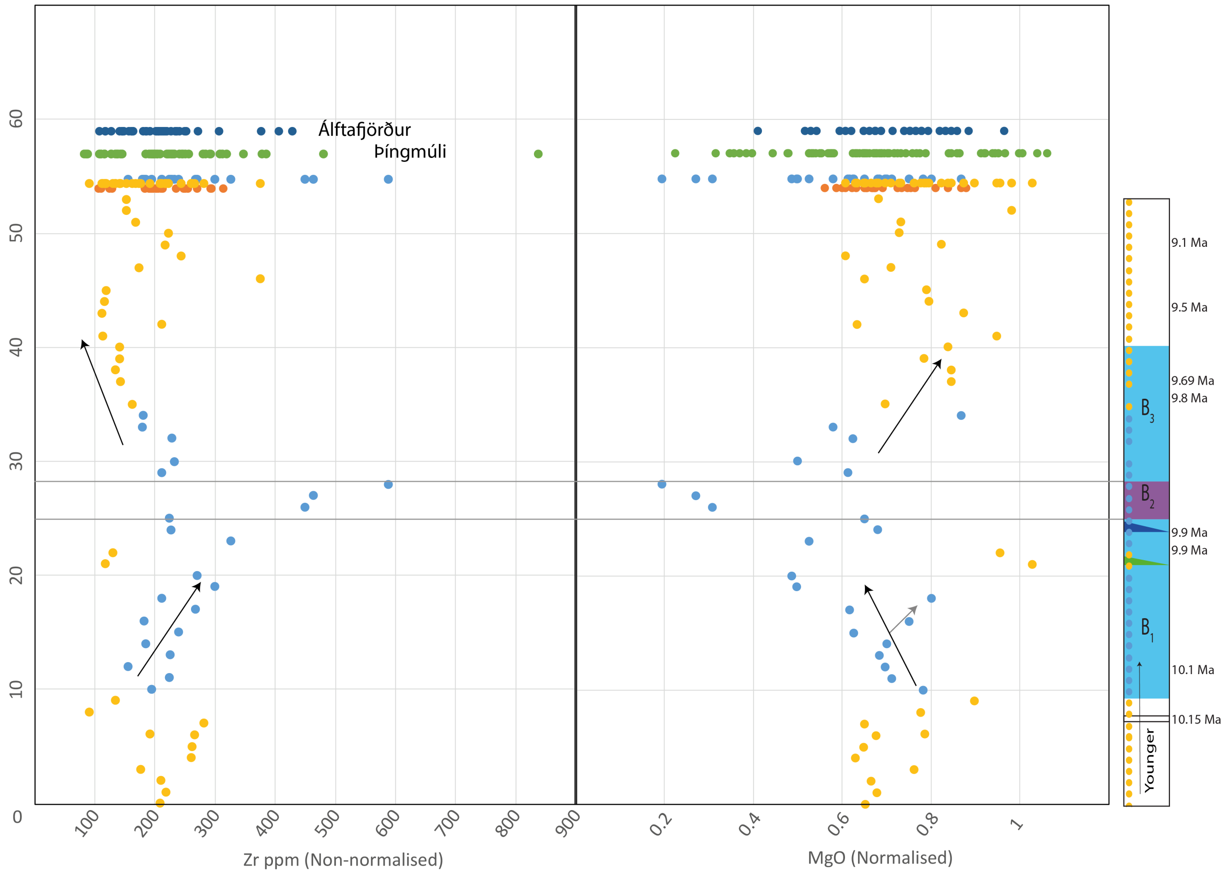

Figure 6: Figure key as in Figure 5. Zr and MgO against stratigraphy in order to compare magmatic evolution through the volcano's stratigraphy. Álftafjörður and Þingmúli (blue and green respectively) data is also shown for comparison with other volcanic systems compositional range (for rocks up to icelandite composition, data cited in Figure 2). Arrows indicate apparent trends.

basaltic icelandites to icelandite and dacite in composition, icelandite is the term for Fe, Ti and Al rich andesites common in Iceland (Carmichael, 1964). Intermediate samples are variable in petrology. They can be fine grained dark rocks, often displaying plagioclase alignment following flow banding, plagioclase is present along with clinopyroxene and oxides. Other intermediate rocks may appear similar to others in hand sample, however they can display mixed texture at thin section scale. Intermediate rocks are present as lavas in the flank sequences, and as intrusions, flows and domes in the caldera sequence.

Composite rocks are seen in the later stages of Breiðdalur volcano, either as mixed intermediate magmas or mingled composite dykes and flows.

4.6. Magmatic variation and trends in the Breiðdalur volcanic system

Major element variation diagrams for all samples are shown in figure 3, the data are separated into dyke, lava and intrusion samples along with extra data from (Schnell, 1994). Al_2O_3 shows little variation across all samples, TiO_2 displays 2 separate distinct trends throughout the samples. The first trend is the typical 'tholeiitic' magma differentiation trends, where more evolved basalts show high TiO_2 before dropping at around 4.5 wt. % MgO with the remaining intermediate to rholitic samples appearing to lie upon a trend of decreasing Ti until the rhyolites at <0.5 wt. % TiO_2. The distinct dog leg is due to the crystallisation of Ti mineral phases when a magma reaches Ti saturation at specific oxidation conditions, a common process within any magma reservoir in Iceland. The second trend displays samples of relatively low TiO_2 for their MgO value, this trend lies between the most primitive samples and the most evolved samples in almost a straight line. Total FeO displays similar trends to TiO_2 with a sharp decrease in the FeO wt. % trend after around 5– 4.5 wt. % MgO. This is again due to the crystallisation and fractionation of FeO bearing oxide minerals within respective melt batches after a melt evolves past 4.5 wt. % MgO. The second straight-line trend is also shown between primitive rocks and evolved rocks. The two oxides are intimately linked throughout the samples, showing that the processes affecting them are due to a mineral(s) that take up both FeO and TiO_2 such as magnetite, illmenite or spinel. Incompatible element oxides NaO and K_2O (in discontinuous magmatic evolution without Na or K feldspars) show expected trends of increasing concentration in more evolved samples. Evolved samples lying 'off-trend' exhibit crystallisation of Na- and K-rich feldspars. CaO displays a decreasing trend, concurrent with its compatibility in the mineral plagioclase which is present throughout the rock series as a crystallising phase. More minor element oxides such as P_2O_5 display a distinct concentration rise and peak at around 3 wt. % MgO. This peak is most likely due to the occurance of the P-compatible mineral apatite, though it is not visible in thin section. Again, a secondary trend (similar to Ti and Fe) is seen with low P values in some samples around 4 wt. % MgO. MnO follows the same trends as Fe and Ti oxides, the same crystallising phases that take up Fe and Ti will also take up Mn.

Origin of major element variation in the Breiðdalur volcanic system, MELTS modelling: Purely utilising major element chemistries, several models were run using the MELTS program (Gualda et al., 2012), in order to determine the origin of evolved rocks and basalts in the Breiðdalur system. The most primitive sample from the oldest Breiðdalur volcano lavas was chosen as the primary magma, the sample (470) is one of the first lavas in the lower flank sequence (B1). Fractional crystallisation and equilibrium crystallisation (later removed as it is considered unrealistic to real-world magma dynamics in the shallow magma reservoirs of Iceland) models were run under reduced conditions FMQ-1 and oxidised conditions at FMQ buffer. Pressure was set to 50 MPa (500 bars) for the initial modelling, this is thought to be a realistic pressure for Icelandic magma to reside beneath a central volcano. This pressure was modified in further runs in order to simulate a deeper magma reservoir where magma for regional dykes and some volcano melts may reside though no significant variation, outwith the sample scatter, was noted.

The models shown (Figures 5 and 3) do not provide the best fit for all samples, however these models are simplified and do not account for all factors affecting magmas in the crust. They fail to meet the highest TiO_2 values of basaltic lavas and dykes. It is possible to model these samples' high TiO_2 values using an assumed pressure of 100 MPa (1000 bars), equilibrium crystallisation at High T in reducing conditions (FMQ-1). This may recreate a magma reservoir at depth where the melt is still in contact with crystals in a crystal mush. In these models the highest Fe and Ti values of the samples is met, however, this cannot be assumed to be the mechanism for the complete magmatic system as equilibrium crystallisation does not recreate the

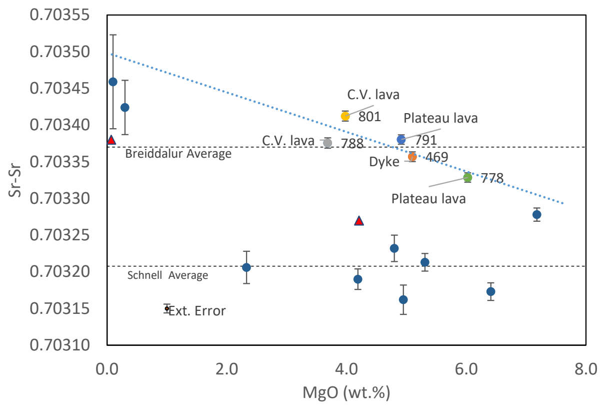

Figure 7: MgO against Sr isotope values for selected samples from the Breiðdalur volcanic system, dark blue symbols are data from Schnell (1994) (unknown external error). 2SD errors shown along with external error for Breiðdalur samples. Red triangles are Breiðdalur samples from Martin and Sigmarsson (2010), low MgO sample is a silicic intrusion from Berufjörður.

most evolved samples (system runs out of melt) and is an unrealistic view of magma in the Icelandic crust. These higher pressure magmas may account for the source of most of the basalts in Breiðdalur, their mineral assemblages also fit the models, assuming that upon ascent olivine is lost from the system.

Trace element variation diagrams are shown in figure 4 for selected trace elements. Elements compatible in olivine and clinopyroxene, such as Ni and Cr, display distinct depletion curves into more evolved samples, there is also significant scatter within the more primitive samples, suggesting the degree of crystallisation of these minerals is variable. Those samples with the highest Cr and Ni values are predominantly regional dykes and plateau basalts, though the most primitive samples (470) from the lower flank sequence lavas also displays high Ni concentration. Incompatible and immobile elements La, Ce, Nd, Nb, Y and Zr all display similar trends: of increasing concentration in more evolved melts. Those elements which display some compatibility in minerals that are present in more evolved melts (e.g. Zircon: Zr and Y) display significant variation in the lower MgO samples. Nb is slightly compatible in clinopyroxene and any accumulation or fractionation of clinopyroxene can affect relative ratios. A single sample lies well off trend in MgO vs La space sample 491, a dyke sample, displays very high La concentration that is difficult to explain but does not change any overall interpretations. Sr is relatively depleted in silicic samples, a factor of its compatibility in plagioclase, Ba, which also displays an affinity for compatibility within the lattice of plagioclase does not show the same variation, instead displaying an almost straight line trend between end member groups. Rb is relatively scattered though shows a general straight-line trend similar to other incompatible elements, again Rb has a slight affinity for compatibility in plagioclase and is also highly mobile in fluids.

4.7. Sr isotopes

The long half life of ^{87}Rb, means that any Sr-Sr ratios in Icelandic basalts, even those of Neogene age, are approximately that of the initial mantle melt. This is useful in determining magmatic relations, fractional crystallisation will not alter the Sr ratio of a primitive magma to a more evolved stage. Equally, a melt produced by partial melting of an existing rock will take up the Sr ratio of the parent rock as both isotopes of Sr are partitioned equally into the melt. A primitive melt, on its way to the shallow crust, is likely to assimilate some of the host material surrounding it. This would also cause a change in the Sr ratio, as the parent magma is essentially mixing with a rock of a different composition, if the mixing is to a significant enough degree then the ratio will be changed. The difficulty comes in unravelling these different source features.

Figure 7 displays samples from Breiðdalur, including published data from Schnell (1994) and Martin and Sigmarsson (2010). Mafic lavas and dykes display similar isotopic ratios within this study's samples, from 0.703329 to 0.70341. These values are similar to the Sr ratio range of silicic samples from other studies but markedly different from the mafic samples analysed by Schnell (1994). If the silicic magmas shown (Low-MgO) were formed from partial melting of a significantly different Sr ratio crust, we would expect the silicic samples to show a markedly different value. If the samples were from fractional crystallisation of the same basaltic magma source feeding basaltic lavas of the volcano, we would expect the values to be the same or similar in basalts and rhyolites. However, our study suggests that the plateau basalts below Breiðdalur even 1-2 km down, may be isotopically similar to the central volcano lavas, any variation in the isotopic ratios is relatively subtle (Kitagawa et al., 2008). This subtle ratio change is significant enough when looking at basaltic magmas that undergo less crustal processes, but silicic magmas will reside in the crust for longer and may undergo assimilation, fractional crystallisation and mixing which will adjust sensitive isotope ratios. This essentially means that magmas formed through fractional crystallisation or partial melting will recreate similar isotopic ratios.

5. Discussion

Breiðdalur volcano is a large, caldera central volcano, in its mature state the volcano had a 10 km wide caldera and broad, shallow sloped flanks. The volcano's activity produced over 600 km^3 of material, spreading over 1000 km^2 and probably creating a 1-2 km high edifice. Most of the activity was mafic, with around 10-15 % being more evolved magmatism. The basement rock is comprised predominantly of tholeiitic basalt plateau lavas. The earliest lavas to erupt from the volcano itself were thin pahoehoe and a'a basalts at around 10.0 Ma, these basalts are relatively uniform with SiO_2 values between 46 – 49 wt. %, FeO_T between 29 – 31 % and MgO between 5.2 – 5.4 wt. %. Similar to the composition of pre-Breiðdalur plateau basalts. There is a notable drop in TiO_2 wt. % in the plateau basalts directly below the first Breiðdalur basalts (Figure 5), a trend which is notable also in FeO_T, Zr, NaO, K_2O, V and inversely visible in MgO wt. %.

The basaltic lavas which are known to be sourced from Breiðdalur all plot within a very confined geochemical space with regards to many major and trace elements. Plateau basalts surrounding and interfingering with the central volcano show varied geochemistry with respect to those lavas known to be sourced from the volcano (Figure 5, includes data from Schnell (1994)). This is likely due to a relatively stable plumbing system feeding lavas to the central volcano, a shallow crustal reservoir where basaltic magma is periodically stored and mixed. Plateau lavas are more varied. Any spatial variation in the magmatic source along a fissure system may create variable geochemical signatures, a signature that is then sampled by the erupting magma. A comparison of plateau lavas and Breiðdalur dyke swarm samples shows a similar degree of variation in geochemistry (Figure 5). The variability in both plateau basalt lavas and dyke swarm magmas, which is not shared by lavas within the central volcano, shows that the plumbing systems for the fissure swarm and the central volcano are not reliant on each other. That is, the central volcano is probably fed by a confined source and each magma batch has similar processes affecting it before it erupts as a basaltic lava flow in the central volcano. The fissure swarms may be fed by the same deep mantle source but are not privy to the same set of processes as the central volcano lavas. The variability in the dyke swarm magmas is probably due to a variety of deep magma source mixing events or simply the differences between a lava erupting 20 km away from another lava on the same 'swarm'.

5.1. Production of magmatic trends in Breiðdalur

Upon first examination, samples from the Breiðdalur volcano display major element geochemistries expected of fractional crystallisation trends such as those seen in Þingmúli volcano (Carmichael, 1964; Charreteur et al., 2013). High TiO_2 basalts may have formed in a deep reservoir (>100 MPa) through equilibrium crystallisation, though this is likely to be a simplified view of the process. Basaltic andesites (icelandites) may be related by fractional crystallisation (Figure 8) of these basalts, presumably as the magma migrated to the surface or in a shallower reservoir (<100 MPa). The model lines indicated in figure 3 (dashed line) suggest that some of the rhyolite compositions can be recreated by fractional crystallisation in a reduced condition (notably, oxidised conditions displayed lowered but similar trends (not shown)). However, the most evolved rhyolites are not recreated in the MELTS models. Both effusive and explosive silicic volcanism occurs at Breiðdalur - the explosive phases must have been volatile rich (water), which requires a high degree of H_2O within the magma (>3-4%) (Owen et al., 2013). This high amount of volatiles could easily be created through partial melting of hydrated basaltic crust, but may be more difficult through fractional crystallisation (Figure 9), though magma mixing and assimilation may increase volatiles. Thus, this question requires further analysis, especially as 2 other separate studies found differing methods of formation of silicic magmas at Breiðdalur. Firstly Schnell (1994) suggested that rhyolites could be formed by fractional crystallisation from a basaltic end-member, assimilating a small amount of low δ18O crust, giving rhyolitic $\delta^{18}O$ values of around 4.5 ‰. Martin and Sigmarsson (2010) however, suggested that the $\delta^{18}O$ values of around 5-5.5 ‰ were purely from partial melting of the hydrated, amphibolite facies basaltic crust. Atlantic MORB δO values are around 5.5 ‰ (+5.45 ± 0.19 = mean and 2sd of 62 fractionation-corrected Atlantic MORB from 33 to 40°N, (Cooper et al., 2004)), meteoric waters in Iceland are depleted in δ18O, so any primitive basaltic magma assimilating the hydrated crust would display lowered δ18O values. Similarly, basaltic crust that is partially melted would also retain these depleted δO values mixed with the original basalts' MORB value. A significant caveat in relying on O isotopes is that the Icelandic mantle itself is not MORB, and may in fact have depleted δ18O values (values as low as 4.5 ‰ are reported in melt inclusions (Thirlwall et al., 2006)). Martin and Sigmarsson (2010) use other trace element methods to come to this conclusion, however, it is our view that we should take care when evaluating isotopes and trace elements as so many factors are at play within the Iceland mantle and crust.

Thus, neither result appears entirely conclusive. Field observations and area to volume estimates of mafic to silicic magmas at Breiðdalur show that rhyolitic rocks make up around 15% of the volcano stratigraphy. And despite the thickness of the B_2 icelandite sequence there is a distinct lack of intermediate magmas (<5% of the volcano area). The rest is comprised of predominately basaltic rocks with some basaltic icelandite lavas in the flanks, the dyke swarm is also entirely basaltic. Fractional crystallisation should produce a decreasing volume of magma as its evolution continues (greater intermediate magma volume than evolved), a trend not mirrored in Breiðdalur or any other mapped volcano in eastern Iceland (e.g. Walker (1958); Gústafsson et al. (1989); Gústafsson (1992); Blake (1970); Gibson (1963); Geirsson (1993)). Partial melting could explain the volume differences, since the predominant input would be mafic magma which crystallises on its way to the surface/shallow crust, and in turn melts the hydrated basaltic crust creating dacite or rhyolite. A mixture of the two could also occur, fractional crystallisation up to icelandite, partial melting creating dacite with fractional crystallisation up to rhyolite and a constant mafic input which explains the mafic lavas high in the summit sequence and mixed magma rocks comprised of basalt and rhyolite.

5.2. Regional geochemistry and Neo-Volcanic zones comparisons

The geochemistry of magmas at a volcanic systems in Iceland is controlled by the proximity of the system to the head of the mantle plume and thus its plume material to MORB ratio, as well as other factors such as the depth of melting and degree of melting. The incompatible in basaltic melts elements of Nb, Zr and Y can be used to discriminate these processes as shown in figure 10. This displays selected basaltic samples from the volcanic systems in the NVZ of Krafla and Askja, due to the proposal that the volcanoes of the east fjords were originally formed along a rift segment similar to the NVZ (Martin and Sigmarsson, 2007). East fjord samples all show a relatively high degree of enrichment compared to active main rift zone volcanoes, though Breiðdalur strongly correlates to a similar magmatic source style (i.e. depth of melting or plume:MORB) as Askja volcanic system. In these respects, Breiðdalur volcano appears to be a geochemically average volcano, rather typical of volcanic systems in Iceland and of lavas in the east fjords. Interestingly, dyke samples from Breiðdalur and the IRDP show higher enrichment than the bulk of lava samples. This may be a factor of clinopyroxene (where Nb has a slight affinity) accumulation or growth during ascent or during cooling.

This apparent similarity between Askja and Breiðdalur samples in the space shown in Figure 10 can be seen to some extent in other plots, though the discrimination is most strongly recognisable in Nb/Y and Zr/Y space. The similarity to an on-rift volcano is not matched in the study by Martin et al. (2011), who show samples of silicic rocks at Breiðdalur and other nearby volcanic systems having a off-rift geochemical signature. Perhaps the Breiðdalur volcano infact lay on the edge of a main-rift, thus having characteristics

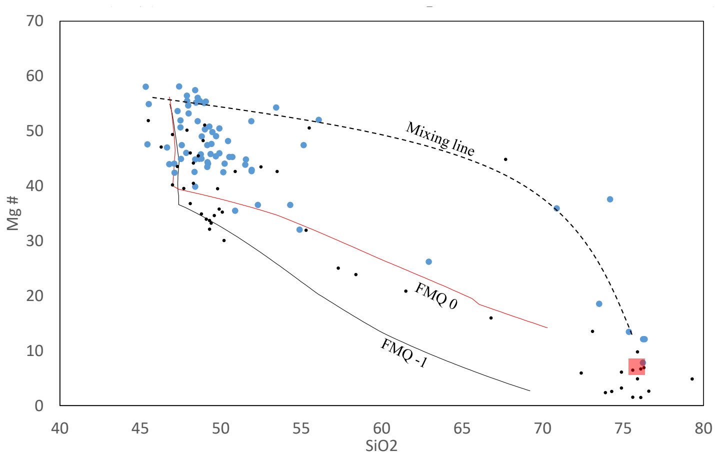

Figure 8: Magmatic trends modelled through MELTS. Simple fractional crystallisation modelling under oxidised and reduced environments are shown over samples from this study (blue) and Schnell (1994). FMQ buffer set to 0 recreates the sample trends well, the magma evolves in early stages with the fractionation of mafic minerals, at around an Mg No. of 40, magnetite and ilmentite begin to form as a fractionating phase, causing the 'dog-leg' trend. An approximate mixing line is indicated for reference and displays a good fit to other samples. One downfall with this modelling is that the apparent fractional crystallisation trends can also be reproduced by direct mixing of less primitive mafic magmas and more evolved silicic magmas.

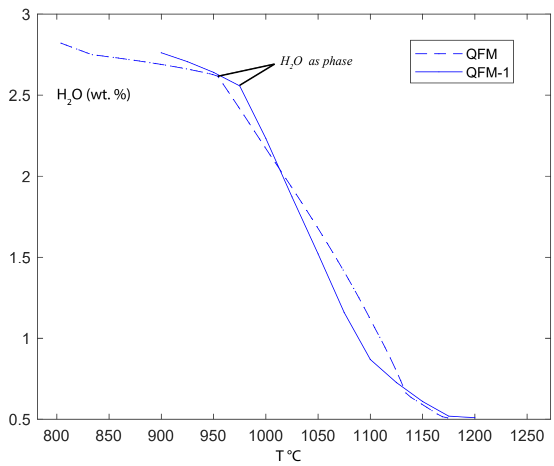

Figure 9: MELTS modelling of H_2O during fractional crystallisation from a basaltic magma containing 0.5 wt.% H2O. At around 975°C H_2O becomes a fractionating phase, causing the slight shift. The final concentration of water in the melt (just over 2.5 wt. %), is realistic for rhyolite magmas in Iceland, though perhaps at the low end of concentration and may be most viable for rhyolites that erupt effusively.

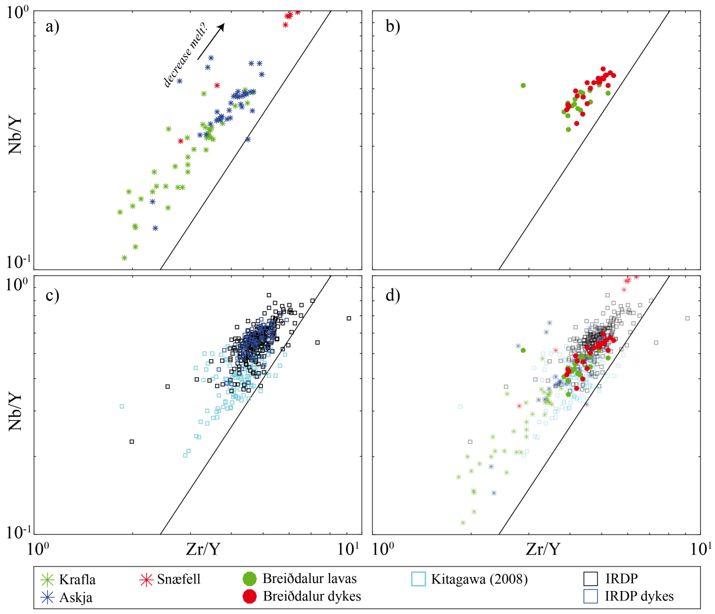

Figure 10: Nb/Y against Zr/Y discrimination plots from Fitton (2007). Samples all have MgO content >5 wt. %. Krafla, Askja and Snæfell samples compiled from the GeoRoc database. IRDP (Iceland Research Drilling Project) samples from Flower et al. (1982); Gibson et al. (1982). Black line is the Northern hemisphere reference line.

of both. In order to better constrain this, further studies on isotope ratios, which would give a higher degree of accuracy and discrimination, in Breiðdalur and nearby systems would need to be undertaken, utilising the entire rock suite from basalts to rhyolites.

6. Conclusions

Breiðdalur is an enriched tholeiitic volcano, it is geochemically similar to the nearby volcanoes of Þingmúli, Álftafjörður and Reyðarfjörður though each may display distinct characteristics in certain elements or isotopes which is beyond the scope of this paper. Breiðdalur is, to a significant degree, more enriched than volcanoes in the Neovolcanic NVZ. Indicative of a more enriched magma feeding the volcano of Breiðdalur than the closest currently active axial volcanic zone. The volcano and EVZ lavas are also distinct from the off-axis zone of Öræfi-Snæfell.

Basaltic lavas erupted from the volcano are relatively evolved and surprisingly homogeneous in composition, suggesting a crustal reservoir(s) where magmas mix prior to eruption. Flood basalt lavas and regional dykes have a wider geochemical range, suggesting they do not share the same plumbing system as the volcano lavas. Intermediate and evolved magmas most likely formed through a predominant process of partial melting and subsequent fractional crystallisation, though mixing and some fractional crystallisation from basaltic magmas can not be excluded. Our evidence for this is based on studies from other volcanoes and on field observations indicating a relative lack of intermediate rocks (5%) vs. mafic (80%) and silicic rocks (15%).

6.1. Current knowledge gaps and further work

The current view of the formation of eastern Iceland evolved and intermediate magmas is split. On the one hand, specific studies of rhyolites from several areas suggest partial melting, and on the other, studies of individual volcanoes suggest fractional crystallisation is the dominant process. In our study, we suggest that partial melting is the dominant process but that fractional crystallisation likely plays a role in forming the more evolved basalts, as well as some of the intermediate to silicic magmatism. The main take away from this, is that we still do not have the complete picture of the processes forming magmas at Icelandic central volcanoes, we likely have to take each volcano as a separate case study and use caution in interpreting trace element and isotope data using over simplified assumptions.

In this study we also found that trace elements appeared to be able to distinguish volcanic systems when ratios of incompatible and immobile elements were analysed. Published datasets of active volcanic systems show that they have distinct signatures which is related to their location or proximity to the mantle plume in Iceland, and also to the depth of melting that is occurring. For example, Krafla is a relatively more depleted volcanic system than Askja, which is closer to the plume and which probably has thicker crust beneath it. This was applied to Neogene volcanic systems, both to compare them with active systems and to compare them to each other in order to investigate Neogene mantle dynamics. Further to this, if they are distinguishable then lavas from each system can be more accurately mapped. Trace elements did show some slight distinguishable features, but for further and more robust analysis, it is suggested that isotopes could be used to analyse this.

Arculus, R. J., 2003. Use and abuse of the terms calcalkaline and calcalkalic. Journal of Petrology 44 (5), 929–935.

Blake, D., 1970. Geology of alftafjordur volcano, a tertiary volcanic centre in south-eastern iceland. Scientia Islandica 2, 43–63.

Carmichael, I. S. E., 1964. The petrology of thingmuli, a tertiary volcano in eastern iceland. Journal of Petrology 5 (3), 435–460.

Charreteur, G., Tegner, C., Haase, K., 2013. Multiple ways of producing intermediate and silicic rocks within thingmúli and other icelandic volcanoes. Contributions to Mineralogy and Petrology 166 (2), 471–490.

Cooper, K. M., Eiler, J. M., Asimow, P. D., Langmuir, C. H., 2004. Oxygen isotope evidence for the origin of enriched mantle beneath the mid-atlantic ridge. Earth and Planetary Science Letters 220 (3-4), 297–316.

Fitton, J., Saunders, A., Larsen, L., Hardarson, B., Norry, M., 1998. Volcanic rocks from the southeast greenland margin at 63°n: composition, petrogenesis, and mantle sources. In Saunders, A.D., Larsen, H.C., and Wise, S.W., Jr. (Eds.), Proc. ODP, Sci. Results, 152: College Station, TX (Ocean Drilling Program), 331–350.

Fitton, J. G., 2007. The oib paradox. Geological Society of America Special Papers 430, 387–412.

Flower, M., Pritchard, R., Brem, G., Cann, J., Delaney, J., Emmerman, R., Gibson, I., Oakley, P., Robinson, P., Schmincke, H.-U., 1982. Chemical stratigraphy, iceland research drilling project, reydarfjordur, eastern iceland. Journal of Geophysical Research: Solid Earth 87 (B8), 6489–6510.

Gallagher, C., 2013. Álftafjörður dyke swarm, petrology, geochemistry and structure. Thesis, School of Earth Sciences, The University of Edinburgh.

Geirsson, K., 1993. Pétrologie d'une série tholéiitique complete: le volcan central de fagridalur, nord-est de l'islande.

Gibson, I. L., 1963. The reydarfjordur acid volcanic centre of eastern iceland. Ph.D. thesis, Imperial College London.

Gibson, I. L., Kirkpatrick, R. J., Emmerman, R., Schmincke, H., Pritchard, G., Oakley, P. J., Thorpe, R. S., Marriner, G. F., 1982. The trace element composition of the lavas and dikes from a 3-km vertical section through the lava pile of eastern iceland. Journal of Geophysical Research: Solid Earth 87 (B8), 6532–6546.

Gualda, G. A., Ghiorso, M. S., Lemons, R. V., Carley, T. L., 2012. Rhyolite-melts: a modified calibration of melts optimized for silica-rich, fluid-bearing magmatic systems. Journal of Petrology 53 (5), 875–890.

Gudmundsson, A., 2002. Emplacement and arrest of sheets and dykes in central volcanoes. Journal of Volcanology and Geothermal Research 116 (3), 279–298.
URL http://www.sciencedirect.com/science/article/pii/S0377027302002263

Gústafsson, L. E., Lapp, B., Thomas, L., Lapp, M., 1989. Tertiary silicic rocks in the area of the kaekjuskörð rhyolitic volcano, eastern iceland. Jökull 39, 75–89.

Gústafsson, L. E., 1992. Geology and petrography of the Dyrfjöll Central Volcano, eastern Iceland. Vol. 138. Selbstverlag Fachbereich Geowissenschaften, FU Berlin.

Kitagawa, H., Kobayashi, K., Makishima, A., Nakamura, E., 2008. Multiple pulses of the mantle plume: evidence from tertiary icelandic lavas. Journal of Petrology 49 (7), 1365–1396.

Le Bas, M., Le Maitre, R., Streckeisen, A., Zanettin, B., Rocks, I. S. o. t. S. o. I., 1986. A chemical classification of volcanic rocks based on the total alkali-silica diagram. Journal of petrology 27 (3), 745–750.

Martin, E., Paquette, J. L., Bosse, V., Ruffet, G., Tiepolo, M., Sigmarsson, O., 2011. Geodynamics of rift–plume interaction in iceland as constrained by new 40ar/39ar and in situ u–pb zircon ages. Earth and Planetary Science Letters 311 (1), 28–38.
URL http://www.sciencedirect.com/science/article/pii/S0012821X11005000

Martin, E., Sigmarsson, O., 2007. Crustal thermal state and origin of silicic magma in iceland: the case of torfajökull, ljósufjöll and snæfellsjökull volcanoes. Contributions to Mineralogy and Petrology 153 (5), 593–605.

Martin, E., Sigmarsson, O., 2010. Thirteen million years of silicic magma production in iceland: links between petrogenesis and tectonic settings. Lithos 116 (1), 129–144.

O'nions, R., Hamilton, P., Evensen, N., 1977. Variations in143nd/144nd and87sr/86sr ratios in oceanic basalts. Earth and Planetary Science Letters 34 (1), 13–22.

Owen, J., Tuffen, H., McGarvie, D. W., 2013. Explosive subglacial rhyolitic eruptions in iceland are fuelled by high magmatic h2o and closed-system degassing. Geology 41 (2), 251–254.

Pearce, J. A., 1996. A user's guide to basalt discrimination diagrams. Trace element geochemistry of volcanic rocks: applications for massive sulphide exploration. Geological Association of Canada, Short Course Notes 12, 79–113.

Riishuus, M., Miggins, D., Koppers, A., Duncan, R., 2010. 40ar/39ar incremental heating experiments on celadonite from the skessa tuff, eastern iceland: Thermochronology of low-temperature alteration of a flood basalt pile during burial metamorphism. In: AGU Fall Meeting Abstracts. Vol. 1. p. 4873.

Schnell, T., 1994. Breiðdalur central volcano, eastern iceland: genesis of the evolved rocks. Thesis, Department of Earth Sciences.

Thirlwall, M., Gee, M., Lowry, D., Mattey, D., Murton, B., Taylor, R., 2006. Low δ18o in the icelandic mantle and its origins: Evidence from reykjanes ridge and icelandic lavas. Geochimica et Cosmochimica Acta 70 (4), 993–1019.

Walker, G. P., 1958. Geology of the reydarfjördur area, eastern iceland. Quarterly Journal of the Geological Society 114 (1-4), 367–391.

Walker, G. P., 1962. Tertiary welded tuffs in eastern iceland. Quarterly Journal of the Geological Society 118 (1-4), 275–290.

Walker, G. P., 1963. The breiddalur central volcano, eastern iceland. Quarterly Journal of the Geological Society 119 (1-4), 29–63.

Walker, G. P., 1964. Geological investigations in eastern iceland. Bulletin Volcanologique 27 (1), 351–363.
URL http://dx.doi.org/10.1007/BF02597532

Winchester, J. A., Floyd, P. A., 1977. Geochemical discrimination of different magma series and their differentiation products using immobile elements. Chemical geology 20, 325–343.

Wood, D. A., 1978. Major and trace element variations in the tertiary lavas of eastern iceland and their significance with respect to the iceland geochemical anomaly. Journal of Petrology 19 (3), 393–436.

Yokoyama, T., Makishima, A., Nakamura, E., 1999. Evaluation of the coprecipitation of incompatible trace elements with fluoride during silicate rock dissolution by acid digestion. Chemical Geology 157 (3), 175 – 187.
URL http://www.sciencedirect.com/science/article/pii/S000925419800206X

Table 1: Standard analyses for trace elements analysed at University of Edinburgh.

		Nb (ppm)	Zr1 (ppm)	Y (ppm)	Sr (ppm)	Rb (ppm)	Zn (ppm)	Cu (ppm)	Ni (ppm)
BCR	Book	14.0	190.0	38.0	330.0	47.2	129.5	19.0	13.0
	Average	12.7	192.4	37.9	333.5	47.6	124.9	17.9	13.5
	1sigma	0.1	1.1	0.3	2.9	0.3	0.8	0.2	0.2
BEN	Book	105.0	260.0	30.0	1370.0	47.0	120.0	72.0	267.0
	Average	117.3	266.8	29.8	1383.3	47.5	133.2	76.6	280.9
		0.3	1.0	0.2	4.7	0.2	0.4	0.6	0.6
BHVO-1	Book	19.0	179.0	27.6	403.0	11.0	105.0	136.0	121.0
	Average	19.4	173.7	27.1	391.8	9.9	103.8	132.7	116.9
		0.1	0.6	0.2	0.8	0.1	0.5	0.2	0.5
BIR	Book	0.6	15.5	16.0	108.0	0.3	71.0	126.0	166.0
	Average	0.7	17.2	16.3	107.7	0.5	66.9	123.7	153.7
		0.0	0.5	0.2	0.3	0.1	0.6	0.8	0.5

		Cr (ppm)	V (ppm)	Ba (ppm)	Sc (ppm)	La (ppm)	Ce (ppm)	Nd (ppm)
BCR	Book	16.0	407.0	681.0	32.6	24.9	53.7	28.8
	Average	4.1	397.8	690.9	30.6			
	1sigma	0.5	0.7	1.1	0.3			
BEN	Book	360.0	235.0	1025.0	22.0	82.0	152.0	67.0
	Average	382.1	248.5	1058.0	24.7	91.9	156.1	69.9
		0.0	1.5	1.6	0.3	1.4	0.6	0.5
BHVO-1	Book	289.0	317.0	139.0	31.8	15.8	39.0	25.2
	Average	283.3	311.3	127.6	32.4	13.5	39.5	26.1
		1.1	2.2	0.4	0.7	1.4	0.9	1.3
BIR	Book	382.0	313.0	7.0	44.0	0.6	2.0	2.5
	Average	369.2	310.0	4.7	40.3	3.5	3.7	2.4
		0.3	1.6	2.9	0.5	0.2	0.8	0.9

Table 2: Sr, Nd and Hf standard analyses

	87Sr/86Sr	error(2sm)	84Sr/86Sr	error(1sd)	Rb87/Sr87	error(2sm).1	frac.(exp)	error(2sm).2
JB2-1Sr	0.703689	0.000006	0.056491	0.000027	0.000008	0.000001	1.003783	0.000049
JB2-2Sr	0.703694	0.000006	0.056486	0.000032	0.000018	0.000002	1.002032	0.000043

A.4 Paper 4: Isotopic geochemistry of Miocene east fjord volcanic systems

Isotopic geochemistry of Miocene east fjord volcanic systems

Robert A. Askew[a], Thorvaldur Thordarson[a]

[a]*Institute of Earth Sciences, University of Iceland, Sturlugata 7, 101, Reykjavik*

1. Introduction

The study undertaken earlier in this thesis (Appendix C Paper 3), touched upon the regional understanding of Neogene volcanoes and their geochemistries. The study showed that Breiðdalur volcano is slightly more enriched in incompatible elements than a typical tholeiite volcano, thus, formulated a hypothesis that Breiðdalur may not have been a typical rift zone volcano. This would have important implications for crustal evolution models, whether the volcanoes of the east were on-rift or off- rift volcanoes (e.g. Harðarson et al., 2008; Óskarsson, 2015; Palmáson and Sæmundsson, 1974). Further to this, the question of being able to discriminate between lavas and dykes of neighbouring volcanoes in the east fjords came about. This question arose because geological mapping relies on regional scale mapping of lavas that have a similar appearance or relating structural contours across fjords. This is an effective but very time consuming process, that may also create errors if assumptions about certain groups and their appearance is incorrect. Therefore, being able to discriminate lavas in the field through geochemistry, may provide a more accurate method of mapping plateau basalt terranes, and discriminating between different volcanic systems which may overlap. Since most neo-volcanic zones and volcanic systems have distinct geochemical signatures, which is related to their location and mantle source (Jakobsson et al., 1979; Halldorsson et al., 2008; Sigmarsson and Halldórsson, 2015), geochemical discrimination diagrams can be used to distinguish between systems. If this is possible in the neovolcanic zones, then trace element and the even more effective tool of isotopes should be able to delimit source characteristics of lavas and dykes in the east fjord volcanoes.

In this paper, we utilise a renewed understanding of the age of the volcanic sequence in eastern Iceland, with the 'fingerprinting' method of delimiting volcanic systems in order to better understand the regional stratigraphic evolution, the magmatic interplay between adjacent volcanic systems and improve geological mapping techniques in the area.

2. Geological background

The east fjords of Iceland contain the exhumed products of Neogene central volcanoes and plateau basalts. The Neogene lava pile in the east of Iceland has a westward dip between 2-12°. This dip is due to excess weight and thickness along the rift zones, which tilts the crust towards these zones, this phenomenon is visible in the west fjords also, but with a dip to the east. This general westward dip, means that further to the east the crust visible at the surface is older than the same altitude to the west, also that lavas visible at sea level are traceable to mountain tops further east. The exposure of deeper volcanic and magmatic edifices at the surface was aided by Plio-Pleistocene glaciations, incising deep fjords in the lava pile. In the south east, estimations from zeolite alteration (Walker, 1960) and magma emplacement depth suggest around 2 km of material was removed through erosion, in the northeast approximately 1 km was removed (Gústafsson, 1992). The difference in erosion rates is due to the proximity to highland areas of Vatnajökull ice cap, which has high crustal accretion rates and high precipitation.

This process also exposes central volcanoes, such as the Breiðdalur volcano (Figure 1). A central volcano is essentially an edifice that forms through repeated eruptions within a confined area and over a relatively short span of time c. 0.5 - 1 My Thordarson and Larsen (2007). Central volcanoes are characterised by the occurrence of silicic magmatism, due to the high heat input below the volcano and subsequent melting of hydrothermally altered basalts (Sigmarsson et al., 1991). A central volcano is also the focus of basaltic activity that builds a large edifice, the shape of the volcano is defined by eruptions and, in modern day Icelandic volcanoes, the presence of ice or water. They may also contain sheet swarms or cone sheets (Anderson, 1937), a large collapse-caldera, silicic or mafic plutons or high hydrothermal heat output. A central volcano may exhibit some or all of these characteristics. Associated with most exposed eastern Iceland central volcanoes is a dyke swarm, containing vertical regional dykes, the sub-surface representation of a fissure swarm. These fissures may be eruptive or purely intrusive and can be traced for many km's (Gudmundsson et al., 2014).

3. Sampling

Samples were taken from 4 major volcanic systems in the east of Iceland. In order to evaluate the relationships between neighbouring volcanic systems dyke swarms' and lavas, samples were taken from dykes, central volcano lavas, plateau basalt lavas and silicic lavas from selected volcanoes. (The samples localities are listed within thesis Appendix).

4. Methods

25 samples were crushed in a jaw crusher and milled in an agate mill, in preparation for trace element and isotope analysis. Several grams of powdered sample was separated into a small sample beaker and taken into the PML clean laboratory. The procedure for trace element analysis by ICP-MS followed Yokoyama et al. (1999) "method 3" except high Mg and Al samples which were digested using a teflon bomb technique (Takei et al., 2001), Sr and Nd analysis by TIMS followed the procedure below, Pb by TIMS followed Kuritani and Nakamura (2002) and Hf by MC-ICP-MS followed Lu et al. (2007). The wet chemistry was supervised by Technician Chie-so Sakaguchi and Prof. Katsura Kobayashi during a research visit to PML, funded by the Watanabe Trust Fund and PML.

Samples were crushed and milled at PML, milling took place for 1 hour using an agate mill to create homogenous powder. The powder was separated for clean lab use and XRF use.

Clean lab:

Between 600 mg to 1 g of sample was taken into 2 batches as duplicate and original.

Acid leaching was undertaken using 8 ml 6M HCl, the sample-acid mix was ultrasonicated for 2 hours, removed and centrifuged for 5 minutes at 3000 RPM. The acid was removed from the beaker and kept in PP bottle for analysis of elements lost. 8 ml USQ water was added to the sample which was then centrifuged again for 5 minutes, the water was removed and discarded. The addition and removal of water was repeated 2 more times (3 total).

Sample decomposition: The leached sample was decomposed using 1 ml $HClO_4$, 1 ml 2D 30M HF and 0.33 ml HCl. Samples were then ultrasonicated for 6 hours, then placed in incubators overnight, the samples were heated at 110°C for several hours to evaporate HCl, the heat was then increased to 160°C to evaporate HF and finally to 195c to evaporate the last of the $HClO_4$. The dried samples were remixed with $HClO_4$ and the heating step repeated. The dried samples were mixed with 1 ml 6M HCl and placed back into the incubators at 110°C, silicic samples were partially separated at this step and placed into Teflon bombs for HP/HT decomposition at 240°C for 3 days.

Samples for trace element analysis were diluted with HNO_3 after drying overnight, the solution was ultrasonicated for 2 hours to ensure complete dissolution. 0.1 ml of the sample + HNO_3 solution was diluted further with 0.9 ml of HNO_3 in a microtube to create a dilution factor of 2000 for use on the ICP-MS. The 12 samples selected for Sr and Nd isotope analysis were diluted with HCl and ultrasonicated for 20–30 minutes. The samples still contained some particulates, so HCl diluted samples were mixed with 1 ml $HClO_4$ and 1 ml HF and left in the ultrasonic bath overnight. After ultrasonication the samples were placed into incubators to dry.

Sr separation After sample decomposition 1.0 ml of 4.0 M HCl was added and to the sample and the sample placed in an ultrasonic bath for up to 30 minutes. The solution was then poured into a concave beaker and centrifuged for 5 minutes. The columns were prepared with BioRad 50W "X10" resin (1.0 ml) and cleaned using 6 M HCl, MilliQ, second 6M HCl and USQ. The resin was conditioned with 1.0 ml of 4.0 M HCl, when the conditioning acid was drained from the resin the 1.0 ml of the sample solution was loaded onto the column. After loading, the column was washed with a total of 2.5 ml of 2.8 M HCl. Once washed a clean flat bottomed beaker was placed under the column and the washing solution discarded. Rb and Sr were eluted with 4.0 ml of 4.0 M HCl, the flat bottomed beaker was removed and set aside for Rb-Sr separation. A second flat bottomed beaker was placed under the column for elution of Sm and Nd with 6.0 ml of 6.0 M Hcl.

Rb-Sr preparation: 3 drops of 0.015N H3PO4 was added to the elutant and set in an incubator at 70°C overnight until 1 drop remained, in the morning a cap was placed on the beakers (not closed) and T increased to 110°C. Once dry, 1-3 drops of Pyridine were added, this solution was dried up at 60°C for 2-3 hours.

Pb and Hf: Follows the procedure outlined in Kuritani and Nakamura (2002). Pb, Nd and Sr were analysed on Thermo Fisher Scientific, Triton Thermal Ionisation Mass Spectrometry (TIMS).

Hf separation:

After leaching and decomposition the samples were centrifuged and the supernate was separated from any precipitates. The separation procedure follows that in Lu et al. (2007), the procedure outlined is a 2 column procedure. The first column uses anion exchange to separate major elements, the second is an extraction resin which purifies Hf from Ti and Zr. Hf was analysed using Thermo Fisher Scientific, Neptune Multi Collector Inductively Coupled Plasma Mass Spectrometer (MC-ICP-MS).

5. Results

5.1. Whole rock geochemistry

A TAS plot of samples in this study is presented in Figure 2. Samples from Breiðdalur, Þingmúli, Reyðarfjörður, Streitishvarf and Álftafjörður are plotted. Results of major, trace element and REE analyses are shown in Figures 3 and 4 (and in Tables in thesis Appendix). All samples follow a similar trend of enrichment of lighter elements and relative depletion of heavier elements. Sr is most prominently depleted in silicic samples, a factor of feldspar fractionation. Some samples show a spike in Ba, which is most likely a factor of plagioclase accumulation especially within intermediate samples. A single sample shows an 'anomalous' trend relative to the rest of the sample set, this lava from Þingmúli is more intermediate in composition and the trend may be a factor of this composition.

Figure 3 outlines the trends in major elements throughout this sampleset, the most concise being Breiðdalur. These volcanoes are very similar in major and trace element (Figure 4) space. Both fractional crystallisation and partial melting of the crust probably play a role in each of these volcanic systems, this is discussed further in Askew and Thordarson, 2019 (Thesis chapter 3). Notably in this sample set, an Icelandite lava from Álftafjörður, sample 674 (circle in Figure 4), is consistently depleted in REE's and incompatible elements compared to the general trends seen through these samples. This is probably due to the fractionation of an element such as apatite (low P in sample), or a similar REE mineral.

5.2. Breiðdalur volcanic system

Lavas and intrusions from this volcanic system were mapped, sampled and analysed in 2014/15, as part of the project to map and characterise the sequences of Breiðdalur. The results from that are detailed in Appendix C (paper 3), the results relevant to this study are trace element data, which indicated that the Breiðdalur volcano may not be a typical tholeiite volcano, with slightly enriched incompatible element ratios compared to those volcanoes e.g. Askja, which are often described as the 'typical' tholeiite trend. Nb and Zr are both relatively enriched in east fjord samples, both elements being incompatible in basaltic melts, and a major constituent of mantle plume material (Fitton et al., 1997), their ratios against Y can contrain relative degrees of mantle plume material entrained in melt. Breiðdalur volcano displays a Nb/Y ratio range between 0.367 – 0.910, a range similar to the volcano of Askja in the Northern Volcanic Zone (Kuritani et al. (2011), Figure 6b). Dykes are slightly enriched in Nb/Y ratio when compared to the bulk of the lava samples.

Breiðdalur samples $^{86}Sr/^{87}Sr$ values lie between 0.703329 – 0.703412, the 3 highest ratio samples are lavas from the Breiðdalur central volcano with ratios between 0.703376 – 0.703412. The lowest value is a basaltic lava which most likely formed outside of the central volcano, probably related to fissure swarm activity on the Breiðdalur system and erupting next to or on the side of the volcano later in the volcano's life. $^{146}Nd/^{148}Nd$ ratios are rather confined, being between 0.513011 – 0.513037. The highest value is from a regional dyke in the Breiðdalur dyke swarm. The central volcano lavas and the dyke form a negative trend in $^{86}Sr/^{87}Sr$ against $^{146}Nd/^{148}Nd$ space, the fissure swarm lava is somewhat off this trend appearing to be an outlier relative to this general trend of samples.

$^{176}Hf/^{177}Hf$ isotope ratios for samples from the Breiðdalur system are between 0.283152 – 0.283256. They show a similar relationship to Nd and Sr isotopic ratios.

Lead isotopic ratios for Breiðdalur are relatively confined (Figure **??**), but displaying a similar 'spread' of values to similar volcanic systems in Iceland, values of $^{206}Pb/^{204}Pb$ are between 18.4684 – 18.6139. $^{207}Pb/^{204}Pb$ values are between 15.4826 – 15.4931 and $^{208}Pb/^{204}Pb$ are between 38.2027 – 38.2850. These values define a slightly enriched, in radiogenic Pb, magmatic source for the Breiðdalur system, when compared to current day volcanic systems Breiðdalur values are more enriched than NVZ volcanoes including Askja. They may be similar to Kverkfjöll volcano but only unpublished data exists for this volcano. Compared to the extensive dataset of Kitagawa et al. (2008), Breiðdalur again displays enriched values with a higher degree of EM2 source component. One sample appears to be an outlier in respect to $^{206}Pb/^{204}Pb$ values, sample 778, which also outlies the dataset in Sr-Nd space (Figure 8).

5.3. Þingmúli volcanic system

The dataset for þíngmúli volcanic system is limited to only 2 samples, but these samples both consistently remain closely grouped in all isotope ratio space. They essentially overlap, or sit within the sample spread of Breiðdalur volcano, meaning, at least with this dataset it is not possible to distinguish the 2 neighbouring volcanic systems. The Þíngmúli samples are displayed in Figures 9, 8 and 7.

5.4. Reyðarfjörður volcanic system

Again a limited dataset, $^{86}Sr/^{87}Sr$ values of the 2 samples are 0.703352, a basaltic dyke from the volcanic system's dyke swarm, and 0.703426, a basaltic lava from the volcano. The dyke displays the most depleted Sr values of all samples in this dataset, and the lava displays some of the most enriched values. In $^{86}Sr/^{87}Sr$ vs $^{146}Nd/^{148}Nd$ space, the dyke sample plots along the same trend line as the majority of this dataset's samples from Breiðdalur, Þíngmúlli, Streitishvarf (below) and one sample from Álftafjörður (below). However, the lava is far from this trend line with relatively elevated Sr ratio by comparison, this is significant in regard to this dataset and the instrument errors, but is still within a very confined space in regards to regional geochemistry.

Reyðarfjörður samples display $^{176}Hf/^{177}Hf$ isotope ratios of 0.283182 (697) and 0.283196 (800), both samples plotting close to the average values of the entire dataset. When coupled against $^{146}Nd/^{148}Nd$ isotopes, Reyðarfjörður plots in the upper right sector (Figure 7), again indicative of a lesser EM component than the other systems in this study.

Reydarfjordur samples are both rather different in Pb - Pb space, sample 800 displays the lowest $_{206}Pb/_{204}Pb$ ratio of 18.3910. This value is markedly lower than any other sample in this dataset (Figure 9), though sits along the 'period I' trend line seen by Kitagawa et al. (2008), suggesting it could be a factor of the volcano's older age. The other sample, 697, is more typical of this dataset $_{206}Pb/_{204}Pb$ ratio of 18.5032, $_{207}Pb/_{204}Pb$ ratio 15.4779 and $_{208}Pb/_{204}Pb$ ratio 38.2134 (Figure 9). This is a basaltic dyke which should sample a similar mantle source to the central volcano lava of 800.

5.5. Álftafjörður volcanic system

Álftafjörður samples are generally the most distinct of this sampleset. They plot well away from the majority of other samples in ϵNd vs $^{86}Sr/^{87}Sr$ space (Figure 8) with $^{146}Nd/^{148}Nd$ values of 0.513005 and 0.513000, lower than any other samples. Sample 673, a basaltic/basaltic icelandite lava from the flank of Álftafjörður volcano, is one of the most distinct in Nd-Sr space. This suggests a higher degree of EM component to the magmas, relative to the rest of the sampleset and to the eastfjord lavas (Figure 8b).

$^{176}Hf/^{177}Hf$ values lie between 0.283148 – 0.283221, the lowest value being sample 674, an intermediate lava, which is also the lowest ratio of all samples in this dataset. The other 3 samples closely resemble to bulk of the other samples in Hf space. However in Hf-Nd space, these samples plot in the bottom left sector of this dataset, again indicating the greatest degree of EM source of these samples (Figure 7).

Pb isotopes measured in Álftafjörður samples display elevated values compared to the sampleset in 3 out of the 4 samples in this subset. The single sample that plots more closely to the rest of the sampleset is 674, the intermediate lava. The elevated values in all other samples agrees with samples from nearby flood basalts (Figure 10, Kitagawa et al. (2008)) and suggests, as the other isotope systems, greater EM magma in the source zone.

6. Discussion

The purpose of our study was to analyse the hypothesis that isotopes could be used to distinguish rocks from different volcanic systems, an important consideration when mapping the volcanic sequences of Iceland, and to delve further into the genesis of volcanic systems in eastern Iceland. Results from trace element analysis show that the volcanoes of Breiðdalur, Reyðarfjörður, Þingmúli and Álftafjörður are slightly enriched in incompatible elements (Figure 6a and 6b). This was previously used to argue that these volcanic systems could be distinguished by high precision geochemistry (Askew and Thordarson, 2019, Thesis), which would aid in geological mapping and further our understanding of the origin of eastern Iceland volcanic systems. Notably, the elements best utilised for these distinctions are Nb, Zr and Y, and to a lesser extent La (Figures 4 and 5). These elements are highly incompatible in basaltic melts, until clinopyroxene becomes a major fractionating phase around MgO 5 - 6 wt.% (Fitton et al., 1997). As such they can give a sense of the degree of mantle melting (and thus depth) and the amount of mantle plume material entering the volcanic systems' plumbing system.

Breiðdalur volcanic system overlaps with the southern NVZ volcano of Askja in Nb/Y vs Zr/Y space (Figure 6b, also seen in Figure 6a). This is somewhat at odds to the view of Martin and Sigmarsson

(2007), who suggest that the Breiðdalur volcano, and other volcanoes in the east fjords, were formed off-rift along segments similar to the Öræfajökull volcanic belt today. Comparisons with an unpublished major and trace element dataset for Álftafjörður (Gallagher, 2013), and the available data for Þíngmúli (Charreteur et al., 2013; Carmichael, 1964) shows these volcanoes all overlap in Nb/Y space (Figure 6a), with some exceptions to this where samples show high Nb enrichment (Álftafjörður and Þíngmúli).

6.1. Pb isotopes

Pb isotopes are one of the most widely used in Iceland, and with their 4 main isotopes used in geology, relatively simple analysis procedure and a good understanding of the mantle processes affecting these isotopes, they offer the best understanding of this sampleset. Their 3 major end members, HIMU, EM1/2, DM, indicate different mantle source material. Pb isotope values for all the samples analysed in this study are shown in Figure 9. The samples are from 5 separate volcanic systems, with this study proposing that Streitishvarf should be treated as an entirely separate system, although previously unrecognised. This new classification is based on the strong evidence displayed by Pb isotopes in this study and coupled with updated age dates (Askew et al, In Prep). Alone, the Pb isotope values from the Breiðdalur, Þingmúli and Streitishvarf samples are almost indistinguishable as separate systems. Reyðarfjörður is difficult to discuss due to the lack of samples available, Sample 800 displays the lowest ^{206}Pb and ^{208}Pb values of the entire sample set, though it still sits along the Period 1 line indicated by Kitagawa et al. (2008) (samples shown in Figure 9). This sample appears to show similar Pb isotopic ratios to lavas in the nearby area, which underlie the volcano of Reyðarfjörður (Figure 10).

Breiðdalur and Álftafjörður display the most enriched Pb isotope sample sets in this subset. Álftafjörðuris the most distinct, plotting with enriched 208 and 207 values suggesting greater input from an EM enriched source than the other systems in this study. Sample 778 is a plateau basalt, sampled above the Breiðdalur volcano but emplaced whilst the volcano was still active. The significant difference between this lava and the other Breiðdalur volcanics in Pb isotope space suggests that the source of this lava was entirely different. The lava was selected due to its proximity to a lava known to be from the volcano itself and was used to test the hypothesis that the lavas burying the Breiðdalur volcano were from the Breiðdalur system itself. Of course, we run into the problem of too small a dataset to effectively discuss this. The lava is clearly from a different magmatic source but that doesn't rule out the possibility that other lavas above this are from the Breiðdalur system. This would need to be resolved with a detailed transect in order to fully comprehend the dynamics of crustal accretion and volcanic system evolution through time.

Reevaluation of age dates in eastern Iceland (Askew and Thordarson, In Prep) indicates that Álftafjörður was active at a similar time to and probably before the Breiðdalur volcanic system. This may be an important factor to note as previously it was suggested that isotopic variation in the east fjords may be due to temporal changes in plume activity. Figure 10 displays the samples Pb isotopic ratios in graphic form on a map of the east fjords.

Notably Álftafjörður's silicic lava plots closely to the older systems of Þingmúli and Breiðdalur, this is possibly a factor of the AFC process forming the silicic magma (Martin and Sigmarsson, 2010; Berg, 2016; Sigmarsson et al., 1991; Schnell, 1994; Charreteur et al., 2013). The magma is presumably assimilating older basalts with similar isotopic fingerprints to those found around Breiðdalur and Þingmúli.

6.2. Hf, Nd and Sr isotopes

Sr and Nd isotopes generally agree with Pb isotopes as to be expected. Álftafjörður magmas plot towards a more enriched end member magma, suggesting a greater deep mantle reservoir source that the other central volcanoes in this study. Hf isotop

6.3. Spatial and temporal context

In order to understand the sample-set in a regional context, we compared the data with available datasets both from the Neogene age sequences in Iceland and Neo-Volcanic lavas. Iceland is the manifestation of MORB magmatism from the MAR mixing with a mantle plume thought to originate in the lower mantle, from a high velocity zone known as FOZO (Stracke et al., 2005). The Iceland rift zones display varying degrees of mixing between these 2 sources, it is believed that plume material flows away from the plume head roughly beneath western Vatnajökull, to the south and mixes with N-MORB. The plume proportion decreases with distance southwards down Reykjanes Ridge. To the north of Vatnajökull the Tjörnes fracture zone, on the northern Iceland coast, is thought to act as a barrier to plume material flowing northwards as little to no plume material is detected along the ridge north of Iceland. The NVZ shows slight mixing trends, with Bárðabunga, Askja and Krafla displaying progressively less enriched plume material. The ÖVZ is isotopically enriched with 208, 207 and 206 Pb, Öræfajökull itself displaying a relatively high EM1 mantle component. EM1 is derived from sedimentary material and may be plume sourced or from a 'slice' of Greenlandic Jurassic sediments trapped when the North Atlantic opened (Torsvik et al., 2015). To the north of the ÖVZ, Snæfell volcano is another enriched volcano. It has a lesser degree of EM1 enrichment to Öræfajökull, Snæfell is likely to not be contaminated with Jurassic sediments and its geochemical signatures a symptom of plume material melting at depth. This geochemical arrangement is important to understand, as the current volcanic system arrangement is a consequence of plume material upwelling beneath Iceland, thus, if we can understand the geochemistry and regional arrangement of Neogene volcanic systems, we have a direct indicator of plume influence through time.

Figure 9 shows the Pb isotope space arrangement of Neogene volcanoes in this study relative to selected neo-volcanic zone volcanoes and a large east-fjords dataset from (Kitagawa, 2006) respectively (Also visualised in Figures 10 and 10). The 12 – 11 My old volcano of Reyðarfjörður, the 10 – 9 My old volcanoes of Þingmúli and Breiðdalur and the dyke from the approx. 11 My old Streitishvarf dyke swarm plot in the most enriched sector of the Kitagawa (2006) array. Álftafjörður volcano however, stands apart from the majority of the other samples in Pb space and away from any potential variation explained through simple binary mixing. Álftafjörður mafic magmas appear more enriched in 207 and 208Pb, these samples do lie closely to some points from the Kitagawa (2006) research paper, samples that are also located close to the Álftafjörður area. Data from Hanan and Schilling (1997) was excluded from comparison due to their analysis age. The enrichment may be explained by a higher EM1 component to the magma source for Álftafjörður.

The enrichment of lavas close to Álftafjörður volcano was thought to be a factor of temporal changes, this hypothesis rests on 2 factors: the age of the lavas close to Álftafjörður are from 9 – 8 Ma, and that the plateau basalts from one fissure system spread evenly throughout the eastfjords stratigraphy. We certainly dispute the first suggestion, and a reevaluation of dates puts these lavas from around 10.5 – 9.5 Ma. The second factor may be true for some eruptions (e.g. Óskarsson, 2015), but is probably not the case for every lava in the whole stratigraphy. Many lavas probably flowed 10's of km's from source but even small topography can dictate the lava flow field growth (Pedersen et al., 2017), so a local scale geochemical signature could stay within tens of km's or less from source. If we take both of these factors along with the published geochemical data and this study's data, we see that lavas of 10 – 10.5 My old from close to Reyðarfjörður are geochemically distinct from similar age lavas to the south near Álftafjörður.

The other volcanoes in this study share geochemical signatures seen in many of the volcanic systems today. However, if we take into account the general picture of Iceland's evolution, it is unlikely that we should compare any east fjord volcanoes with Western Volcanic Zone (WVZ) or Reykjanes Peninsula. The current southern Eastern Volcanic Zone (EVZ) and South Iceland Volcanic Zone shares little in common, geochemically, with the volcanoes of the east fjords this study focuses on. Thus, our main comparable focus is on the volcanoes of the Northern Volcanic Zone (NVZ) or the northern EVZ (Figure 10). Breiðdalur, Þingmúli and Reyðarfjörður show similarities in Pb characteristics with the volcanoes of Askja or Snæfell (Figure 9; (Kuritani et al., 2011)). When comparing this study's Neogene samples with the active Neo-Volcanic zones, Álftafjörður overlaps with the Snæfell volcanic system of the ÖVZ in ^{207}Pb space and also with unpublished samples from Kverkfjöll volcanic system in both ^{208}Pb and ^{207}Pb space (Eemu Ranta, pers. comm.). Our proposal is that the Álftafjörður system once shared a similar mantle source to these systems to the north of Vatnajökull.The question then turns to if the mantle plume beneath Iceland was the same or similar to today or if it was larger (Óskarsson, 2015; Harðarson et al., 2008; Spice et al., 2016; Fitton et al., 1997; Hanan and Schilling, 1997). The enriched nature of the small set of samples we have from Álftafjörður plus the location of the system almost directly east of Kverfjöll suggests that the Neogene plume and volcanic system setup may be similar to today, though this may not be fully backed up by data from other studies.The suggestion is thus that the geochemical traits seen in both lavas close to, and lavas known to be from Álftafjörður are most likely the result of a local geochemical fingerprint, which is still visible today, not a regional scale mantle variation.

Our dataset also suggests that samples from Þingmúli and Breiðdalur are geochemically indistinct. The hypothesis this study tested hoped to find a method of geochemically fingerprinting and characterising lavas and dykes from neighbouring volcanoes in order to aid in geological mapping, understanding of rift evolution and how neighbouring volcanic systems might interact with one another. This is a possibility in volcanic systems such as Álftafjörður and Breiðdalur which clearly show a differential mantle source, but Þingmúli and Breiðdalur must share some mantle source characteristics. This in of itself is not a surprising find, the 2 volcanoes are very closely spaced and lavas overlap, as does the dyke swarm. If the volcanoes are sampling a broad overlapping area within the aesthenosphere, and rising magma is held within shallow reserviors, then the geochemical signatures could be affected by subsequent mixing.

7. Conclusions

Our study of 5 Neogene volcanic systems has revealed a spatial and temporal link to isotopic characteristics affecting magmatism at these systems. The enriched nature of the rocks in eastern Iceland provides support to crustal accretion models and crustal evolution models that suggest the volcanic systems of eastern Iceland were constructed on the edge of a main rift zone in Northern Iceland.

- Breiðdalur, Reyðarfjörður and Þingmúli volcanoes are closely spaced in isotope variation diagrams. The suggestion is that there must have been a relatively uniform source zone for these central volcanoes from at least 12 to 9 Ma. The slight depletion in Pb isotopes for the Reyðarfjörður volcano lava, may be due to a temporal plume waning.
- Breiðdalur and Þingmúli volcanic systems may have formed along the edge of a main rift axis, similar to the Kverkfjöll system in the NVZ today.
- Álftafjörður volcano is more geochemically enriched than the other volcanoes in this study, it is suggested that Snæfell is a close analogue to the magmatic source of Álftafjörður. Silicic magma for this volcano is probably sourced through AFC of country rock from older volcanoes such as Breiðdalur and Þingmúli.
- Streitishvarf dyke swarm is not related to Álftafjörður, it is at least 1 My older and geochemically distinct. The magma for the Streitishvarf composite dyke is unlikely to be sourced from Álftafjörður.

8. Figures

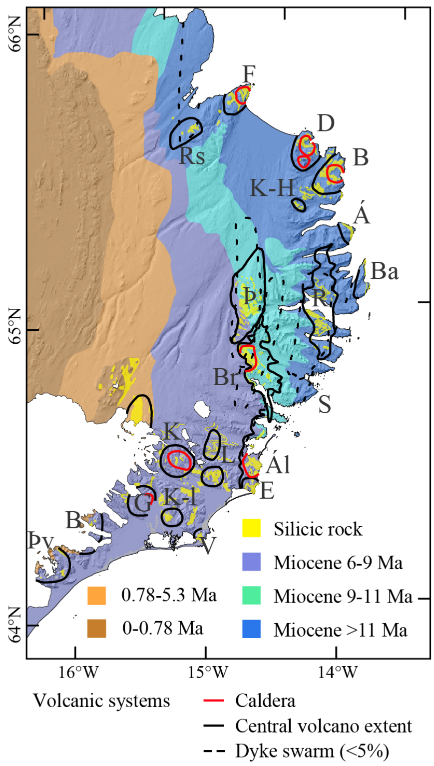

Figure 1: East fjord central volcanoes: Fagridalur - F; Refsstaðir - Rs; Dyrfjöll - D; Breiðavík - B; Álfavík - Á; Kækjuskörð - K-H; Herfell - K-H; Barðsnes - Ba; Reyðarfjörður - R; Þingmúli - Þ; Breiðdalur - Br; Streitishvarf - S; Álftafjörður - Ál; Lón L; Kollumúli - K; Eystrahorn - E; Vestrahorn - V; Ketil-laugarfjall - K-l; Geitafell - G; Birnudalstindur - B; Thverartindur - Þv. The oldest systems are in the north and the youngest in the south. The central volcanoes of Breiðdalur, Þingmúli, Álftafjörður and Reyðarfjörður have their approximate full extents outlined, other volcanoes are outlined as presented by data from Náttúrufræðistofunun's geology GIS shapefiles. The extents of dyke swarms were mostly presented by Walker (1964), the Streitishvarf dyke swarm has been added and the Álftafjörður swarm slightly altered from the original mapping which originally suggested it extented up to Barðsnes.

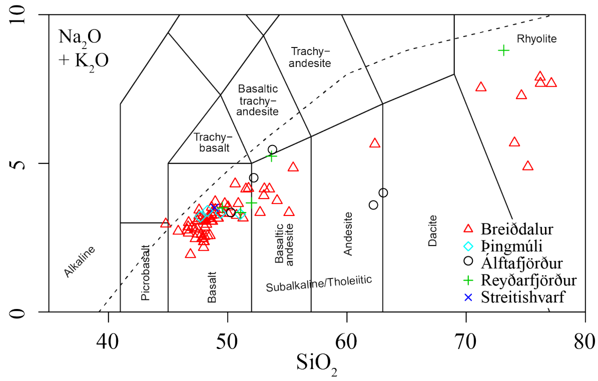

Figure 2: TAS diagram (Le Bas et al., 1986) for all samples, including samples from Breiðdalur volcano (Askew, Thesis).

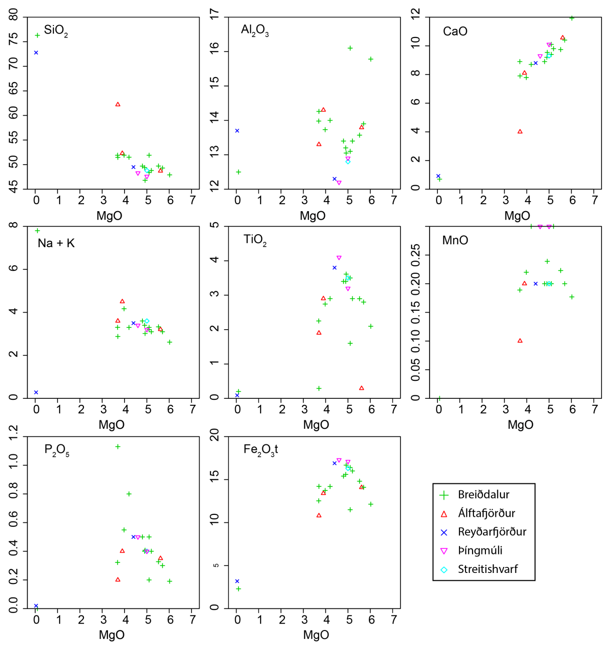

Figure 3: MgO vs Major elements for samples from this study.

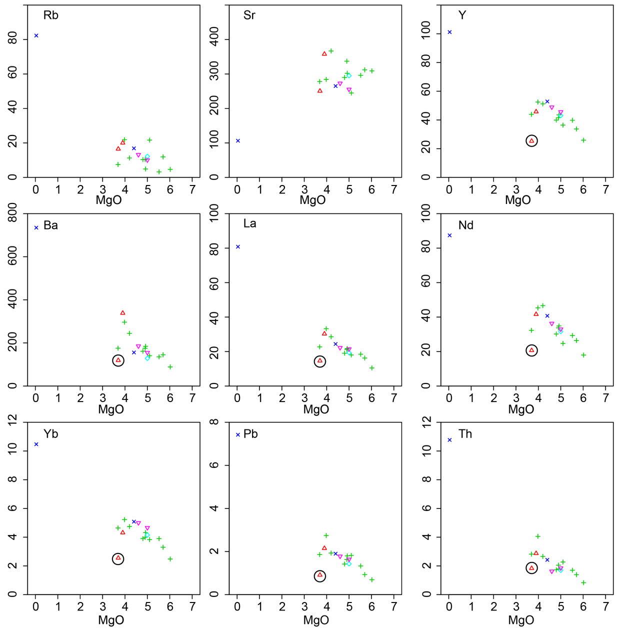

Figure 4: MgO (wt %.) vs trace elements. Symbols as for Figure 3

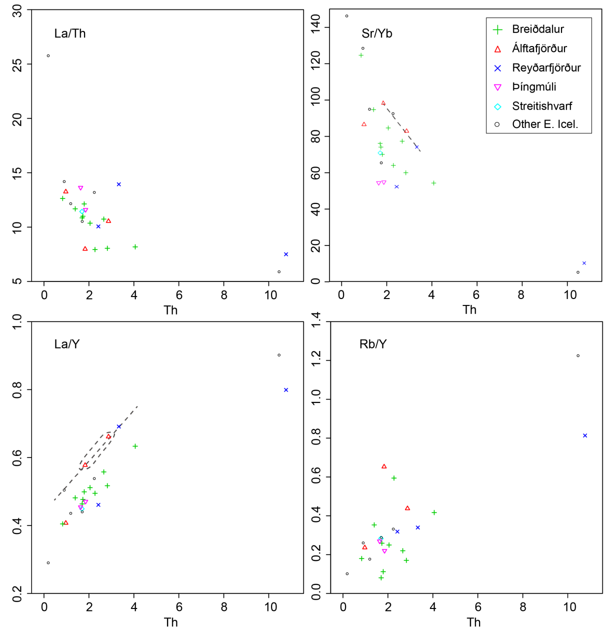

Figure 5: Th (ppm) against trace and REE ratios, elements that are used to discriminate volcanic systems in Iceland. Rb appears to be mobile. La/Y ratios appear to discern 2 main trends in basaltic samples, where the volcanic systems of Reyðarfjörður and Álftafjörður are picked out (dashed lines). Similarly with Sr/Yb, the same samples discern a slight trend though no other trends or groups are realistically seen.

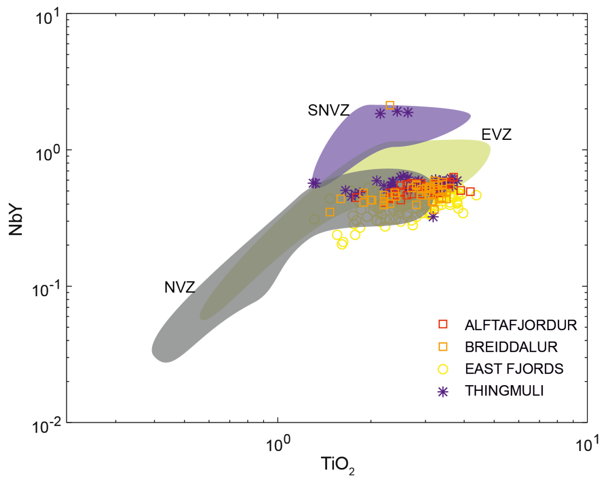

(a) TiO_2 (wt.%) vs Nb/Y ratios in basaltic samples from Breiðdalur, Álftafjörður (Extended sample set from Gallagher 2012, Thesis), Þíngmúli (Charreteur et al., 2013; Carmichael, 1964)

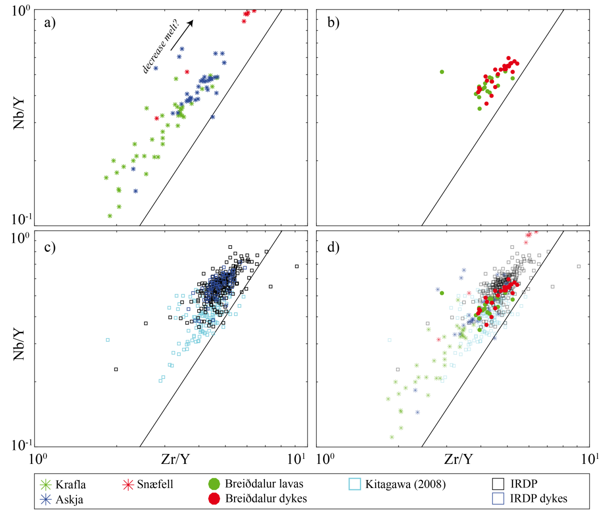

(b) Nb and Zr ratios for Breiðdalur, showing the ability of certain incompatible elements to distinguish volcanic systems. Samples from Breiðdalur volcano are shown with other values from the GeoRoc database. More enriched volcanic systems plot to the uper right. Black line: Northern Hemisphere reference line.

Figure 6: Incompatible trace element discrimination plots

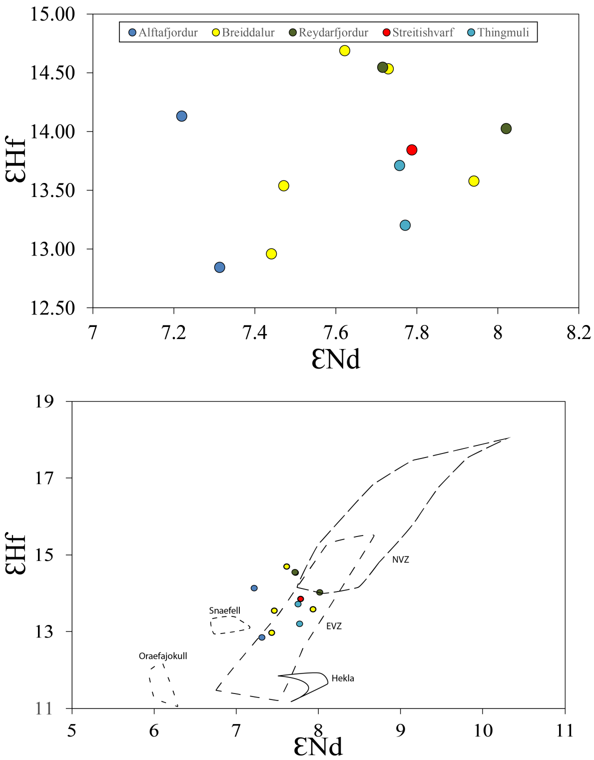

Figure 7: ϵHf isotopes against ϵ Nd. Left: Samples from this study. Right: This study relative to volcanic zones in Iceland.

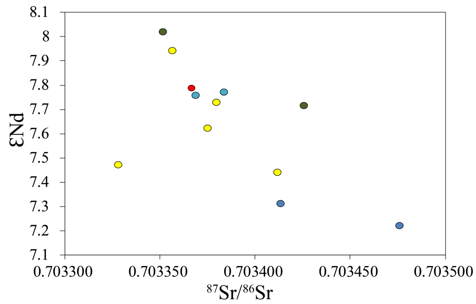

(a) Samples from this study

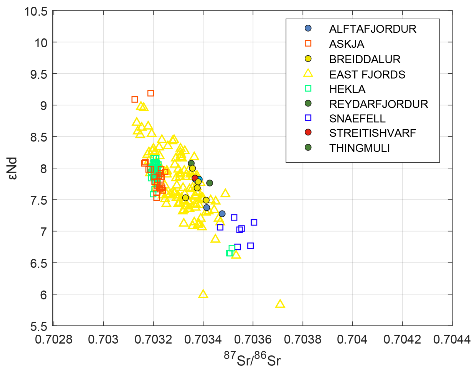

(b) Comparison with data from the east fjords (Kitagawa et al., 2008), Askja (Kuritani et al., 2011), Hekla (Chekol et al., 2011) and Snæfell.

Figure 8: Sr-ϵNd plots.

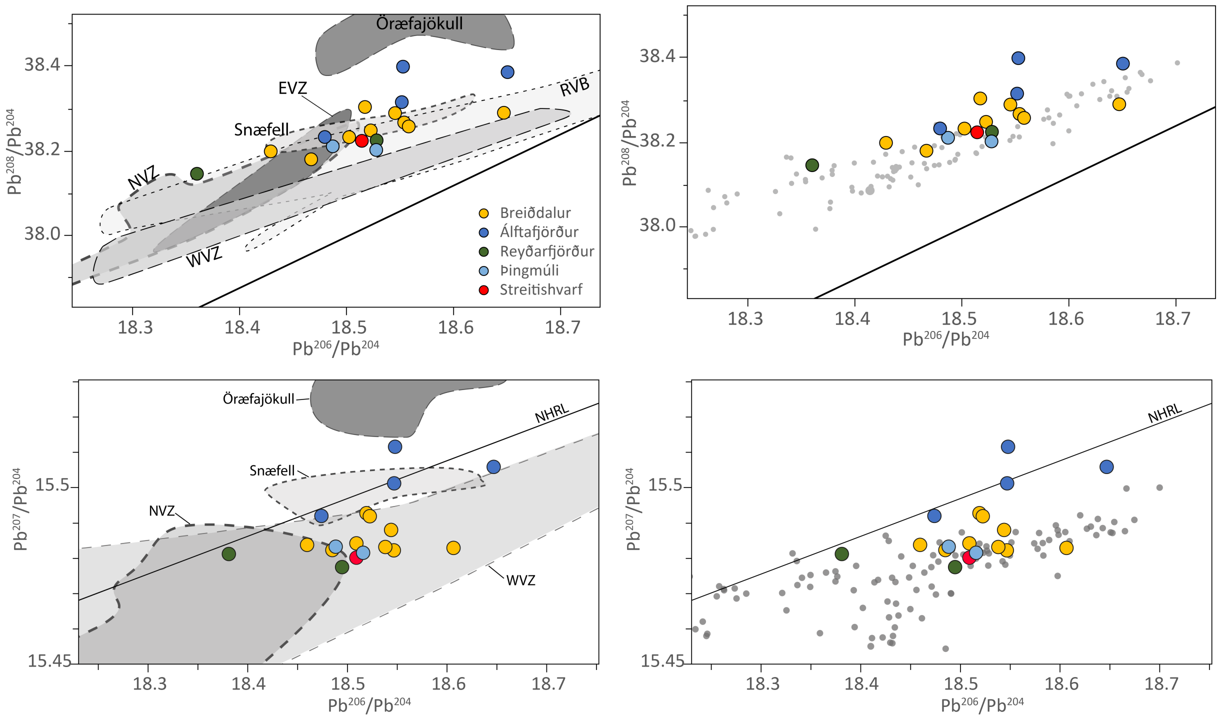

Figure 9: Figure key in top left graph. Top left: $^{208}Pb/^{204}Pb$ isotopic variability in samples from this study in relation to the geochemistry of active volcanic zones in Iceland. Top right: Samples from this study against the comprehensive dataset of plateau basalt lavas in the east fjords of Kitagawa (2006) (grey points). Of interest is the ^{208}Pb enrichment displayed by Álftafjörður (blue) and some samples from Breiðdalur.
Bottom left: $^{207}Pb/^{204}Pb$ isotopic variability in samples from this study in relation to the geochemistry of active volcanic zones in Iceland. Bottom right: the same sample set against the dataset of Kitagawa (2006), again the same samples show enrichment in ^{207}Pb even against east fjord plateau lavas. Errors are presented in tables in thesis appendix though mostly are represented by the point size. Figure data fields are a combined geochemical dataset compiled using the GeoRoc database, see text for references.

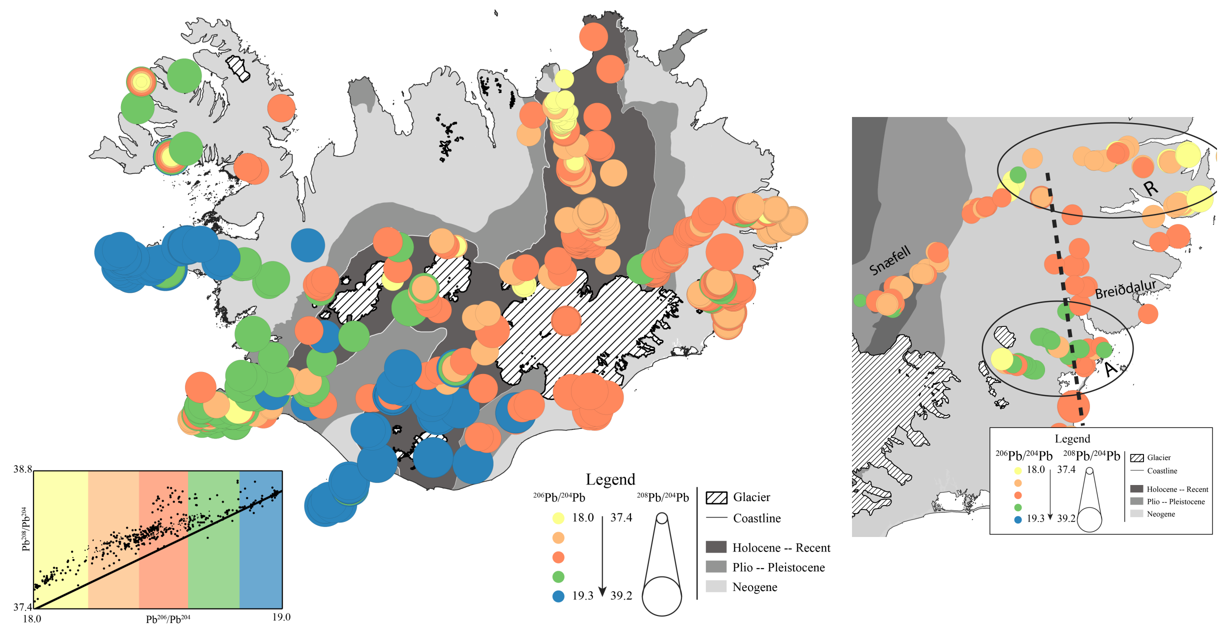

Figure 10: Pb isotopic variability map for Icelandic basaltic samples. The colours and symbol sizes indicate relative ratios, which gives a simple visualisation of mantle properties. Notably eastern Iceland is most isotopically similar to the NVZ and northern EVZ. To the right is a close-up map of east fjord Pb isotopic samples. Notably, The areas to the south east (Álftafjörður, A. Lower ellipse), are more enriched than much of the east fjords. Upper ellipse displays the more depleted samples relative to the Álftafjörður region, most depleted to the east, more enriched to the west.

9. References

References

Anderson, E.M., 1937. Ix.—the dynamics of the formation of cone-sheets, ring-dykes, and caldron-subsidences. Proceedings of the Royal Society of Edinburgh 56, 128–157. doi:10.1017/S0370164600014954.

Berg, S.E., 2016. Silicic Magma Genesis in Basalt-dominated Oceanic Settings : Examples from Iceland and the Canary Islands. Doctoral thesis, comprehensive summary. Department of Earth Sciences.

Carmichael, I.S.E., 1964. The petrology of thingmuli, a tertiary volcano in eastern iceland. Journal of Petrology 5, 435–460.

Charreteur, G., Tegner, C., Haase, K., 2013. Multiple ways of producing intermediate and silicic rocks within thingmúli and other icelandic volcanoes. Contributions to Mineralogy and Petrology 166, 471–490.

Chekol, T.A., Kobayashi, K., Yokoyama, T., Sakaguchi, C., Nakamura, E., 2011. Timescales of magma differentiation from basalt to andesite beneath hekla volcano, iceland: constraints from u-series disequilibria in lavas from the last quarter-millennium flows. Geochimica et Cosmochimica Acta 75, 256–283.

Fitton, J., Saunders, A., Norry, M., Hardarson, B., Taylor, R., 1997. Thermal and chemical structure of the iceland plume. Earth and Planetary Science Letters 153, 197–208.

Gústafsson, L.E., 1992. Geology and petrography of the Dyrfjöll Central Volcano, eastern Iceland. volume 138. Selbstverlag Fachbereich Geowissenschaften, FU Berlin.

Gudmundsson, A., Pasquarè, F., Tibaldi, A., 2014. Dykes, Sills, Laccoliths, and Inclined Sheets in Iceland. Springer Berlin Heidelberg. book section 1. Advances in Volcanology, p. 1–14.

Halldorsson, S.A., Oskarsson, N., Gronvold, K., Sigurdsson, G., Sverrisdottir, G., Steinthorsson, S., 2008. Isotopic-heterogeneity of the thjorsa lava—implications for mantle sources and crustal processes within the eastern rift zone, iceland. Chemical Geology 255, 305–316.

Hanan, B.B., Schilling, J.G., 1997. The dynamic evolution of the iceland mantle plume: the lead isotope perspective. Earth and Planetary Science Letters 151, 43 – 60.

Harðarson, B.S., Fitton, J.G., Hjartarson, A., 2008. Tertiary volcanism in iceland. Jökull 58, 161–178.

Jakobsson, S.P., et al., 1979. Petrology of recent basalts of the eastern volcanic zone, iceland .

Kitagawa, H., 2006. Petrological and geochemical study of the Icelandic Tertiary lavas: Implications for the evolution of Iceland mantle plume. Ph.D. thesis. Department of Earth and Planetary Sciences.

Kitagawa, H., Kobayashi, K., Makishima, A., Nakamura, E., 2008. Multiple pulses of the mantle plume: evidence from tertiary icelandic lavas. Journal of Petrology 49, 1365–1396.

Kuritani, T., Nakamura, E., 2002. Precise isotope analysis of nanogram-level pb for natural rock samples without use of double spikes. Chemical Geology 186, 31 – 43.

Kuritani, T., Yokoyama, T., Kitagawa, H., Kobayashi, K., Nakamura, E., 2011. Geochemical evolution of historical lavas from askja volcano, iceland: implications for mechanisms and timescales of magmatic differentiation. Geochimica et Cosmochimica Acta 75, 570–587.

Le Bas, M., Le Maitre, R., Streckeisen, A., Zanettin, B., Rocks, I.S.o.t.S.o.I., 1986. A chemical classification of volcanic rocks based on the total alkali-silica diagram. Journal of petrology 27, 745–750.

Lu, Y., Makishima, A., Nakamura, E., 2007. Purification of hf in silicate materials using extraction chromatographic resin, and its application to precise determination of 176hf/ 177hf by mc-icp-ms with 179hf spike. Journal of Analytical Atomic Spectrometry 22, 69–76. doi:10.1039/b610197f.

Martin, E., Sigmarsson, O., 2007. Crustal thermal state and origin of silicic magma in iceland: the case of torfajökull, ljósufjöll and snæfellsjökull volcanoes. Contributions to Mineralogy and Petrology 153, 593–605.

Martin, E., Sigmarsson, O., 2010. Thirteen million years of silicic magma production in iceland: links between petrogenesis and tectonic settings. Lithos 116, 129–144.

Óskarsson, B.V., 2015. Volcanological studies of Neogene flood basalt groups in eastern Iceland. Thesis. Department of Earth Sciences. URL: http://hdl.handle.net/1946/22929.

Palmáson, G., Sæmundsson, K., 1974. Iceland in relation to the mid-atlantic ridge. Annual review of earth and planetary sciences 2, 25.

Pedersen, G., Höskuldsson, A., Dürig, T., Thordarson, T., Jonsdottir, I., Riishuus, M.S., Óskarsson, B., Dumont, S., Magnússon, E., Gudmundsson, M.T., et al., 2017. Lava field evolution and emplacement dynamics of the 2014–2015 basaltic fissure eruption at holuhraun, iceland. Journal of Volcanology and Geothermal Research 340, 155–169.

Schnell, T., 1994. Breiðdalur central volcano, eastern Iceland: genesis of the evolved rocks. Thesis. Department of Earth Sciences.

Sigmarsson, O., Halldórsson, S.A., 2015. Delimiting bárðarbunga and askja volcanic systems with sr- and nd-isotope ratios. Jökull 65, 17–27.

Sigmarsson, O., Hémond, C., Condomines, M., Fourcade, S., Oskarsson, N., 1991. Origin of silicic magma in iceland revealed by th isotopes. Geology 19, 621–624.

Spice, H.E., Fitton, J.G., Kirstein, L.A., 2016. Temperature fluctuation of the iceland mantle plume through time. Geochemistry, Geophysics, Geosystems 17, 243–254.

Stracke, A., Hofmann, A.W., Hart, S.R., 2005. Fozo, himu, and the rest of the mantle zoo. Geochemistry, Geophysics, Geosystems 6.

Takei, H., Yokoyama, T., Makishima, A., Nakamura, E., 2001. Formation and suppression of alf₃ during hf digestion of rock samples in teflon bomb for precise trace element analyses by icp-ms and id-tims. Proceedings of the Japan Academy, Series B 77, 13–17. doi:10.2183/pjab.77.13.

Thordarson, T., Larsen, G., 2007. Volcanism in iceland in historical time: Volcano types, eruption styles and eruptive history. Journal of Geodynamics 43, 118–152.

Torsvik, T.H., Amundsen, H.E., Trønnes, R.G., Doubrovine, P.V., Gaina, C., Kusznir, N.J., Steinberger, B., Corfu, F., Ashwal, L.D., Griffin, W.L., et al., 2015. Continental crust beneath southeast iceland. Proceedings of the National Academy of Sciences 112, E1818–E1827.

Walker, G.P., 1960. Zeolite zones and dike distribution in relation to the structure of the basalts of eastern iceland. The Journal of Geology 68, 515–528. doi:10.1086/626685.

Walker, G.P., 1964. Geological investigations in eastern iceland. Bulletin Volcanologique 27, 351–363. URL: `http://dx.doi.org/10.1007/BF02597532`, doi:10.1007/bf02597532.

Yokoyama, T., Makishima, A., Nakamura, E., 1999. Evaluation of the coprecipitation of incompatible trace elements with fluoride during silicate rock dissolution by acid digestion. Chemical Geology 157, 175 – 187. doi:https://doi.org/10.1016/S0009-2541(98)00206-X.

Appendix B

Map Units

Here we describe mapped units from the geological map in approximate chronological order, see map key for reference to labels (if applicable) and label colour.

Skessa Tuff Regional welded ignimbrite. Crops out throughout eastern Iceland though a complete section is rarely found. One of the main outcrops is at the foot of Skiðudalur on the banks of the Skriðuá. Lithic rich silicic ignimbrite; clasts include welded fiamme, angular white rhyolite fragments, mafic angular clasts within a grey, fine tuff. At Skriduá the lowermost visible section is 3 m below the top of the ignimbrite. The welded tuff is at least 2 m thick and quickly grades into a lithic poor ash tuff of around 1–1.5 m thickness. The upper section of the ignimbrite is oxidised and has the appearance of a "red bed" paleosol. Ar/Ar dates 10.15 My (±0.2) My (Riishuus et al., 2014).

Regional plateau lavas. Undifferentiated, these are a short sequence of basaltic lava flows with minimal defining characteristics. They are pahoehoe lavas, interbedded with paleosol making up a stratigraphic thickness of around 30 m.

Grænavatn Porphyritic group (Gr). Definable group of regional lavas, notable for the abundance of plagioclase macrocrysts within the lavas.

B_1, Lower Breiðdalur flank lavas. Aphyric fine grained plagioclase, clinopyroxene, oxide basalts. Predominantly a'a lava morphology with characteristic rubbly bases and tops. Thicknesses vary from 1 to 2 m with rubbly bases of 10's of cm up to 40 cm and rubbly tops taking up approximately $\frac{1}{3}$ of the lava thickness. The cores are 10's of cm thick. In the field, the lavas are very dark grey to black in colour. A distinct difference is seen between these lavas and the plateau basalts below.

Breiðdalur Flaga (Fl). The group is part of the lower sequence of Breiðdalur flows, but differs from the general sequence below due to its pahoehoe flow morphology. The group crops out across the Breiðdalur but is best exposed at Flaga waterfall (Flögufoss), where a 15 m sequence of lobes bearing no paleosols is present. The group does not differ petrographically from flows around it, being a plagioclase, augite, oxide basalt with minor (5 %) phenocrysts of plagioclase. Geochemically the lavas of the group contain: SiO2 48.8 wt %; FeO(t) 17.8 wt %; MgO 5.2 wt %; Na2O 2.7 wt %; K2O 0.4 wt %; TiO2 2.9 wt %. The group may be traceable to the north of Breiðdalur but appears to thin to the south. The lack of the group in Berufjörður may potentially be a factor of exposure.

Fagridalur Olivine Basalt Group (Fa). Olivine bearing basalt group on the south eastern flank of Breiðdalur.

Breiðdalur Stöng Group (St). Structurally notable group of basaltic lavas, though individual flows appear to show no real relation to one another. The structural group is most visible from the southern side of Berufjörður facing north, where a group of lavas noticeably "bends" and terminates 50–100 m below the mountain of Stöng. The group thins towards a termination point, at which a coarse, angular, clast supported basaltic breccia is poorly exposed and is subsequently cross cut by a silicic dyke, presumably a feeder dyke for the Stöng rhyolite.

B_2, Breiðdalur Flaga Andesites. A sequence comprised predominantly of andesitic lavas sourced from the central volcano. The number of lava flows decreases to the east. The lavas are each around 10 m thick, a feature which is distinguishable in the mountainsides of Breiðdalur. Andesite lavas are found above and in the mountains to the north of the mapped group, but these often occur interdigited with mafic lavas, rather than a single stack of predominantly andesites. Hence why they are not differentiated at this scale of mapping.

B_3, Upper Breiðdalur flank lavas. Overlying the B_2 group, this is the youngest sequence of lavas on the eastern flank of the volcano. Comprised of <5 m thick basaltic lavas, the group is well exposed below Flögutindur, up Selá and on the scar of Svartagíl.

B_{ne}, Breiðdalur north eastern flank lavas. Overlying the B_1 group, this sequence is well exposed on southern side of Tóatindur and Breiðitindur. This sequence of lavas is stratigraphically equivalent to B_2 but is comprised of thin basaltic lavas and icelandite lavas rather than mostly icelandite lavas. Presumably B_2 and B_{ne} formed separate cones on the main edifice.

South Eastern Rhyolites (SER). See Schnell (1994) for further information and detailed descriptions of the units, brief descriptions will be outlined here as taken from the 1994 publication which are concurrent with the current authors' own observations. The SER sit atop the basaltic lavas of the Breiðdalur flank sequence, the eruptions appear to be forceful, breaking the lavas below and show signs of post-eruptive subsidence. The SER and upper Breiðdalur flank lavas show lesser degree of dip than those lower down, an expected consequence of less load stress on the higher stratigraphic lavas (Walker, 1960).

Stöng Rhyolite (St). The rhyolite of Slöttur and Stöng forms 2 distinct peaks of rhyolite each with cliffs of 200 m and 150 m high respectively. The Stöng lava is a continuation of the Slöttur, with the former peak also showing what is believed to be the agglomerate from the eruption vent. The rhyolite is well jointed and completely aphyric, it has a spherulitic texture where sperulites are around 1mm in diameter.

Flögutindur Rhyolite (Flö). Plagiocalse phyric lava with strong cleavage and flow structure. The rhyolite rests directly atop an agglomerate, the lava may be a continuation of the lava at Röndulfur or may have a separate, now eroded vent.

Smátindur Rhyolite (Smá). A large rhyolite flow or dome erupted effusively after an initial explosive event created a layer of agglomerate below the lava. The rhyolite is glassy and aphyric with a spherulitic texture. The lava's contact zone with the agglomerate is often chilled pitchstone, the agglomerate and blocks of rhyolite suggest the initial phase of the eruption event was explosive and an effusive lava phase proceeded it.

Caldera group basalts. Mapped lavas within the inferred caldera fault boundary. Many of the lavas are hydrothermally altered with poor exposures, and with a few exceptions, tracing lavas for any distance can be difficult.

Caldera fill facies. The major constituent of the caldera sequence is lapilli (pumice) tuff, previously called 'agglomerate' by Walker (1963). The entire caldera group is altered to various degrees causing discolouration depending on the degree of alteration and the type of secondary mineral precipitated. The highest grade of alteration seen is chlorite-epidote. The lapilli tuff consists of non-welded pumice clasts, angular basaltic and rhyolitic clasts in a fine grained ash matrix. Bedding is seen throughout but any structure is impossible to trace due to the amount of variability in bedding dip and strikes between exposures. Clast ratio within the agglomerate sequence is variable along with the matrix to clast ratio but largely looks similar from one area to the next, disregarding the alteration colour. Further to the lapilli tuff, the group contains layered tuffs, siltstones some of which display trace fossils, breccias and a multitude of intrusions. The variable dips, sedimentary structures, siltstones and trace fossils indicate the presence of multiple smaller subsidence events (or upwards deformation) indicative of nested calderas forming from smaller eruptions in the caldera itself.

Þórgrímsstaðir Rhyolite (Þó). Part of the summit sequence. The Þórgrímsstaðir rhyolite forms a steep, 3.5 km long, 20 – 30 m high, orange to pink cliff above the farm of Þórgrímsstaðir. A second, smaller rhyolite sits atop this obvious cliff but is less well exposed. The rhyolite lavas are sandwiched between tuffs. The underlying tuff is white and silicic in composition, exhibiting some degree of alteration, and the overlying is a red to black basaltic tuff. Petrographically the rhyolite lava is hypocrystalline, composed of quartz and feldspar with little to no macrocrysts. This lava is undated but relative dating suggests an age of around 9.2 (±0.2) My.

Berufjarðartindur Rhyolite. (BFTR) Part of the summit sequence. A thick red rhyolite flow visible most obviously from the south. The rhyolite is exposed for around 2–3 km around the peak of BFT but is thought to cover an area of up to 14 km2. It forms an impressive 30–50 m high cliff of jointed and fissile red rhyolite with a typical upward steepening flow structure. To the north west the rhyolite overlies the Matarhnjúkur ignimbrite and links up with a potential source intrusion on the western side of the mountain. The rhyolite and ignimbrite are suggested to be formed in the same eruption (Schnell 1994). As with the ÞGSR, the rhyolite is aphyric, hypocrystalline composed of quartz and feldspar. The rhyolite is overlain by olivine basalts from Heiðarvatn group (9.1 ±0.2 My), and appears to have tholeiitic plateau basalts banking up against it to the western side. Below BFTR is a sequence of around seven basaltic lavas, including one hyaloclastite, with a total thickness of 50 m.

Matarhnjúkur Ignimbrite. Part of the summit sequence. The upper caldera sequence is capped by a distinct, layered ignimbrite well exposed up the mountain Matarhnjukur. Though the base is not directly exposed, it can be inferred that the ignimbrite overlies a sequence of breccias, tuffs, and lavas with a dip of 15 degrees south west. The ignimbrite is red to pink in colour, with sub-horizontal layering dipping with surrounding lavas. It is exposed in sections on the mountainside, in total the thickness is around 150 m with a visible area of 0.6 km2. The ignimbrite rapidly thins away from the mountain. (Walker, 1963) suggested that a thin tuff traceable across to Fossárfell is linked to Matarhnjúkur, whilst Schnell (1994) suggests the BFTR is the effusive equivalent of the ignimbrite. The small area to thickness makes this a high aspect ratio ignimbrite suggesting deposition in a large depression within the caldera. In hand specimen, the ignimbrite contains white fiamme in a fine, glassy tuff matrix. The fiamme are of very high density (>50 %) in the lower portion of the ignimbrite. Lithic fragments are seen throughout but always highly outnumbered by the fiamme. Lithic fragments are variable: small (2–3 cm) basaltic fragments are seen throughout, along with mineral fragments, notably large dark clinopyroxenes (2–3 cm). Though layering is present in the 150 m thick ignimbrite, there is very little variation between each layer. There is a general decrease in the density of fiamme versus matrix but high at the top it is still on the order of 40 %.

Rauðafell Composite intrusion (Ra). Part of the summit sequence. 9.3 (±0.2) My (Martin and Sigmarsson, 2010). Considered to be the feeder vent for Fossárvík Composite flow, the intrusion is visible from the valley floor, where it is a 2 m wide dyke, up to Rauðafell, a dome-like peak below BFT. Rauðafell consists of both basalt and rhyolite end members, with a complex zone of mixing between the two. The rhyolite end member crops out in the central portion of the dyke and vent. It is comprised of unzoned macrocrysts of oligoclase, ferroaugite, and oxides in a fine grained K-feldsapr and quartz matrix. The basalt end member crops out on the outer portions of the feeder dyke. It is a plagioclase, clinopyroxene, and oxide basalt with up to 15 % zoned bytownite macrocrysts up to 1 cm in size (Charreteur and Tegner, 2013; Gibson and Walker, 1963). For further descriptions and information see specific publications by Charreteur and Tegner (2013); Gibson and Walker (1963).

Kelduskogar Intrusion (Keld). 9.3 My (±0.2) (Martin et al., 2011). A large intrusion ringed by agglomerate, presumably a feeder for a silicic flow (now eroded) similar to those exposed as the SER). Similar in age to the Rauðafell intrusion, this also appears to be one of the earliest silicic events though at the end of the volcano's lafe. Kelduskogar intrusion is easily visible by the coast, though is very poorly exposed as a yellow-white scree on flat ground.

Fossárvík Porphyrytic Basalt Group. Onlapping onto the upper (young) southern flank of

Breiðdalur, the porphyritic group consists of several lobes and flows of similar petrography which interfinger with the composite lava of Fossárvík.

Fossárvík Composite Flow (Fo). Exposed from Berufjörðurá across Fossárfell and into Fossárdalur, the composite flow is the type-exposure of mixed magma eruptions in eastern Iceland. Gibson and Walker (1963) suggest the flow is sourced from Rauðafell intrusion to the north. The following description is based on a detailed study by Askew and Gallagher (Unpublished, 2013) which in turn is based upon the observations made by Gibson and Walker (1963) and Charreteur and Tegner (2013).

Below the lava is 6 cm of red, laminated/finely bedded, sediment. The contact between the two is coherent. The mafic base contains small vesicles of around 20 % density which rapidly decreases upwards to around 10 % density at 30 cm vertically into the flow, and continues at this density to the contact at the flow top. The vesicle size ranges from 3 mm to 60 mm with an average 11–20 mm. The larger vesicles are elongate along a strike bearing 120°/300°. There is a lack of "rubble" or clinker at the base suggesting a general pahoehoe morphology.

The lower mafic flow is composite in character; there are distinct enclaves of material within the flow which are more mafic in character than their host. The host flow contains around 15– 20 % of zoned bytownite macrocrysts and <5 % clinopyroxene glomerocrysts in a matrix of plagioclase, clinopyroxene, oxide, and glass. It is lighter in colour than the enclaves it hosts. The phenocrysts are of 1–3 mm in size, averaging 2 mm and the glomerocrysts range up to around 8 mm in size.

Mafic enclaves within the mafic flow: The enclave sizes range from 1–8 cm throughout the flow. There is a range of compositions within the enclaves themselves. Some are plagioclase phyric only, others have plagioclase phenocrysts with some subordinate clinopyroxene, and others are aphyric. An approximate density of 20 % of phenocrysts throughout the different enclaves was found, and sizes range from 1–3 mm. Some enclaves appear apyhric and though this may be a factor of size and exposure, upon examination of 2D and 3D samples, enclaves were found to be wholly aphyric. None of the enclaves throughout the mafic flow are vesicular and all of the mafic enclaves have rounded shapes, none of them are angular or fractured. The host flow and enclaves are more easily distinguished on the more weathered surfaces of the mafic flow, as the hydrothermal alteration strongly brings out the contrasts between the two.

The mafic and rhyolite boundary is difficult to define. There is no basaltic flow top crust visible and no presence of a quenched pitchstone base of the rhyolite above. Instead, there is a visual mixing boundary between these two flows which seems to dominate the transition between mafic and silicic. It's a thin, 10–15 cm, gradational boundary which shows an interfingering and mixing of colours and compositions, as the upper silicic layer appears to interdigitate into the lower mafic flow. There are, however, anomalies to this narrow, gradational, mixing boundary; on the western side of the Fossárfell outcrop, fractured and angular fragments of silicic material are clearly seen within the upper section of the mafic flow for 60 cm vertically. How dominant and extensive each boundary is across the flow is hard to distinguish due to lack of outcrops but it suggests there are differing environments/conditions in localised regimes which results in two mixing types.

The silicic upper section of the flow is heavily weathered with very limited good, unbrecciated, exposure. It weathers into flat, angular slabs and creates a medium angled and unconsolidated scree. However, when clearing sections of the scree one can find more solid, less weathered and in situ sections of the flow. The silicic member of the composite flow is around 20–21 m thick, including the pitchstone flow top. In hand specimen, the rhyolite is grey to white in colour with obvious, dark, mafic blobs within the host flow. The mafic inclusions are rounded in shape, often elongate but in no preferential orientation. Phenocrysts in the silicic flow have been subject to hydrothermal alteration and jasper grade alteration can be seen throughout this sequence. The phenocrysts present are a mix of altered oligoclase feldspars (often bright red or green) and quartz. There is complex flow banding of grey to cream white bands of 2 to 5 cm thick. The vesicle density visibly increases vertically from 20 % to greater throughout this section of the outcrop, however the weathering out of macrocrysts, and the presence of infilling clays within vesicles makes taking a true vesicle density difficult. Those vesicles which were positively identified were elongated and consistently around 5mm in size. A raft of larger scale, angular, basalt appears high up in the rhyolite, the basalt is sharp and fissile and therefore easily distinguishable from the crumbly rhyolite flow and its enclaves. Hydrothermal alteration has been focused around this raft which also enhances the differences between the raft and its host. This basaltic contains large, elongate vesicles (unlike the enclaves) which are oriented vertically.

The mafic enclaves within the silicic part of the flow have the same range of compositions as the ones incorporated within the mafic flow. The size range is however slightly different. These enclaves have a larger size range from 1 mm to as much as 60 cm, but still display convolute, rounded margins. There are no fractured or angular enclaves. Their density is generally less than 10 % in the whole flow and does not vary greatly throughout.

The composite flow displays a pitchstone crust. Its contact is undulating and ranges from 3–5 m in thickness at the Fossárfell locality. The phenocryst percentage is around 25 % with a size range from 1 mm to 4 mm. Vesicles do not appear to be present, though this may be a factor of devitrification, weathering of the crumbly pitchstone, or infilling with zeolites mistaken in the field. The weathering is pervasive in this section of the flow. Mafic enclaves within the pitchstone are of a similar size to those seen in the rhyolite body, with a maximum size of 30 cm and a similar range of sizes. A xenolith of dacitic rock is present in the pitchstone top. The dacite shows flow banding which is oriented vertical to the section. The whole xenolith is 4 m by 1 m in size and is >20 % feldspar phyric.

Summit Breiðdalur lavas. Lavas based within the summit group area of the geological map. Their grouping does not appear to define a chemical or petrological relationship as there are many different lavas within this group. These lavas may be sourced from nearby fissure eruptions or from Breiðdalur sources, but their limited extents and difficulty in tracing for any distance makes any source inference impossible with current knowledge. Some of the lavas appear to fill in depressions found in the upper caldera sequence, between rhyolite flows, agglomerates or perhaps vent depressions.

One such example is the BFT hyaloclastite, formed from brecciated pillow basalts which created a hyaloclastite delta within a depression in the caldera.

Appendix C

Geochemical data

Table C.1: Geochemical data for Thesis presented in full

Sample name	340	348	376	381	388	389	392
Latitude	64.799837	64.898317	64.854612	64.926697	64.926025	64.925673	64.925075
Longitude	-14.498381	-14.502201	-14.499336	-14.404284	-14.399124	-14.394553	-14.392401
Location	Raudafellsgil	Hrafnaskrida	Innri Ljosá	Nordurdal.	Nordurdal.	Nordurdal.	Nordurdal.
Type	Dyke	Dyke	Dyke	Dyke	Dyke	Dyke	Dyke
Age							8.1
SiO2	49.9	54.9	47.3	49.2	49.7	48.6	48.4
Al2O3	13.8	12.8	14.1	13.0	13.4	13.3	13.1
Fe2O3	14.0	14.8	15.0	16.5	15.4	16.4	16.4
FeO	1.6	1.6	1.7	1.8	1.7	1.8	1.8
FeOT	15.6	16.4	16.7	18.3	17.1	18.2	18.3
MgO	5.6	2.8	6.7	4.9	4.8	5.1	5.1
CaO	10.1	7.0	10.3	9.1	8.9	9.4	9.4
Na2O	2.6	2.8	2.4	2.6	2.6	2.6	2.6
K2O	0.6	1.0	0.4	0.6	0.9	0.6	0.7
Na + K	3.2	3.8	2.8	3.2	3.6	3.2	3.3
TiO2	2.7	2.4	3.1	3.2	3.4	3.3	3.5
MnO	0.2	0.3	0.2	0.2	0.2	0.2	0.2
P2O5	0.3	1.0	0.3	0.4	0.5	0.4	0.5
LOI	20.4	21.9	21.2	23.4	22.4	23.2	23.4
Total	99.8	99.8	99.8	99.8	99.8	99.8	99.9
Zn	114.0	189.9	135.9	139.9	139.5	122.6	97.9
Cu	132.2	16.1	112.5	101.3	81.4	197.4	166.2
Ni	47.1	5.9	34.3	35.3	34.7	87.1	74.9
Cr	56.4	3.4	7.6	10.2	29.4	163.4	200.1
V	355.7	56.5	405.9	387.4	391.1	344.4	317.1
Ba	146.3	341.2	158.6	223.6	160.3	114.4	91.3
Sc	30.5	31.8	31.4	33.5	35.0	32.4	36.4
La	15.2	35.6	14.4	21.8	15.1	10.9	5.5
Ce	50.0	97.0	51.0	65.6	51.0	42.2	26.0
Nd	29.7	62.1	31.9	38.0	31.5	27.2	18.4
Nb	22.8	41.9	22.4	31.8	23.2	19.9	11.7
Zr	212.4	371.3	200.9	269.7	196.5	183.4	106.2
Y	43.0	84.2	47.8	53.4	47.2	39.7	27.0
Sr	300.4	335.3	262.5	276.8	282.8	306.6	255.9
Rb	13.4	21.7	11.7	29.7	11.9	9.0	4.9
U							
Th							
Pb							
Co							
146Nd/148Nd							
86Sr/87Sr							
206Pb/204Pb							18.5461
207Pb/204Pb							15.4835
208Pb/204Pb							38.2753
208Hf/206Hf							0.283213

Sample name	402	404	405	413	421	426	427
Latitude	64.896707	64.896913	64.897076	64.843498	64.903481	64.839324	64.839393
Longitude	-14.491021	-14.491399	-14.491053	-14.350366	-14.536577	-14.471698	-14.472685
Location	Merkigil	Merkigil	Merkigil	Baejargil	Storalaekjargil	Ytri Ljósá	Matarhnjúkur
Type	Inclined sheet	Dyke	Lava	Lava	Dyke	Dyke	Lava
Age							
SiO2	54.3	49.9	75.4	47.9	48.7	49.5	48.6
Al2O3	13.4	13.1	12.6	13.1	13.3	14.1	15.4
Fe2O3	14.4	15.5	3.7	16.7	16.2	14.3	12.7
FeO	1.6	1.7	0.4	1.9	1.8	1.6	1.4
FeOT	16.0	17.2	4.1	18.5	18.0	15.9	14.1
MgO	2.9	5.0	0.3	5.4	5.0	5.5	6.5
CaO	7.1	9.2	2.6	9.8	10.4	10.2	11.9
Na2O	3.7	2.4	3.2	2.5	2.2	2.5	2.1
K2O	0.5	0.8	1.7	0.4	0.2	0.6	0.1
Na + K	4.2	3.2	4.9	2.8	2.4	3.1	2.3
TiO2	2.3	3.3	0.3	3.4	3.2	2.8	2.2
MnO	0.3	0.2	0.1	0.3	0.2	0.2	0.2
P2O5	1.0	0.4	0.0	0.5	0.3	0.3	0.2
LOI	21.8	22.1	9.4	23.2	22.2	20.5	17.8
Total	99.8	99.8	99.8	99.8	99.8	99.8	99.9
Zn	178.2	132.3	155.6	141.6	134.9	112.5	99.1
Cu	7.4	111.6	13.8	110.6	147.6	105.3	138.8
Ni	5.7	37.6	2.1	47.4	38.9	55.4	62.4
Cr	0.7	31.6	0.0	34.6	17.3	48.4	185.6
V	67.5	403.9	8.7	431.3	469.6	359.6	332.4
Ba	292.3	188.5	620.4	187.0	234.4	141.2	60.3
Sc	25.6	31.3	3.3	39.5	33.2	31.2	39.9
La	38.2	19.2	92.5	18.0	15.2	14.0	8.4
Ce	96.4	57.2	204.7	56.2	51.0	47.8	29.7
Nd	62.5	38.7	109.6	36.6	32.6	28.4	18.6
Nb	41.5	28.0	99.5	26.7	22.8	22.2	13.3
Zr	366.3	254.7	618.8	253.6	202.0	205.6	123.8
Y	86.5	50.9	145.7	51.6	41.5	40.6	31.4
Sr	382.8	283.8	141.8	295.9	403.8	311.3	263.4
Rb	31.5	19.1	67.3	6.0	1.7	12.8	1.0
U							
Th							
Pb							
Co							
146Nd/148Nd							
86Sr/87Sr							
206Pb/204Pb							
207Pb/204Pb							
208Pb/204Pb							
208Hf/206Hf							

Sample name	440	446	448	451	463	469	470
Latitude	64.845544	64.827005	64.827269	64.824026	64.887403	64.877263	64.877342
Longitude	-14.450656	-14.440187	-14.441849	-14.449095	-14.540316	-14.399055	-14.399355
Location	Ketilhnjukur	BFT	BFT	BFT		Jorvík	Jorvík
Type	Lava	Lava	Lava	Lava	Lava	Dyke	sheet
Age			9.7	9.8			8.5
SiO2	56.1	76.3	48.7	49.0	45.52	51.9	62.9
Al2O3	15.5	12.5	14.4	14.4	13.91	16.1	13.6
Fe2O3	9.7	2.3	13.2	13.1	13.33	11.5	9.8
FeO	1.1	0.3	1.5	1.5	1.5	1.3	1.1
FeOT	10.8	2.5	14.6	14.6	14.8	12.8	10.9
MgO	4.2	0.1	6.5	6.4	6.32	5.1	1.5
CaO	7.5	0.7	11.8	11.7	11.77	10.1	4.3
Na2O	2.1	4.6	2.2	2.3	1.82	2.6	3.9
K2O	2.8	3.1	0.2	0.3	0.056	0.6	1.8
Na + K	4.8	7.8	2.4	2.6	1.878	3.2	5.7
TiO2	1.7	0.2	2.4	2.3	2.525	1.6	1.3
MnO	0.2	0.0	0.2	0.2	0.190	0.2	0.2
P2O5	0.2	0.0	0.3	0.2	0.167	0.2	0.5
LOI	16.7	10.5	18.5	18.6	14.0	17.2	17.7
Total	99.8	99.8	99.8	99.9	99.80	99.9	99.8
Zn	125.2	152.0	119.9	109.7	106.9	114.5	199.4
Cu	96.8	9.1	155.2	134.3	153	120.1	10.0
Ni	54.7	0.8	64.1	66.3	62.3	142.1	5.3
Cr	104.6	0.6	205.0	209.8	191	76.2	4.5
V	277.1	4.8	365.5	335.5	376.9	237.2	13.3
Ba	383.3	617.4	55.4	84.6	40.9	150.9	453.5
Sc	36.0	0.7	43.7	42.3	39.1	22.9	20.2
La	30.9	79.3	7.8	7.0	2.6	16.8	59.3
Ce	72.1	175.6	36.2	30.9	21.1	51.8	141.7
Nd	38.1	93.0	23.6	18.3	14.3	27.9	82.0
Nb	26.6	93.8	16.7	13.7	11.2	18.9	67.4
Zr	185.8	406.0	152.3	129.5	96.4	194.3	795.0
Y	53.2	132.7	36.7	33.7	25	43.1	108.6
Sr	216.6	65.4	258.4	252.5	164.3	239.9	258.4
Rb	66.2	67.9	6.3	5.3	1.2	22.0	55.3
U					0		
Th					0.3		
Pb					1.2		
Co							
146Nd/148Nd						0.513037	
86Sr/87Sr						0.703357	
206Pb/204Pb		18.5546				18.55186	
207Pb/204Pb		15.4826				15.48839	
208Pb/204Pb		38.2541				38.26053	
208Hf/206Hf		0.283183					

Sample name	472	476	478	491	492	493	496
Latitude	64.818147		64.703513	64.784224	64.786648	64.790815	64.803604
Longitude	-14.376627		-14.389718	-14.487015	-14.509945	-14.525155	-14.52951
Location	Flogufoss		Berufjordur	Berufjordur	Berufjordur	Berufjordur	Berufjordur
Type	Lava	Lava	Dyke	Dyke	Dyke	Dyke	Dyke
Age	10.1				9.3		
SiO2	48.8	45.33	48.4	50.5	49.3	51.6	49.1
Al2O3	13.4	15.79	16.7	13.3	13.9	13.4	15.0
Fe2O3	16.0	13.41	11.3	15.0	14.1	14.5	12.8
FeO	1.8	1.5	1.3	1.7	1.6	1.6	1.4
FeOT	17.8	14.9	12.6	16.6	15.7	16.1	14.2
MgO	5.2	7.66	6.1	4.6	5.7	4.4	6.3
CaO	9.8	10.15	12.4	8.6	10.4	8.4	11.4
Na2O	2.7	2.43	2.2	2.8	2.5	2.8	2.3
K2O	0.4	0.255	0.3	0.9	0.6	0.9	0.3
Na + K	3.1	2.688	2.6	3.7	3.1	3.7	2.6
TiO2	2.9	1.924	1.9	3.4	2.8	3.1	2.2
MnO	0.3	0.191	0.2	0.2	0.2	0.2	0.2
P2O5	0.4	0.225	0.2	0.5	0.3	0.5	0.2
LOI	22.7	16.6	16.5	22.0	20.4	21.5	18.3
Total	99.8	99.9	99.9	99.8	99.8	99.8	99.9
Zn	130.0	108.2	99.6	133.2	133.2	114.8	99.8
Cu	86.9	64.5	139.2	42.9	64.9	146.9	124.8
Ni	33.7	127.5	62.3	19.0	23.1	51.7	59.0
Cr	39.8	100.2	183.7	14.1	9.0	74.0	89.4
V	413.2	308.2	335.3	320.5	338.6	366.4	336.2
Ba	158.6	79.1	60.2	213.4	189.2	153.2	91.7
Sc	43.2	34.3	40.1	29.8	30.1	34.3	34.4
La	15.7	6.6	6.6	83.8	22.2	14.8	5.0
Ce	52.0	27.7	30.6	67.5	66.7	45.9	28.5
Nd	33.0	19.4	19.4	41.0	41.2	29.5	18.8
Nb	23.8	12.4	13.1	31.6	30.5	20.9	13.6
Zr	224.9	120.2	124.0	292.0	293.8	192.0	128.2
Y	51.3	28	31.7	54.9	54.1	39.4	29.2
Sr	264.7	244.4	262.8	330.8	308.2	303.3	303.2
Rb	4.3	2.9	0.8	15.4	20.0	13.8	5.9
U		0					
Th		0.1					
Pb		0.8					
Co							
146Nd/148Nd							
86Sr/87Sr							
206Pb/204Pb	18.4937						
207Pb/204Pb	15.4827						
208Pb/204Pb	38.2027						
208Hf/206Hf	0.283256						

Sample name	498	500	501	503	504	507	510
Latitude	64.804544	64.808963	64.811722	64.813538	64.813501	64.772942	64.774337
Longitude	-14.557525	-14.580037	-14.5892	-14.586737	-14.587352	-14.357459	-14.367796
Location	Berufjordur	Berufjordur	Berufjordur	Berufjordur	Berufjordur	Stong	Stong
Type	Dyke	Dyke	Dyke	Dyke	Dyke	Dyke	Lava
Age							9.9
SiO2	51.5	50.2	48.8	48.4	49.4	49.4	50.2
Al2O3	14.0	13.0	13.6	13.0	13.2	13.4	13.3
Fe2O3	14.2	16.4	15.2	16.4	15.6	15.2	15.6
FeO	1.6	1.8	1.7	1.8	1.7	1.7	1.7
FeOT	15.7	18.3	16.9	18.2	17.4	16.8	17.3
MgO	4.2	4.7	5.7	4.5	4.9	5.2	4.8
CaO	8.7	8.2	10.3	10.1	9.2	9.5	8.8
Na2O	3.0	2.6	2.4	2.6	2.7	2.6	2.8
K2O	0.3	0.8	0.5	0.6	0.7	0.7	0.7
Na + K	3.3	3.4	2.8	3.2	3.4	3.4	3.5
TiO2	2.9	3.2	2.8	3.6	3.4	3.2	3.0
MnO	0.3	0.3	0.2	0.2	0.2	0.2	0.2
P2O5	0.8	0.4	0.3	0.5	0.4	0.4	0.4
LOI	20.6	23.5	21.4	23.2	22.5	21.9	22.5
Total	99.8	99.8	99.9	99.8	99.8	99.8	99.8
Zn	125.8	136.3	115.8	138.7	129.1	123.4	131.2
Cu	46.0	95.1	154.8	107.2	82.7	104.4	130.0
Ni	18.8	19.8	43.8	39.5	31.2	37.3	38.6
Cr	14.0	16.4	27.2	20.4	17.2	34.5	9.7
V	205.5	345.7	378.0	382.5	385.5	395.1	391.8
Ba	256.4	164.7	103.9	142.3	179.0	168.0	183.9
Sc	26.1	38.7	33.2	33.7	33.4	32.1	33.7
La	28.6	17.1	11.7	14.7	18.4	17.3	19.3
Ce	79.3	52.1	39.8	51.2	55.9	55.8	58.0
Nd	50.6	34.5	27.3	33.3	35.5	33.9	37.1
Nb	30.9	21.9	16.7	24.4	27.1	25.7	26.2
Zr	313.1	249.3	183.1	208.7	247.8	234.6	244.6
Y	59.9	59.5	41.8	46.2	48.4	45.4	53.1
Sr	358.9	232.4	287.2	325.2	327.0	310.3	271.1
Rb	12.4	17.5	7.6	12.7	11.9	14.9	15.5
U							
Th							
Pb							
Co							
146Nd/148Nd							
86Sr/87Sr							
206Pb/204Pb							
207Pb/204Pb							
208Pb/204Pb							
208Hf/206Hf							

Sample name	515	518	519	678	747	776	777
Latitude	64.818016	64.817614	64.888376	64.887396		64.754879	64.757396
Longitude	-14.347589	-14.350011	-14.565322	-14.557113		-14.483211	-14.502421
Location	Near Skridá	Near Skridá	Hesthálsá	Hesthálsá		Fossardalur	Fossardalur
Type	Dyke	Lava	Sill	Int	Lava	Lava	Lava
Age		11.2	10.0				
SiO2	49.0	47.5	52.3	50.89	76.23	47.41	48.00
Al2O3	13.4	13.6	13.4	13.32	11.79	15.90	13.73
Fe2O3	14.9	15.1	15.2	15.56	2.13	11.97	14.17
FeO	1.7	1.7	1.7	1.7	0.2	1.3	1.6
FeOT	16.5	16.7	16.9	17.3	2.4	13.3	15.7
MgO	5.8	6.0	3.4	3.45	0.08	6.62	6.36
CaO	10.3	11.5	7.2	7.26	0.55	11.98	11.62
Na2O	2.4	2.4	3.3	2.83	4.27	2.46	2.41
K2O	0.6	0.3	0.9	1.504	3.326	0.343	0.244
Na + K	3.0	2.7	4.2	4.331	7.596	2.798	2.649
TiO2	3.0	3.0	2.9	2.649	0.181	2.044	2.556
MnO	0.2	0.2	0.3	0.322	0.033	0.170	0.212
P2O5	0.3	0.4	0.9	1.039	0.027	0.195	0.237
LOI	21.2	21.1	22.8	22.3	8.9	16.6	19.6
Total	99.8	99.8	99.9	99.90	99.90	99.90	99.90
Zn	118.6	135.7	165.0	194.5	83.1	87.4	114
Cu	108.7	120.6	13.8	16.2	6.8	152.5	143.5
Ni	41.8	66.2	5.4	5.7	0	63.4	57.8
Cr	31.8	86.5	0.0	0	4.2	220	91
V	396.0	426.6	139.5	132.2	4.3	287.5	377.1
Ba	142.0	128.4	227.8	233.6	563.6	89	86.7
Sc	33.1	44.8	30.8	31.3	1.6	37.3	41.9
La	13.1	11.4	25.2	28.5	58.1	5.4	8.3
Ce	45.5	40.2	72.9	82.7	155.5	26.4	31.6
Nd	28.9	27.7	48.5	55.5	68.9	18.2	20.1
Nb	21.1	20.7	34.4	36.3	73.9	12.5	15.2
Zr	189.6	191.5	316.5	368.3	350.1	111.8	141
Y	40.0	41.6	72.0	82.3	100.4	26.5	33.3
Sr	305.1	292.5	314.6	305.3	47.2	283.1	284.2
Rb	12.9	2.3	19.0	40.4	69.8	3.6	1.7
U				0	2.6	0	0
Th				2	9.1	0.6	0.6
Pb				2.8	8.9	1.1	1
Co							
146Nd/148Nd							
86Sr/87Sr							
206Pb/204Pb							
207Pb/204Pb							
208Pb/204Pb							
208Hf/206Hf							

Sample name	778	779	780	781	782	783	785
Latitude	64.757996	64.759022	64.80545	64.808072	64.810743	64.810607	64.823157
Longitude	-14.502869	-14.516634	-14.558228	-14.57298	-14.5893	-14.600635	-14.651802
Location	Fossardalur	Fossardalur	Oxi	Oxi	Oxi	Oxi	Oxi
Type	Lava	Lava	Lava	Lava	Lava	Lava	Lava
Age	9.5						9.1
SiO2	47.91	47.97	50.45	55.14	50.72	45.44	49.71
Al2O3	15.78	15.37	15.48	15.47	13.29	14.33	13.57
Fe2O3	12.14	12.40	12.85	9.97	15.19	17.46	14.81
FeO	1.4	1.4	1.4	1.1	1.7	1.9	1.6
FeOT	13.5	13.8	14.3	11.1	16.9	19.4	16.5
MgO	6.02	5.98	4.93	5.38	4.60	6.24	5.52
CaO	11.93	11.66	9.88	7.94	8.57	9.24	9.74
Na2O	2.31	2.25	2.91	2.82	3.04	2.59	2.86
K2O	0.308	0.288	0.434	0.526	0.546	0.413	0.463
Na + K	2.615	2.533	3.344	3.347	3.591	3.007	3.328
TiO2	2.095	2.098	1.900	1.330	3.061	3.166	2.898
MnO	0.177	0.187	0.231	0.154	0.230	0.250	0.223
P2O5	0.191	0.203	0.360	0.160	0.445	0.389	0.327
LOI	16.4	16.2	18.6	14.5	22.0	24.0	21.7
Total	99.90	99.90	99.90	99.90	99.90	99.90	99.90
Zn	102.5	99.5	126	86.8	141.2	155.8	135.1
Cu	129.8	98.8	91.9	94	92.9	165	94.5
Ni	68.1	57.3	49.9	86.8	29.5	78.9	46.9
Cr	186.2	81.4	125.8	62	10.9	38.8	48.1
V	328	314.5	233.7	206.9	333.4	379.1	412.7
Ba	84.4	85.3	157.4	204.4	183.5	103.7	134.4
Sc	39.2	37.7	36.3	25.4	38.5	34	38.1
La	4.6	5.5	18.4	18.6	17.9	11.3	15.2
Ce	27.1	31.5	55.3	48.1	55.6	45.6	49.9
Nd	17.1	18.2	33.4	22.2	35.8	30.7	31.4
Nb	12.8	13.1	21.4	13.6	24.3	21.9	23.2
Zr	116.2	119.5	375.2	174.1	244.2	217.1	222.1
Y	27.8	28	49	36.1	56.1	49.3	45.8
Sr	287.6	290.5	273.5	192.3	255.5	246	279.1
Rb	5.5	3.4	4.1	18.3	4.6	6.3	3.7
U	0	0	0.4	1	0	0	0
Th	0	0.4	1.8	4.5	2	0.8	1.1
Pb	1.3	0.8	2.1	3.1	2.6	1.5	2.2
Co							
146Nd/148Nd	0.513013						
86Sr/87Sr	0.703329						
206Pb/204Pb	18.61393						
207Pb/204Pb	15.48331						
208Pb/204Pb	38.2759						
208Hf/206Hf							

Sample name	786	788	789	790	791	792	793
Latitude	64.897805	64.87955	64.860462	64.856243	64.8206	64.819328	64.81816
Longitude	-14.645367	-14.442106	-14.40738	-14.382463	-14.357854	-14.357227	-14.356568
Location	Oxi						
Type	Lava	Lava	Lava	Lava	Lava	Lava	Lava
Age							
SiO2	53.44	51.91	48.41	47.49	46.80	47.52	47.10
Al2O3	15.27	13.98	14.34	13.87	13.05	12.80	12.51
Fe2O3	11.33	12.53	14.55	14.55	16.68	16.40	16.32
FeO	1.3	1.4	1.6	1.6	1.9	1.8	1.8
FeOT	12.6	13.9	16.2	16.2	18.5	18.2	18.1
MgO	5.54	3.69	3.77	6.07	4.92	5.13	4.92
CaO	7.92	8.90	8.85	10.22	9.54	9.29	9.27
Na2O	2.82	2.65	3.10	2.60	2.52	2.62	2.51
K2O	1.126	0.649	0.571	0.201	0.495	0.457	0.535
Na + K	3.942	3.303	3.676	2.798	3.017	3.081	3.047
TiO2	1.658	2.251	2.728	2.889	3.612	3.376	3.512
MnO	0.173	0.189	0.223	0.240	0.239	0.298	0.253
P2O5	0.192	0.322	0.751	0.364	0.407	0.463	0.485
LOI	17.4	15.8	18.8	19.2	21.8	21.6	20.5
Total	99.90	99.90	99.90	99.90	99.90	99.90	99.90
Zn	102.2	133.1	155.1	139.5	169.4	157.1	164.4
Cu	86.2	90.5	50.3	131.8	150.1	158.9	152.8
Ni	83.1	30.6	29.6	41	48.3	44.5	35.8
Cr	62.8	43.1	23.8	55.5	42.5	27.5	0.1
V	249.9	342.2	204.4	423	468	444	451.9
Ba	185	187.5	215.8	114.6	184.2	176.9	197
Sc	28	38.6	41.1	42.8	41.7	40.1	40.6
La	18	20.8	27.3	13.4	15.7	18.2	19.5
Ce	48.9	61.4	77.8	48.7	57.4	61.4	63.8
Nd	27.6	34	49	31.7	35.1	37.4	40.9
Nb	16.8	26.8	31.7	22.3	29.1	28.7	30.8
Zr	168.3	270.6	300.1	211.5	262.3	265.7	281.1
Y	40.3	51	65.4	44.3	49.8	52.5	54.7
Sr	212.6	254.9	275.8	304.4	277.1	284.8	290.6
Rb	26.2	8.5	5.2	0.9	4.8	7.3	12.2
U	0.7	0.05	0	0	0	0	0
Th	1.7	2.4	2.1	1.3	1.2	1.6	1.8
Pb	3.1	2.4	2.3	1.8	3.5	2.4	2.3
Co							
146Nd/148Nd		0.513021			0.513026		
86Sr/87Sr		0.703376			0.703380		
206Pb/204Pb		18.46844			18.51735		
207Pb/204Pb		15.48417			15.48458		
208Pb/204Pb		38.21479			38.23735		
208Hf/206Hf							

Sample name	794	795	796	799	801	802	803
Latitude	64.82004	64.819772	64.836127	64.824458	64.772455	64.798824	64.748679
Longitude	-14.377328	-14.37946	-14.328561	-14.216565	-14.41319	-14.488982	-14.449624
Location							
Type	Lava	Lava	Lava	Lava	Lava	Lava	Lava
Age					9.9		
SiO2	47.57	46.66	49.17	49.15	51.92	48.76	49.21
Al2O3	13.10	14.65	12.77	13.73	13.73	13.55	13.04
Fe2O3	15.31	14.92	16.31	14.85	13.73	15.60	16.27
FeO	1.7	1.7	1.8	1.7	1.5	1.7	1.8
FeOT	17.0	16.6	18.1	16.5	15.3	17.3	18.1
MgO	5.39	5.28	5.04	5.14	3.98	5.15	4.93
CaO	9.47	10.85	9.30	9.39	7.79	9.78	9.29
Na2O	2.70	2.58	2.62	2.98	3.18	2.82	2.90
K2O	0.348	0.285	0.563	0.579	0.993	0.322	0.365
Na + K	3.045	2.862	3.187	3.554	4.169	3.138	3.263
TiO2	2.903	2.543	3.136	2.970	2.742	2.907	3.248
MnO	0.240	0.224	0.240	0.210	0.220	0.241	0.239
P2O5	0.380	0.273	0.359	0.339	0.549	0.459	0.388
LOI	19.3	19.4	22.7	21.1	19.9	21.9	23.1
Total	99.90	99.90	99.90	99.90	99.90	99.90	99.90
Zn	139.4	127	145.6	128.3	145.7	148.9	150.2
Cu	112.9	143.7	111.3	100.1	92	120.5	108.3
Ni	44.6	41.7	34.4	35.6	25.1	39.2	38.4
Cr	41.7	92.1	21	16.9	12.9	35.6	20.2
V	416.9	455.8	447.8	393.6	313	390.1	446.9
Ba	163.7	123.3	158.5	164.9	278	164.7	161.5
Sc	41.4	45	38.2	36.2	30.1	39	38.2
La	14.8	9.7	17.7	23.9	29.8	16.2	15.3
Ce	51.8	35.3	50.3	52.4	79.9	55.3	54.7
Nd	32.8	23.9	31	31.3	47.4	35.8	32.6
Nb	23.6	16.7	22.7	25.1	37.1	25.4	25.9
Zr	224.1	155.8	210.2	218.3	326.3	227	223.7
Y	47.9	37.8	45.9	41.8	59.9	50.9	49.6
Sr	274.7	260.3	280.4	317.3	267.4	275.7	280.4
Rb	4.8	2.7	11.6	7.3	21.2	1.6	3.8
U	0	0	0	0	0.8	0	0
Th	1.8	1	1.6	1.3	3.7	1.7	1.7
Pb	1.8	1.4	2	2	2.9	2.1	1.6
Co							
146Nd/148Nd					0.513011		
86Sr/87Sr					0.703412		
206Pb/204Pb					18.52737		
207Pb/204Pb					15.49312		
208Pb/204Pb					38.28501		
208Hf/206Hf							

Sample name	20140712a	20140713a	Ct.D6 334	Gunn1	M10	St0714	Stong
Latitude	64.84465	64.810567	64.854142	64.84465			64.77695
Longitude	-14.366633	-14.332367	-14.475613	-14.366633			-14.355917
Location	Gunnarsgil	Skridá		Gunnarsgil		Storalækjargil	Stong
Type	Dyke	Lava	Lava	Dyke	Dyke	Lava	Lava
Age				9.2			
SiO2	47.9	48.5	73.52	74.2	47.12	70.87	76.2
Al2O3	15.5	14.0	13.78	12.7	12.96	13.25	12.7
Fe2O3	12.5	13.7	2.41	2.8	16.56	3.99	2.1
FeO	1.4	1.5	0.3	0.3	1.8	0.4	0.2
FeOT	13.9	15.2	2.7	3.1	18.4	4.4	2.3
MgO	6.6	6.8	0.25	0.8	4.74	0.92	0.1
CaO	12.5	11.8	0.78	3.4	8.56	1.62	0.6
Na2O	2.2	2.3	3.90	2.3	2.61	4.55	4.5
K2O	0.3	0.2	3.269	3.4	0.788	2.953	3.4
Na + K	2.5	2.5	7.169	5.7	3.398	7.500	7.9
TiO2	2.0	2.2	0.191	0.2	3.178	0.679	0.2
MnO	0.2	0.2	0.086	0.1	0.247	0.127	0.0
P2O5	0.2	0.2	0.025	0.0	0.437	0.124	0.0
LOI	17.8	19.2	8.4	9.1	20.9	11.6	10.5
Total	99.9	99.9	99.9	99.8	99.9	99.9	99.8
Zn	100.3	107.2	121.2	98.4	162.9	110.8	94.1
Cu	170.8	157.6	7.8	9.1	101.4	3.9	7.7
Ni	76.1	62.2	0	2.8	32.2	0	0.2
Cr	210.2	79.8	1.1	0.4	0.2	1.7	0.9
V	325.9	362.9	2.5	0.9	438.1	1.4	3.2
Ba	95.4	93.4	712.9	417.9	172.8	544	605.1
Sc	37.0	43.4	1.6	2.7	35.3	10.3	1.4
La	5.2	5.8	83.5	86.5	16.5	62.2	65.4
Ce	29.5	29.8	165.5	173.0	54.5	152.1	154.7
Nd	15.7	19.7	91.8	86.3	32.7	81.3	68.2
Nb	11.9	13.2	81.5	67.3	25.5	77.9	75.3
Zr	110.1	124.7	385.4	406.3	227.8	810.9	346.2
Y	27.7	30.2	137	128.3	52.2	101.3	82.8
Sr	263.6	285.3	63.1	21.9	214.4	146.8	45.9
Rb	5.0	1.2	72.3	79.6	13.1	67.1	78.2
U			3		0	2.2	
Th			9.8		2.1	8.7	
Pb			6.2		2.7	4.6	
Co							
146Nd/148Nd							
86Sr/87Sr							
206Pb/204Pb							
207Pb/204Pb							
208Pb/204Pb							
208Hf/206Hf							

Sample name	T-688	T-690	A-675	A-699	A-674	A-001	B-678
Latitude	65.01545	65.01742	64.60865	64.93679	64.49891	64.51562	64.8874
Longitude	-14.4284	-14.4192	-14.4104	-13.7581	-14.4849	-14.5735	-14.5571
Location	T	T	A	A	A	A	B
Type							
Age							
SiO2	48.88	47.76	48.71	49.48	61.82	52.35	51.47
Al2O3	12.63	13.8	13.79	13.9	14.76	14.23	14.26
Fe2O3							
FeO							
FeOT	15.38	15.35	14.09	12.72	10.3	13.06	14.21
MgO	5.27	5.05	5.61	5.8	3.57	3.14	3.7
CaO	9.61	10.79	10.56	11.19	3.12	7.63	7.9
Na2O	2.57	2.63	2.96	2.71	3.26	4.52	3.44
K2O	0.58	0.59	0.28	0.53	0.67	0.83	0.58
Na + K	4.09	3.16	3.21	2.98	2	2.71	2.88
TiO2	0.25	0.28	0.29	0.2	0.14	0.33	0.29
MnO							
P2O5	0.59	0.42	0.35	0.34	0.22	1.07	1.13
LOI							
Total	100	100	99.99	100	99.99	99.99	100
Zn	147.4	134.9	122.2	114.5	87.5	150.2	178.1
Cu	87.2	135.3	117.7	165.1	112.6	16.6	26
Ni	26.1	24.3	42.9	67.8	43	5	0.2
Cr	15.3	27	42.7	117.5	77.4	8.3	9
V	459.8	448.2	400.5	358.8	240.9	65.4	138.7
Ba	159.6	158	157.5	107.1	130.9	259.1	244.8
Sc	43.7	43.9	41.9	39.3	29.8	21.3	31.2
La							
Ce							
Nd							
Nb							
Zr	232.4	239.6	189.7	199.7	188.2	230.9	360.2
Y	56.3	53.9	40.2	40.5	29.9	66.6	87.8
Sr	267.6	244.6	306.1	258.9	277.5	429.7	333.3
Rb							
U							
Th							
Pb							
Co	74.8	69.3	68.9	64.7	47.5	37.6	46.5
146Nd/148Nd							
86Sr/87Sr							
206Pb/204Pb			18.5548				18.5308
207Pb/204Pb			15.5016				15.4923
208Pb/204Pb			38.3169				38.2478
208Hf/206Hf		0.283158	0.283221				0.283198

Sample name	R-700	R-007	R-697	R-800
Latitude	64.98464	64.99574	64.92554	64.995736
Longitude	-13.9064	-13.904	-13.8801	-13.903998
Location	R	R	R	R
Type			basalt dyke	basalt lava
Age				
SiO2	72.79	52.02	49.88	
Al2O3	13.7	13.59	13.02	
Fe2O3				
FeO				
FeOT	3.19	14.36	14.81	
MgO	0.04	3.51	4.71	
CaO	0.92	6.88	9.23	
Na2O	5.23	3.64	2.71	
K2O	3.53	1.44	0.81	
Na + K	0.28	2.89	3.89	
TiO2	0.09	0.3	0.24	
MnO				
P2O5	0.02	1.19	0.53	
LOI				
Total	99.97	99.99	99.99	
Zn	131.5	168	143.4	
Cu	19.2	26.6	220.9	
Ni	0.3	1.1	32.5	
Cr	3.7	3.2	20.2	
V	5.9	99.4	398.5	
Ba	734	445.1	156.9	
Sc	3.8	30	38	
La				
Ce				
Nd				
Nb				
Zr	730.6	451.5	308.9	
Y	136.8	85.5	62.2	
Sr	102.2	434.7	248.4	
Rb				
U				
Th				
Pb				
Co	1.2	43.1	69.9	
146Nd/148Nd				0.5130
86Sr/87Sr				0.7034
206Pb/204Pb			18.5032	18.3910
207Pb/204Pb			15.4778	15.4815
208Pb/204Pb			38.2133	38.1607
208Hf/206Hf			0.283182	

Table C.2: Standard analysis undertaken alongside U-Pb zircon analysis for samples 470 and Gunn1.

Primary Standard for Pb/U ratio:	Measured Pb/U Age		95% C.I. Uncertainty	Published age:	Error
91500	1064	±	3.6	1062.4	1.6
Secondary standard zircon - Analysed as unkowns:	**Measured Pb/U Age**		**95% C.I. Uncertainty**	**Published age:**	**Error**
Mudtank	706		13	732	5.0
Monastery	85.3	±	2.5	90.1	0.5
Penglai	3.94	±	0.39	4.1	0.11
Temora	420	±	6.7	416.8	3.2
AusZ-2	38.34	±	0.45	38.8963	0.0044
AusZ-5	38.18	±	0.55	38.9022	0.0035

Table C.3: Standard analyses for trace elements analysed at University of Edinburgh.

		Nb (ppm)	Zr1 (ppm)	Y (ppm)	Sr (ppm)	Rb (ppm)	Zn (ppm)	Cu (ppm)	Ni (ppm)
BCR	Book	14.0	190.0	38.0	330.0	47.2	129.5	19.0	13.0
	Average	12.7	192.4	37.9	333.5	47.6	124.9	17.9	13.5
	1sigma	0.1	1.1	0.3	2.9	0.3	0.8	0.2	0.2
BEN	Book	105.0	260.0	30.0	1370.0	47.0	120.0	72.0	267.0
	Average	117.3	266.8	29.8	1383.3	47.5	133.2	76.6	280.9
		0.3	1.0	0.2	4.7	0.2	0.4	0.6	0.6
BHVO-1	Book	19.0	179.0	27.6	403.0	11.0	105.0	136.0	121.0
	Average	19.4	173.7	27.1	391.8	9.9	103.8	132.7	116.9
		0.1	0.6	0.2	0.8	0.1	0.5	0.2	0.5
BIR	Book	0.6	15.5	16.0	108.0	0.3	71.0	126.0	166.0
	Average	0.7	17.2	16.3	107.7	0.5	66.9	123.7	153.7
		0.0	0.5	0.2	0.3	0.1	0.6	0.8	0.5

		Cr (ppm)	V (ppm)	Ba (ppm)	Sc (ppm)	La (ppm)	Ce (ppm)	Nd (ppm)
BCR	Book	16.0	407.0	681.0	32.6	24.9	53.7	28.8
	Average	4.1	397.8	690.9	30.6			
	1sigma	0.5	0.7	1.1	0.3			
BEN	Book	360.0	235.0	1025.0	22.0	82.0	152.0	67.0
	Average	382.1	248.5	1058.0	24.7	91.9	156.1	69.9
		0.0	1.5	1.6	0.3	1.4	0.6	0.5
BHVO-1	Book	289.0	317.0	139.0	31.8	15.8	39.0	25.2
	Average	283.3	311.3	127.6	32.4	13.5	39.5	26.1
		1.1	2.2	0.4	0.7	1.4	0.9	1.3
BIR	Book	382.0	313.0	7.0	44.0	0.6	2.0	2.5
	Average	369.2	310.0	4.7	40.3	3.5	3.7	2.4
		0.3	1.6	2.9	0.5	0.2	0.8	0.9

Table C.4: Sr, Nd and Hf standard analyses

	87Sr/86Sr	error(2sm)	84Sr/86Sr	error(1sd)	Rb87/Sr87	error(2sm).1	frac.(exp)	error(2sm).2
JB2-1Sr	0.703689	0.000006	0.056491	0.000027	0.000008	0.000001	1.003783	0.000049
JB2-2Sr	0.703694	0.000006	0.056486	0.000032	0.000018	0.000002	1.002032	0.000043

	143Nd/144Nd	error(2sm)	150Nd/144Nd	error(2sm).1	Sm144/Nd144	error(2sm).2	frac.(exp)	error(2sm).3
JB2-1Nd	0.513112	0.000007	0.236512	0.000009	0.000032	0.000000	0.998827	0.000055

	176Hf/177Hf	error(2sm)	multiple applied
JMC 14374	0.282173	0.000005	1.000066
JB2-1Hf	0.283206	0.000015	
JB2-2Hf	0.283233	0.000005	

Table C.5: Pb isotope standard analysis

	208/204c	2SE	207/204c	2SE	206/204c	2SE
JB-3 Iceland	38.2571	0.0018	15.5392	0.0007	18.2952	0.0007
JB-3 Japan	38.1000	0.0046	15.5000	0.0042	18.3000	0.0043
NBS981	36.5957	0.0038	15.4582	0.0034	16.9118	0.0031

C.1 Breiðdalur volcano geological map

Geological Map of the Breiðdalur Central Volcano

Basemap: 20 m contours sourced from Landmælingar Íslands

Based upon previous mapping by Walker (1963)

CRS: WGS 84; Datum Lambert 2004

Breiðdalur, eastern Iceland

Robert A. Askew, Thorvaldur Thordarson, Ármann Höskuldsson

Institute of Earth Science, University of Iceland, Askja, Sturlugata 7, 101 Reykjavík

UNIVERSITY OF ICELAND

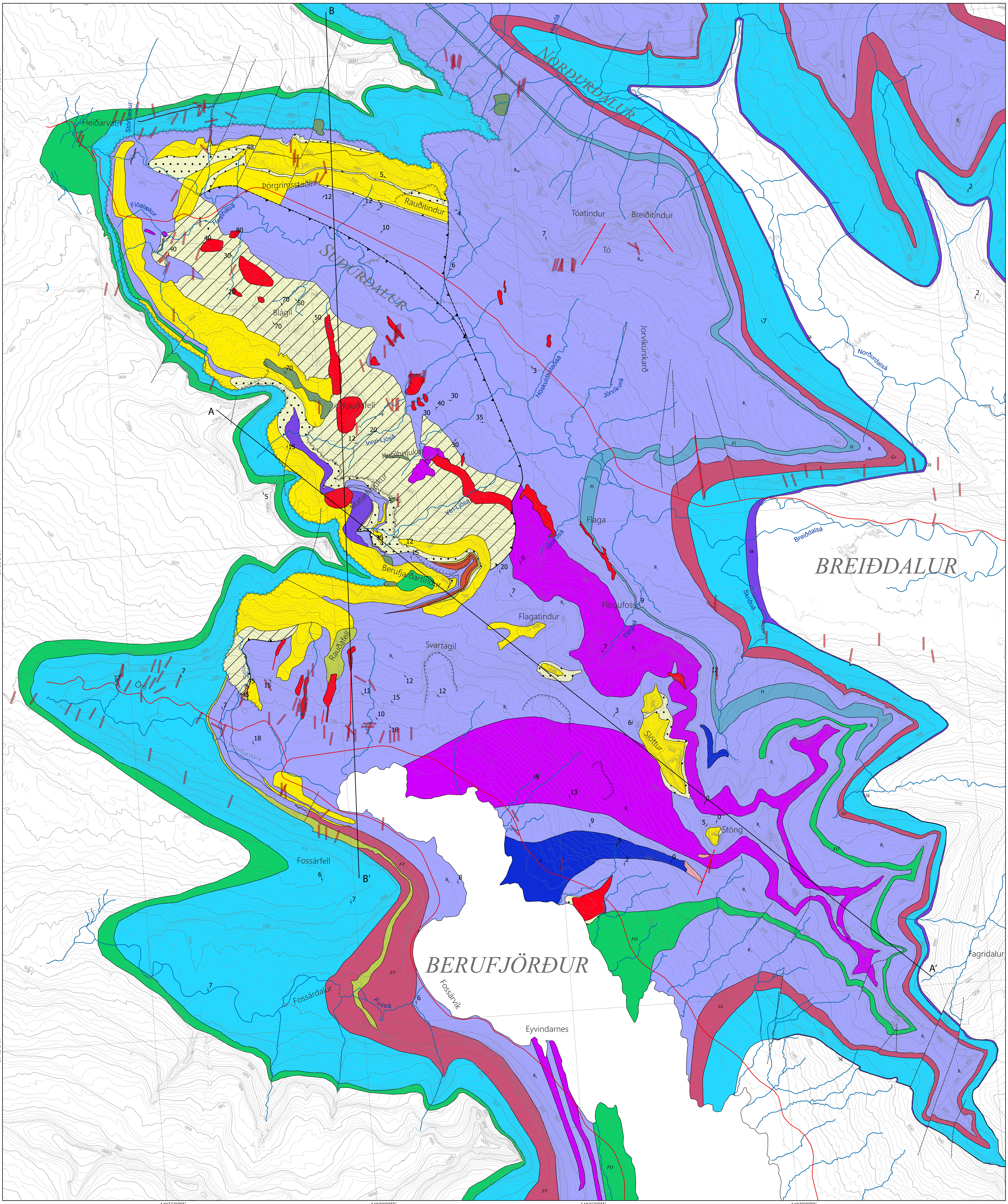

Legend

Contact Type

- Contact
- Disconformity
- Caldera fault (displacement to arrow)
- Caldera fault (inferred) (displacement to arrow)
- Normal fault
- Mass movement scarp
- Minor contour (20 m); Major contour (100 m)
- River (River name); Road
- Cross section line
- Bedding (dip in degrees)

Scale (Km): 0 – 2.5 – 5

N

Units

Breiðdalur Lavas

- B_1 Lower Eastern Flank
- Fl Breiðdalur Flögufoss Group
- St Breiðdalur Stöng Group
- Icelandite Lavas
  - B_2 Flaga Icelandite lavas
- B_3 Upper Eastern Flank
- B_{ne} North Eastern Flank
- Silicic Lava
- Composite Lava
- Hyaloclastite
- Caldera Fill Deposits
- Silicic Lapilli Tuff or Tuff
- Ignimbrite
  - Sk Skessa Tuff Ignimbrite

- Mafic Intrusion
- Silicic Intrusion
- Silicic dyke
- Icelandite Intrusion
- Composite intrusion
- Dykes

Other groups

- Plateau Basalt Lavas
  - Olivine Basalt Group
  - FO Fagridalur Olivine Basalt Group
  - FV Fossárvik Porphyritic Basalt Group
  - Gr Grænavatn porphyrytic group
- Volcaniclastic Sediment